by

Andrew John Bond

MA, MSc, DIC, CEng, MICE

12th August 1989

A thesis submitted to the University of London
(Imperial College of Science, Technology, and Medicine)
in partial fulfillment of the requirements for the degree of
Doctor of Philosophy in the Faculty of Engineering

BIBL.
LONDIN.
UNIV.

Volume 2

Table of Contents

APPENDIX 1

Cavity expansion solutions

A1.1 FORMULAE FOR INCREASE IN STRESS INSIDE PLASTIC ZONE . . 504
A1.2 NOTES AND REFERENCES 507

APPENDIX 2

Survey of previous instrumented pile tests

A2.1 INTRODUCTION 512
A2.2 SURVEY OF INSTRUMENTED PILE TESTS 513
A2.3 NOTES AND REFERENCES 518

APPENDIX 3

Fundamental properties of London clay

A3.1 INTRODUCTION 526
A3.2 COMPOSITION 527
A3.3 BEHAVIOUR IN ONE DIMENSIONAL COMPRESSION 528
A3.3.1 Introduction 528
A3.3.2 Reconstituted clay 528
A3.3.3 Intact London clay 529
A3.4 BEHAVIOUR IN UNDRAINED SHEAR 530
A3.4.1 Reconstituted London clay 530
A3.4.2 Intact Samples 533
A3.5 INTERFACE BEHAVIOUR AT LARGE SHEAR STRAINS 534
A3.5.1 The basic shear mechanisms 534
A3.5.2 Sliding shear behaviour 535
A3.5.3 Transitional shear 535
A3.5.4 Special tests to simulate pile installation and testing 536
A3.6 NOTES AND REFERENCES 538

APPENDIX 4

Geology of the Canons Park area

A4.1 GEOLOGY OF THE STANMORE AREA 542
A4.1.1 Six-inch and one-inch geological maps 542
A4.1.2 Well records 542
A4.1.3 Estimating the past overburden 546
A4.2 ESTIMATING THE PRE-CONSOLIDATION PRESSURE OF THE LONDON CLAY 547
A4.2.1 From standard oedometer tests 547
A4.2.2 From high pressure oedometer tests 547
A4.3 NOTES AND REFERENCES 549

APPENDIX 5

Earth and pore pressure cells: a review

A5.1 PILE-MOUNTED EARTH PRESSURES CELLS 555
A5.1.1 Introduction 555
A5.1.2 Reese and Seed (1955) 555
A5.1.3 Φien (1962) 556
A5.1.4 Agarwal and Venkatesan (1965) 558
A5.1.5 Koizumi and Ito (1967) 558
A5.1.6 BP/BRE instrumented pile (1976) 558
A5.1.7 Johnston (1979) 559
A5.1.8 Taylor Woodrow's EP cells (1982) 560
A5.1.9 O'Neill et al. (1982) 560
A5.1.10 Maddocks (1983) 561
A5.1.11 Francescon (1983) 562
A5.1.12 The Piezo-Lateral Stress cell 562
A5.1.13 Wersching (1987) 564
A5.1.14 The Oxford University IMP (1987) 565
A5.1.15 NGI's instrumented piles (1989) 566
A5.2 ASSESSMENT OF CELL ACTION EFFECTS 569
A5.2.1 Definition of cell action 569
A5.2.2 Factors that affect cell action 570
A5.2.3 Cell action in stiff soils 570
A5.2.4 Comparing designs of earth pressure cell 572
A5.2.5 Cell action effects during pile installation 575
A5.2.6 Laboratory studies of cell action effects 575
A5.3 PILE-MOUNTED PIEZOMETERS 578
A5.3.1 Introduction 578
A5.3.2 Reese and Seed (1955) 578
A5.3.3 Hanna (1967) 579
A5.3.4 Kenney (1967) 579
A5.3.5 Laboratory tests at Cambridge University (1981-83) 580
A5.3.6 O'Neill et al. (1982) 580
A5.3.7 The Oxford University IMP (1987) 580
A5.3.8 NGI's instrumented piles (1989) 582
A5.4 RESPONSE TIMES OF PILE-MOUNTED PIEZOMETERS 583
A5.4.1 Sources of error in pore pressure measurement 583
A5.4.2 Comparing pile-mounted piezometers 584
A5.5 NOTES AND REFERENCES 589

APPENDIX 6

Details of instrument design: axial load cells

A6.1 AXIAL LOAD CELLS MKS I-III 596
A6.2 TECHNICAL DATA: AXIAL LOAD CELLS 597
A6.2.1 General information 597
A6.2.2 Basic properties 597
A6.2.3 Calibration coefficients 598

A6.2.4 Other properties 598
A6.3 DESIGN DRAWING 599
A6.4 NOTES AND REFERENCES 600

APPENDIX 7

Details of instrument design: surface stress transducers

A7.1 SURFACE STRESS TRANSDUCERS MKS. I-IV 606
A7.1.1 Background 606
A7.1.2 Circuit diagram 607
A7.2 TECHNICAL DATA: SURFACE STRESS TRANSDUCERS 608
A7.2.1 General Information 608
A7.2.2 Details of the main housing 608
A7.2.3 Basic features of the load cells 608
A7.2.4 Radial total stress circuits 609
A7.2.5 Shear stress circuits 609
A7.2.6 Calibration coefficients 610
A7.2.7 Load cell compliance 610
A7.3 DESIGN DRAWINGS 611
A7.4 NOTES AND REFERENCES 617

APPENDIX 8

Details of instrument design: pore pressure probes

A8.1 PORE PRESSURE PROBES MKS I-IV 624
A8.1.1 Background 624
A8.2 TECHNICAL DATA: PORE PRESSURE PROBES 626
A8.2.1 General information 626
A8.2.2 Housing 626
A8.2.3 Pore pressure block 626
A8.2.4 Fluid used in system 626
A8.2.5 Transducer 627
A8.3 DESIGN DRAWINGS 628
A8.4 NOTES AND REFERENCES 632

APPENDIX 9

Notes on instrumented pile tests CP0-5

A9.1 JARDINE'S PILOT TEST (CP0F) 638
A9.1.1 Main sequence of events 638
A9.1.2 Instrument performance 639
A9.2 TEST SERIES CP1s - REJUVENATING THE SOUTHAMPTON PILE . . 640
A9.2.1 Aims of the first Test Series 640
A9.2.2 Main sequence of events 640
A9.2.3 Instrument performance 641
A9.3 TEST SERIES CP2f - INAUGURATION OF THE IMPERIAL COLLEGE INSTRUMENTED PILE 644

A9.3.1 Aims of the second Test Series 644
A9.3.2 Main sequence of events 645
A9.3.3 Instrument performance 645
A9.4 TEST SERIES CP3fs - PROVING THE SIGNIFICANCE OF JACKING RATE 647
A9.4.1 Aims of the third Test Series 647
A9.4.2 Main sequence of events 648
A9.4.3 Instrument performance 648
A9.5 TEST SERIES CP4f - LONG-TERM MEASUREMENTS OF PORE PRESSURE 649
A9.5.1 Aims of the fourth Test Series 649
A9.5.2 Main sequence of events 649
A9.5.3 Special procedure for installing CP4f 650
A9.5.4 Instrument performance 651
A9.6 TEST SERIES CP5f - "CONTROL" EXPERIMENT FOR DRIVEN PILES 652
A9.6.1 Main aims of the fifth Test Series 652
A9.6.2 Main sequence of events 652
A9.6.3 Instrument performance 652
A9.7 ORIENTATION OF INSTRUMENTS 653
A9.8 CONFIGURATION OF INSTRUMENTS 654
A9.8.1 Test Series CP0-2 654
A9.8.2 Test Series CP3-5 655
A9.9 NOTES AND REFERENCES 656

APPENDIX 10

Instrument performance (tests CP1-5)

A10.1 INSTRUMENT RELIABILITY: TEST SERIES CP1S 660
A10.2 INSTRUMENT RELIABILITY: TEST SERIES CP2F 661
A10.3 INSTRUMENT RELIABILITY: TEST SERIES CP3FS 662
A10.4 INSTRUMENT RELIABILITY: TEST SERIES CP4F 663
A10.5 INSTRUMENT RELIABILITY: TEST SERIES CP5F 664

APPENDIX 11

Further test results: pile installation

A11.1 PORE PRESSURE RESPONSE DURING PILE INSTALLATION 668
A11.1.1 Introduction 668
A11.1.2 Test Series CP1s 668
A11.1.3 Test Series CP2f 669
A11.1.4 Test Series CP3fs 670
A11.1.5 Test Series CP4f 671
A11.2 RELIABILITY OF THE PORE PRESSURE READINGS 673
A11.3 SUMMARY OF RESULTS FROM CANONS PARK EXPERIMENTS 675
A11.4 NOTES AND REFERENCES 676

APPENDIX 12

Further test results: equalization

A12.1 PORE PRESSURE DISSIPATION CURVES CP1-4 680
A12.2 LONG-TERM MEASUREMENTS WITH FLUSHABLE PROBES 684

APPENDIX 13

Further test results: pile loading

A13.1 LOAD-DISPLACEMENT DIAGRAMS 688
A13.2 FURTHER INSTRUMENTED PILE DATA: TEST SERIES CP5f 700
A13.3 FURTHER INSTRUMENTED PILE DATA: TEST SERIES CP3fs . . . 704

APPENDIX 14

Notes on the preparation of thin sections

A14.1 PREPARATION OF THIN SECTIONS 710
A14.1.1 Sampling procedure 710
A14.1.2 Sample impregnation 710
A14.2 NOTES AND REFERENCES 712

APPENDIX 15

Notes on the measurement of soil suction

A15.1 FILTER PAPER TECHNIQUE 716
A15.1.1 Sampling procedure 716
A15.1.2 Testing procedure 716
A15.1.3 Notes on the formulae used to calculate soil suction 717
A15.1.4 Further test results 720
A15.2 PRESSURE-PLATE MEASUREMENTS 723
A15.2.1 Testing procedure 723
A15.3 NOTES AND REFERENCES 724

LIST OF FIGURES: VOLUME 2

APPENDIX 1

Figure A1.1 Relationship between extent of plastic zone and clay's rigidity index 506

APPENDIX 3

Figure A3.1 Schematic map of London clay depositional environment 526
Figure A3.2 Grading curve envelope for Canons Park London clay 527
Figure A3.3 Mineral suite for typical lower London clay . 527
Figure A3.4 One-dimensional compression and swelling characteristics of London clay 528
Figure A3.5 Variation of secant bulk modulus with strain for K_0-swelling (reconstituted soil) 529
Figure A3.6 Effective stress paths for K_0-consolidated reconstituted London clay 531
Figure A3.7 Stress-strain curves for K_0-consolidated reconstituted London clay: (a) triaxial compression; (b) triaxial extension tests . . 532
Figure A3.8 Normalized undrained stiffness characteristics of reconstituted London clay 532
Figure A3.9 Variation of undrained small strain stiffness index with OCR: re-constituted samples 533
Figure A3.10 Undrained stress paths for intact samples of London clay 533
Figure A3.11 Undrained stiffness characteristics of intact samples 534
Figure A3.12 Rate effects shown by interface ring shear tests on London clay from Canons Park 537

APPENDIX 4

Figure A4.1 Six-inch geological maps for Canons Park . . . 543
Figure A4.2 Cross-section from Stanmore Common to Hampstead Heath 544
Figure A4.3 Construction of the rebound curve for the London clay at Canons Park 548

APPENDIX 5

Figure A5.1 Earth and pore pressure cells employed by Reese and Seed 555
Figure A5.2 NGI's earth pressure gauge of the 1960s . . . 556
Figure A5.3 Agarwal and Venkatesan's surface stress transducer 557
Figure A5.4 BP's cell for Forties Field 558
Figure A5.5 Johnston's Cambridge-type "local load cell" . 559
Figure A5.6 Taylor Woodrow's EP cell 560
Figure A5.7 Earth pressure cell designed by Maddocks to measure radial effective stress acting on a pile 561

Figure A5.8 The PLS cell 563
Figure A5.9 Detail of the Piezo-Lateral Stress cell 564
Figure A5.10 Werseching's "Boundary Orthogonal Stress Transducer" 565
Figure A5.11 Earth pressure cells on the Oxford University model pile 565
Figure A5.12 NGI's A-, B-, & C- piles 567
Figure A5.13 Instrument units for the NGI's A- & C- piles . 567
Figure A5.14 Cell action effects for rigid piston earth pressure cell 569
Figure A5.15 Effect of cell compli-ance, loading platen radius, and soil stiff-ness on cell factor . . 571
Figure A5.16 Cell action effects as determined in laboratory tests at TRRL 576
Figure A5.17 Hanna's pile piezometer 579
Figure A5.18 Strain-gauged diaphragm pore pressure cell mounted on the Oxford University model pile . . 581
Figure A5.19 Instrument units for the NGI's B- piles 582
Figure A5.20 Problems associated with measuring pore pressures in soil 583

APPENDIX 6

Figure A6.1 Design drawing for Mk III axial load cell . . . 599

APPENDIX 7

Figure A7.1 The "Oval" Cambridge earth pressure cell . . . 606
Figure A7.2 Circuit diagram for surface stress transducers. axial load cells, and pore pressure probes . . 607
Figure A7.3 Surface stress transducer: design drawing AJB/PSST/1 611
Figure A7.4 Surface stress transducer: design drawing AJB/PSST/2 612
Figure A7.5 Surface stress transducer: design drawing AJB/PSST/3 613
Figure A7.6 Surface stress transducer: design drawing AJB/PSST/4 614
Figure A7.7 Surface stress transducer: design drawing AJB/PSST/5 615
Figure A7.8 Surface stress transducer: design drawing AJB/PSST/6 616

APPENDIX 8

Figure A8.1 Pore pressure probes, Mks I and II 624
Figure A8.2 Pore pressure probes: design drawing AJB/PPU/1 628
Figure A8.3 Pore pressure probes: design drawing AJB/PPU/2 629
Figure A8.4 Pore pressure probes: design drawing AJB/PPU/3 630
Figure A8.5 Pore pressure probes: design drawing AJB/PPU/4 631

APPENDIX 9

Figure A9.1 Configuration of instruments - Pilot Test . . 638
Figure A9.2 Configuration of instruments - pile CP1 . . . 640
Figure A9.3 Pore pressures recorded during installation, Test CP1 641
Figure A9.4 Erratic pore pressure signals during Test Series CP1s 642
Figure A9.5 Erratic pore pressure observations reported by DiBiaggio 643
Figure A9.6 Configuration of Pile CP2 644
Figure A9.7 Configuration Pile CP3 647
Figure A9.8 Configuration of Pile CP4 649
Figure A9.9 Orientation of instruments, Test Series CP1-5 653

APPENDIX 11

Figure A11.1 Pore pressures recorded at leading instrument positions during pile installation, Test Series CP1s 668
Figure A11.2 Pore pressures recorded at leading instrument positions during pile installation, Test Series CP2f 669
Figure A11.3 Pore pressures recorded at leading instrument positions during pile installation, Test Series CP3fs 670
Figure A11.4 Pore pressures recorded at leading instrument positions during pile installation, Test Series CP4f 672

APPENDIX 12

Figure A12.1 Pore pressure dissipation curves for Test Series CP1s 680
Figure A12.2 Pore pressure dissipation curves for Test Series CP2f 681
Figure A12.3 Pore pressure dissipation curves for Test Series CP3fs 682
Figure A12.4 Pore pressure dissipation curves for Test Series CP4f 683
Figure A12.5 Pore pressures recorded by flushable probes in Test Series CP4f 684

APPENDIX 13

Figure A13.1 Load-displacement diagram for load test CP1s/L1C 688
Figure A13.2 Load-displacement diagram for load test CP2f/L1C 689
Figure A13.3 Pattern of loads applied in load test CP2f/L2C 689
Figure A13.4 Load-displacement diagram for load test CP2f/L2C 690
Figure A13.5 Load-displacement diagram for load test CP2f/L3T 691
Figure A13.6 Load-displacement diagram for load test

CP3fs/L1C 692
Figure A13.7 Load-displacement diagram for load test CP3fs/L2T 693
Figure A13.8 Load-displacement diagram for load test CP3fs/L3C 694
Figure A13.9 Load-displacement diagram for load test CP4f/L1T 695
Figure A13.10 Load-displacement diagram for load test CP4f/L2C 696
Figure A13.11 Load-displacement diagram for load test CP5f/L1T 697
Figure A13.12 Load-displacement diagram for load test CP5f/L2C 698
Figure A13.13 Load-displacement diagrams for load tests CP6d/L1T and CP7do/L1T 699
Figure A13.14 Variations in pore pressure with pile displacement during load test CP5f/L1T 700
Figure A13.15 Variations in pore pressure with pile displacement during load test CP5f/L2C 701
Figure A13.16 Changes in radial total stress, load test CP5f/L2C 702
Figure A13.17 Coefficients of friction, load test CP5f/L2C . 703
Figure A13.18 Changes in radial total stress, load test CP3fs/L2T 704
Figure A13.19 Coefficients of friction, load test CP3fs/L2T . 705

APPENDIX 15

Figure A15.1 Bench of clay for obtaining filter-paper samples 716
Figure A15.2 Filter-paper measurements of soil suction next to the driven pile CP6d 721
Figure A15.3 Filter-paper measurements of soil suction next to Kitching's jacked pile 722

LIST OF TABLES: VOLUME 2

APPENDIX 1

Table A1.1 Formulae for stress changes in plastic zone due to cavity expansion 505

APPENDIX 4

Table A4.1 Well records for Stanmore and surrounding areas 545

APPENDIX 5

Table A5.1 Properties of various pile-mounted earth pressure cells 573
Table A5.2 Response times of various piezometer systems, as used on piles and piezocones 586

APPENDIX 11

Table A11.1 Pore pressure response in CP4f/EQ 674
Table A11.2 Summary of results from the Canons Park pile tests 675

Appendix 1

Cavity expansion solutions

CONTENTS OF APPENDIX 1

A1.1 FORMULAE FOR INCREASE IN STRESS INSIDE PLASTIC ZONE . . 504
A1.2 NOTES AND REFERENCES 507

A1.1 FORMULAE FOR INCREASE IN STRESS INSIDE PLASTIC ZONE

Table A1.1 lists various formulae, derived from cylindrical cavity expansion analyses, for the stress changes caused by pile installation. The references to accompany this table are given at the end of this appendix.

The stress changes have been normalized by the clay's undrained shear strength, herein given the symbol k. Many of the formulae for $\Delta\sigma_{11}/k$ are expressed in terms of the parameter (r_p/R), where r_p is the radius of the plastic (yielded) zone around the pile, and R is the pile's radius.

Figure A1.1 shows the relationship between (r_p/R) and the clay's rigidity index G/k, for the various solutions given in the table. G is the shear modulus of the soil. Note the significance of the parameter Δ (the average volumetric strain in the plastic zone) on the results of Vesic's analysis.

Table A1.1 Formulae for stress changes in plastic zone due to cavity expansion

Author(s)	Stress change within PLASTIC ZONE ($r_p \leq r \leq \infty$) $\Delta\sigma_{rr}/k$	$\Delta\sigma_{zz}/k$	$\Delta\sigma_{\theta\theta}/k$	$\Delta u/k$	Extent of plastic zone (r_p/R)
Bishop et al. (1945)	-	-	-	-	$3^{\frac{1}{4}}\sqrt{(G/k)}$
Hill (1950)	$2Ln(r_p/r)+1$	$2Ln(r_p/r)$	$2Ln(r_p/r)-1$	-	$\sqrt{\{[2(1+\mu)/(5-4\mu)](G/k)\}}$
Gibson & Anderson (1961)	$2Ln(r_p/r)+1$	$2Ln(r_p/r)$	$2Ln(r_p/r)-1$	-	$\sqrt{(G/k)}$
Ladanyi (1963)	Weald Clay (at r = R) for G/k = 8.3-9.6				
	3.05	2.05	1.05	0.48	≈2.8-4.0
	Drarren Clay (at r = R) for G/k = 172-259				
	6.15	5.15	4.15	7.06	≈12-20
Mishida (1964)	$2Ln(r_p/r)+1$	0 (1)	$2Ln(r_p/r)-1$	$4Ln(r_p/r)/3^*$	$\sqrt{(G/k)}$
Butterfield & Banerjee (1970)[#]	$2Ln(\Omega r_p/r)+2w_r-w_p$	$2Ln(\Omega r_p/r)+w_r-w_p$	$2Ln(\Omega r_p/r)-w_p$	$2Ln(\Omega r_p/r)+w_r-w_p+0.81\alpha_H$	$(2/\sqrt{w_p})\sqrt{(G/k)}$
Vesic (1972)[$]	$(F'_q-1)\cot\phi$	-	$(K_a F'_q-1)\cot\phi$	$2Ln(r_p/r)+0.81\zeta'_v$	$\sqrt{[\zeta'_v I_r \sec\phi]}$
Randolph & Wroth (1979)	Assumes solution by Hill (1950)			$2Ln(r_p/r)$	$\sqrt{(G/k)}$
Carter et al. (1979)	Model (a) (at r = R) for G/k = 50				
	4.9			$2Ln(r_p/r)$	$\sqrt{(G/k)}$
	Model (b) (at r = R) for G/k = 74				
	≈5.0	≈2.7	≈3.0	≈4.2	$\sqrt{(G/k)}$
Randolph et al. (1979)	Boston Blue clay (at r = R) for various G/k				$\sqrt{(G/k)}$ =
	5.02	2.68	3.02	4.20	8.60, 5.48
	5.24	3.74	3.24	3.96	9.11
	5.44	4.44	3.44	3.90	9.54
	5.49	4.67	3.49	3.72	10.00
	5.46	4.72	3.46	3.42	10.86
	$(\sigma'_{rr}/k)_c = \{\sqrt{3}/M\}+1$	$(\sigma'_{zz}/k)_c = \sqrt{3}/M$	$(\sigma'_{\theta\theta}/k)_c = \{\sqrt{3}/M\}-1$		
Wroth et al. (1979)	London clay (at r = R) for various G/k				$\sqrt{(G/k)}$ =
	4.67	2.26	2.67	3.59	6.93, 6.00
	5.12	3.46	3.12	3.45	7.68
	5.44	4.35	3.44	3.45	8.49
	5.71	4.93	3.71	3.45	9.22
	5.87	5.24	3.87	3.20	10.95
	3.97	3.15	1.97	2.21	4.69
	$(\sigma'_{rr}/k)_c = \{\sqrt{3}/M\}+1$	$(\sigma'_{zz}/k)_c = \sqrt{3}/M$	$(\sigma'_{\theta\theta}/k)_c = \{\sqrt{3}/M\}-1$		
Mishida (1980)	Plane stress assumption			Function[†]	Function of G/k and μ
	Plane strain assumption			Function[‡]	$\sqrt{[2(G/k)-1]}$ for $\mu = 0.5$
Banerjee et al. (1983)	$2Ln(r_p/r)+1$	$2Ln(r_p/r)$	$2Ln(r_p/r)-1$	$2Ln(r_p/r)+0.82\alpha_H$	$1.08\sqrt{(G/k)}$

*Mishida assumes there is zero increase in vertical total stress - hence $\Delta u/k$ is as given here. Previously (1962), he had derived the equation $\Delta u/k = 4Ln(r_p/r)/3 + (A - 1/3)\sqrt{[3 + 4Ln^2(r_p/r)]}$

#The symbols used in these formulae are: $w_r = 1 - (\alpha R/r)^2$; $w_p = 1 - (\alpha R/r_p)^2$; $\Omega = (1 + w_p)/(1 + w_r)$; α_H = Henkel's (1960) pore pressure parameter; α = proportion of shear strength mobilized at pile face

$Vesic's parameters are: $F'_q = (1 + \sin\phi)(r_p/R)^{2\lambda}$, where $\lambda = \sin\phi/(1 + \sin\phi)$; $K_a = (1 - \sin\phi)/(1 + \sin\phi)$; ζ'_v = "volume change factor for a cylindrical cavity" (see Table 4 and equation 29 of original Paper); $\zeta'_v = I_r/(1 + I_r\Delta\sec\phi)$, where $I_r = G/k$ and Δ = average volumetric strain in plastic zone

†Function = $4Ln(r_p/r)/3 + (A-1/3)\sqrt{[3 + 4Ln^2(r_p/r)]}$
‡Function = $4(1+\mu)Ln(r_p/r)/3 + (A - 1/3)\sqrt{[3 + 4(1-2\mu)^2Ln^2(r_p/r)]}$

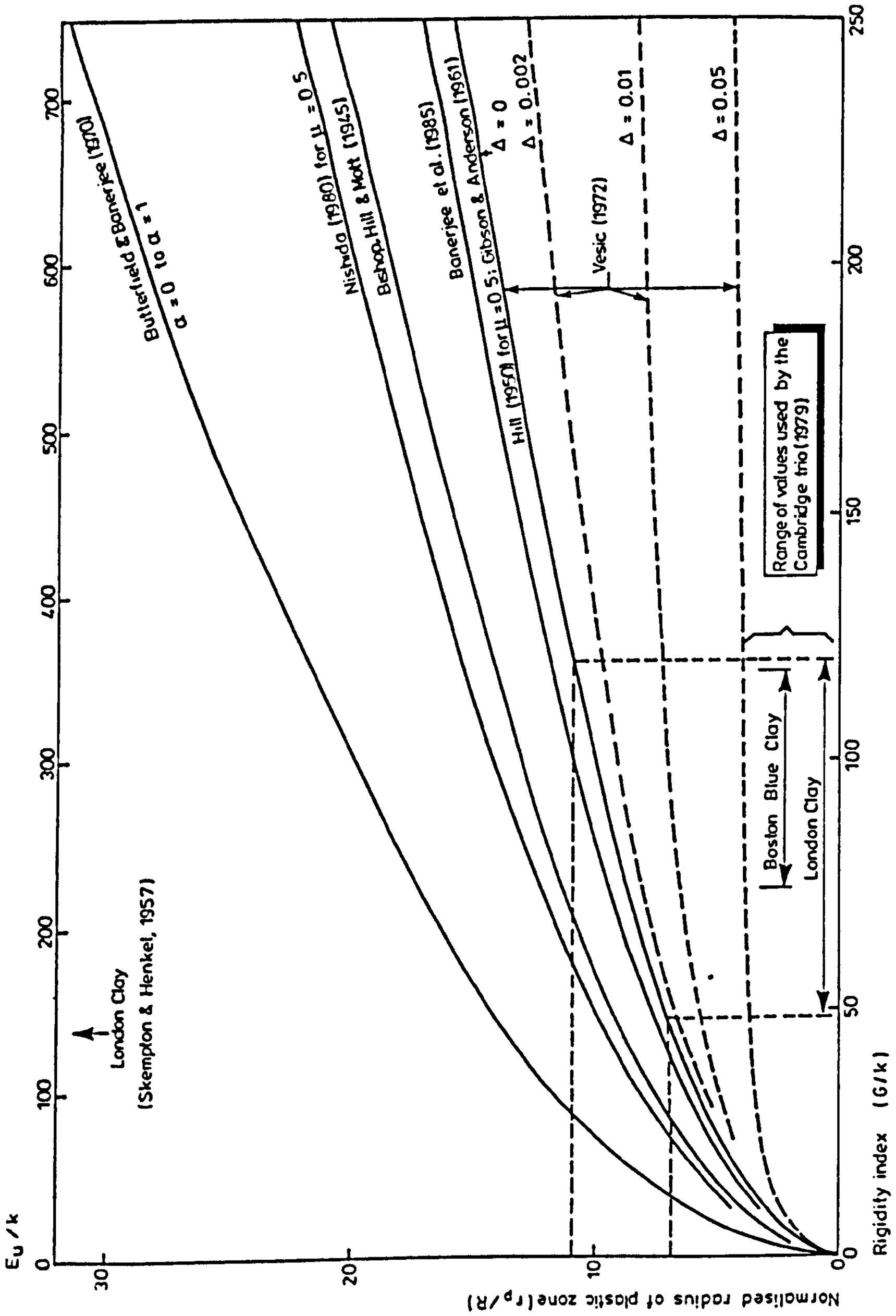


Figure A1.1 Relationship between extent of plastic zone and clay's rigidity index

A1.2 NOTES AND REFERENCES

Bishop R.F., Hill R., and Mott N.F. (1945). The theory of indentation and hardness tests. Proc. Phys. Soc., 57, Part 3, No 321, pp147-159.

Hill R. (1950). The mathematical theory of plasticity. Oxford Univ. Press, London, 356pp.

Gibson R.E. and Anderson W.F. (1961). In-situ measurement of soil properties with the pressuremeter. Civ. Engng & Publ. Works Review, 56(658), May 1961, pp615-618.

Ladanyi B. (1963). Expansion of a cavity in a saturated clay medium. J. Soil Mech. & Fdns Div., Am. Soc. Civ. Engrs, 89(SM4), pp127-161.

Nishida Y. (1962). Correspondence. Géotechnique, 13(1), pp90.

Nishida Y. (1964). A basic calculation of the failure zone and the initial pore pressure around a driven pile in clay. Proc. 2nd Asian Regional Conf. Soil Mech. & Fdn Engng, Tokyo, 1, pp217-219.

Butterfield R. and Bannerjee P.K. (1970). The effect of porewater pressures on the ultimate bearing capacity of driven piles. Proc. 2nd Southeast Asian Conf. Soil Mech. & Fdn Engng, Singapore, pp385-384.

Vesic A.S. (1972). Expansion of cavities in infinite soil mass. J. Soil Mech. & Fdns Div., Am. Soc. Civ. Engrs, 98(SM3), pp265-290.

Randolph M.F. and Wroth C.P. (1979). An analytical solution for the consolidation around a driven pile. Int. J. Num. & Anal. Methods in Geomechanics, 3, pp217-229.

Carter J.P., Randolph M.F., and Wroth C.P. (1979). Stress and pore pressure changes in clay during and after the expansion of a cylindrical cavity. Int. J. Numer. Anal. Methods Geomech., 3, pp305-322.

Randolph M.F., Carter J.P., and Wroth C.P. (1979). Driven piles in clay - the effects of installation and subsequent consolidation. Géotechnique, 29(4), pp361-393.

Wroth C.P., Carter J.P., and Randolph M.F. (1979). Stress changes around a pile driven into cohesive soil. In "Recent developments in the design and construction of piles", Instn Civ. Engnrs, London, pp345-354.

Nishida Y. (1980). Discussion of "Driven piles in clay - the effects of installation and subsequent consolidation" by Randolph et al. (1979). Géotechnique, 30, pp293-294.

Banerjee P.K., Davies T.G., and Fathallah R.C. (1983).
Behaviour of axially loaded driven piles in saturated clay from model studies. In "Developments in Soil Mechanics and Foundation Engineering - 1. Model Studies." (Ed. P.K. Banerjee and R. Butterfield.) Applied Science Publishers, London, 266pp. (pp169-195).

Henkel D.J. (1960). The shear strength of saturated remoulded clays. Proc. Research Conf. Shear Strength of Cohesive Soils, Boulder, Colorado, p551ff.

Appendix 2

Survey of previous instrumented pile tests

CONTENTS OF APPENDIX 2

A2.1 INTRODUCTION 512
A2.2 SURVEY OF INSTRUMENTED PILE TESTS 513
A2.3 NOTES AND REFERENCES 518

A2.1 INTRODUCTION

This appendix contains detailed notes about more than fifty instrumented pile tests in clay soils. In each case, information is given about the location of the test site and its soil conditions; the pile dimensions and method of installation; the instrumentation employed; and the load tests performed. At the end of each entry a note is made of the Category of the pile test - see Chapter 4 for details about the classification system used. The references from which this information has been compiled are listed at the end of the appendix.

Standard format for recording the pile tests

Authors (date)
- • Site (soil type)
- o Pile type (& number)
  Installation method (energy/blow)
- D Diameter
- L Embedded length
- h Wall thickness
- L/D Length to diameter (aspect) ratio
- D/h Diameter to thickness ratio
- $ Instruments (EP = earth pressure; PP = pore pressure; AL = axial load; SS = shear stress; ES = effective radial stress; SG =strain gauges; GM = measurements of (deep) ground movements; Acc = accelerometer; Inc = inclinometer; TS = temperature sensor; R_{remote})
- ¶ Load tests (L#C or L#T, where C = compression, T = tension; # = order of test, 1 = first, 2 = second, etc.)
- ‡ Notes

Category (A to E) - see Chapter 4

A2.2 SURVEY OF INSTRUMENTED PILE TESTS

Airhart et al. (1969)
- • Beaumont, Texas, USA (Beaumont clay)
- • 1 closed-ended steel pipe
- V Driven (Delmag D-12)
- D 406mm
- L 15.2m
- h 9.53mm
- L/D 37.5
- D/h 42.7
- § 6SG, 5PP, 3Acc
- ¶ L1C, L2C (13d); L3C, L4C (30d)
- ¦ v_{max} during driving = 4.4m/s (-0.9m/s rebound); no info. about u_o; incomplete equalization after 25d

Category B

Appendino, Jamiolkowski, & Lancellotta (1979)
- • Porto Tolle, Italy (Porto Tolle clay)
- • 9000 closed-ended steel tubes
- V Driven (drop hmr: 175-440kNm)
- D 508mm
- L 37-43m
- h ?
- L/D ≈78.7
- D/h ?
- § FP; PP^R; 4SG; 4Acc; AL^{toe}
- ¶ Load tests not reported
- ¦ See also Appendino (1977)

Category B

Arroyo and Lutz (1986)
- • Empire, Louisiana, USA (Empire clay)
- • 2 cone-ended PLS cell profiles
- V Jacked (20mm/s)
- D 38.4mm
- L 1.9m*
- h ?
- L/D 48.6*
- D/h ?
- § 1EP, 1PP, 1AL
- ¶ L1T, L2T
- ¦ *Distance of sensors from "pile" tip

Category A

Arroyo and Morrison (1988)
- • Saugus, Massachusetts, USA (Boston blue clay)
- • 6 cone-ended PLS cell profiles
- V Jacked (20mm/s)
- D 38.4mm
- L ?
- h ?
- L/D 25-50*
- D/h ?
- § 1EP; 1PP; 1AL
- ¶ None (penetration data only)
- ¦ *Distance of sensors from tip

Category A

Beradahl and Hult (1981)
- • Ska-Edeby, nr Stockholm, Sweden (Glacial varved clay)
- • 5 closed-ended timber piles
- V Driven (Borroram: 1.1kNm)
- D 100mm[8,9]
- L 15m
- h Solid
- L/D 150
- D/h -
- § AL^{head}
- ¶ L1C-L5C
- ¦ CRP, ML, & cyclic load tests

Category E

Bjerrum and Johannessen (1960)
- • Southern Norway (Homo. soft marine clay)
- • >100 open-ended steel box section
- V Driven
- D 200mm[8,9]
- L 20-23m
- h ?
- L/D 100-115
- D/h ?
- § $7PP^R$
- ¶ Load tests not reported
- ¦ Piles installed next to abutment

Category C

Blanchet, Tavenas, & Garneau (1989)
- • Maskinongé, Quebec, Canada (Champlain silty clay)
- • 1 closed-ended timber pile (in group of 9)
- V Driven (drop hmr)
- D Butt: 375mm; Tip: 222mm
- L 15.25m
- h Solid
- L/D 51.1 (av)
- D/h -
- § $2PP^{R*}$
- ¶ L1C
- ¦ *Gloetzl cells

Category C

Bond (1989)
- • Canons Park, north London, England (London clay)
- • 2 (5 tests) cone-ended steel pipes
- V Jacked (1.35-8.1mm/s)
- D 102mm
- L 3.18-4.07m
- h 9.53mm
- L/D 31.4-40.0
- D/h 10.7
- § 3EP/SS; 6PP; 4AL; 3TS
- ¶ Various (compression & tension)
- ¦ Profiles of w, c_u, p_k with radius; X-ray & micro-fabric studies

Category A

BP "Superteste"
- • [A]Pentre, Shropshire, England (silty glacial NC clay); [B]Tilbrook Grange, Cambridgeshire, England (boulder clay over Oxford clay)
- • 3 open-ended steel pipes
- V Driven ([A]BSP 357; [B,C]BSP HA40)
- D 762mm
- L A_{40}; B_{30}; C_{31m}
- h A_{15-20}; $B,C_{30-40mm}$
- L/D $A_{52.5}$; $B_{39.4}$; $C_{40.7}$
- D/h 19-51
- § >10 levels of SG, EP, PP; Acc (over 100 instruments in total)
- ¶ [A,B]L1C, Creep, 1-way cyclic, L2C? [C]L1T, Creep, L2T
- ¦ Data currently confidential; info. provided by Dr G. Symons (pers. comm., March 1989); see also Offshore Research Focus No 66, Aug 1988

Category A

BRE (1986)
- • RAF Cowden, North Humberside, England (Cowden glacial till)
- • 9 closed- and open-ended steel pipes
- V Driven (BSP HA: 2.5t drop hmr)
- D $C\text{-}F_{304.8}$; $G\text{-}K_{203.2mm}$
- L 8.85m
- h $C\text{-}F_{9.53}$; $G\text{-}K_{6.35mm}$
- L/D $C\text{-}F_{31.7}$; $G\text{-}K_{47.5}$
- D/h 32.0
- § $D.I_{4EP}$, 4PP, 6SG, 1Inc; D_{6PP^R}
- ¶ Tension (monotonic and cyclic)
- ¦ Profiles of w, c_u with radius; see also reports by Ove Arup (1986 & 1987)

Category A

Burghignoli and Caruana (1979)
- • Lab. tests, Univ. of Rome, Italy (Fiumicino clay: w_L = 65%; I_p = 25%)
- • 1 cone-ended perspex tube
- V Jacked (0.5mm/s)
- D 30mm
- L 0.2m
- h ?
- L/D 6.7
- D/h ?
- § $6PP^R$
- ¶ ?
- ¦ Installed into chamber ϕ600mm x 200mm

Category C

Chandler and Martins (1982)
• Laboratory tests, Imperial College, London, England (Speswhite kaolin)
o 17 closed-ended grouted brass piles
▽ "Wished-in-place"*; driven; & jacked
D 15mm
L 0.110-0.132m
h Solid
L/D 7.3-8.8
D/h -
§ $15,17_{1EP}$
¶ L1C (24h) - slow (drained) test
ǂ *Piles grouted into pre-bored holes; tests conducted in large txl cell ϕ102mm x 150mm
Category A

Clark and Meyerhof (1972 & 1973)
• Calgery, Alberta, Canada (Stiff clayey & sandy silt)
o 5 closed-ended timber
▽ Driven (28.5kNm)
D 304.8mm
L 6.9m
h -
L/D 22.6
D/h -
§ SG, EP^R
¶ Compression
Category E

Clark and Meyerhof (1972 & 1973)
• Edmonton, Alberta, Canada (Soft-firm clay)
o 5 closed-ended timber
▽ Driven
D 304.8mm
L 7.5m
h -
L/D 24.6
D/h -
§ SG, EP^R
¶ Compression
Category E

Cooke and Price (1973)
• Hendon, north London, England (London clay)
o 1 cone-ended steel tubing
▽ Jacked (0.083mm/s)
D 168mm
L 3.5m
h 6.4mm
L/D 20.8
D/h 26.25
§ 9AL; extensive measurements of GM
¶ L1C (21d); L2T
Category D

Cooke, Price, & Tarr (1979)
• Hendon, north London, England (London clay)
o 3 cone-ended steel tubes
▽ Jacked (0.25mm/s)
D 168mm
L 4.6m
h 6.4mm
L/D 27.4
D/h 26.25
§ ^{A,B}9AL, extensive measurements of GM
¶ Various loading tests, incl.: vert. & horiz. (as a group^{A-C}); horiz. static and cyclic^{A}; followed by compression^{B,C} and tension^{A-C} tests
Category D

Coop (1987)
• Madingley, Cambridge (Gault clay); Canons Park, north London (London clay); Huntspill, Somerset, England (soft blue-grey silty clay)
o 1 (several tests) open-/closed-ended segmented brass model pile
▽ Jacked (3.7-9mm/s)
D 80mm
L 5-9m (depending on test)
h ?
L/D 65-110
D/h -
§ 4EP; 5PP; 3AL; TS
¶ L1C-L3C
Category A

Cox, Kraft, & Verner (1979)
• Empire, Louisiana, USA (Empire clay)
o 4 open-ended steel pipes
▽ Driven (Vulcan 020)
D 355.6mm
L ^{1,2}15.24m; ^{3,4}12.2m
h ?
L/D ^{1,2}42.9; ^{3,4}34.3
D/h ?
§ 4SG
¶ ^{1,2}LCT//TCT; ^{3}LCTC//TCT; ^{4}LCT//CTC*
ǂ *≈310days pause at //
Category D

Coyle and Reese (1966)
• Laboratory tests, Univ. of Texas, USA (Taylor Marl No 2)
o 10 open-ended steel tubings
▽ "wished-in-place"*
D 12.7mm; 9.525mm
L 101.6mm
h ?
L/D 8.0; 10.7
D/h ?
§ AL^{head}
¶ Load transfer
ǂ *Soil consolidated around pile in triaxial cell; two ϕ12.7mm piles had roughened surfaces, others smooth
Category E

Flaate (1972)
• Nitsund, Norway (silty clay)
o 2 closed-ended timber piles (in group of 8)
▽ Driven (hmr ?)
D *Butt 370, tip 180mm; ^{II}330mm
L ^{I}11.7; ^{II}13.7m
h -
L/D ^{I}42.5; ^{II}53.7
D/h -
§ None
¶ L1C-L5C
ǂ Profiles of w, c_u with radius
Category E

Fox, Parker, & Sutton (1970); Clarke, Rigden, & Semner (1985)
• 'WC' platform, West Sole, southern North Sea (0-13m: Boulder clay; >13m: Lias clay)
o 2 open-ended steel pipes
▽ Driven
D 762mm
L 18.3m
h 31.75mm
L/D 24.0
D/h 24.0
§ -
¶ L1C, L2T*
ǂ Pile A with driving shoe (acted as "cookie cutter"); Pile B without (10.5m plug for L = 18m); *loading tests also conducted during installation
Category E

Francescon (1983)
• Lab. tests, Cambridge Univ., England (Speswhite kaolin)
o ^{A}4Series A; ^{B}12Series B closed-ended stainless steel tubes
▽ Jacked (^{A}100; ^{B}6.7mm/s)
D 18.9mm
L ^{A}≈0.4m; ^{B}≈0.3m
h 3.2mm
L/D ^{A}21.2; ^{B}15.9
D/h 5.9
§ 6EP/SS; 4PP; 5AL; $10PP^R$; GM
¶ LCTTCCCTCCTcyc
ǂ Profiles of w & soil displacements with radius; X-rays
Category A

Grosch and Reese (1980)
• Sabine, Texas, USA (soft, organic, highly plastic clay)
o 1 closed-ended aluminium tubing
▽ Jacked?
D 25.4mm
L 0.787m*
h .0.711mm
L/D 31
D/h 35.7
§ 1PP; 2SG
¶ Cyclic (two-way)
ǂ *Extended by ϕ50.8mm steel pipe, allowing penetrations of 3.0-3.7m
Category B

Hanna (1967)
• Lambton, Ontario, Canada (firm-stiff silty clay)
o 1 open-ended steel pipe
▽ Driven (Vulcan 000: 52.9kNm)
D 324mm
L ≈4.3m
h 7.92mm
L/D ≈13
D/h 40.9

§ 1PP
¶ None
‡ Instrumented pile installed in group of 53 piles; PP gauge at 27.4m; u_{max} ≈ 380kPa; u_o ≈ 200kPa?; 100% dissipation after 170h

Category B

Heerema (1979)
• Kontich, Belgium (Boom clay)
• 16 (2 tested) open-ended steel pipes
V Driven (Delmag D-12: 30.6kNm; Delmag D-15: 36.8kNm)
D 609.6mm
L " 18.6m; 66' 21.9m
h ", 6.2-25.4mm,
L/D " 36.0; 66' 30.5
D/h 24-80
§ SG,
¶ " L1C (2d), L2T (26d); 66' L1C (12d), L2T (16d)
‡ 1.5m deep starter pit

Category D

Bousel (1950)
• Detroit, Michigan, USA (soft plastic lacustrine clay)
• 1 ?-ended steel pipe
V Driven
D 406mm
L 20.0m
h ?
L/D 49.2
D/h ?
§ None
¶ L1C-L21C (2h; 3, 4, 6, 7, 9, 10, 11, 14d; then re-driven)

Category E

Ismael and Klym (1979)
• Pickering, Ontario, Canada (firm clayey-sandy-silt)
• 1 open-ended H-section pile (in group of 5)
V Driven (diesel hmr: 48.8kNm)
D ?
L 7.68m
h -
L/D ?
D/h -
§ 1PP*; 4PP^R**
¶ L1T
‡ *Hanna's (1967) device; **Geonor piezos

Category B

Jardine (1985)
• Canons Park, north London, England (London clay)
• 1 closed-ended steel pipe
V Jacked (≈8mm/s?)
D 102mm
L 3.11m
h 9.53mm
L/D 30.6
D/h 10.7
§ 8EP/SS; 4PP; 5AL
¶ L1T
‡ Pilot Test for current series of experiments

Category A

Johnston (1972): Butterfield and Johnston (1973 & 1980)
• Wellington Sports Ground, Southampton University, England (London clay [Hampshire Basin])
• 1 (3 tests) closed-ended steel tube
V Jacked (0.35mm/s in; 0.2mm/s out)
D 102mm
L 3.5m
h 9.53mm
L/D 34.4
D/h 10.7
§ 8EP/SS; 5AL
¶ None
‡ 3 experiments without electro-osmosis; installation and extraction only

Category B

Karlsrud and Haugen (1985a & 1985b)
• Høga, near Oslo, Norway (Høga clay)
• 18 closed-ended steel pipes
V Jacked (≈1.2mm/s)
D 153mm
L 5.15m
h 4.5mm
L/D 33.7
D/h 34.0
§ 4EP; 4PP; 6SG
¶ Various (incl. L1C and L1T)
‡ Vibrating wire devices; profiles of w and c_u with radius; X-ray and micro-fabric studies

Category A

Kenney (1967)
• Oslo, Norway (^K Kjelsås, ^M Manglerud III, and ^T Tønsberg) (Oslo quick clay)
• 1 open-ended pile made from sheet pile section
V Free fall under own weight!
D 470mm wide
L ^K≈9m; ^M≈10m; ^T≈6m
h ?
L/D ^K19; ^M21; ^T13
D/h ?
§ 8EP; 4PP
¶ None
‡ Kenney's aim was to measure σ'_{ho}

Category A

Koizumi and Ito (1967)
• Otemachi, Tokyo, Japan (soft, plastic clay)
• 4 cone-ended steel pipes (3^{1-3} in group of 9; 1 isolated[4])
V Jacked (1.67mm/s)
D 300mm
L 5.55m
h 3.2mm
L/D 18.5
D/h 93.8
§ 1,2 16EP; 1,2 8PP; 1,2 9SG; 3,4 18SG; 10PP^R
¶ [4]L1C

Category A

Lo and Stermac (1964)
• Toronto, Ontario, Canada (T, F Jane St; P Black Creek) (Sft-frm silty-clay)
• 2 closed-ended timber piles[T,P] and 1 closed-ended Franki pile[F]
V Driven (drop hammer: T 142kNm; F 28.5kNm)
D T,P Butt 368mm, tip ≈220mm; F 610mm
L T 7.7m; P 11.3m; F 4.3m*
h T,P Solid; F conc. filled
L/D T 25.9; P 38.6; F 7.0
D/h -
§ 4PP^R
¶ L1C, L2C
‡ *Length in silty-clay only; PP readings not reported in full

Category C

McAnoy et al. (1982); Pomnlah and McAnoy (1985)
• RAF Cowden, North Humberside, England (Cowden glacial till)
• 4 open-ended steel pipes[1-4]
V Jacked
D 193mm
L 10m
h 9mm
L/D 51.8
D/h 21.4
§ 1 4SG; 2 10SG; 3 3EP, 6PP, 3PP^R, 14SG, 4TS; 4 4SG
¶ Cyclic tension

Category A

Morrison (1984)
• MIT Campus, Boston, Massachusetts, USA (Boston blue clay)
• 1 cone-ended PLS cell profiles
V Jacked (20mm/s)
D 38.4mm
L ?
h ?
L/D 25-50*
D/h ?
§ 1EP; 1PP; 1AL
¶ None (penetration data only)
‡ *Distance of sensors from tip

Category A

Nauroy, Brucy, & Le Tirant (1985)
• Cran, Brittany, France (very plastic clay)
• 2 closed-ended steel pipes
V Driven
D 273mm
L 17m
h 6.3mm
L/D 62.3
D/h 43.3
§ 3EP; 2PP; ≈15SG
¶ Various tests (static, cyclic, storm-loading): incl. L1T
‡ See also Puech and Jezequel (1980)

Category A

NGI tests (1)
- • Onsøy, Norway (plastic marine clay)$^{A1-4,B1,C1-2}$; Lierstranda, Norway (lean silty marine clay)$^{A7-10,B2}$; Pentre, Shropshire, England (silty glacial clay)$^{A5-6}$
- o 12 closed-ended steel pipes$^{A1-10,C1-2}$ and 2 open-ended^{B1-2} steel pipes
- ∇ Driven
- D $^{A,C}219$; $^{B}812mm$
- L $^{A}5_{25}$; $^{A}6_{32.5}$; $^{C1-2}30$; others$_{10m}$
- h $^{A,C}8.3$; $^{B}9.5mm$
- L/D $^{A}47.7-148$; $^{B}12.3$; $^{C}137$
- D/h $^{A,C}26.4$; $^{B}85.5$
- § ^{A}6EP, 6PP, 6AL; ^{B}6EP, 6PP, 12SG; ^{C1}14EP, 14PP, 14AL; ^{C2}None
- ¶ L1T + 1-way cyclic tension
- ‡ Data currently confidential; information provided by Dr G. Symons (pers. comm. March 1989); see also Offshore Research Focus No 66, Aug 1988 and Borg Hansen et al. (1989)

Category A

NGI tests (2)
- • Tilbrook Grange, Cambridgeshire, England (Boulder clay over Oxford clay)
- o 3 closed-ended steel pipes^{A-C} and 1 open-ended^{D} steel pipe
- ∇ Driven
- D $^{A-C}219$; $^{D}273mm$
- L $^{A}9.5$; $^{B}10$; $^{C}16.5$; $^{D}17.5m$
- h $^{A}8-16$; $^{B,C}16-25$; $^{D}16-32mm$
- L/D $^{A}43.4$; $^{B}45.7$; $^{C}75.3$; $^{D}64.1$
- D/h Varies
- § ^{A}4EP, 8PP, 4ES, 8AL; ^{B}3EP, 6PP, 3ES, 6AL; ^{C}2EP, 4PP, 2ES, 4AL; ^{D}None
- ¶ L1T + 1-way cyclic tension
- ‡ Data currently confidential; info. provided by Dr G. Symons (pers. comm., March 1989); see also Offshore Research Focus No 66, Aug 1988

Category A

O'Neill et al. (1982a & 1982b)
- • Beaumont, Texas, USA (Beaumont clay)
- o 9 closed-ended steel pipes
- ∇ Driven (Raymond 1S: 26.5kNm)
- D 273.1mm
- L 10.1m
- h 9.27mm
- L/D 36.8
- D/h 29.5
- § 11SG; 1Inc; 4EP; 4PP; 4Acc; 4TS; 13PP^{R}; GM
- ¶ L1C-L4C (18, 80, 108, 114d); L5T (?d)

Category A

Orrje and Broms (1967)
- • Gothenburg, Sweden (*Backa, **Gullberg River) (Gothenburg clay)
- o 230 ?-ended r. conc. piles*; ? closed-ended timber piles**
- ∇ Driven
- D ?
- L *22.6m; **≈20.6m total
- h ?
- L/D ?
- D/h ?
- § *3PP^{R}; **6PP^{R}
- ¶ ?

Category C

Pelletier & Doyle (1982)
- • Aquatic Park, Long Beach, California (Aquatic Park clay)
- o 1 open-ended steel pipe
- ∇ driven (Delmag D62-12)
- D 762mm
- L 22.6m
- h 38.1mm
- L/D 29.6
- D/h 20.0
- § 3SG
- ¶ L1T (1h); re-driven 0.3m; L2T (60d); L3T? (90d)
- ‡ The "Beta" pile tests

Category D

Price and Wardle (1982)
- • Canons Park, London, England (London clay)
- o 2 cone-ended steel pipes
- ∇ 1 driven^{d} (3t air hmr) & 1 jacked^{J} (0.33mm/s)
- D 168mm
- L 4.5m
- h 6mm
- L/D 26.8
- D/h 28
- § ^{J}4AL; ^{d}displacement lugs (for AL)
- ¶ L1C

Category D

Reese and Seed (1955); Seed and Reese (1955)
- • San Francisco, California, USA (San Francisco Bay mud)
- o 1 cone-ended steel pipe
- ∇ Driven (drop hmr: 68kg)
- D 152.4mm
- L 4.57m
- h 2.0mm
- L/D 30.0
- D/h 76.2
- § 6EP; 6PP; SG
- ¶ L1C-L7C (3, 21h; 3, 7, 14, 23, 33d)

Category A

Rigden et al. (1979); Gallagher & St John (1980)
- • Cowden, North Humberside, England (Cowden glacial till)
- o 1 open^{A}-ended and 1^{B} closed-ended steel pipe
- ∇ Driven (BSP HA: 3.5t)
- D 457mm
- L 9.14m
- h 19mm
- L/D 20.0
- D/h 24.1
- § 3EP, 3PP, 12SG, 2Acc
- ¶ L1C (1), L2C (13), L3T (20mmth)
- ‡ Large zero shifts for several instruments

Category A

Roy et al. (1981); Konrad and Roy (1987)
- • St Alban, Quebec, Canada (Champlain clay)
- o 6 closed-ended steel pipes
- ∇ Jacked (^{1,2}0.17; ^{3,4}0.33; ^{5,6}1.17mm/s)
- D 219mm
- L 6.6m
- h 8mm
- L/D 30.1
- D/h 27.4
- § $^{1-6}$1EP^{toe}, 1,3,6$_{8PP}$, 2,5$_{4PP}$; not ^{5}7PP^{R}
- ¶ ^{A}L1C-L4C (4, 8, 20, 33d); ^{B}L1C (2y)
- ‡ See also Roy and Lemieux (1986)

Category B

Steenfelt, Randolph, & Wroth (1981)
- • Laboratory tests, Cambridge Univ., England (Speswhite kaolin)
- o 4 cone-ended duraluminium tubes
- ∇ Jacked (≈50mm/s)
- D 19.05mm
- L 0.372-0.443m
- h 0.91mm
- L/D 19.5-23.3
- D/h 20.9
- § 4EP, 4PP, 5AL, 6PP^{R}
- ¶ L1C, L2T, L3T, cyclic tests, L4C, L5C, L6T, L7T...
- ‡ Test chamber ϕ250mm x 600mm

Category A

Stermac, Selby, & Devata (1969)
- • Toronto, Ontario, Canada (Jane St) (Firm-v.stiff clayey silt)
- o 2 closed-ended conc.-filled steel tubes^{3,5} & 1 closed-ended timber pile^{9}
- ∇ Driven (Delmag D-12: 30.5kNm)
- D ^{3,5}324mm; ^{9}381mm butt, 203mm tip
- L ^{3,5}15.3m; ^{9}14.5m
- h -
- L/D ^{3,5}47.2; ^{9}49.6
- D/h -
- § ^{A}L^{head}
- ¶ ^{3,9}L1C, L2T//L3C, L4T; ^{5}L1C, L2T, L3C//L4C, L5T*
- ‡ ^{3}with oversized end-plate ϕ343mm; *≈400day time interval at //

Category E

Sutton et al. (1979)
- FD Platform, Forties Field, North Sea (Forties clay)
- 1 open-ended steel pipe
- ∇ Driven (Menck 3000/7000)
- D 1372mm
- L 71.2m
- h 50.8mm
- L/D 51.9
- D/h 27
- § 10SG; 9Acc; 3PP; 3EP
- ¶ Re-drive 2m

Category A

A2.3 NOTES AND REFERENCES

Airhart T.P., Coyle H.M., Hirsch T.J., and Buchanan S.J. (1969). Pile-soil system response in a cohesive soil. Am. Soc. for Testing & Materials, Special Tech. Publ. 444, "Performance of Deep Foundations", pp264-294.

Appendino M. (1977). Analysis of data from instrumented driven piles. Proc. 9th Int. Conf. Soil Mech. & Fdn Engng, Tokyo, 1, pp359-370.

Appendino M., Jamiolkowski M., and Lancellotta R. (1979). Pore pressure of NC soft silty clay around driven displacement piles. Proc. Conf. on Recent Developments in the Design and Construction of Piles, Instn Civ. Engnrs, London, pp169-175.

Azzouz A.S. and Lutz D.G. (1986). Shaft behavior of a model pile in plastic Empire clays. J. Geotech. Engng, Am. Soc. Civ. Engrs, 112(4), pp389-406.

Azzouz A.S. and Morrison M.J. (1988). Field measurements on model pile in two clay deposits. J. Geotech. Engng, Am. Soc. Civ. Engrs, 114(1), pp104-121.

Bergdahl U. and Hult G. (1981). Load tests on friction piles in clay. Proc. 10th Int. Conf. Soil Mech. & Fdn Engng, Stockholm, 2, pp625-630.

Bjerrum L. and Johannessen I. (1960). Pore pressures resulting from driving piles in soft clay. Proc. Conf. on Pore Pressure and Suction in Soils, London, pp108-111. Butterworths, London, 1961. (Also NGI Publ. 41.)

Blanchet R., Tavenas F., and Garneau R. (1980). Behaviour of friction piles in soft sensitive clays. Can. Geotech. J., 17(2), pp203-224.

Borg Hansen S., Solheim K., and Norum P. (1989). Instrumentation of driven model test piles for determination of capacity of cyclically loaded offshore piles. Proc. Conf. on Geotech. Instrumentation in Civ. Engng Projects, Nottingham, April 1989, Paper 53 (in press).

Building Research Establishment (1986). Research on the behaviour of piles as anchors for buoyant structures. Final Report, Dept of Energy Offshore Technology Report, OTH 86 222, HMSO, London.

Burghignoli A. and Caruana R. (1979). Indagine sperimentale sugli effetti dell'infissione di pali in terreni coesivi teneri. Rivista Italiana di Geotechnica, 13(2), Aprile-Giugno 1979, pp87-93.

Butterfield R. and Johnston I.W. (1973). The stress acting on a continuously penetrating pile. Proc. 8th Int. Conf. Soil Mech. & Fdn Engng, Moscow, 2.1, pp39-45.

Butterfield R. and Johnston I.W. (1980). The influence of electro-osmosis on metallic piles in clay. Géotechnique, 30(1), pp17-38.

Chandler R.J. and Martins J.P. (1982). An experimental study of skin friction around piles in clay. Géotechnique, 32(2), pp119-132.

Clark J.I. and Meyerhof G.G. (1972). The behavior of piles driven in clay. I. An investigation of soil stress and pore water pressure as related to soil properties. Can. Geotech. J., 9(4), pp351-373.

Clark J.I. and Meyerhof G.G. (1973). The behavior of piles driven in clay. II. Investigation of the bearing capacity using total and effective stress parameters. Can. Geotech. J., 10(1), pp86-102.

Clarke J., Rigden W.J., and Senner D.W.F. (1985). Reinterpretation of the West Sole platform 'WC' pile load tests. Géotechnique, 35(4), pp393-412.

Cooke R.W. and Price G. (1973). Strains and displacements around friction piles. Proc. 8th Int. Conf. Soil Mech. & Fdn Engng, Moscow, 2, pp53-60.

Cooke R.W., Price G., and Tarr K. (1979). Jacked piles in London Clay: a study of load transfer and settlement under working conditions. Géotechnique, 29(2), pp113-147.

Coop M.R. (1987). The axial capacity of driven piles in clay. DPhil Thesis, Univ. of Oxford.

Cox W.R., Kraft L.M., and Verner E.A. (1979). Axial load tests on 14-inch pipe piles in clay. Proc. 11th Offshore Technology Conf., Houston, Texas, 2, pp1147-1158 (Paper OTC 3491).

Coyle H.M. and Reese L.C. (1966). Load transfer for axially loaded piles in clay. J. Soil Mech. & Fdns Div., Am. Soc. Civ. Engrs, 92(SM2), pp1-26.

Flaate K. (1972). Effects of pile driving in clays. Can. Geotech. J., 9(1), pp81-88.

Fox D.A., Parker G.F., and Sutton V.J.R. (1970). Pile driving into North Sea Boulde Clays. Proc. 11th Offshore Technology Conf., Houston, Texas, 1, pp353-548.

Francescon M. (1983). Model pile tests in clay. Stresses and displacements due to installation and axial loading. PhD Thesis, Univ. of Cambridge, 110pp + figures.

Gallagher K.A. and St John H.D. (1980). Field scale model studies of piles as anchorages for buoyant platforms. Proc. European Offshore Petroleum Conf. and Exhibition, London, Paper EUR 135, pp

Grosch J.J. and Reese L.C. (1980). Field tests of small-scale pile segments in a soft clay deposit under repeated axial loading. Proc. 12th Offshore Technology Conf., Houston, Texas, 4, pp143-151 (Paper OTC 3869).

Hanna T.H. (1967). The measurement of pore water pressures adjacent to a driven pile. Can. Geotech. J., 4(3), pp313-325.

Heerema E.P. (1979). Pile driving and static load tests on piles in stiff clay. Proc. 11th Offshore Technology Conf., Houston, Texas, 2, pp1135-1145 (Paper OTC 3490).

Housel W.S. (1950). Discussion of paper by Cummings, Kerkoff, and Peck (1948). Trans. Am. Soc. Civ. Engnrs, 115, pp339-346.

Ismael N.F. and Klym T.W. (1979). Pore-water pressures induced by pile driving. J. Geotech. Engng Div., Am. Soc. Civ. Engrs, 105(GT11), pp1349-1354.

Jardine R.J. (1985). Investigations of pile-soil behaviour, with special reference to the foundations of offshore structures. PhD Thesis, Univ. of London (Imperial College), 2 vol., 789pp.

Johnston I.W. (1972). Electro-osmosis and porewater pressures; their effect on the stresses acting on driven piles. PhD Thesis, Southampton Univ.

Karlsrud K. and Haugen T. (1985a). Axial static capacity of steel model piles in overconsolidated clay. Proc. 11th Int. Conf. Soil Mech. & Fdn Engng, San Francisco, 3, pp1401-1406.

Karlsrud K. and Haugen T. (1985b). Behaviour of piles in clay under cyclic axial loading - results of field model tests. Proc. 4th Int. Conf. on the Behaviour of Offshore Structures (BOSS 1985), Delft, pp589-600. Elsevier, Amsterdam.

Kenney T.C. (1967). Field measurements of in situ stresses in quick clays. Proc. Geotech. Conf. on Shear Strength Properties of Natural Soils and Rocks, Oslo, 1, pp45-55.

Koizumi Y. and Ito K. (1967). Field tests with regard to pile driving and bearing capacity of piled foundations. Soils and Foundations, 7(3), pp30-53.

Konrad J.-M. and Roy M. (1987). Bearing capacity of friction piles in marine clay. Géotechnique, 37(2), pp163-175.

Lo K.Y. and Stermac A.G. (1964). Some pile loading tests in stiff clay. Can. Geotech. J., 1(2), pp63-80.

McAnoy R.P.L., Cashman A.C., and Purvis D. (1982). Cyclic tensile testing of a pile in glacial till. Proc. 2nd Int. Conf. on Num. Methods in Offshore Piling, Austin, Texas, pp257-291.

Morrison M.J. (1984). In-situ measurements on a model pile in clay. PhD Thesis, Massachusetts Institute of Technology, c687pp.

Nauroy J.-F., Brucy F., and Le Tirant P. (1985). Pieux battus sollicités en tension. Proc. 11th Int. Conf. Soil Mech. & Fdn Engng, San Francisco, 3, pp1607-1610.

O'Neill M.W., Hawkins R.A., and Audibert J.M.E. (1982a). Installation of pile group in overconsolidated clay. J. Geotech. Engng Div., Am. Soc. Civ. Engrs, 108(GT11), pp1369-1386.

O'Neill M.W., Hawkins R.A., and Mahar L.J. (1982b). Load transfer mechanisms in piles and pile groups. J. Geotech. Engng Div., Am. Soc. Civ. Engrs, 108(GT12), pp1605-1623.

Orrje O. and Broms B. (1967). Effects of pile driving on soil properties. J. Soil Mech. & Fdns Div., Am. Soc. Civ. Engrs, 93(SM5), pp59-73.

Ove Arup and Partners (1986). Research on the behaviour of piles as anchors for buoyant structures. Dept of Energy, Offshore Technology Report, OTH 86 215. HMSO, London, 80pp.

Ove Arup and Partners (1987). Comparison of British and Norwegian research on the behaviour of piles as anchors for buoyant structures. Dept of Energy, Offshore Technology Report, OTH 86 218. HMSO, London, 43pp.

Pelletier J.H. and Doyle E.H. (1982). Tension capacity in silty clays - bata pile test. Proc. 2nd Int. Conf. on Num. Methods in Offshore Piling, Austin, Texas, pp163-181.

Ponniah D.A. and McAnoy R. (1985). Pile jacking in glacial tills. Proc. Int. Conf. on Construction in Glacial Tilss and Boulder Clays, Edinburgh University, pp137-146.

Price G. and Wardle I.F. (1982). A comparison between cone penetration test results and the performance of small diameter instrumented piles in stiff clay. Proc. 2nd Eur. Symp. on Penetration Testing (ESOPT II), Amsterdam, 2, pp775-780. A.A. Balkema, Rotterdam, 1982.

Puech A. and Jezequel J.-F. (1980). The effects of log time cyclic loadings on the behaviour of a tension pile. Proc. 12th Offshore Technology Conf., Houston, Texas, 4, pp153-162 (Paper OTC 3870).

Reese L.C. and Seed H.B. (1955). Pressure distribution along friction piles. Proc. Am. Soc. for Testing Materials, 55, pp1156-1182.

Rigden W.J., Pettit J.J., St John H.D., and Poskitt T.J. (1979). Developments in piling for offshore structures. Proc. 2nd Int. Conf. on the Behaviour of Offshore Structures (BOSS '79), Imperial College, London, pp279-296.

Roy M., Blanchet R., Tavenas F., and La Rochelle P. (1981). Behaviour of a sensitive clay during pile driving. Can. Geotech. J., 18(1), pp67-85.

Roy M. and Lemieux M. (1986). Long-term behaviour of reconsolidtaed clay around a driven pile. Can. Geotech. J., 23(1), pp23-29.

Seed H.B. and Reese L.C. (1955). The action of soft clay along friction piles. Proc. Am. Soc. Civ. Engrs, 81(SM), Dec. 1955, Paper 842, 28pp.

Steenfelt J.S., Randolph M.F., and Wroth C.P. (1981). Instrumented model piles jacked into clay. Proc. 10th Int. Conf. Soil Mech. & Fdn Engng, Stockholm, 2, pp857-864.

Stermac A.G., Selby K.G., and Devata M. (1969). Behaviour of various types of piles in a stiff clay. Proc. 7th Int. Conf. Soil Mech. & Fdn Engng, Mexico, 2, pp239-245.

Sutton V.J., Rigden W.J., James E.L., St John H.D., and Poskitt R.J. (1979). A full scale instrumented pile test in the North Sea. Proc. 11th Offshore Technology Conf., Houston, Texas, 2, pp1117-1133 (Paper OTC 3489).

Appendix 3

Fundamental properties of London clay

CONTENTS OF APPENDIX 3

A3.1 INTRODUCTION 526
A3.2 COMPOSITION 527
A3.3 BEHAVIOUR IN ONE DIMENSIONAL COMPRESSION 528
A3.3.1 Introduction 528
A3.3.2 Reconstituted clay 528
A3.3.3 Intact London clay 529
A3.4 BEHAVIOUR IN UNDRAINED SHEAR 530
A3.4.1 Reconstituted London clay 530
A3.4.2 Intact Samples 533
A3.5 INTERFACE BEHAVIOUR AT LARGE SHEAR STRAINS 534
A3.5.1 The basic shear mechanisms 534
A3.5.2 Sliding shear behaviour 535
A3.5.3 Transitional shear 535
A3.5.4 Special tests to simulate pile installation and testing 536
A3.6 NOTES AND REFERENCES 538

A NOTE ABOUT APPENDIX 3

This appendix has been taken from a forthcoming Offshore Technology Report, published through HMSO by the UK Government's Department of Energy. The report is entitled "Behaviour of displacement piles in an overconsolidated clay", and has been jointly written by Dr Richard Jardine and myself. Section 3, *Properties of London clay*, was written mainly by Dr Jardine. It is reproduced here with only a few changes (to the lay-out and figure numbering, etc.), since it neatly summarizes those aspects of the behaviour of London clay that are relevant to the understanding of the pile tests at Canons Park.

A3.1 INTRODUCTION

The London clay sequences found in the Thames basin consist of medium to high plasticity, stiff to hard clays. These layers were laid down in Eocene times (≈30 million years before present) as marine sediments over the extensive area shown in Figure A3.1. Much of this material has since been eroded, but, before this occurred, the clays were compressed under the weight of a considerable depth of overburden. The clay layers at Canons Park are from the lowest 20m of this sedimentary sequence.

This part of the Report provides a description of the fundamental behaviour of London clay. This background information is needed for the

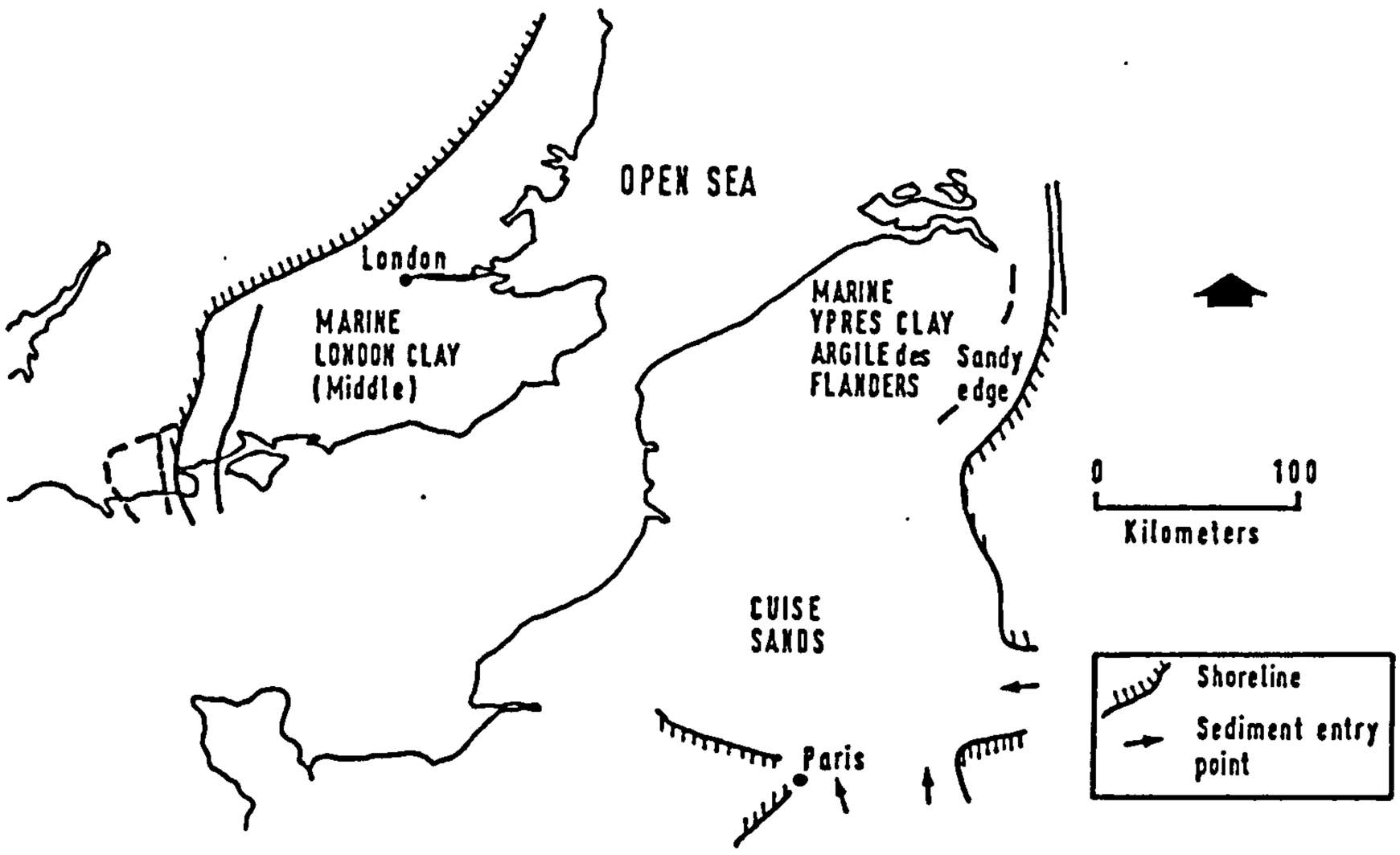


Figure A3.1 Schematic map of London clay depositional environment

following purposes:

- To help identify those features of the clay's behaviour that might have a significant bearing on the performance of displacement piles
- To assist the interpretation of the pile tests at Canons Park
- To provide the necessary parameters for any future theoretical analysis of the pile tests

The review is limited to describing those features of the properties of London clay that are of greatest importance to the Canons Park pile tests, and considers the following aspects:

- Composition (grading, Atterberg limits, mineralogy, etc.)

- Drained one-dimensional compression and swelling characteristics
- Undrained stress-strain and strength behaviour under triaxial conditions
- Residual strength properties when the clay is sheared against a rigid interface

The information used to do this has been taken from various published reports and recent research carried out at Imperial College.[1,2,3,4,5,6]

A3.2 COMPOSITION

The grading curves for the Canons Park London clay show the deposit to be composed predominantly of silt and clay sized particles (Figure A3.2).

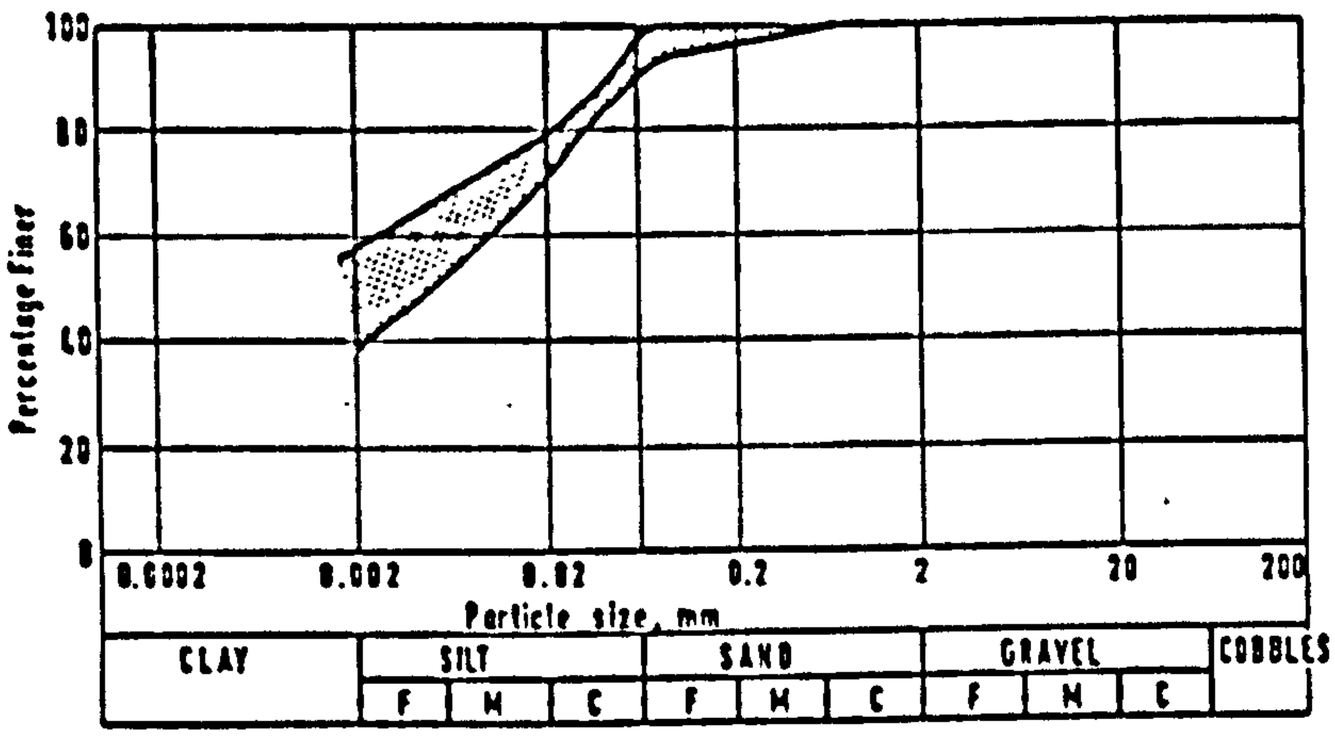


Figure A3.2 Grading curve envelope for Canons Park London clay (five tests)

A summary of the clay minerals expected at Canons Park is shown in Figure A3.3. This combination of minerals leads to an average activity (plasticity index divided by percentage clay) slightly greater than unity. Below the superficial weathered clay the plastic limit (w_P) falls between 25 and 27%, whilst the liquid limit (w_L) varies between 72 and 67%. w_P and w_L have been increased (to ≈29% and ≈83% respectively) in the upper four metres by the effects of chemical weathering. This upper zone has also been disturbed mechanically by periglacial and other processes.

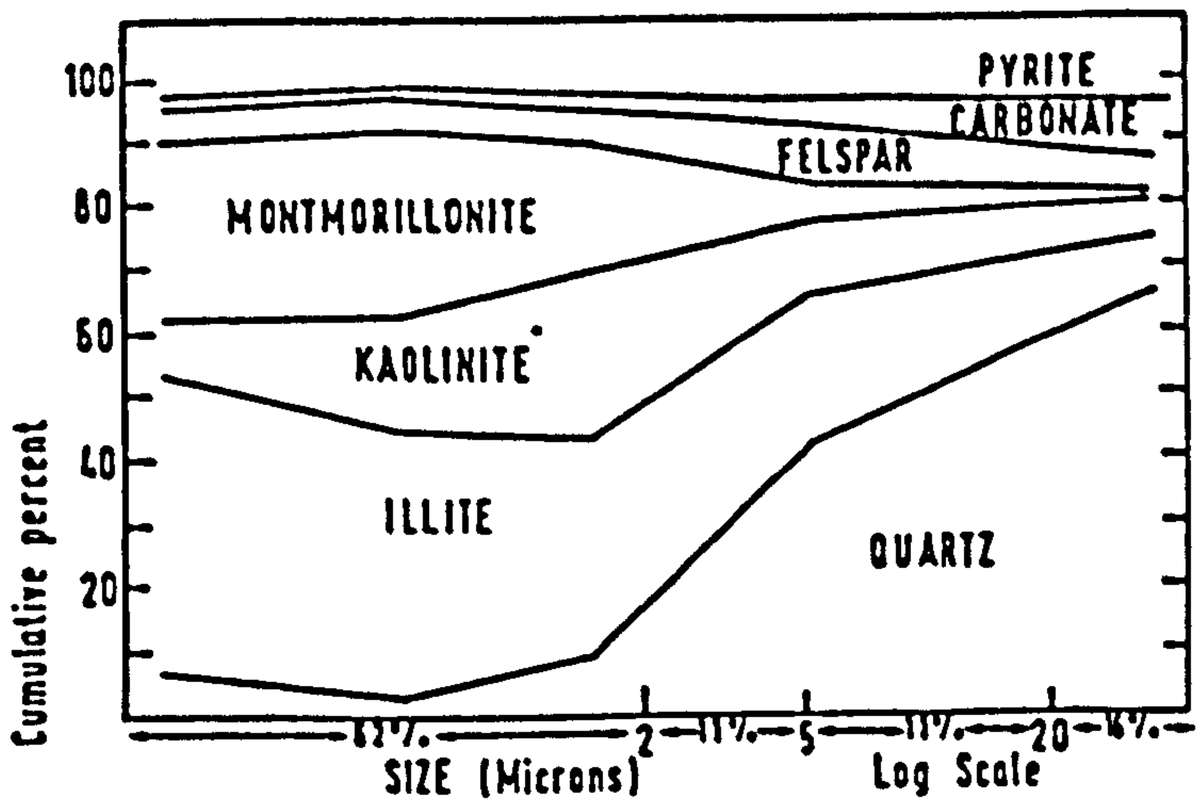


Figure A3.3 Mineral suite for typical lower London clay

A3.3 BEHAVIOUR IN ONE DIMENSIONAL COMPRESSION

A3.3.1 Introduction

The oedometer characteristics of the London clay are illustrated by the four voids ratio (e) vs log stress (σ'_v) plots shown in Figure A3.4, and attention will be drawn first to the two tests on reconstituted soil.

A3.3.2 Reconstituted clay

Curves A and B show the traces for reconstituted samples that were remixed as a slurry and compressed from very low stresses. The K_0 virgin consolidation lines (VCLs) show variations in gradient with stress, but in the region of greatest interest the compression index C_c (= $-\Delta e/\Delta[\log_{10} \sigma'_v]$) can be taken as 0.4. The swelling portion of curve A is initially very flat, but becomes steeper unloading continues. That is, C_s increases markedly with OCR. The clay also exhibits creep after the completion of primary consolidation.[7]

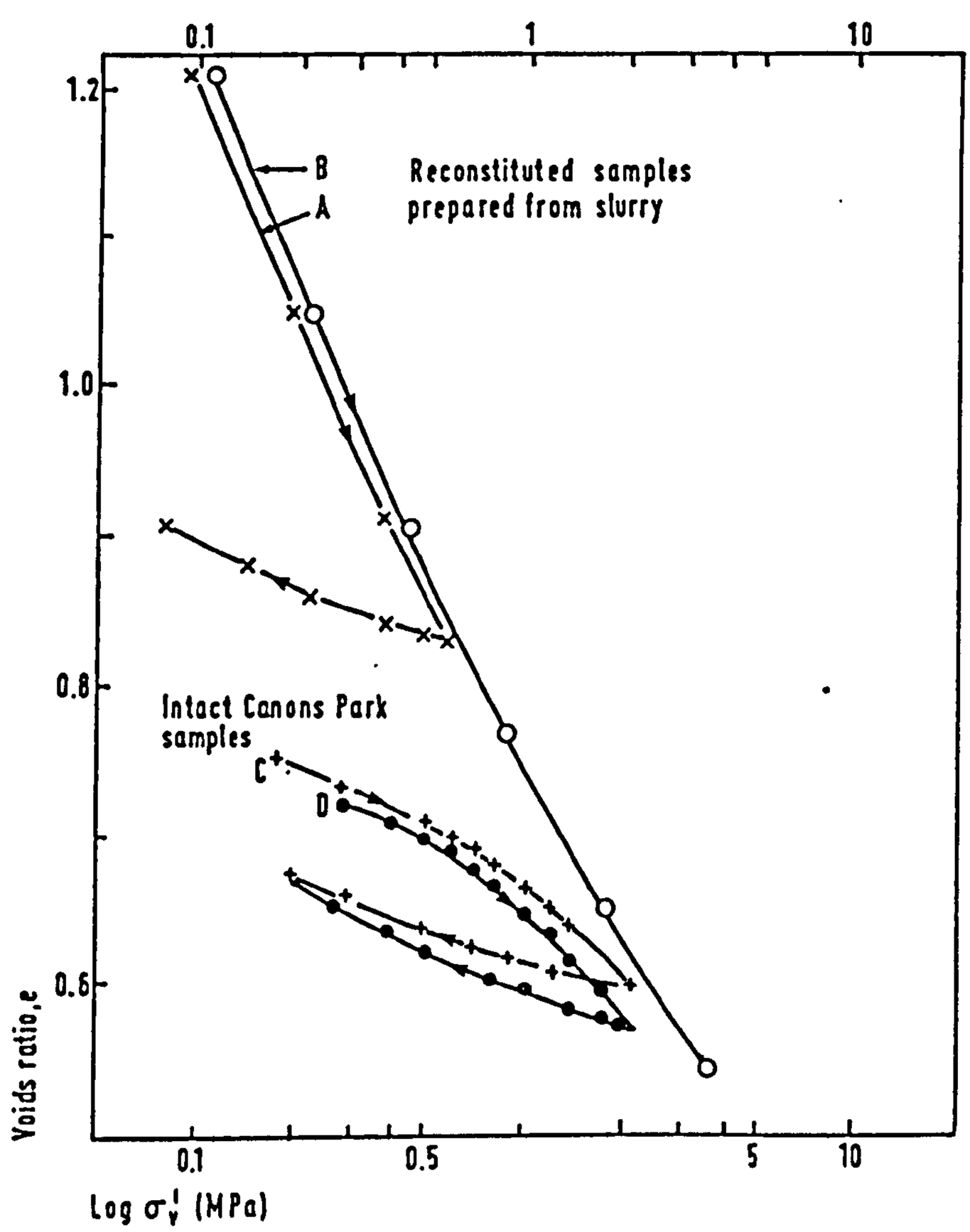


Figure A3.4 One-dimensional compression and swelling characteristics of London clay

A more detailed picture of the swelling and recompression characteristics is given in Figure A3.5, which shows the steep reductions of K' (the elastic bulk modulus) with volumetric strain ϵ_v as noted in specially instrumented, triaxial, K_0-swelling tests.

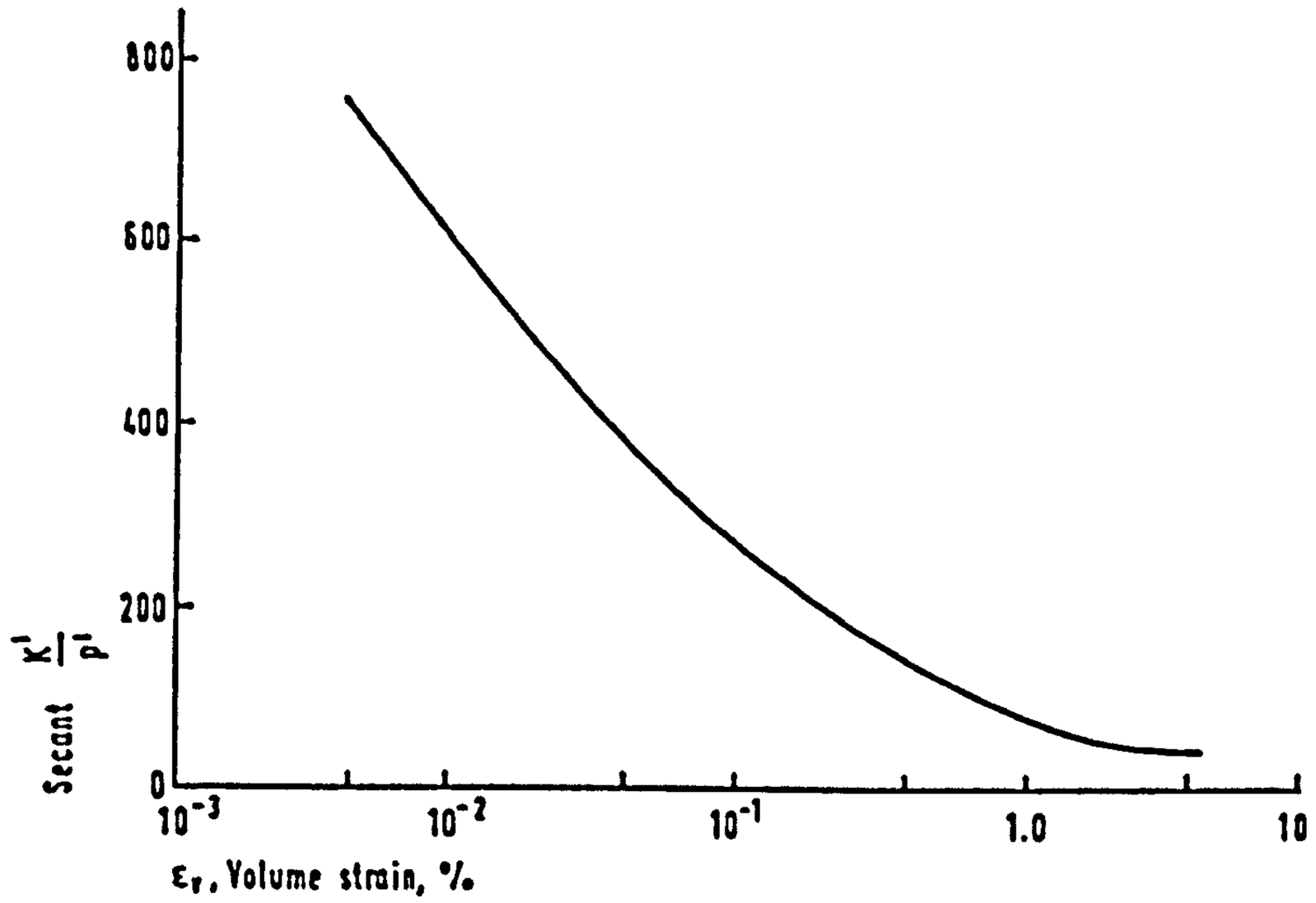


Figure A3.5 Variation of secant bulk modulus with strain for K_0-swelling (reconstituted soil)

The compressibility characteristics have an important influence on the stresses developed by pile installation, and on the times taken for pore pressure equalization; the values of c_v deduced in the normally consolidated range are around $0.2m^2/yr$, but values up to 50 times higher are found when unloading to low OCRs.

A3.3.3 Intact London clay

The curves for two intact samples are also shown on Figure A3.4. The swelling, creep, and consolidation characteristics of these samples conform with the behaviour shown by overconsolidated reconstituted London clay. Indeed, when compressed from their highly overconsolidated in situ state, the traces for C and D tend towards the VCL of Test B and indicate possible pre-consolidation pressures in the range 1.5-2MPa. Since the London clay is an aged stratum, the yield stresses are likely to exceed the maximum geological overburden stresses, due to secondary consolidation, bonding, and other phenomena.

A3.4 BEHAVIOUR IN UNDRAINED SHEAR

A3.4.1 Reconstituted London clay

As with the oedometer characteristics, it is useful to consider the behaviour of reconstituted London clay before moving on to consider the properties of intact material.

Figure A3.6 shows the results of a suite of tests on K_0-consolidated samples which were prepared in the same way as the reconstituted oedometer samples. These 'stress path' experiments included the use of local instrumentation to obtain precise measurements of the stresses, strains, and pore water pressures during consolidation and undrained shearing. The most important features to note are:

- The behaviour is strongly anisotropic, quite different patterns of behaviour are seen in extension and compression tests
- Samples with OCR less than approximately 2 contract when sheared beyond their yield points (when strains exceed 0.2-0.4%)
- More heavily overconsolidated samples dilate when sheared to strains greater than approximately 0.5%
- The stress paths for the low OCR samples indicate a critical state ϕ value of around 22.5 degrees
- High OCR samples fail before reaching this state and show apparent cohesion at peak strength. This tendency is believed to result from shear band formation involving softening through both water content change and fabric reorientation
- The soil experiences only small strains before yielding

The stress-strain curves for these tests are given in Figure A3.7. Semi-logarithmic axes are used as the curves are highly non-linear and little can be seen of the pre-yield characteristics when the data is plotted to a natural scale. In each case the stiffnesses fall rapidly with strain; these features are emphasized on Figure A3.8, which shows the strong dependency of secant stiffnesses on axial strain (for the compression tests). Figure A3.9 illustrates how the small strain stiffness index, $(E_u/p'_o)_{0.01}$, varies with OCR.

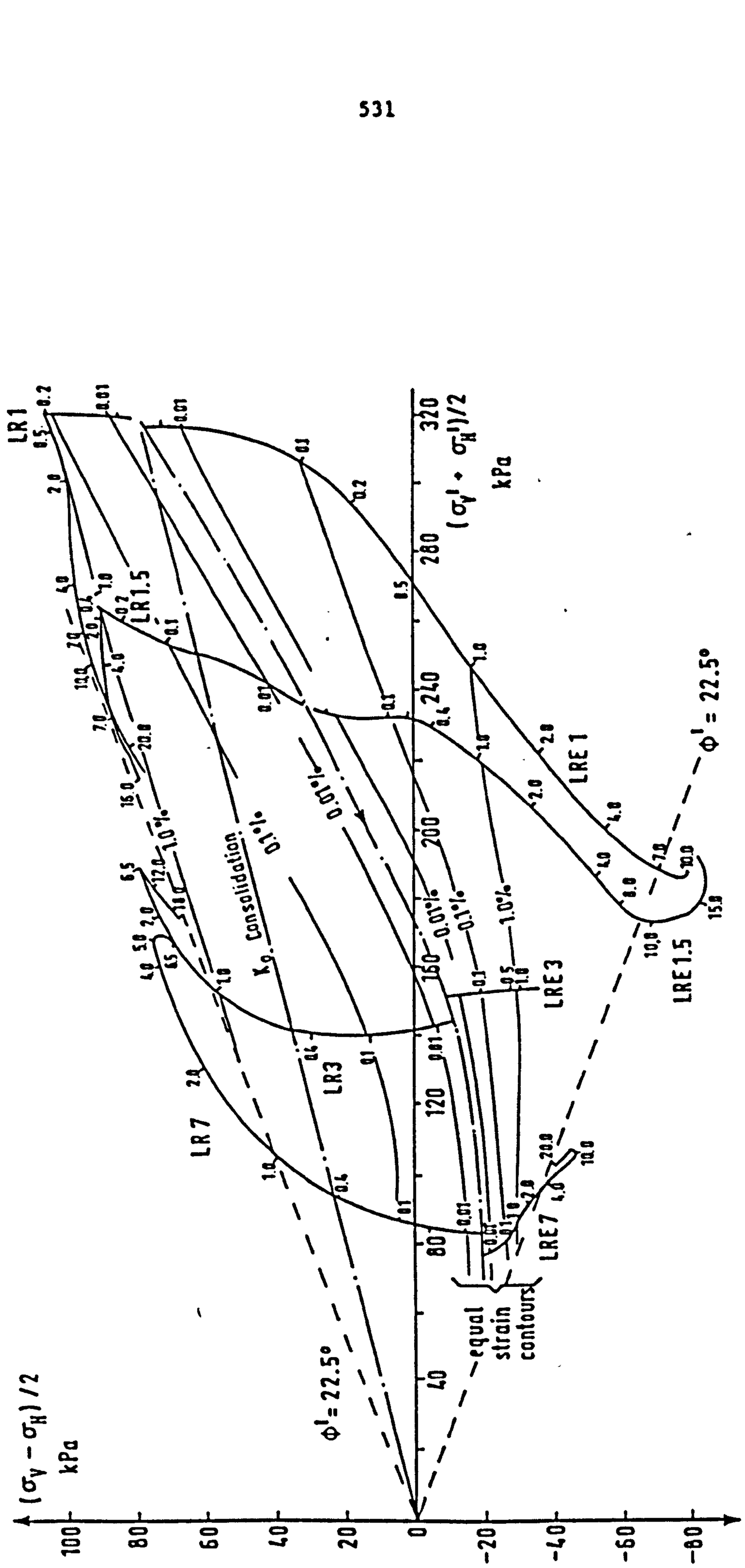


Figure A3.6 Effective stress paths for K_0-consolidated reconstituted London clay (OCRs 1, 1.5, 3, and 7)

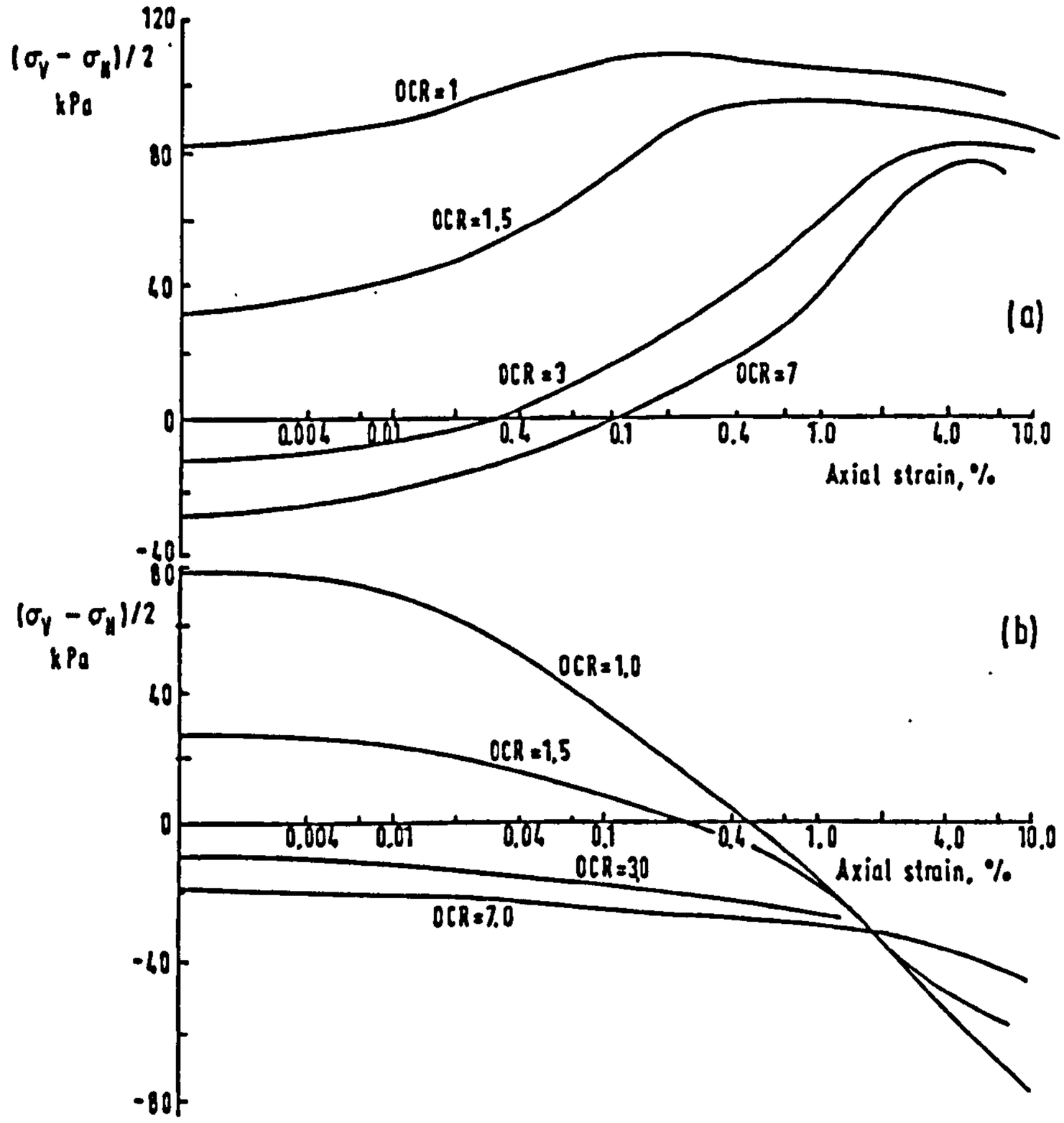


Figure A3.7 Stress-strain curves for K_0-consolidated reconstituted London clay: (a) triaxial compression; (b) triaxial extension tests

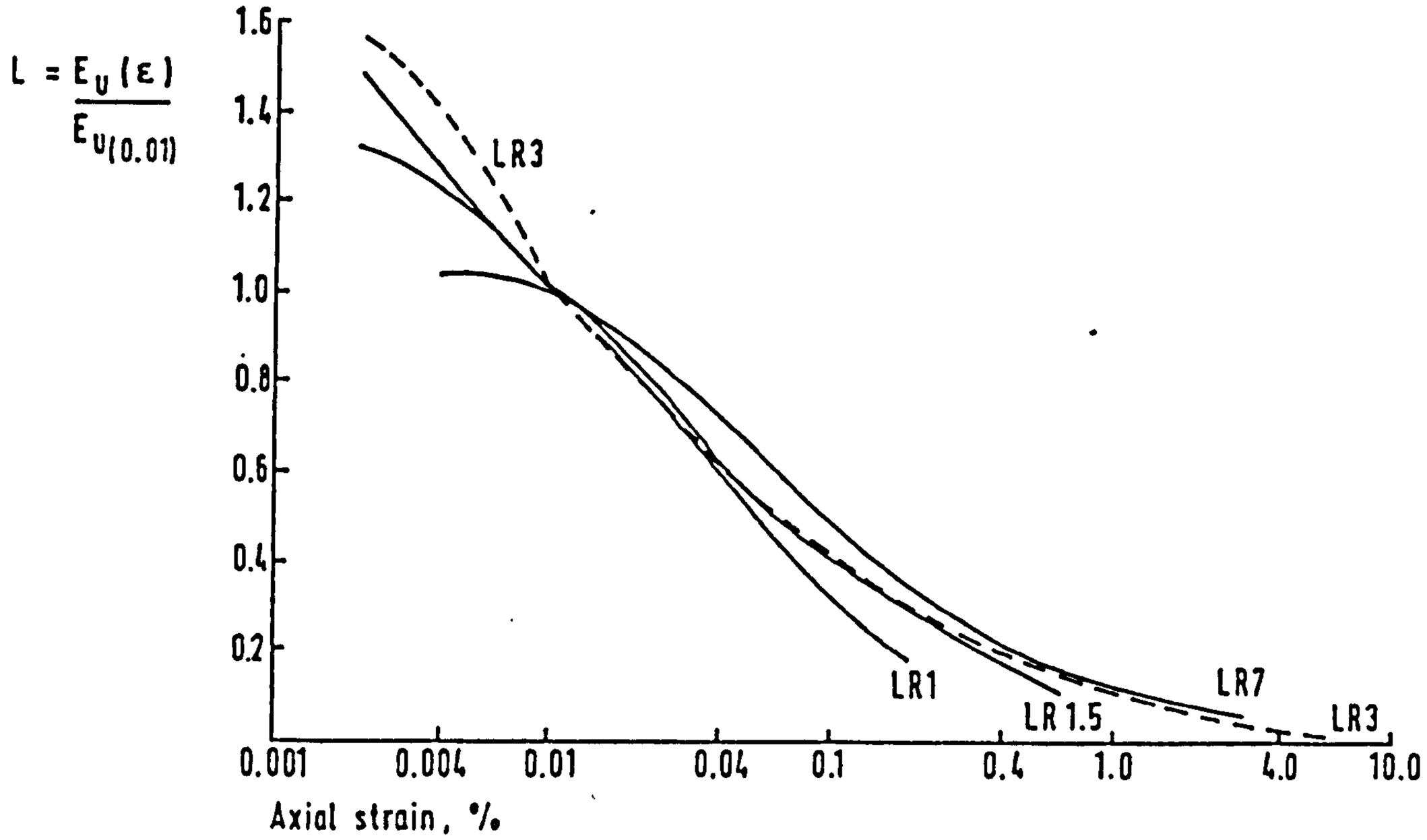


Figure A3.8 Normalized undrained stiffness characteristics of reconstituted London clay

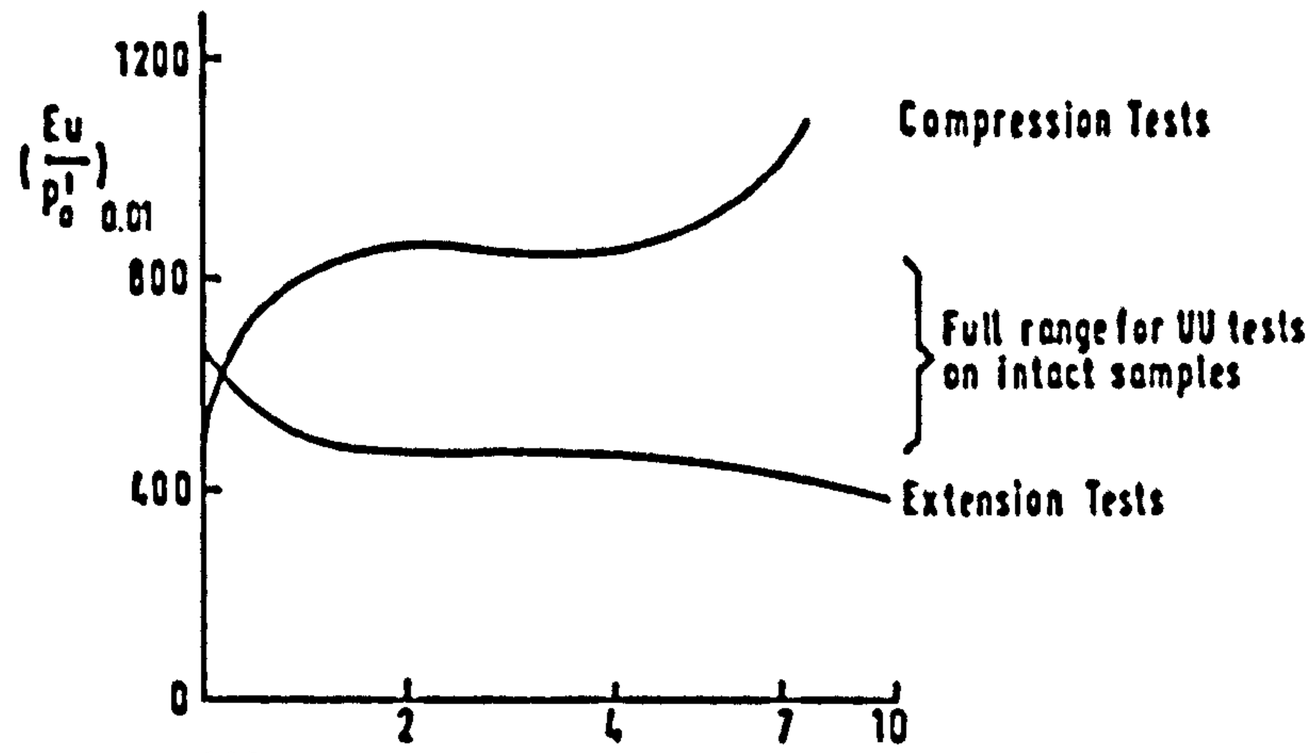


Figure A3.9 Variation of undrained small strain stiffness index with OCR: reconstituted samples

A3.4.2 Intact Samples

The stress-strain and strength behaviour of intact London clay can be illustrated using the results of a suite of unconsolidated undrained (UU) triaxial compression tests on high quality samples from Canons Park. Although the intact samples' behaviour matches many of the features

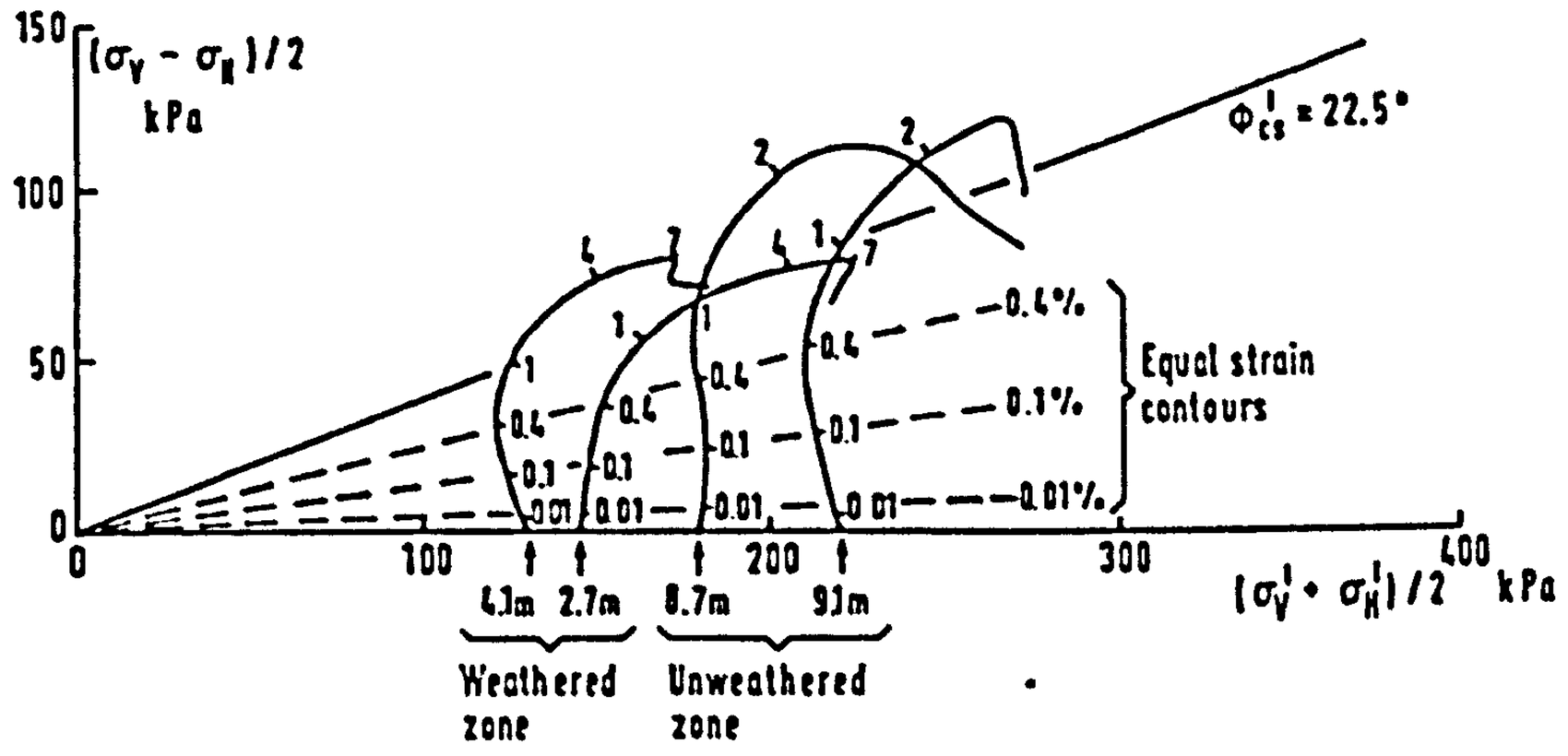


Figure A3.10 Undrained stress paths for intact samples of London clay

shown by the reconstituted clay, there are some important differences - particularly in the behaviour at large strains.The undrained stress paths and secant stiffness curves for groups of weathered and un-weathered samples are shown in Figure A3.10 and Figure A3.11; these should be compared with the tests on the highest OCR reconstituted samples (LR7 and LRE7). The main points to note regarding the stress paths are:

- The stress paths for the un-weathered samples show far less dilation than the reconstituted material

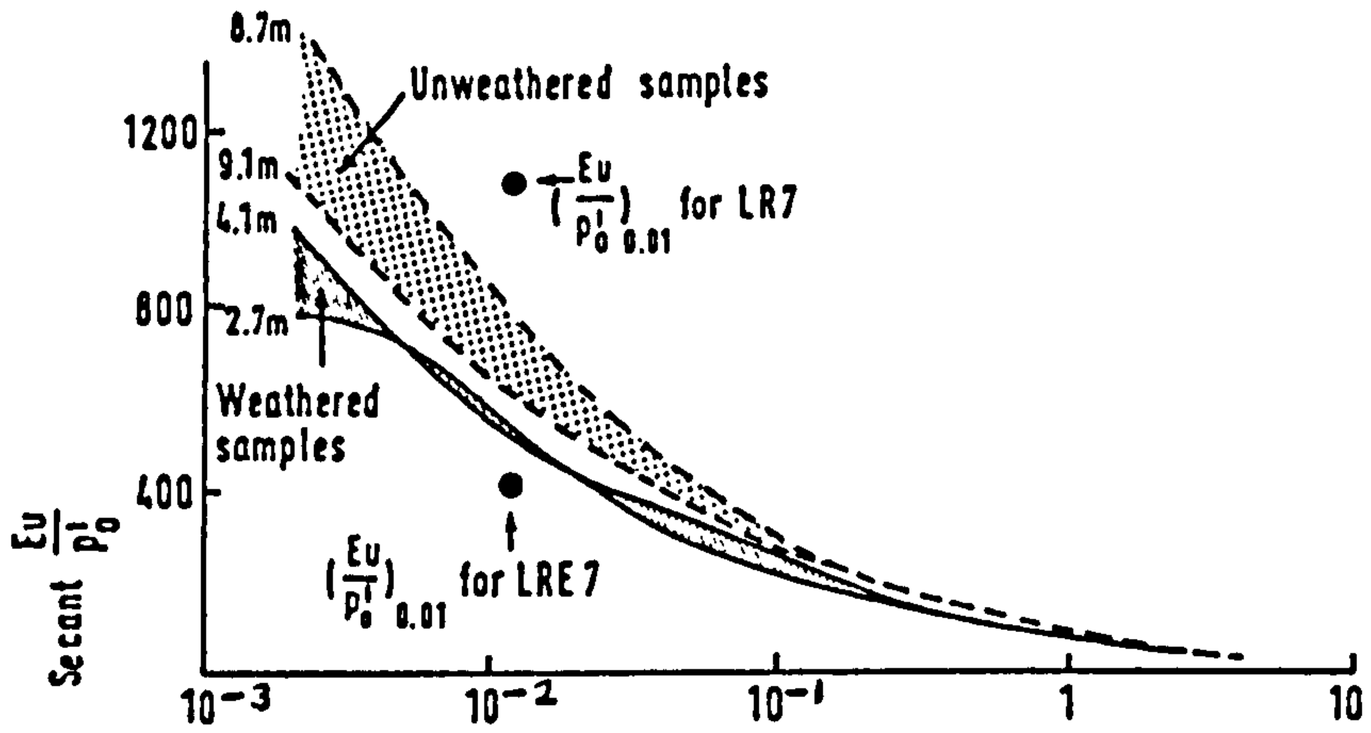


Figure A3.11 Undrained stiffness characteristics of intact samples

- The well-defined fissures and bedding features found in intact samples appear to concentrate stresses and to initiate the formation of polished sliding surfaces (through particle reorientation) after comparatively small strains
- Local softening on shear zones allows the samples to move towards their residual strengths long before the mass of soil reaches critical state conditions - this leads to an apparent cohesion c' (at peak strength) of up to 30kPa
- The disturbed fabric of the weathered soil retards the formation of residual fabric and allows more dilation than is possible for in un-weathered clay; this produces less cohesion at peak strength

Considering the pre-yield behaviour it is useful to note that the normalized stiffness characteristics are similar to those of the reconstituted samples; the spread of data from the UU tests falls between limits defined by the K_0-consolidated extension and compression tests LR7 and LRE7.

A3.5 INTERFACE BEHAVIOUR AT LARGE SHEAR STRAINS

A3.5.1 The basic shear mechanisms

The triaxial tests on London clay showed that reoriented fabric can be developed in intact samples after relatively small deformations (i.e. shear strains <5%). However, much larger shear distortions are developed close to the shafts of displacement piles during installation and, as will be shown in later sections of this Report, the soil's residual strength characteristics can be of key importance in determining shaft capacity. This section has been included to summarize the background research into residual strength and to present the results of special tests carried out as part of the Canons Park programme.

Experiments in the ring shear apparatus have demonstrated how a clay's residual frictional resistance depends on, amongst other things, the rate of shearing. To understand why certain factors govern the soil's behaviour it is necessary to distinguish between the different mechanisms that can be involved when soil is sheared to large displacements, either against a hard interface or in soil-on-soil tests.

Lupini[8] described two basic shear mechanisms that govern the residual strength behaviour of soils in the ring shear apparatus. "Turbulent" shearing (mode T) occurs typically in soils with a low clay content and hence low plasticity index I_p; whereas "sliding" shear (mode S) occurs in soils with a high plasticity index. A "transitional" mode (T_R) of shearing exists, part turbulent and part sliding, for soils with intermediate plasticity. Soils which would normally fail in a turbulent way may also undergo sliding shear when failed against a smooth interface - this mode of behaviour has been designated S_1. When sheared very quickly, viscous phenomena may cause soils that normally slide to fail in the transitional - or even the turbulent - mode.

When subjected to large shear strains, the London clay usually fails by shearing in the sliding mode, but may also fail in modes T_R and S_1 when loaded at a fast rate.

A3.5.2 Sliding shear behaviour

Sliding shear involves the formation of a polished surface of strongly oriented clay particles. An oriented shear surface, once formed, is a permanent feature of the soil and is substantially unaffected by subsequent stress history.[9] Typical residual angles of friction (as found in slow tests) for the London clay fall between 7 and 11° (for mode S).

A plastic clay, which suffers preferred particle orientation when sheared to large strains, will be brittle even when sheared after normal consolidation. Once a shear surface has formed, the clay will fail without brittleness on this surface even after overconsolidation (provided that displacement on the surface in monotonic and without reversal).[10]

A3.5.3 Transitional shear

Soils undergoing transitional shear exhibit the behaviour observed for both the turbulent* and sliding modes, although in muted form. Transitional behaviour involves discontinuous sliding shear surfaces and pockets of soil behaving in the turbulent mode, both contained within a thick shear zone. If a soil of the turbulent type is sheared against a smooth interface which locally reduces interlocking and interference, then partial sliding on the boundary might occur, with local orientation of the platy particles and a low residual strength.[11]

---

*Soils exhibiting turbulent shear show a high residual strength, typically with $\phi'_R \approx \phi_{cs}$ (for London clay ≈ 23°)

A3.5.4 Special tests to simulate pile installation and testing

A special series of ring-shear tests on the London clay from Canons Park have been performed[12,13] at Imperial College, in order to complement the field experiments with the instrumented piles. Remoulded samples of the un-weathered London clay were sheared against a stainless-steel interface that had previously been grit-blasted to give the same surface roughness (≈8μm centre-line average) as the instrumented piles.

The samples were first consolidated under K_0-conditions to a normal stress (σ_n) of ≈500kPa, and then sheared at a constant velocity in a series of five or six identical stages, each stage involving ≈1m of relative displacement between the soil and the interface. The samples were allowed to consolidate for 10 minutes between each stage. This procedure was intended to simulate the installation of a pile by jacking; the velocities were varied between 1 and 5000mm/min.

At the end of the "installation" stages, the samples were left to consolidate for 16-18h, and were then re-sheared <u>at a slow rate</u> (≈0.005 mm/min) - thereby simulating subsequent compression load tests, starting from fully equalized conditions.

The results of these tests are shown in simplified form on Figure A3.12. The peak ratios* of (τ/σ_n) as measured during the final stages of installation and during subsequent slow shearing are plotted against the rate of displacement <u>during "installation"</u>. Considering the fast shearing stages first: the stress ratio (and hence the coefficient of friction) depends strongly on the rate of shearing. Increasing the velocity from 10 to ≈2000mm/minute doubles the shearing resistance.

If this behaviour was caused solely by rheological (i.e. viscous) phenomena, then the rate of displacement during installation should have little or no effect on the subsequent behaviour in slow shear. In fact the lower curve on Figure A3.12 implies that, although there is an important viscous component, the subsequent frictional strength is also strongly influenced by the rate of displacement during installation. This suggests that shearing irretrievably alters the soil's fabric and that the way in which it is changed depends upon the shearing rate. The mechanism appears to switch from <u>sliding</u> (at rates less than ≈100mm/min) to a <u>transitional</u> mode (at velocities greater than ≈200mm/min).

It is also valuable to note that the ratio (τ/σ_n), as measured in slow loading, does not approach tan ϕ'_{cs}, even after pre-shearing at 8000mm/min. Although it may be transitional, the failure mechanism is

---

*Note that σ_n is equal to the normal effective stress during consolidation and slow shearing. Excess pore pressures may develop during fast shearing that could cause σ'_n at the interface to be less than, or greater than, this value.

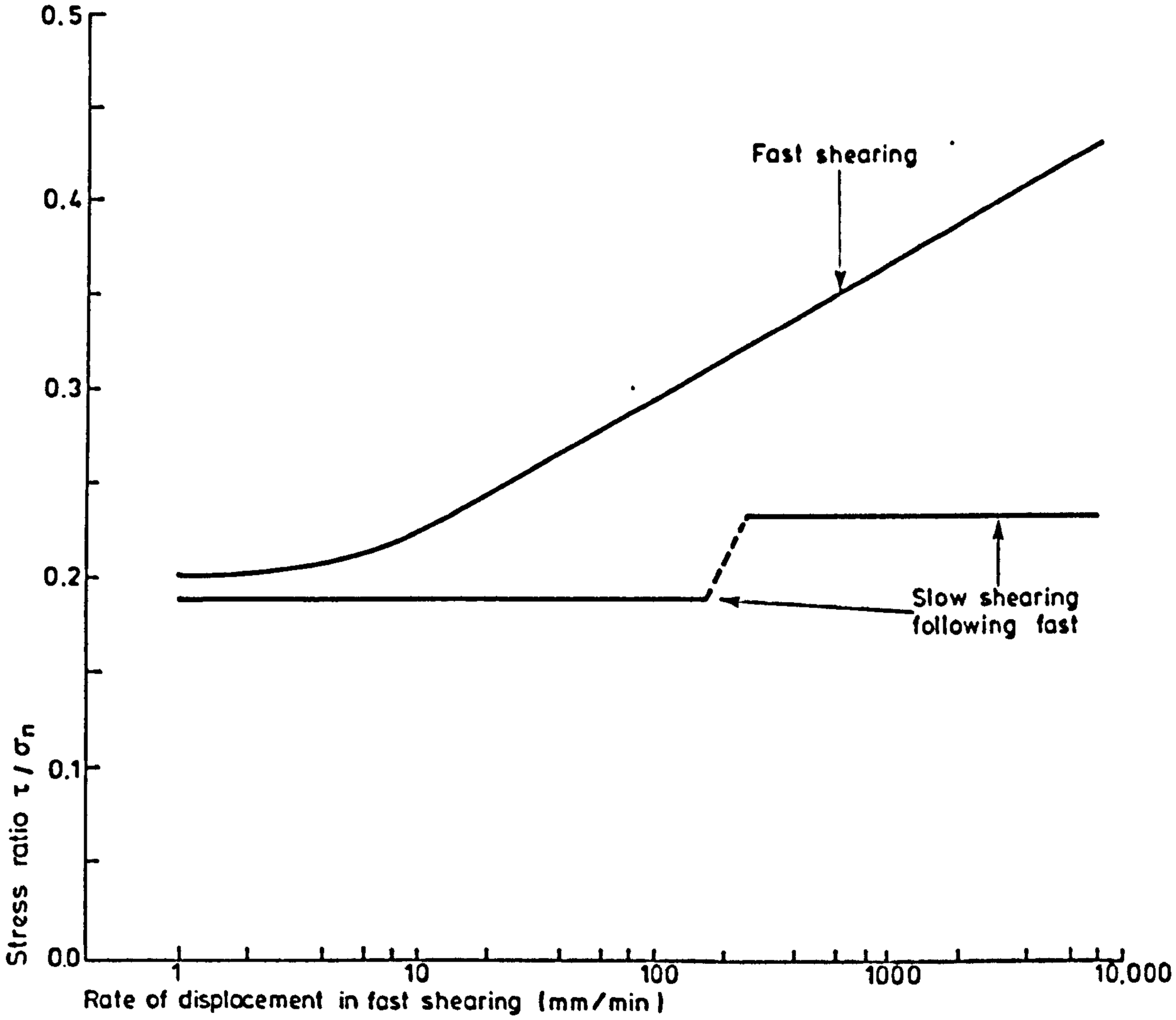


Figure A3.12 Rate effects shown by interface ring shear tests on London clay from Canons Park

closer to residual sliding than to turbulent (continuum) shear.

A3.6 NOTES AND REFERENCES

[1]Som N.N. (1968). The effect of stress path on the deformation and consolidation of London Clay. PhD Thesis, Univ. of London (Imperial College), 2 vols, 409pp + figures.

[2]Lupini J.F. (1981). The residual strength of soils. PhD Thesis, Univ. of London (Imperial College), 462pp.

[3]Jardine R.J. (1985). Investigations of pile-soil behaviour, with special reference to the foundations of offshore structures. PhD Thesis, Univ. of London (Imperial College), 2 vol., 789pp.

[4]Lemos L.J.L. (1986). The effect of rate on residual strength of soil. PhD Thesis, Univ. of London (Imperial College), 540+pp.

[5]Tika T. (1989). The effect of fast shearing on the residual strength of soils. PhD Thesis, Univ. of London (Imperial College).

[6]Burnett A.D. and Fookes P.G. (1974). A regional engineering geological study of the London clay in the London and Hampshire Basins. Q. Jl Engng Geol., 7, pp257-295.

[7]The drained creep rates vary with the state of stress. The coefficients $C_{\alpha e}$ (defined as the change in voids ratio per log cycle of time) are roughly 0.02 of the 'primary' compressibility (C_c or C_s) developed for any particular loading increment. The highest rates of creep are therefore found when undergoing normal consolidation or swelling back to very low stresses.

[8]Lupini (1981), loc. cit.

[9]Lupini J.F., Skinner A.E., and Vaughan P.R. (1981). The drained residual strength of cohesive soils. Géotechnique, 31(2), pp181-213. See p206.

[10]Lupini, Skinner, and Vaughan (1981), loc. cit., p185.

[11]Lupini, Skinner, and Vaughan (1981), loc. cit., p205.

[12]Tika T. (1989), loc. cit.

[13]Lemos L.J.L. (1986), loc. cit.

Appendix 4

Geology of the Canons Park area

CONTENTS OF APPENDIX 4

A4.1 GEOLOGY OF THE STANMORE AREA 542
A4.1.1 Six-inch and one-inch geological maps 542
A4.1.2 Well records 542
A4.1.3 Estimating the past overburden 546
A4.2 ESTIMATING THE PRE-CONSOLIDATION PRESSURE OF THE LONDON CLAY 547
A4.2.1 From standard oedometer tests 547
A4.2.2 From high pressure oedometer tests . 547
A4.3 NOTES AND REFERENCES 549

A4.1 GEOLOGY OF THE STANMORE AREA

A4.1.1 Six-inch and one-inch geological maps

The geology of the Canons Park area was surveyed in 1899 by A.C.G. Cameron and in 1922 by C.N. Bromehead, resulting in the four six-inch geological maps[1] from which Figure A4.1 has been compiled. The Canons Park site, which was established by the Building Research Establishment (BRE) as a test-bed facility for research into the London clay, is situated near the top left hand corner of London Sheet 1 NW (see Figure A4.1).

The uppermost deposit over the area covered by Figure A4.1 is the London clay, which is "up to 100ft"[2] thick (30.5m). Below it are the Woolwich and Reading Beds of "sand, loam & pebbles",[3] and, in some places below that, Thanet sand. Underlying these Eocene deposits is the soft white Upper Chalk of the Cretaceous Period.

The London clay was deposited around 40 million years ago (i.e. during the Eocene Period), and is therefore an "aged" clay. Its geotechnical properties are reviewed in Appendix 3.

On top of the London clay there are several recent (i.e. Quaternary) alluvial deposits. In the vicinity of the BRE's site, there is a large tract of alluvium (Stanmore Marsh), just to the west; and further deposits along the route of Dean's Brook and Silk Stream, to the east. Water from Stanmore Marsh runs easterly along Edgware Brook towards Burnt Oak, where it joins that coming south along Dean's Brook. The two waterways merge to form into the Silk Stream, which links into the River Brent and ultimately the Thames.[4]

A4.1.2 Well records

A great wealth of knowledge about the geology of London has been gleaned from the records of boreholes and wells that were sunk during the last century. The records for the Stanmore and Edgware areas were catalogued

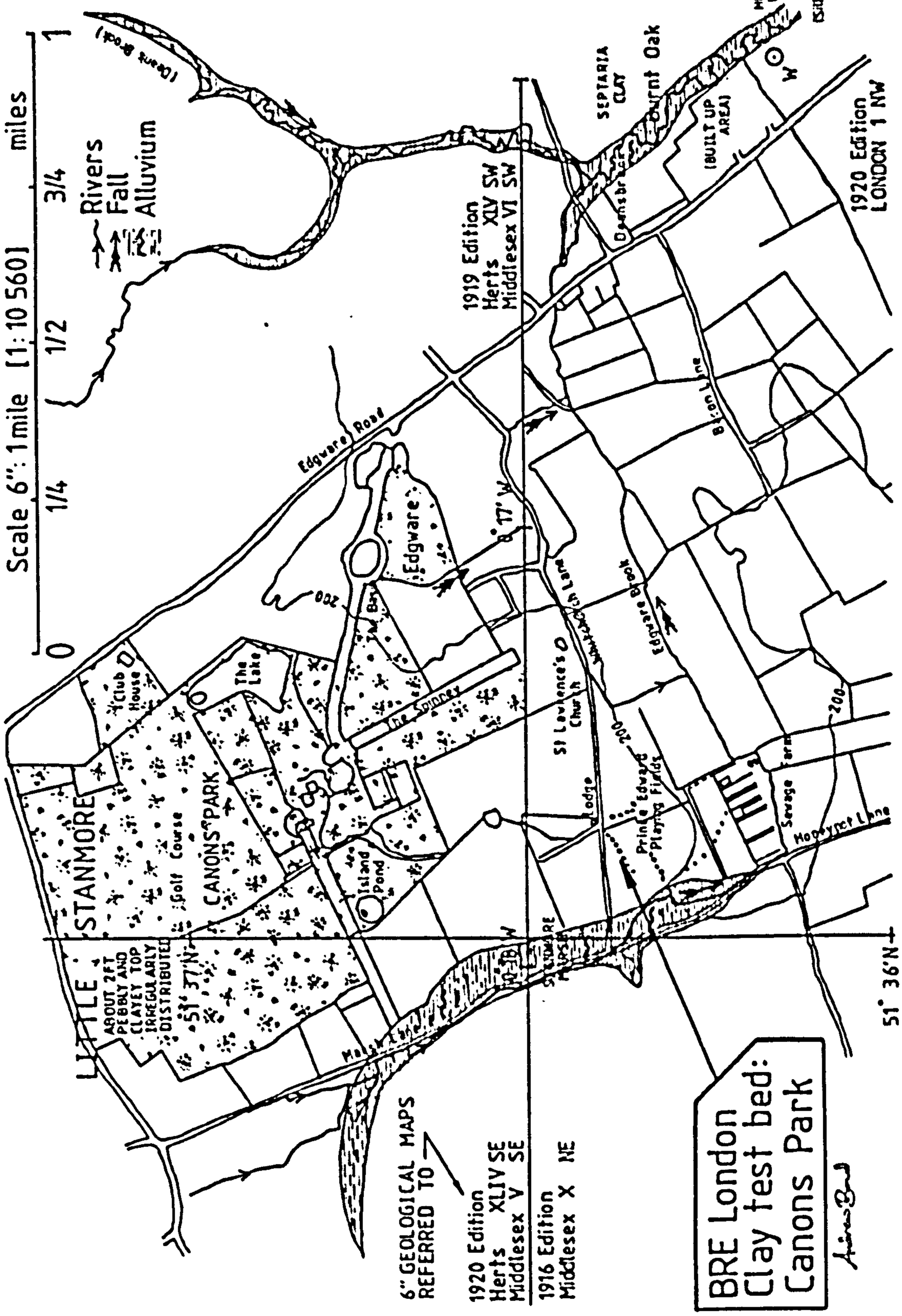


Figure A4.1 Six-inch geological maps for Canons Park

in 1889 and 1897,[5,6] and those for Golders Green in 1913[7]; in addition, there exists an extremely helpful wartime publication[8] which combines many disparate well catalogues into one document.

The well records themselves are summarized in Table A4.1, which lists the thickness of each deposit (in feet, 1ft = 0.3048m) and the reference numbers of the records from which the information was obtained.

Figure A4.2 shows a (vertical) cross-section along a line from Stanmore Common to Hampstead Heath, with some of the well records superimposed. The upper part of the diagram gives the registered number of each well, and the lower part indicates, on plan, where they were located. As Figure A4.2 reveals, the London clay thickens along the line of

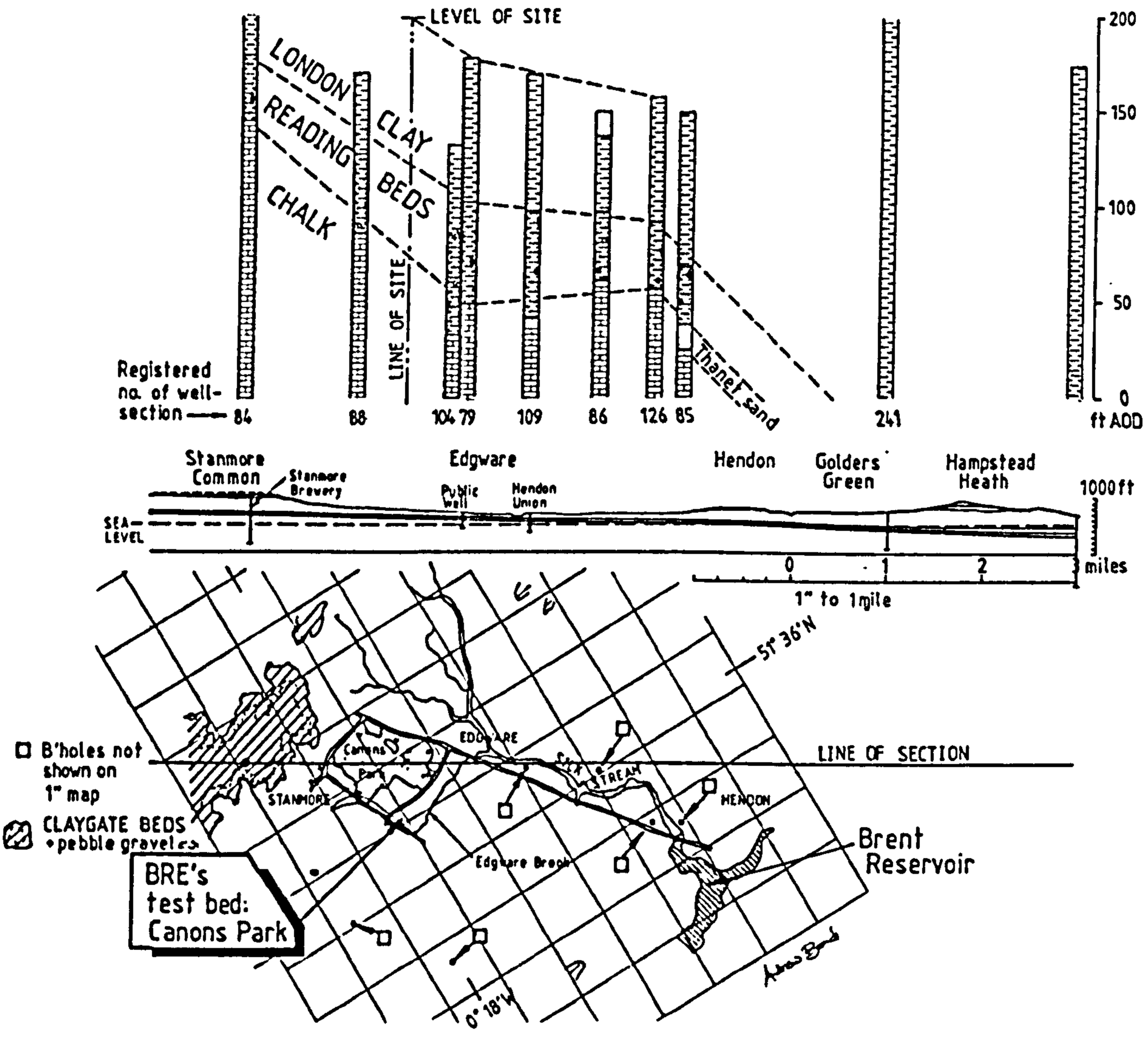


Figure A4.2 Cross-section from Stanmore Common to Hampstead Heath

Table A4.1 Well records for Stanmore and surrounding areas

	256/84 Stanmore Brewery	256/70 Edgware Public Well	256/100 Hendon Union	256/83 Edgware Convalescent Hospital	256/88 Kenton Lane Farm	256/104 Kenton Grange
Gl	+470	+178	+170	?	+172	+132
Wt	?	+88	+83	?	+62	+75
Tp	4	-	-	-	1	1
LC	284	76	72	108	43	98½
RB	36	54	56	46	41½	inc in LC
TS	-	-	-	-	-	-
Ch	239	160	197	100	164½	22½
Ref	W89	W89	W89	B40	B40	B40

	256/126 The Hyde, Edgware Rd	256/85 Messrs Schweppes, Hendon	256/86 Presdale Ltd, Collindale Avenue	256/241 Golder's Green	256/? Kentish Town Waterworks	256/? Hampstead Brewery
Gl	+158	+157	+150	+240	+174	+315
Wt	?	+79	?	+20	-36	-10
Tp	-	10	13	-	-	?
LC	66	82	39½	259	236	353
RB	34½	30	36½	49	61½	53
TS	-	13	-	15	27	31
Ch	37	175	214	329	?	?
Ref	W89	B40	B40	B13	W97	W97

Key

256/84 registered number of original well-record in Geological Survey collection (see B40)
Gl ground level (above Ordnance Datum)
Wt level of water table (above Ordnance Datum)
Tp topsoil, drift, or made ground
LC London Clay
RB Reading Beds
TS Thanet Sand
Ch Chalk

References

W89 Whitaker (1889)
W97 Whitaker (1897)
B13 Barrow & Wills (1913)
B40 Buchan et al. (1940)

All thicknesses/levels given in feet (1ft = 0.3048m)

In his Thesis, Som suggests a method for determining the pre-consolidation pressure of a heavily overconsolidated clay by re-constructing the rebound curve for the intact, in situ, material. Figure A4.3 shows the rebound curve for the Canons Park London clay, as given by a simplified version[18] of Som's method.

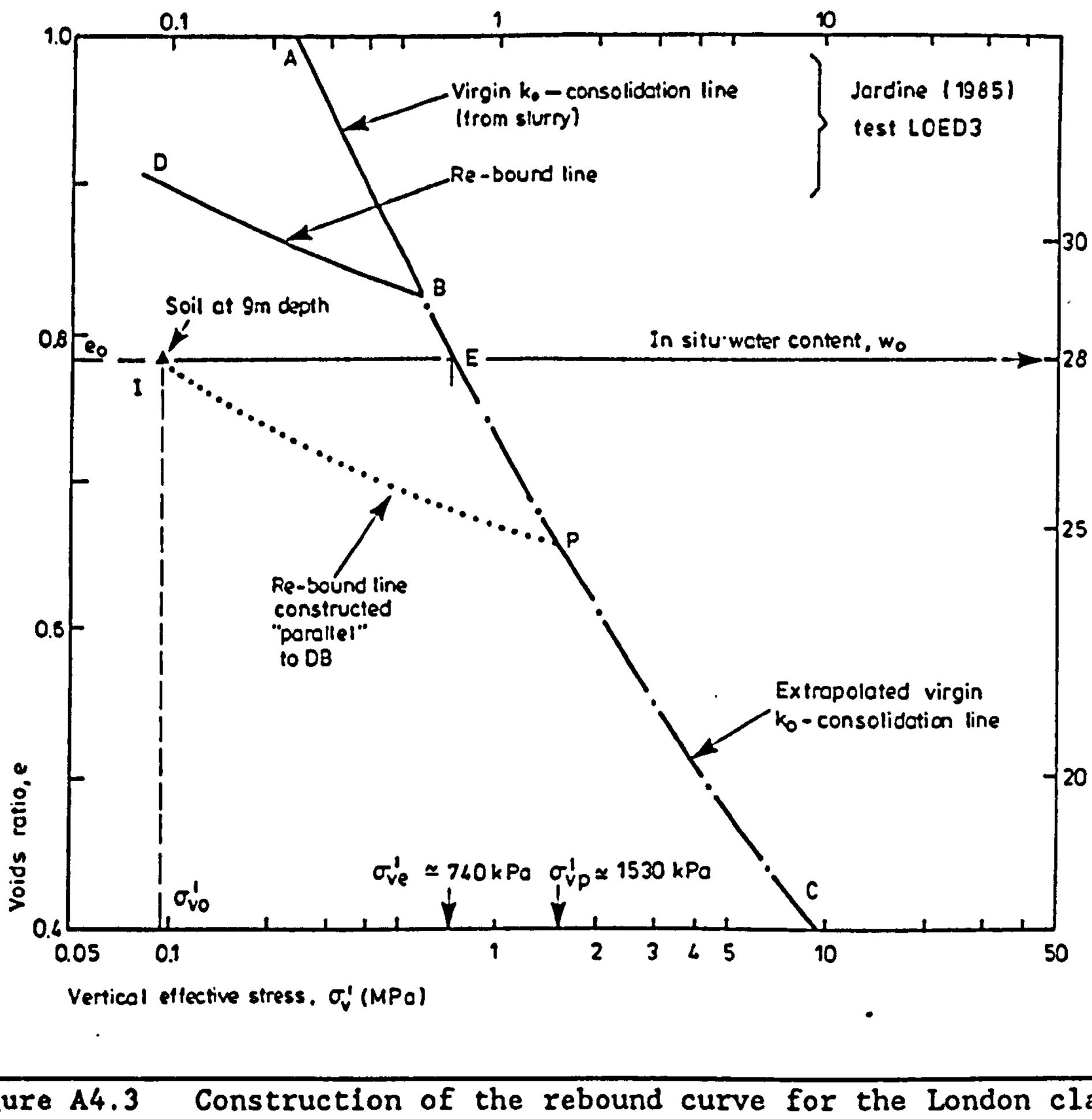


Figure A4.3 Construction of the rebound curve for the London clay at Canons Park

Based on this construction the pre-consolidation pressure at Canons Park is estimated to be between 1530 and 1870kPa (for soil at 9m), suggesting that 155-190m of past overburden has been removed from the site.

A4.3 NOTES AND REFERENCES

[1]All of the maps referred to are now out of print. Existing copies may be inspected at the British Geological Survey's library at the Geological Museum in South Kensington. There is also a one-inch geological map for North London (Sheet 256, Drift Edition) which covers the entire compass of the six-inch maps.

[2]According to the Six Inch London Sheet 1 NW.

[3]Institute of Geological Sciences (1951). One-inch geological maps of England and Wales. Sheet 256, North London, drift edition.

[4]Barton N.J. (1962). The lost rivers of London. Phoenix House Ltd, London, & Leicester Univ. Press, 148pp. See Map I. This book gives an interesting account of London's "lost" rivers, many of which now exist in culverts and sewers.

[5]See volume 2 of Whitaker W. (1889). The geology of London and part of the Thames Valley. Mem. Geol. Survey, England & Wales (explanation of Sheets 1,2, and 7), HMSO, London. 2 vols: 1, Descriptive geology, 556pp; 2, Appendices, 352pp.

[6]Whitaker W. (1897). Some Middlesex well-sections. Trans. British Assoc. Waterworks Engnrs, 2nd Annual Meeting, pp76-103 (& discussion pp104-109).

[7]Barrow G. and Wills L.J. (1913). Records of London wells. Mem. Geol. Survey, England & Wales, HMSO, London, 215pp.

[8]Buchan S., Robbie J.A., Holmes S.C.A., Earp J.R., Bunt E.F., and Morris L.S.O. (1940). Water supply of South-East England from underground sources (quarter-inch geological sheets 20 and 24). Part I. Catalogues of wells on One-Inch Sheet 256.

[9]Cf. the thicknesses at the Edgware Public Well (number 79) and at Hendon Union (no 109): 76 and 72ft respectively.

[10]Bromehead C.E.N. (1925). The geology of North London. Memoirs Geol. Survey, England & Wales (explanation of Sheet 256). HMSO, London, 63pp.

[11]Fookes P.G. (1966). Correspondence on London basin tertiary sediments. Géotechnique, 16(3), pp260-263. On Figure 1, Canons Park is approximately 14 miles NNE of Ashford and 10 miles NW of Central London. This places it just outside the 300ft contour.

[12]Bromehead (1925), loc. cit.

[13]See the One-Inch Series, Sheet 256, Drift Edition.

[14]Fookes (1966), loc. cit., Table 1.

[15]Jardine R.J. (1985). Investigations of pile-soil behaviour, with special reference to the foundations of offshore structures. PhD Thesis, Univ. of London (Imperial College), 2 vol., 789pp. See vol. 1, Section 7.3 (pp159-161); and vol. 2, Figures 7.10, 7.11, and 7.13. Test LOED1 (on soil from 9.4m depth) gave σ'_{vp} = 630kPa; test LOED2 (4.7m depth) gave 540kPa. See also Table 9 of: Fourie A.B. (1984). The behaviour of retaining walls in stiff clay. PhD Thesis, Univ. of London (Imperial College), 437pp.

[16]See any standard text book on soil mechanics, for example: Terzaghi K. and Peck R.B. (1967). Soil mechanics in engineering practice (2nd edition). John Wiley and Sons Inc., New York, 729pp.

[17]Som N.N. (1968). The effect of stress path on the deformation and consolidation of London Clay. PhD Thesis, Univ. of London (Imperial College), 2 vols, 409pp + figures.

[18]The precise details are as follows:

Lines A-B and B-D come from Jardine's oedometer test LOED3. Line A-B has been extrapolated along B-C by following the shape of Som's virgin consolidation curve for High Ongar clay.

Line P-I has been drawn "parallel" to B-D, by sliding A-B down the virgin line (B-C) until the extension to B-D (not shown) meets point I. In this configuration, point P is given by the position of B along B-C.

Appendix 5

Earth and pore pressure cells: a review

CONTENTS OF APPENDIX 5

A5.1 PILE-MOUNTED EARTH PRESSURES CELLS 555

A5.1.1 Introduction 555

A5.1.2 Reese and Seed (1955) 555

A5.1.3 Φien (1962) 556

A5.1.4 Agarwal and Venkatesan (1965) 558

A5.1.5 Koizumi and Ito (1967) 558

A5.1.6 BP/BRE instrumented pile (1976) 558

A5.1.7 Johnston (1979) . . 559

A5.1.8 Taylor Woodrow's EP cells (1982) 560

A5.1.9 O'Neill et al. (1982) 560

A5.1.10 Maddocks (1983) 561

A5.1.11 Francescon (1983) 562

A5.1.12 The Piezo-Lateral Stress cell 562

A5.1.13 Wersching (1987) 564

A5.1.14 The Oxford University IMP (1987) 565

A5.1.15 NGI's instrumented piles (1989) 566

A5.2 ASSESSMENT OF CELL ACTION EFFECTS 569

A5.2.1 Definition of cell action 569

A5.2.2 Factors that affect cell action 570

A5.2.3 Cell action in stiff soils 570

A5.2.4 Comparing designs of earth pressure cell 572

A5.2.5 Cell action effects during pile installation 575

A5.2.6 Laboratory studies of cell action effects 575

continued....

A5.3 PILE-MOUNTED PIEZOMETERS 578
A5.3.1 Introduction 578
A5.3.2 Reese and Seed (1955) 578
A5.3.3 Hanna (1967) 579
A5.3.4 Kenney (1967) 579
A5.3.5 Laboratory tests at Cambridge University (1981-83) 580
A5.3.6 O'Neill et al. (1982) 580
A5.3.7 The Oxford University IMP (1987) 580
A5.3.8 NGI's instrumented piles (1989) . 582
A5.4 RESPONSE TIMES OF PILE-MOUNTED PIEZOMETERS 583
A5.4.1 Sources of error in pore pressure measurement 583
A5.4.2 Comparing pile-mounted piezometers . 584
A5.5 NOTES AND REFERENCES 589

A5.1 PILE-MOUNTED EARTH PRESSURES CELLS

A5.1.1 Introduction

The first part of this appendix describes previous designs of earth pressure cells, as used for measuring the stresses acting on displacement piles in clay soils. The instruments' technical details are summarized in Table A5.1 (p573). An assessment of cell action effects is given in Section A5.2.

A5.1.2 Reese and Seed (1955)

The earth and pore pressure cells employed by Reese and Seed[1] in San Francisco Bay mud are illustrated in Figure A5.1. Both devices relied upon ϕ38mm strain-gauged diaphragms to sense the pressure, the pore pressure gauges incorporating a porous bronze filter and a large, water-filled space in front of the diaphragm (to prevent its contact with the soil). Because of the diaphragm's flexibility, the cell action effects are quite severe: the under-registration of changes in radial total stress ($\Delta\sigma_{rr}$) acting on the pile could be as much as 43% in the soft San Francisco Bay mud (assuming c_{uo} ≈ 12kPa and E_u/c_{uo} = 1000).* The cell's technical details are given in Table A5.1.

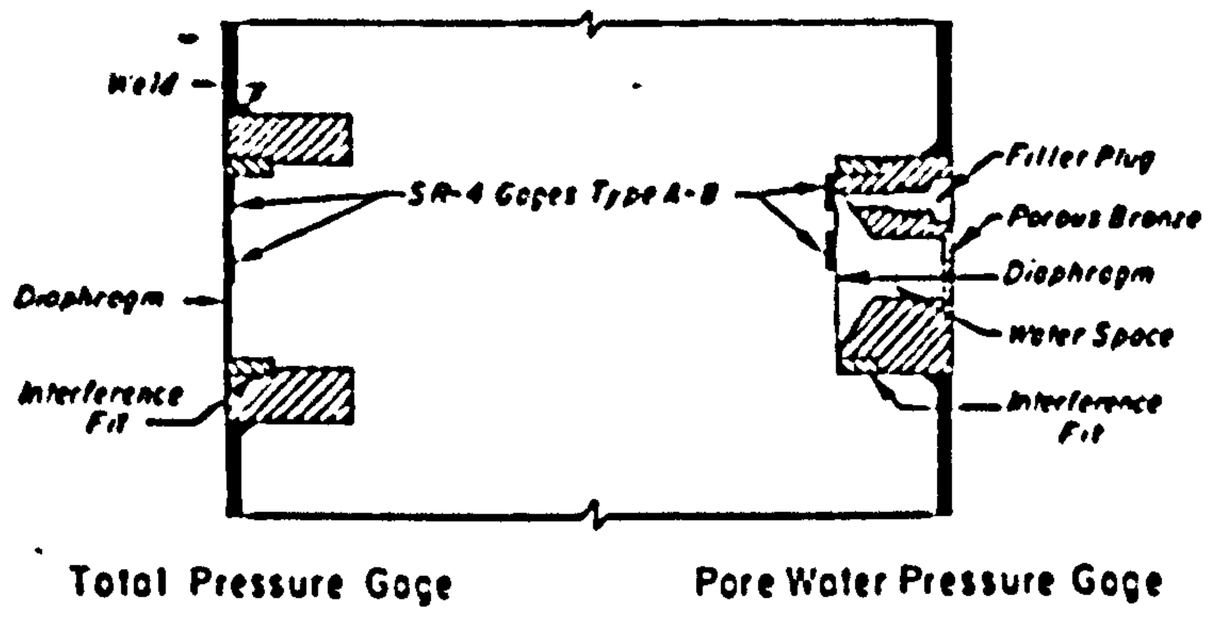


Figure A5.1 Earth and pore pressure cells employed by Reese and Seed

*This, and all the following calculations of cell action are based on the formulae given on p569 et seq.

A5.1.3 Φien (1962)

Kenney[2] employed a number of vibrating-wire earth pressure cells on steel piles installed in the quick clay in and around Oslo. The instrument that Kenney used has been described in detail by Φien,[3] and is shown here in Figure A5.2 (the components are described in a note[4] at the end of the appendix).

The earth pressure causes the transducer's diaphragm to bend, thus changing the natural frequency of the vibrating wire. Although the diaphragm is reasonably large (ϕ75mm), it is also quite flexible. In the Oslo clays in which they were installed, the error in the instruments' readings would have been < 1% (c_{uo} = 5kPa and E_u/c_{uo} = 1000 assumed).

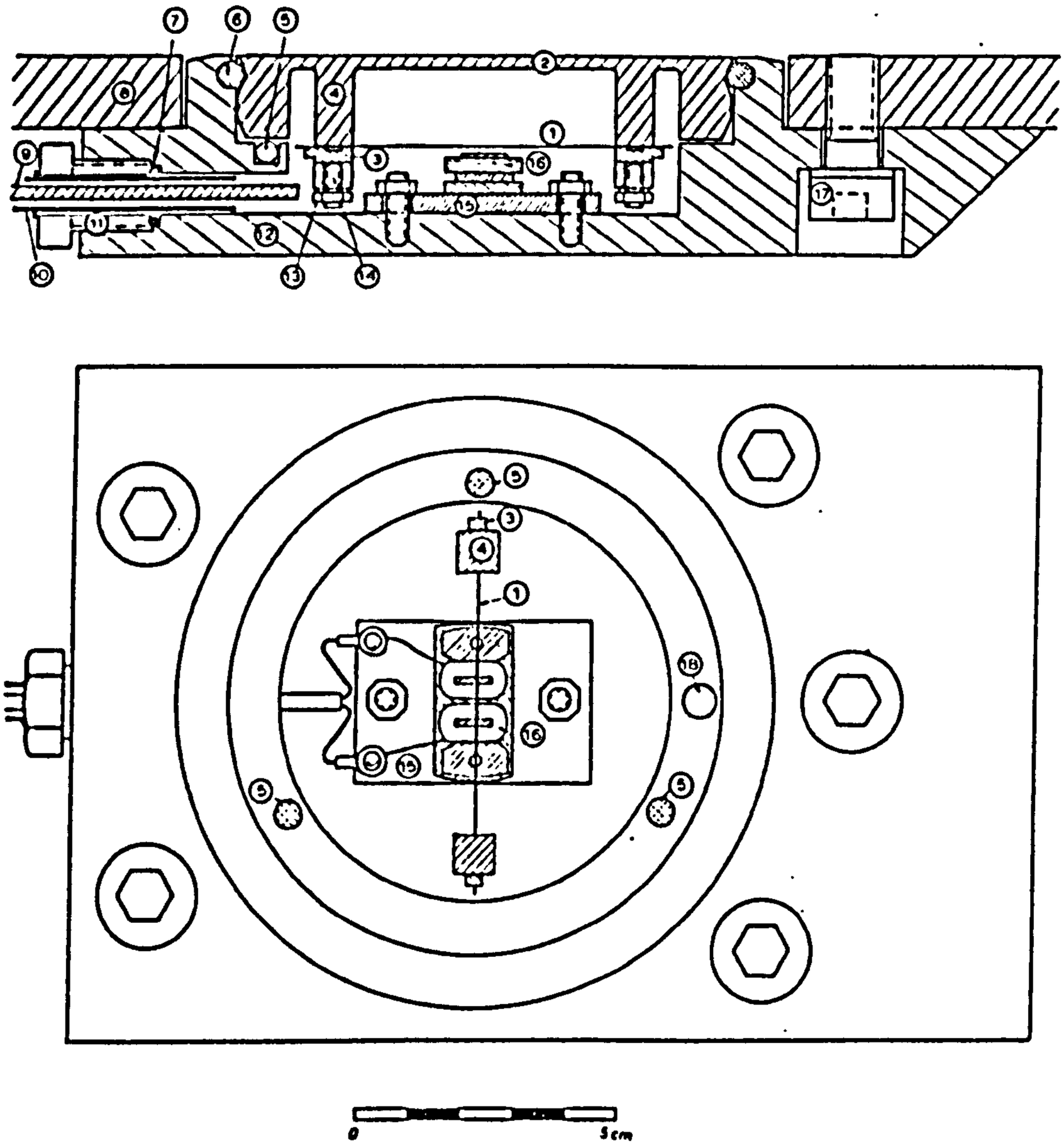


Figure A5.2 NGI's earth pressure gauge of the 1960s

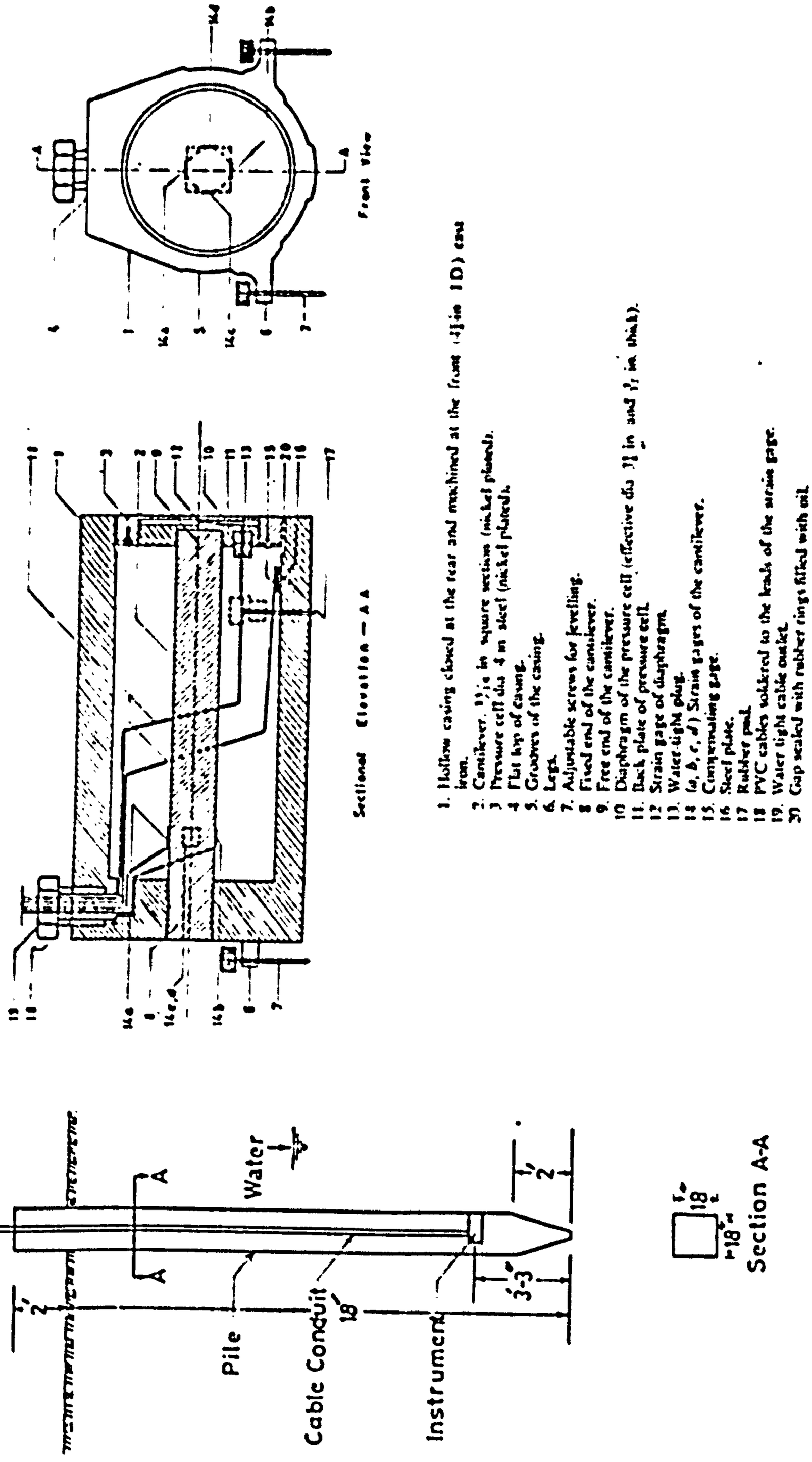


Figure A5.3 Agarwal and Venkatesan's surface stress transducer

A5.1.4 Agarwal and Venkatesan (1965)

Agarwal and Venkatesan[5] describe an instrument to measure the normal stress and skin friction on the surface of a 457mm (square) precast concrete pile. Figure A5.3 gives information about this unusual device. The radial total stress is sensed by a strain-gauged diaphragm in the conventional way; but the skin friction is measured by the bending of a solid steel cantilever, ≈230mm long x 24mm square. The instrument is not very stiff in either direction, and would seriously under-register changes in radial total stress and shear stress in stiff soils (see Table A5.1).

A5.1.5 Koizumi and Ito (1967)

Koizumi and Ito[6] give very few technical details about the EP cells employed for their pile tests. They utilized "magnet-type" diaphragm pressure cells with a working range of 98-294kPa and a maximum central deflection of 1μm. Hence these devices were very stiff, and would have under-registered $\Delta\sigma_{rr}$ in the soft Tokyo clay in which they were installed by 1% at most (assuming c_{uo} = 30kPa and E_u/c_{uo} = 1000).

A5.1.6 BP/BRE instrumented pile (1976)

In 1976, British Petroleum carried out a full-scale instrumented pile test on their FD platform, located in the North Sea Forties Field. The results are described by Sutton et al.,[7] and the instrumentation by St John.[8] The same devices were used at the Building Research Establishment's site at Cowden, on ϕ450mm steel pipe piles (see Rigden et al.,[9] and Gallagher and St John[10]).

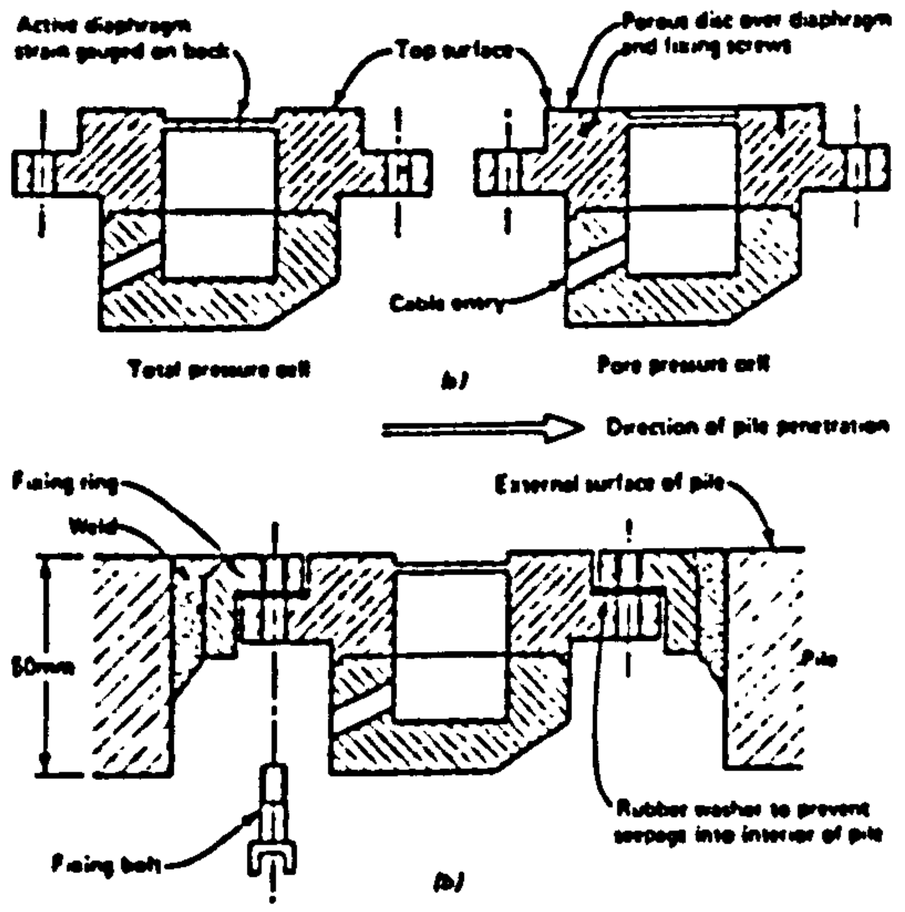


Figure A5.4 BP's cell for Forties Field

Figure A5.4 shows cross-sections through the earth and pore pressure cells. These instruments were

identical, save for the addition of a porous disk at the front of the PP cell. Both were (commercially manufactured) strain-gauged diaphragm devices, with an operating range of 0 to ≈4000kPa. The diaphragm's radius to thickness ratio (r/h) must have been around 20. Based on this value, I estimate that the EP cells could have under-registered changes in σ_{rr} in the (stiff) Cowden clay by about 26% (assuming G = 33MPa). The main cause of this large error is the small size of the strain-gauged diaphragm (only 28mm in diameter).

A5.1.7 Johnston (1979)

Johnston[11] employed Cambridge-type boundary stress transducers in a ϕ100mm diameter pile, for tests in London clay at Southampton University. (This was the pre-cursor of the Imperial College Instrumented Pile, which is described in full in Chapter 6.) Figure A5.5 shows, on the left, the general arrangement of the Southampton pile; and, on the right, a section

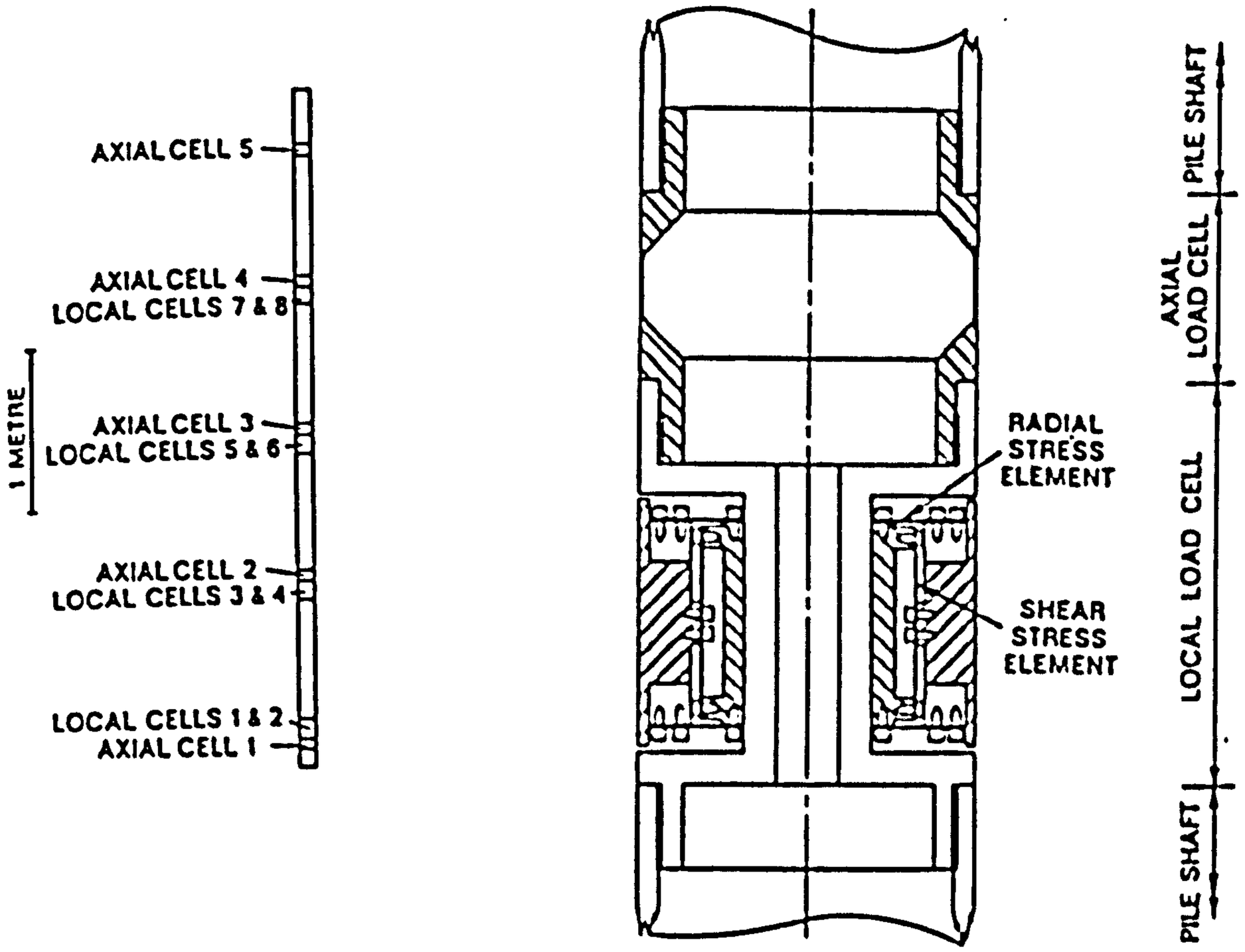


Figure A5.5 Johnston's Cambridge-type "local load cell"

through one of Johnston's instrument clusters. Each cluster (except that at the top) incorporated one axial load cell and two "local load cells" (or surface stress transducers, as I prefer to call them). The latter measure both the radial total stress and shear stress acting on the pile, via the appropriate strain-gauged elements shown on Figure A5.5.

Johnston's transducers were extremely stiff devices and his measurements in London clay contain negligible errors due to cell action.

A5.1.8 Taylor Woodrow's EP cells (1982)

Taylor Woodrow Research Laboratories performed tests[12] on four open-ended steel piles, also at the BRE's test-bed site at Cowden. Pile 3 was equipped with three levels of earth and pore pressure cells, as described by Ponniah and McAnoy.[13] One of the EP cells is shown in Figure A5.6. The instruments were housed inside a cover plate welded to the outside of the pile. Unfortunately, Ponniah and McAnoy give no other technical details.

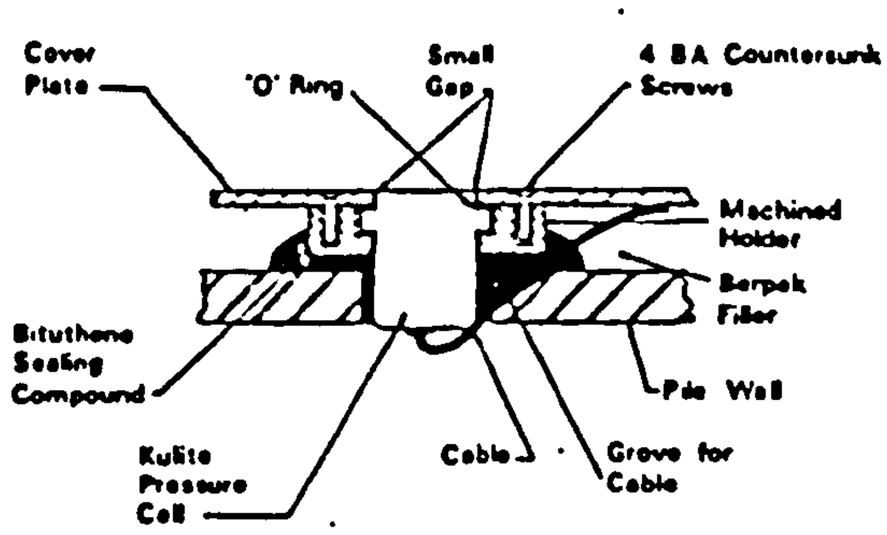


Figure A5.6 Taylor Woodrow's EP cell

A5.1.9 O'Neill et al. (1982)

O'Neill et al.[14,15] performed a number of compression load tests on closed-ended steel pipe piles, in the heavily overconsolidated Beaumont clay. Each of the instrumented piles carried both earth and pore pressure cells, at four levels. The Authors state in one paper that the pressure cells were pneumatic, and in the other that they were hydraulic[16] - but otherwise give very little technical information about the instruments.

One piece of information that is given concerns the EP cells' sensitivity to changes in temperature, which was extremely high (≈83kPa/°C). To allow the readings of σ_{rr} to be corrected for changes in temperature, the piles were fitted with thermistors, but because they had a resolution no better

than ±0.5°C, the "corrected" values of σ_{rr} were still only accurate to ±48kPa.

A5.1.10 Maddocks (1983)

Maddocks[17] designed an instrument for measuring the radial effective stress acting on a ϕ305mm pile, by transferring the pore pressure in the soil (u) to the back face of the load cell, and acts against the total

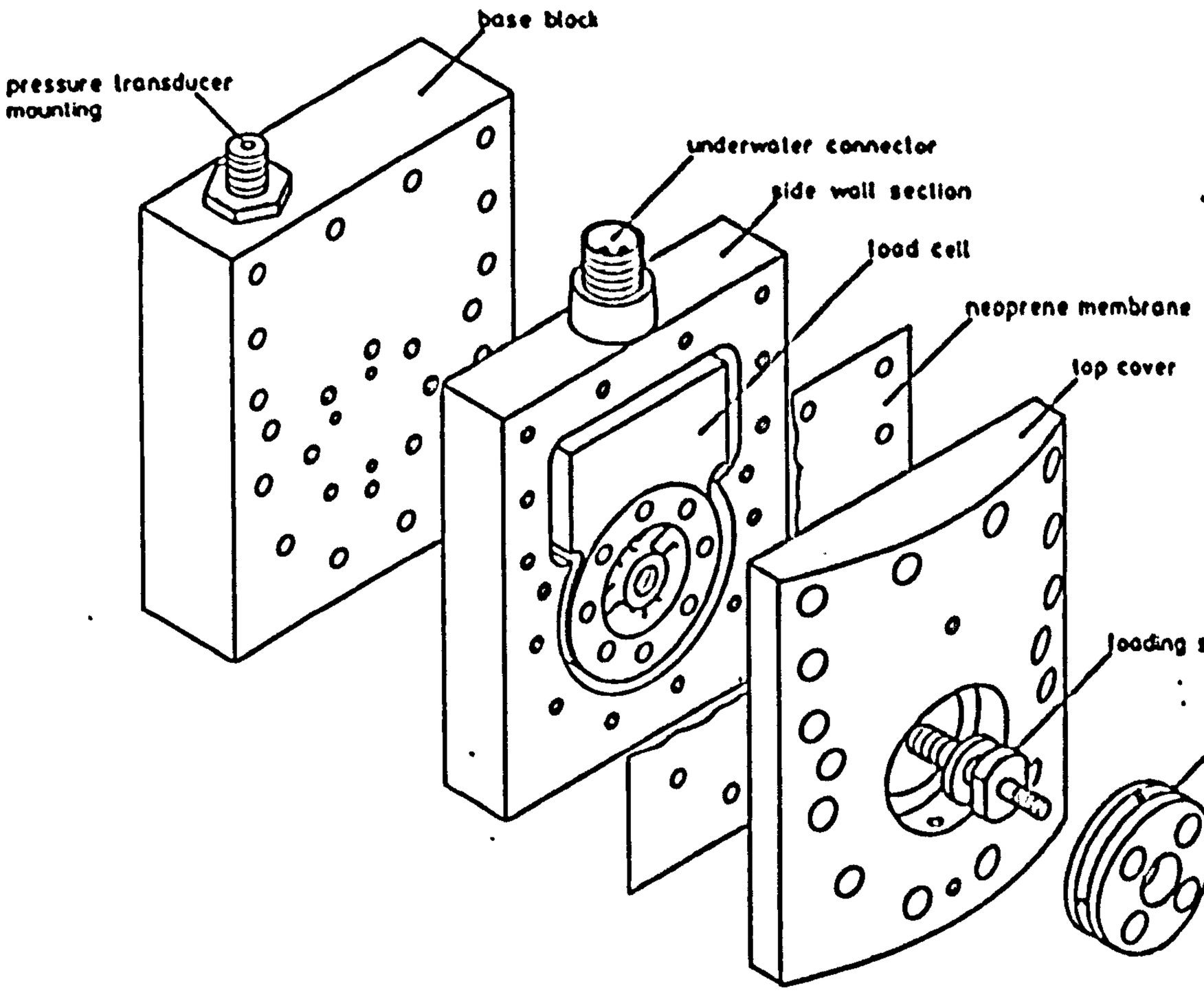


Figure A5.7 Earth pressure cell designed by Maddocks to measure radial effective stress acting on a pile

radial stress (σ_{rr}) applied to the front. Thus the load cell measures the nett force - i.e. the radial effective stress ($\sigma'_{rr} = \sigma_{rr} - u$).

Figure A5.7 shows a blow-up of Maddocks' effective stress transducer. The radial total stress σ_{rr} pushes against the load cell, via a loading stud which screws into the back of the porous face. Oil, which surrounds the load cell, is pressurized by the neoprene membrane that separates it from the water behind the porous element. Because the load cell's face

is porous, the pressure in the water inside the cell is the same as that in the soil. The load cell is a commercially produced (Strainsert) flat load cell, which can withstand the rigours of pile driving.

Maddocks designed the effective stress cell for tests in the Gault clay, and the instrument appears capable of performing extremely well in this material, provided that the fluid inside the instrument does not cavitate due to the soil dilating. If it does, then the pore pressure acting on the back face of the load cell (≈ -100kPa) may not match the suction in the soil (low permeability clays can sustain suctions well in excess of -100kPa). The nett effect would be for the instrument to <u>under</u>-estimate the radial effective stress σ'_{rr}.

I am not aware of any field tests in which Maddocks' EP cell has been used, despite (apparently) successful calibration and testing in the laboratory.

A5.1.11 Francescon (1983)

The earth pressure cell designed by Francescon,[18] for laboratory tests on ϕ18.9mm model piles, is similar in concept to the cell employed on the Oxford University Model Pile (see Figure A5.11). The radial total stress causes a fully encastré beam to deflect, and strain-gauges convert the resulting bending strains into an electrical signal, via a Wheatstone bridge arrangement. The compliance of the instrument is rather high, and since the design made no provision for applying a back-pressure to the loading platen (whereas the Oxford cell did), the potential cell action effects are quite large.

A5.1.12 The Piezo-Lateral Stress cell

The Piezo-Lateral Stress (PLS) cell was conceived, designed, and built at Massachusetts Institute of Technology (MIT) in the late 1970s, as a tool for investigating the fundamental aspects of pile/soil interaction. The main features of the instrument are described by Baligh et al.[19]; information about the latest version can be found in the PhD Thesis by

Morrison.[20] In many ways the PLS cell is similar to a model pile, as can be seen from Figure A5.8.

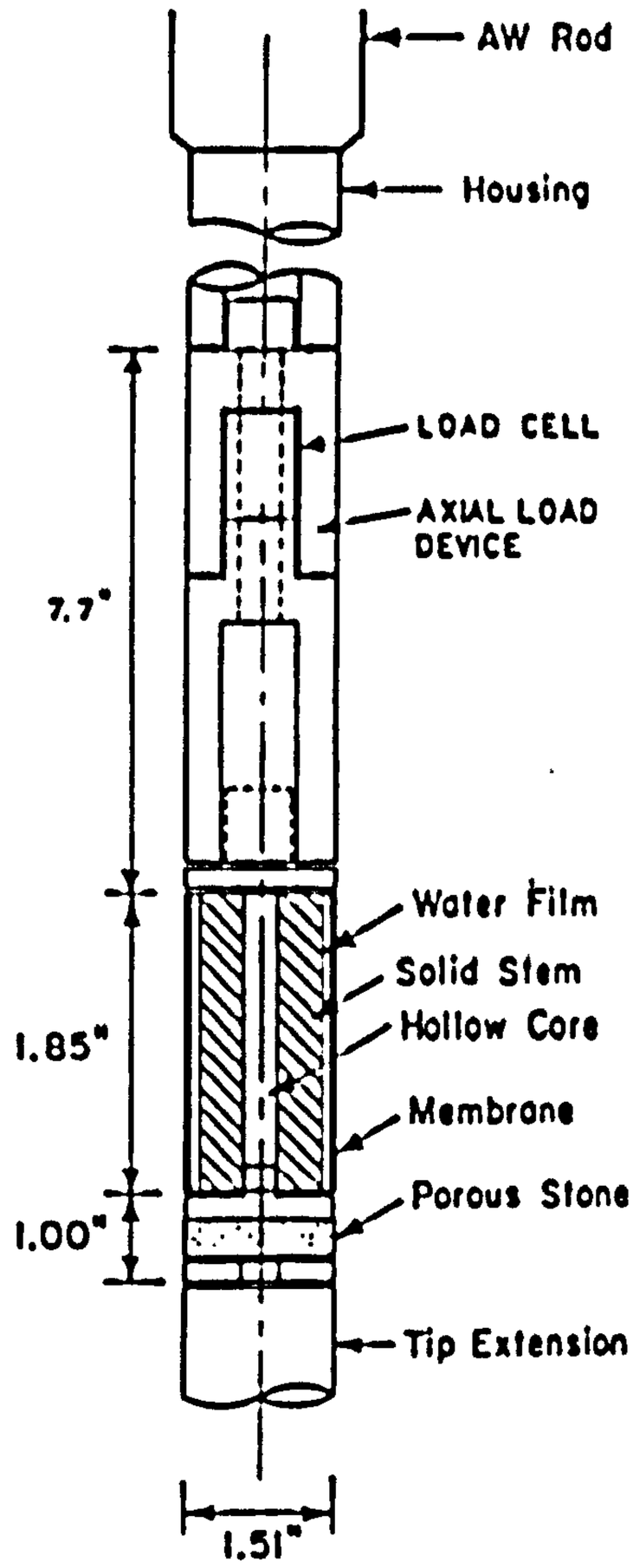


Figure A5.8 The PLS cell

The Piezo-Lateral Stress cell is capable of measuring the radial total stress (σ_h on the figure), the pore water pressure (u), and the axial stress (σ_a) at a solitary position far behind the "pile" tip. The distance L is normally 50-60 times the radius of the pile.

The instrument's pore pressure sensing element contains a high air-entry porous ring linked to a transducer. The lateral stress cell operates as follows (see Figure A5.9):

- The earth pressure σ_{rr} acting on the instrument pressurizes the thin film of water, that is trapped between the cell's (thin) outer membrane and its solid steel core
- A transducer measures the pressure in the water, which, because the membrane is thin, equals σ_{rr} almost exactly

The PLS cell will faithfully record the earth pressures only if the film of water is thoroughly de-aerated. In this case, the instrument's radial compliance is minimal and there should be no under-registration of σ_{rr} in even the stiffest of clays. The requirement that the lateral stress cell is thoroughly de-aerated obviously hinders its use in routine geotechnical investigations.

There is no doubt that the PLS cell is capable of providing (and, indeed, has already provided) valuable information about the behaviour of piles in soft clays. Unfortunately, the outside of the cell is rather fragile

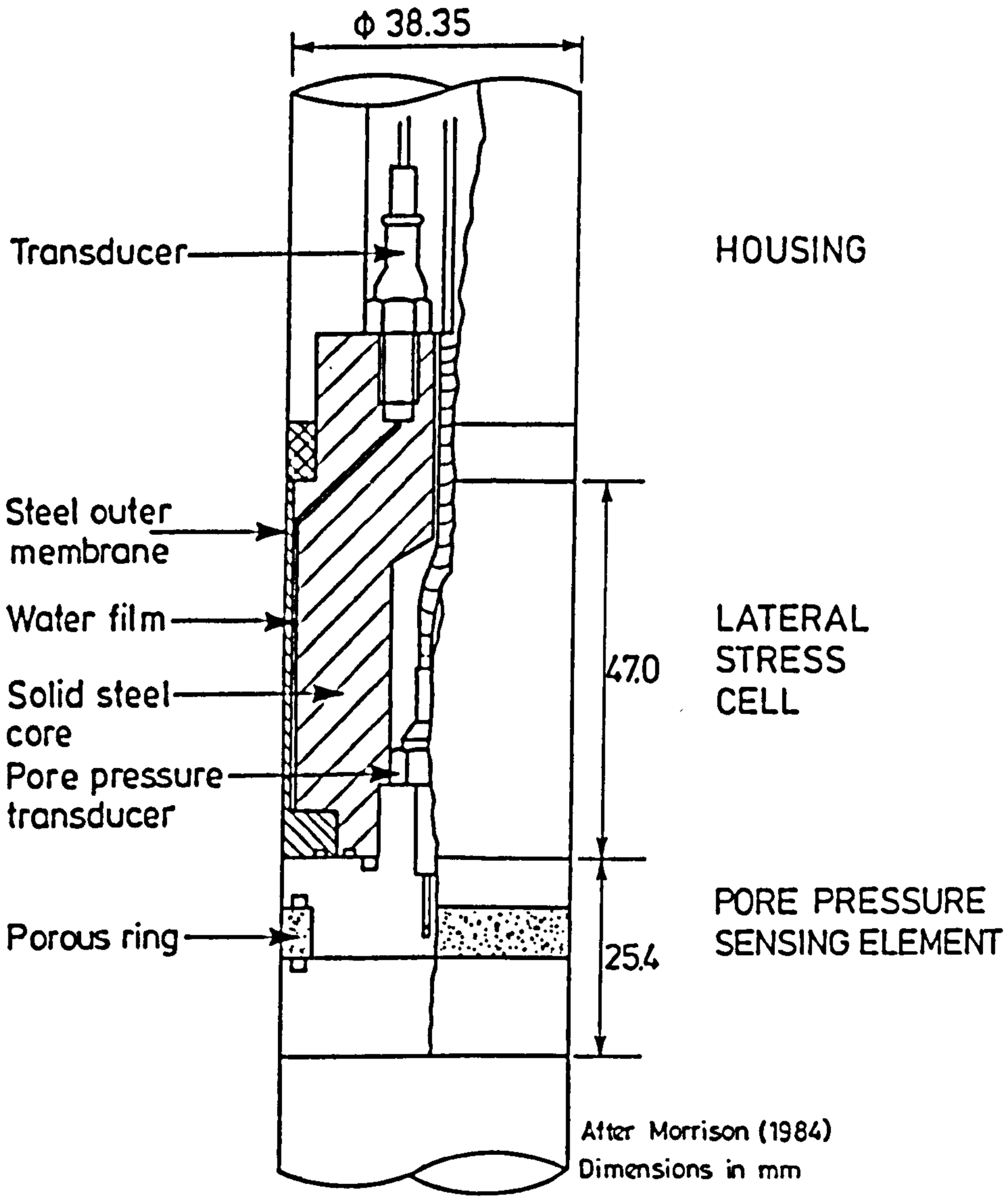


Figure A5.9 Detail of the Piezo-Lateral Stress cell

(because of the thin steel membrane), and so it is not ideally suited for tests in stiff clays, or in soils containing hard inclusions (such as stones, etc.). For this reason, there have been no PLS cell soundings in heavily overconsolidated clays.

A5.1.13 Wersching (1987)

Wersching[21] designed and manufactured a "Boundary Orthogonal Stress Transducer" (BOST) for a ϕ114mm model pile, which was used for laboratory experiments in dry sand and in dry sand overlying clay. The BOST (see Figure A5.10) is similar in concept to the Cambridge boundary stress cell, although the shear forces are measured by bending of thin webs as

as opposed to their axial compression or extension. Figure A5.10 shows the main features of this particular instrument.

(It is worth noting here that the chamber in which Werscking's tests were performed was rather small - only 3m in diameter by 3m high.* It is highly likely that the proximity of the confining walls would have had a significant influence on Werscking's results.)

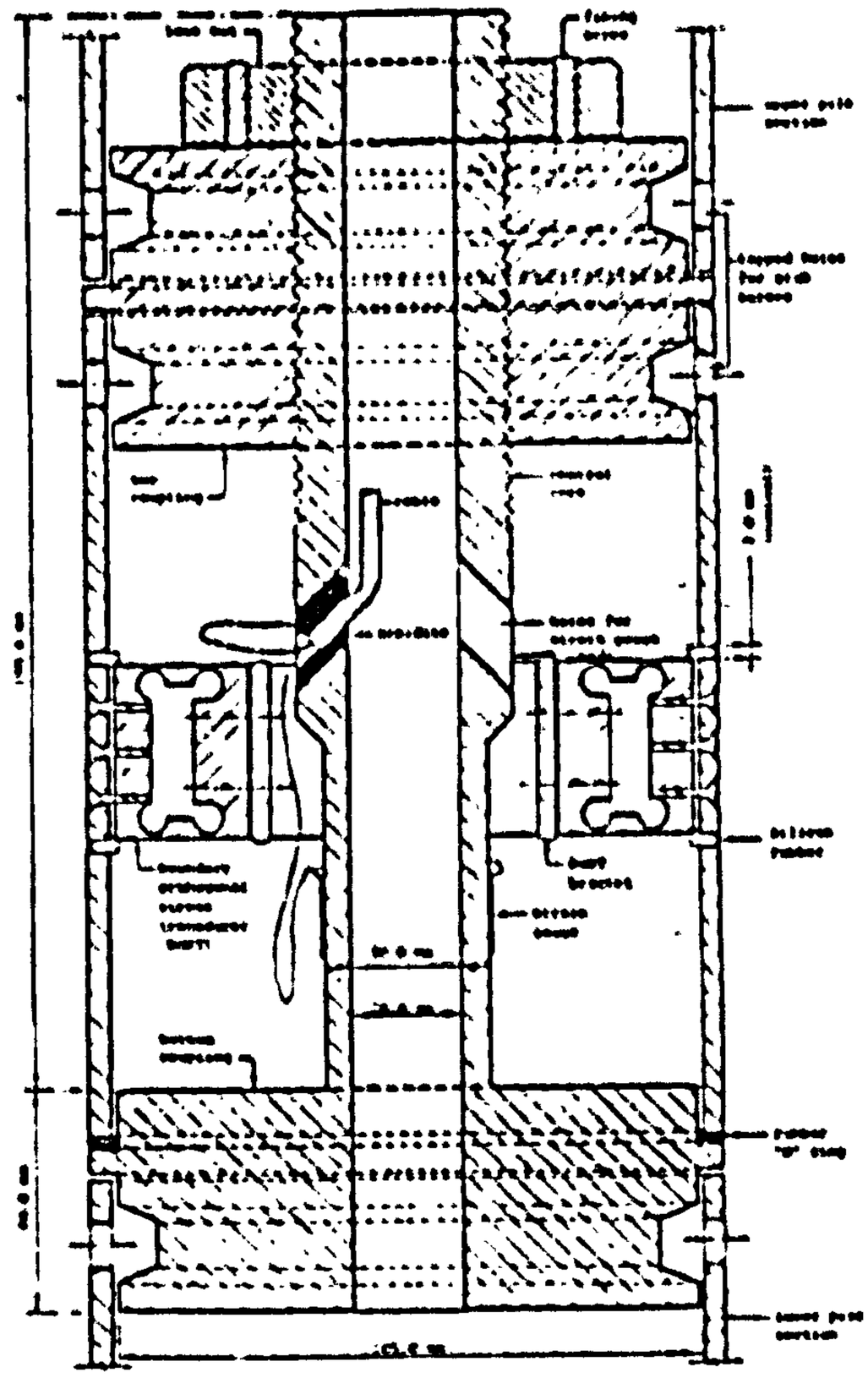


Figure A5.10 Werscking's "Boundary Orthogonal Stress Transducer"

A5.1.14 The Oxford University IMP (1987)

Coop[22] has performed field tests in heavily overconsolidated clays, using the Oxford University "In-situ Model Pile" (IMP). This device carries a total of four miniature EP cells, one of which is shown in Figure A5.11.

The EP cells operate in the following way. The radial total stress acting on the stainless steel cap causes the strain-gauged beam to deflect; the gauges' resistance changes and a Wheatstone bridge arrangement converts these changes into an electrical signal. The radial compliance of the EP cell is rather high (see Table A5.1), and in theory could lead to an under-registration of $\Delta\sigma_{rr}$ of up to 29% in a stiff clay.

*The clay was contained within a smaller tank, which was placed co-axial with, and at the bottom of, the larger (sand-filled) chamber

Since most of Coop's experiments were in the heavily overconsolidated Gault clay (with one test in the London clay at Canons Park), cell action was potentially a serious problem in his field tests. Therefore Coop applied a back-pressure to the EP cell, and attempted to keep the loading platen from moving. In this case the cell has negligible radial compliance, and the necessary changes in back-pressure are equal to the changes in σ_{rr}.

Coop dispensed with the back-pressure system during pile installation, since it was impracticable to keep the loading platen stationary whilst the radial total stresses were changing. He argued that the instrument's compliance was not a problem, in these circumstances, "since the transducer is continually moving into fresh soil. Whilst fluctuations during penetration may be subject to a small error, the mean reading will be correct."[23] However, he does not justify this statement or explain why the mean reading should be correct whilst changes in σ_{rr} are wrongly measured. This subject is discussed at greater length in Section A5.2.

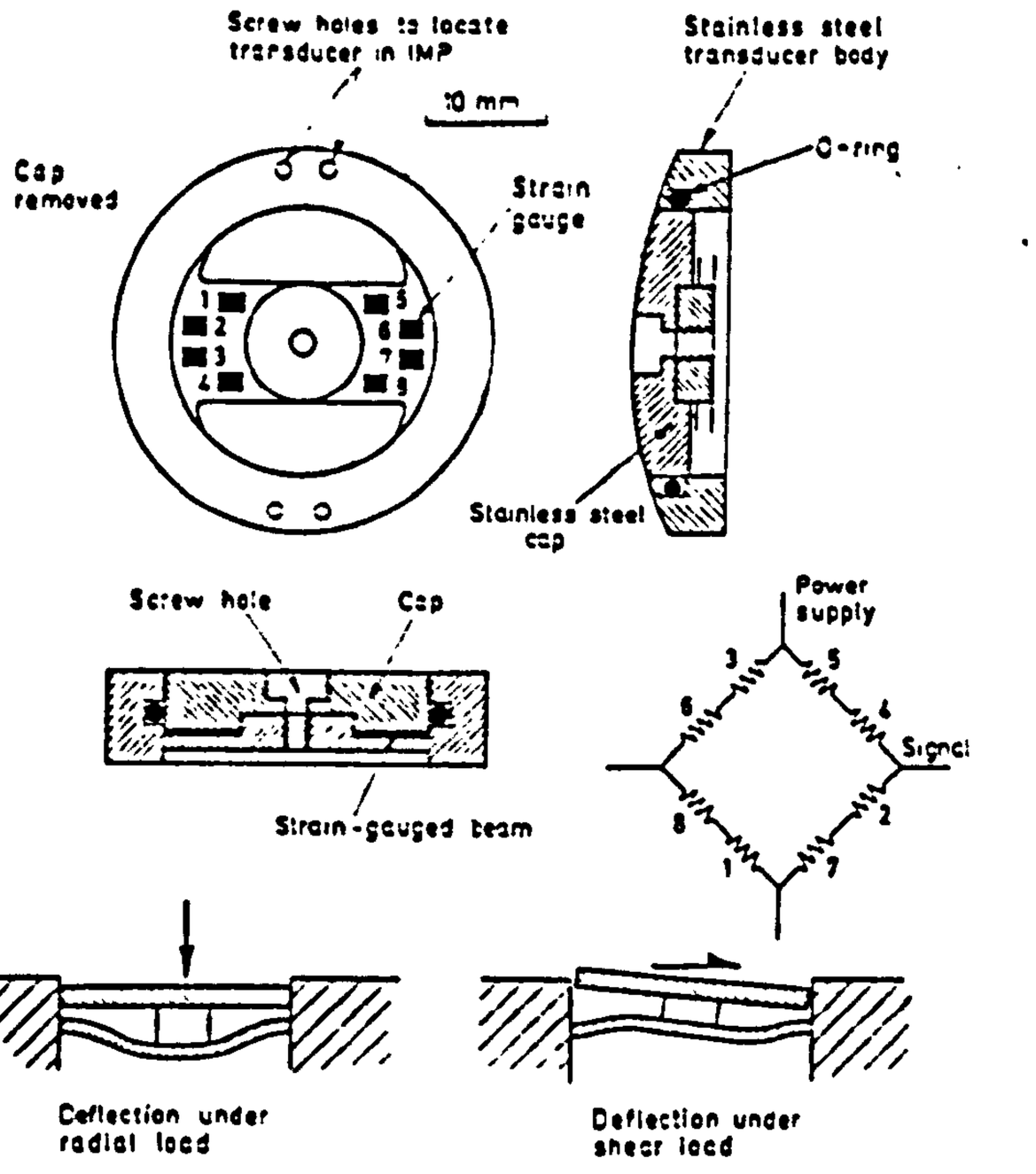


Figure A5.11 Earth pressure cells on the Oxford University model pile

A5.1.15 NGI's instrumented piles (1989)

The Norwegian Geotechnical Institute (NGI) has conducted a number of instrumented pile tests, mainly in Norway (Haga, Onsøy, Lierstranda), but also in the United Kingdom (Pentre, Tilbrook Grange). Details about the earth pressure cells employed at Haga have not been published, but some

information has appeared regarding the instruments used at the other sites.[24]

Figure A5.12 shows the instrumentation scheme adopted for the tests at Onsøy, Lierstranda, and Pentre. The A- and C- piles contain two axial load, two earth pressure, and two pore pressure cells at each level (marked "2" on the diagram). Except for their difference in length, these 219mm diameter piles are identical in every respect. The B- piles are 820mm in diameter, and carry three levels of instrumentation (marked "4"), each one containing 8 strain gauge circuits, 2EP, and 2PP cells.

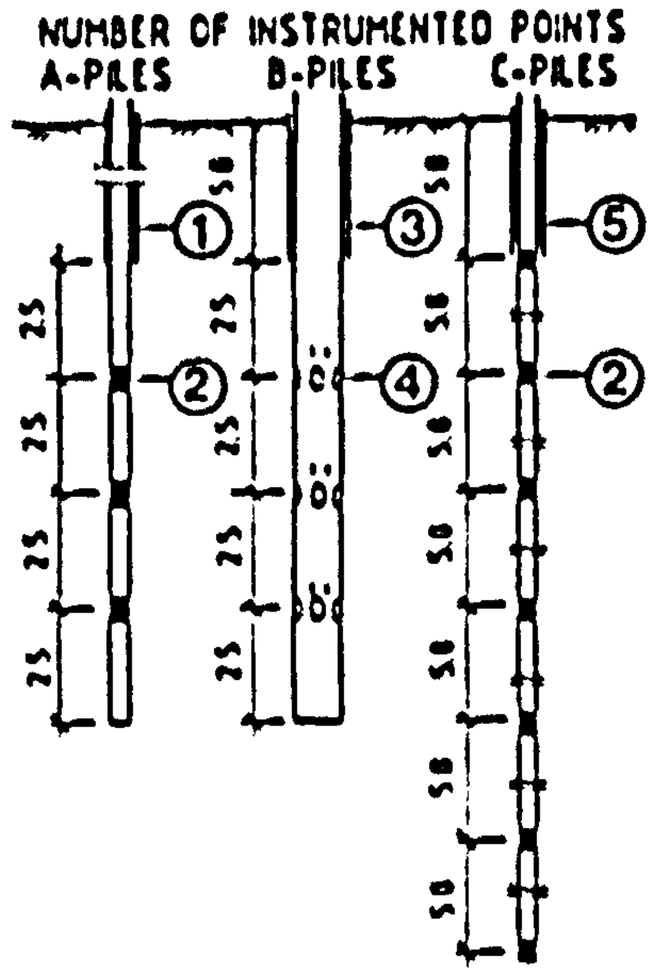


Figure A5.12 NGI's A-, B-, & C- piles

All the pressure cells are vibrating wire devices. Those on the B- piles were adapted from instruments used for measuring the stresses on sheet pile walls (i.e. similar to the Φien cell, see Section A5.1.3).

The earth and pore pressure sensors employed on the A- and C- piles are illustrated in Figure A5.13. The sensors fit into special transducer housings, which also act as joining pieces for the adjacent (un-instrumented) pile segments (see Figure A5.12). Glued to the membrane of each EP cell is a hard rubber disk, which is shaped to match the curvature of the pile. The design is

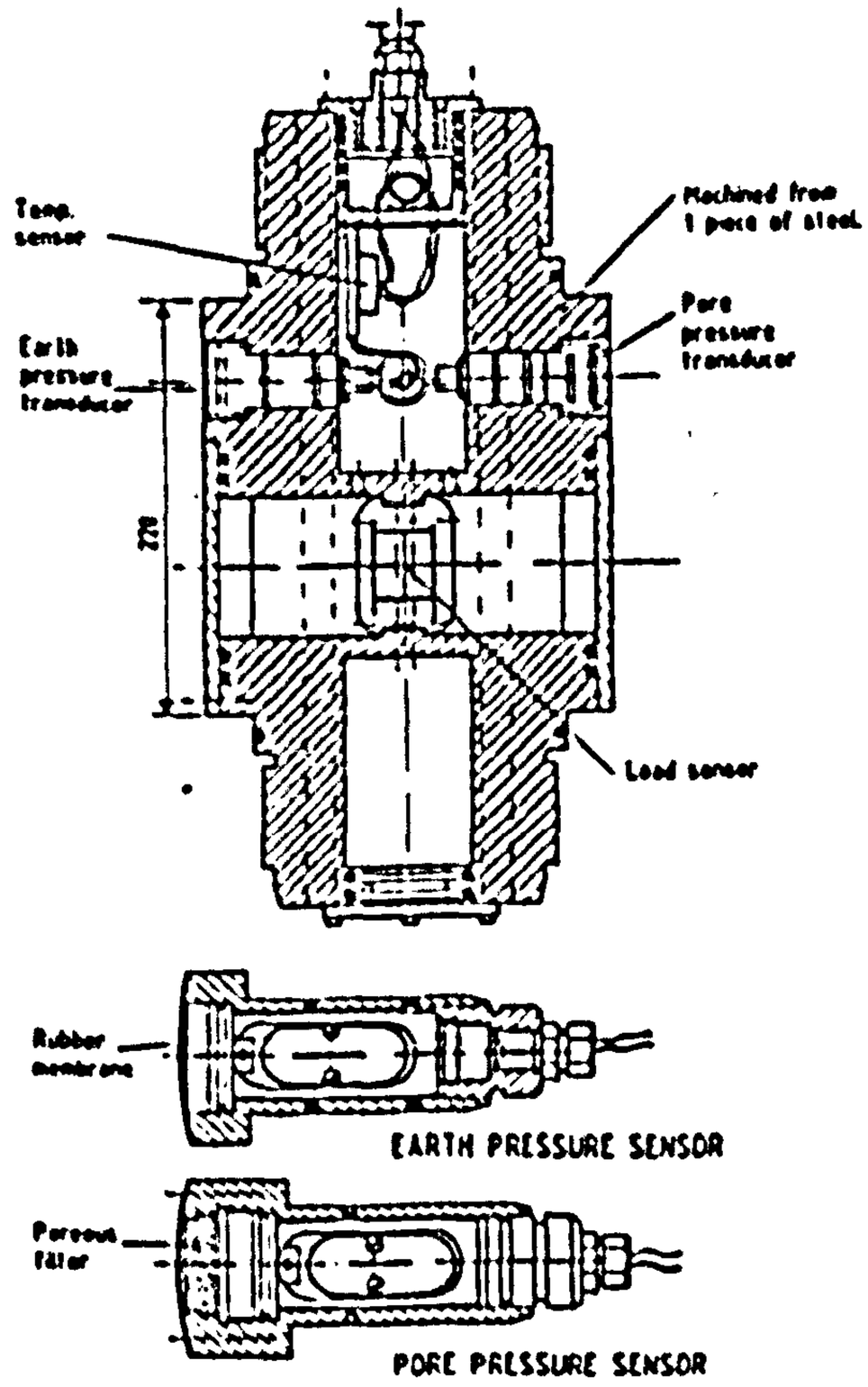


Figure A5.13 Instrument units for the NGI's A- & C- piles

sufficiently robust for the instruments to survive the high accelerations caused by pile driving, and, from the little information that has been published to date, they appear to give excellent results in the soft, plastic clay at Onsøy. The data is currently confidential to the NGI's sponsors, but should begin to appear in the Literature later this year (1989).

A5.2 ASSESSMENT OF CELL ACTION EFFECTS

A5.2.1 Definition of cell action

An important aspect in the design of earth pressure cells is the assessment of "cell action": in order to register a load, the cell's loading platen must deflect by a finite amount (δ) under the pressure exerted by the soil; simultaneously, this deflection reduces the earth pressure, and leads to an error (ϵ) in the measurement of the true load.

This phenomenon is illustrated in Figure A5.14 for the case of a rigid piston earth pressure cell, and is analogous to the classical "trap-door" problem. As the loading platen deflects away from the soil, so the earth

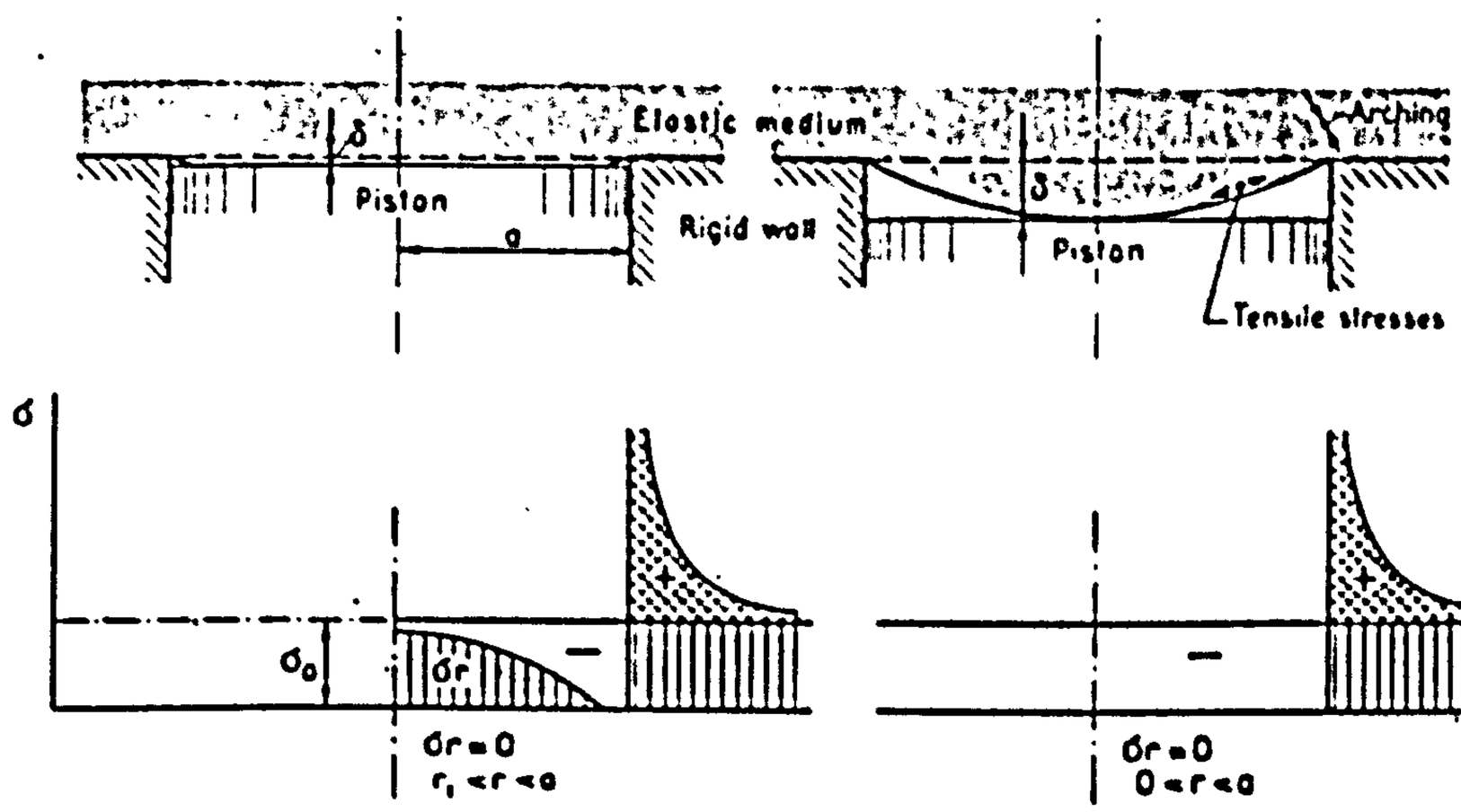


Figure A5.14 Cell action effects for rigid piston earth pressure cell

pressure reduces by an amount $\Delta\sigma_{rr}$. If the measured stress is σ_{rr}, then the original stress in the soil (prior to arching) was $\sigma_{rr} + \Delta\sigma_{rr}$. Hence the error in the measurement is:

$$\epsilon = -\Delta\sigma_{rr}/(\sigma_{rr} + \Delta\sigma_{rr}) \approx -\Delta\sigma_{rr}/\sigma_{rr} \text{ (if } \Delta\sigma_{rr} \text{ is small)}$$

If we assume that the soil is a semi-infinite, isotropic, linear-elastic medium, then, for a circular surface of radius a:[25]

$$\Delta\sigma_{rr}/\sigma_{rr} = (f/a)(G/[1-\mu])C$$

where f is the radial compliance* of the load cell ($f = \delta/\sigma_{rr}$); G is the shear modulus of the soil; and μ its Poisson's ratio; and C is a (non-dimensional) factor that depends on the shape and deformation of the loading platen. Values of C may be obtained from the book by Poulos and Davis[28] (some of the more relevant values are given in Table A5.1 herein).

Of course, real soils differ from the ideal linear-elastic medium in several important respects, for instance:

- Clay soils have a limited shear strength, and often a negligible tensile strength
- Soils are anisotropic, elasto-plastic materials whose elastic behaviour is highly non-linear (see Appendix 3)
- Soils are not infinite in extent

A5.2.2 Factors that affect cell action

As the equation above demonstrates, the scale of any cell action effects depends on a combination of factors, which include the cell's compliance (f), the radius of its loading platen (a), and the stiffness of the soil ($G = E_u/3$). The significance of each of these parameters is illustrated in Figure A5.15 for the case of a Cambridge-type surface stress transducer in contact with a sandy clay. The diagrams are based on a linear-elastic finite element study into the performance of rigid piston earth pressure cells. The study was undertaken at the Transport and Road Research Laboratory, in parallel with a series of laboratory tests (as described in Section A5.2.6).

A5.2.3 Cell action in stiff soils

In stiff soils cell action is potentially a serious problem: to reduce the errors in the earth pressure measurements, the transducer must be made as stiff as possible (thereby reducing f) and the loading platen as

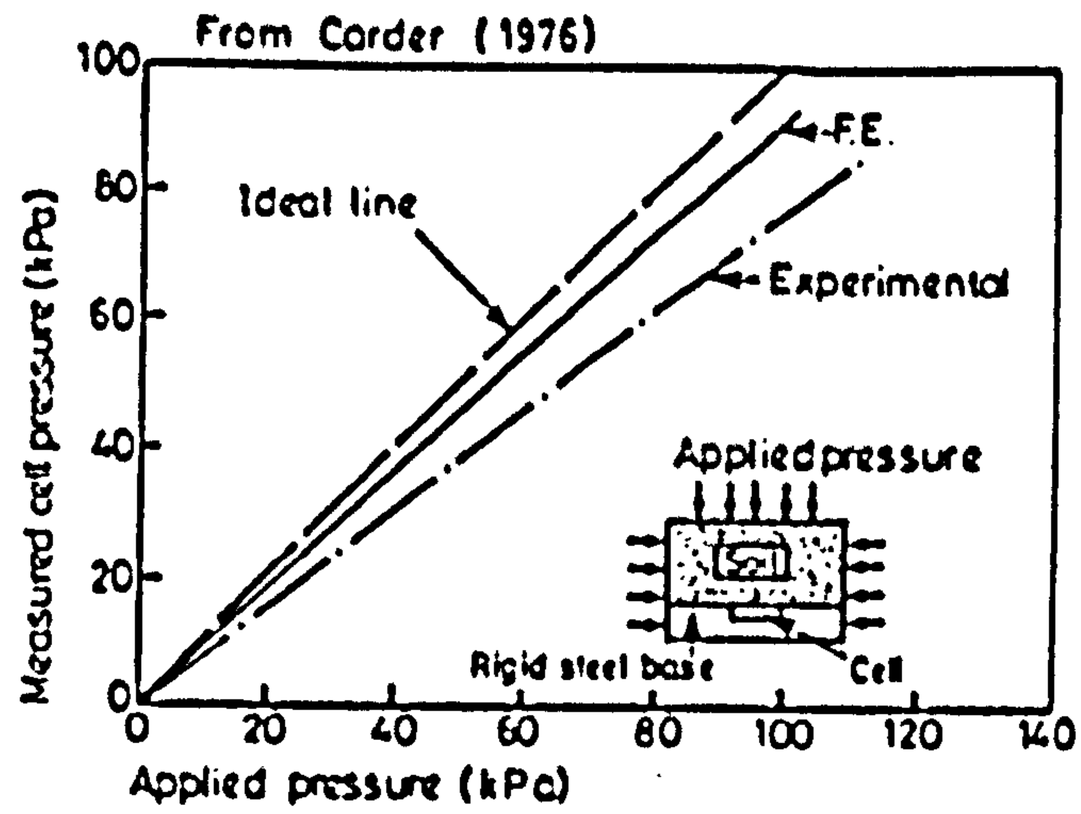
---

*f for 'flexibility'

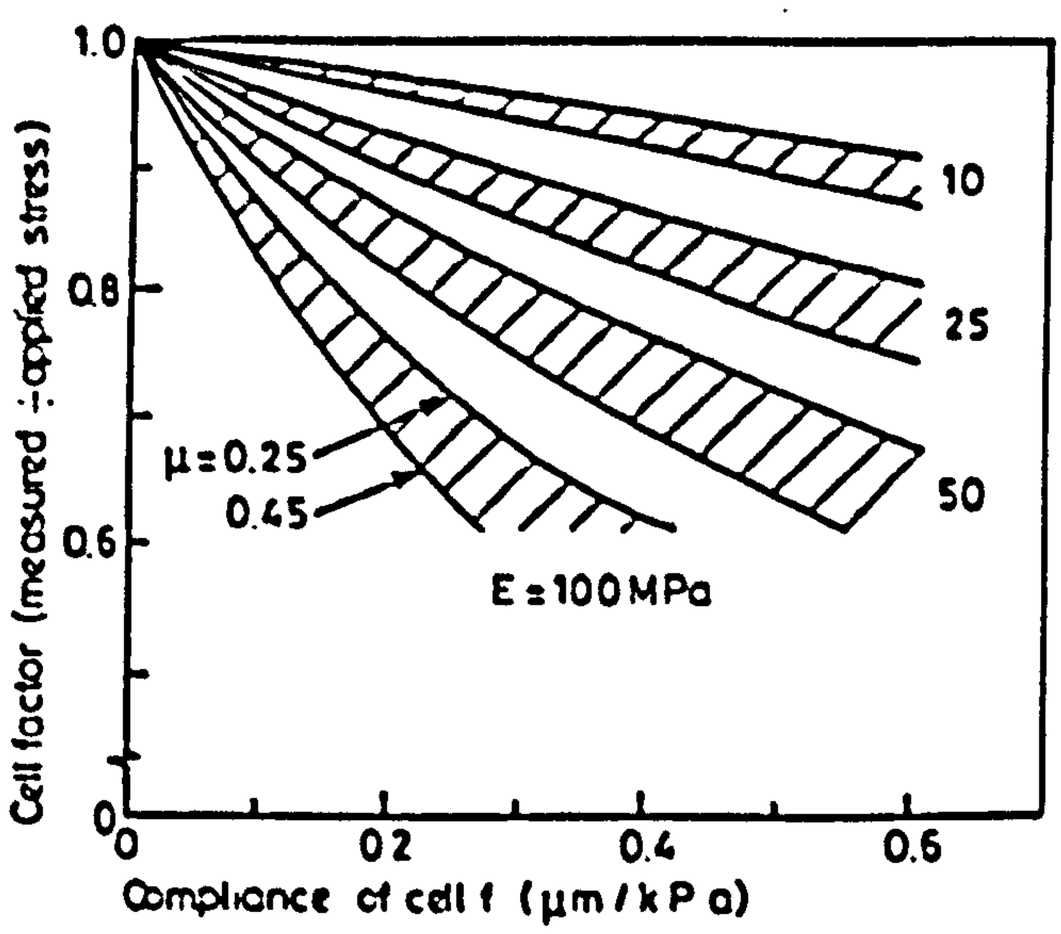
large as possible (thereby increasing a). However, reducing the compliance of a cell also reduces its sensitivity (s), all other things being equal. Hence it is useful to define an "Optimization Factor" (O_f) to help in quantifying the trade-off that must be made. O_f is defined as the sensitivity of the cell (s) divided by the ratio (f/a).

Despite its limitations, the simple linear-elastic formula for $\Delta\sigma_{rr}/\sigma_{rr}$ does give an indication of whether an earth pressure cell will suffer from significant cell action effects. However, the calculation of ϵ depends strongly on the value chosen to characterize the soil's stiffness. How does the designer select an appropriate value for G?

The soil's shear modulus will not be the same next to the pile as it is in the free-field. If Baligh's 'Simple Pile'[27] approach is correct, then the soil could well be on an unload-reload portion of its stress-strain curve, as it passes along the pile's shaft. Because the soil's elastic behaviour is highly non-linear, values of G



Tests in a sandy clay E=20MPa, μ=0.405, f=0.2μm/kPa



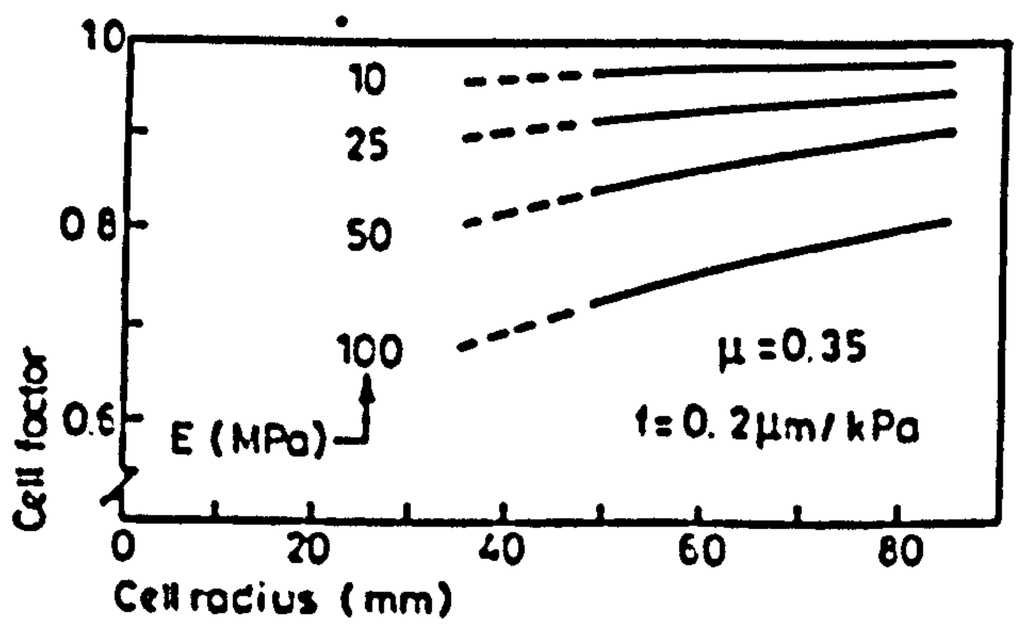


Figure A5.15 Effect of cell compliance, loading platen radius, and soil stiffness on cell factor

depend on the level of straining involved. At 1% axial strain in a triaxial test, the secant stiffness G is of the order of 4MPa for London clay. To err on the safe side, however, we might choose the value of G at 0.01% axial strain: for London clay this is ≈33MPa (see Appendix 3). This is close to the value of 30MPa assumed by Maddocks[28] for the stiff Gault clay. (Note that for the London clay at Canons Park c_{uo} is ≈100kPa, so this implies that $E_u/c_{uo} \approx 1000$.)

A5.2.4 Comparing designs of earth pressure cell

Table A5.1 compiles data for a number of earth pressure cells that have been mounted on full-size and on model piles (as reviewed in Section A5.1). Included in the Table is an estimate of each cell's compliance, its sensitivity, and the under-registration of load that might be expected if the instrument had been installed into stiff London Clay at Canons Park. Several points are worth noting:

- Many of the EP cells that operate by bending (e.g. the diaphragm devices) are far too compliant for reliable measurements in the stiff London clay
- The "well-tuned" strain-gauged devices (such as Johnston's and Maddocks') have Optimization Factors in the range $2.7 < O_f < 4.1$
- Many of the high compliance instruments have very low Optimization Factors ($O_f < 0.25$) - in these cases, reduced radial rigidity has not been traded for an increase in sensitivity

Table A5.1(a) Properties of various pile-mounted earth pressure cells

	Authors	Reese & Seed (1955)	ϕien (1962)/ Kenney (1967)	Agarwal & Venkatesan (1965)	Koizumi & Ito (1967)	Johnston (1979)	Maddocks (1983a)	
2	Organization	Univ. of California	NGI	Central BRI, Roorkee, India	BRI, Tokyo	Southampton University	Cambridge University	
3	Instrument	Pile	Pile	Pile	Pile	Model pile	Pile	
4	Diameter D (mm)	ϕ152.4	470 wide	457.2 sq	ϕ300	ϕ101.6	ϕ304.8	
	Loading platen							
5	Type	Flexible membrane	Flexible membrane*	Flexible membrane	Flexible membrane*	Rigid piston	Rigid piston	
6	Shape	Circle	Circle	Circle	Circle	Rectangle	Circle	
7	Size (mm)	ϕ38.1	ϕ75	ϕ101.6	30	63.5 x 76.2	ϕ50.8	
	Load cell							
8	Design type	Strain-gauged diaphragm	Vibrating wire diaphragm	Diaphragm/ cantilever[ϕ]	Magnet type	Cambridge load cell	Strainsert cell FL2.5U	Strainsert cell FL1U
9	Cell senses...	Bending	Bending	Bending	(Deflection?)	Compression	Bending	Bending
	Radial stress							
10	Capacity (kPa)	(98.5)	245	(98.5)[$]	98-294	(3182)	5489	2197
11	Compliance f (μm/kPa)	2.12*	0.107	(5.16)	0.010max	0.0095	0.004	0.0086
12	Sensitivity s ([μV/V]/kPa)	(8.88)	5600Hz²/kPa	(2.13)**	?	(≈0.77)	0.55	0.91
13	Under-reading ε (%)	-86	-13.7	-85	-3.7max	-1.9	-1.3	-2.8
14	O_f	≈0.09	?	≈0.09	?	≈3.2	≈3.5	≈2.7
	Shear stress							
15	Capacity (kPa)	Not able to measure shear	Not able to measure shear	?	Not able to measure shear	(900)	Not able to measure shear	Not able to measure shear
16	Compliance f (μm/kPa)			5.84		0.06		
17	Sensitivity s ([μV/V]/kPa)			?		(≈4.00)		
18	Under-reading ε (%)			-86		-8.0		
19	O_f			?		≈2.6		

*r/h = 15

ϕStrain-gauged diaphragm (r/h = 50) senses radial total stress; cantilever senses shear stress

$Calibrated up to 690kPa!

*This figure implies r/h ≈ 50

**One strain gauge only, for which $s = (3k[1-\mu^2]/32E)(r/h)^2$, where k = strain gauge factor (≈ 2.1)

*r/h ≈ 6.5

Table A5.1(b) Properties of various pile-mounted earth pressure cells

	1	Rigden et al. (1979)	Francescan (1983)	Baligh et al. (1985)	Wersching (1987)
	2	BP/BRE	Cambridge University	MIT	Polytechnic of Wales
	3	Pile	Model pile	PLS cell	Model pile
	4	ϕ450	ϕ18.9	ϕ38.35	ϕ114
	5	Loading platen Flexible membrane*	Rigid piston	Thin steel membrane	Rigid piston
	6	Circle	Circle	Cylinder	Square
	7	ϕ28	ϕ10	ϕ38.35 x 47	30 x 30
	8	Load cell Strain gauged diaphragm	Strain gauged beam	Fluid behind membrane	Boundary stress cell
	9	Bending	Bending	Pressure	Compression
	10	Radial stress 4137	?	3180	
	11	(≈0.09)	0.068	0.0095	(0.001?)
	12	(≈1.4)	2.16	?	
	13	-26	-53	-0.07[#]	
	14	0.22	0.16	?	
	15	Shear stress Not able to measure shear	?	Not able to measure shear	16.3?
	16		?		≈1.53
	17		0.98		
	18		?		
	19		?		

*r/h ≈ 20

[#]Applying Gibson & Anderson's pressuremeter analysis, ε = 4Gf/D

	1	Coop (1987)		Borg Hansen et al. (1989)	This Thesis
	2	Oxford University		NGI	Imperial College
	3	Model pile		Pile	Model pile
	4	ϕ80		ϕ219	ϕ101.6
	5	Rigid piston		Flexible membrane*	Rigid piston
	6	Circle		Circle	Rectangle
	7	ϕ21.85			75 x 95
	8	Strain gauged beam		Vibrating wire diaphragm	Cambridge load cell
	9	Bending			Compression
	10	No b/p[@] (1630)	With b/p ∞		870
	11	(0.054)	0		0.023
	12	≈1	?		2.41
	13	-41.5	0		-3.8
	14	≈0.20	∞		≈4.1
	15	Not able to measure shear	Not able to measure shear	Not able to measure shear	262
	16				0.076
	17				15.7
	18				-8.3
	19				≈9.8

*Hard rubber disk glued to flexible membrane

[@]b/p - back pressure; this instrument works as a null device: the back pressure is increased until there is no deflection of the loading platen relative to its original (unloaded) position

Notes to accompany Table A5.1

BRE = Building Research Establishment; BRI = Building Research Institute; NGI = Norwegian Geotechnical Institute; MIT = Massachusetts Institute of Technology.

The general formula for the under-registration of radial stress is:

$$\epsilon = 1/(1 + 1/\Phi),$$

where $$\Phi = (f/a)(G/(1-\mu))C.$$

C depends upon the shape of the loading platen, and the manner in which it deforms. f is the load cell compliance (or flexibility); G the soil's shear modulus (taken as 33MPa for the London clay); and μ is the soil's Poisson's ratio (0.5). For a rigid circular platen $C = 4/\pi$; for a flexible circular membrane $C = 8/3\pi$; and for a rectangular rigid platen $C = 2.14/\sqrt{\pi}$ (all for radial stress). For a rectangular rigid platen in shear $C = 1.4/\sqrt{\pi}$. See Kallstenius and Bergau (1956) and Poulos and Davis (1974).

O_c ("optimization factor") is defined as the cell's sensitivity, s, divided by the ratio (f/a), where f is the cell's compliance and a is the equivalent radius of the loading platen.

For circular membranes: capacity = $[8E/3(1-\mu^2)](h/r)^2$, where r = radius, h = thickness, E = Young's modulus, and μ = Poisson's ratio of membrane; compliance $f = 3(1-\mu^2)r^4/16Eh^3$; and with suitable strain gauge patterns, the sensitivity, $s = [0.82(1-\mu^2)/E](r/h)^2$.

A5.2.5 Cell action effects during pile installation

The tabulated values of ϵ correspond to the errors expected in measuring instantaneous changes in the earth pressures acting on a stationary pile after installation in London clay. When the pile is static (i.e. during equalization or load testing), very stiff transducers are required if stress changes are to be resolved accurately. Various arguments can be put forward[29] to suggest that these linear-elastic calculations grossly over-predict the real errors for a moving pile. Experimental evidence to support this statement is provided by comparing the results obtained independently at Canons Park by Coop and in the current research programme (see Chapter 9). Despite the far higher flexibility of Coop's device (used without back-pressure adjustments during installation), the measurements of σ_{rr} agree to within 15%.

A5.2.6 Laboratory studies of cell action effects

The performance of various kinds of earth pressure cell has been assessed in a series of laboratory tests at the Transport and Road Research Laboratory (TRRL).[30] One of the cells investigated was the Cambridge-type surface stress transducer shown in Figure A5.16. The instrument was mounted in a recess at the centre of a ϕ540mm rigid steel base, and soil was compacted against the cell inside a 300mm high cylindrical mould.

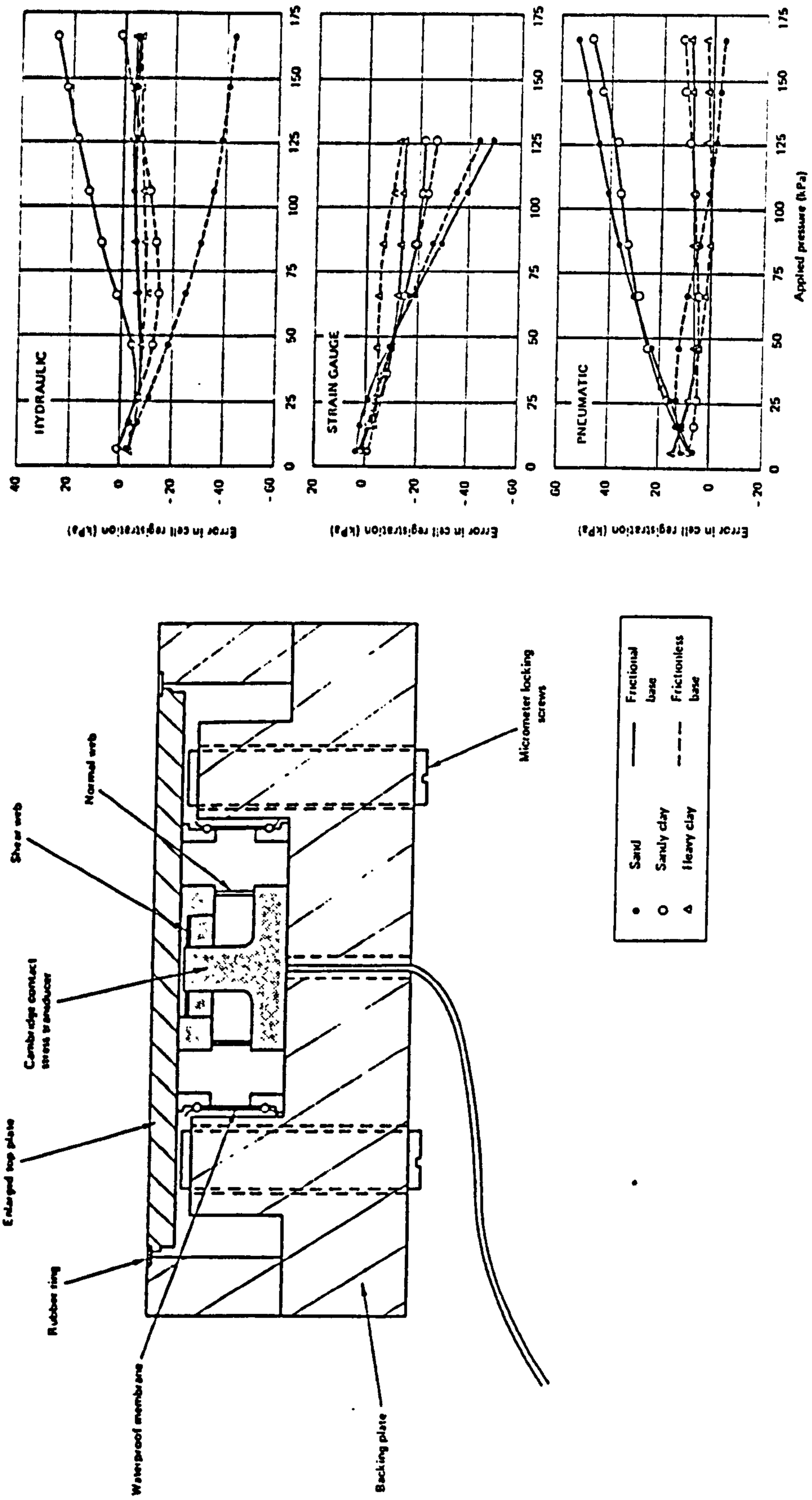


Figure A5.16 Cell action effects as determined in laboratory tests at TRRL

Three different soils were employed: a washed sand; a sandy clay; and a heavy clay. Similar tests were performed on a hydraulic and a pneumatic earth pressure cell.

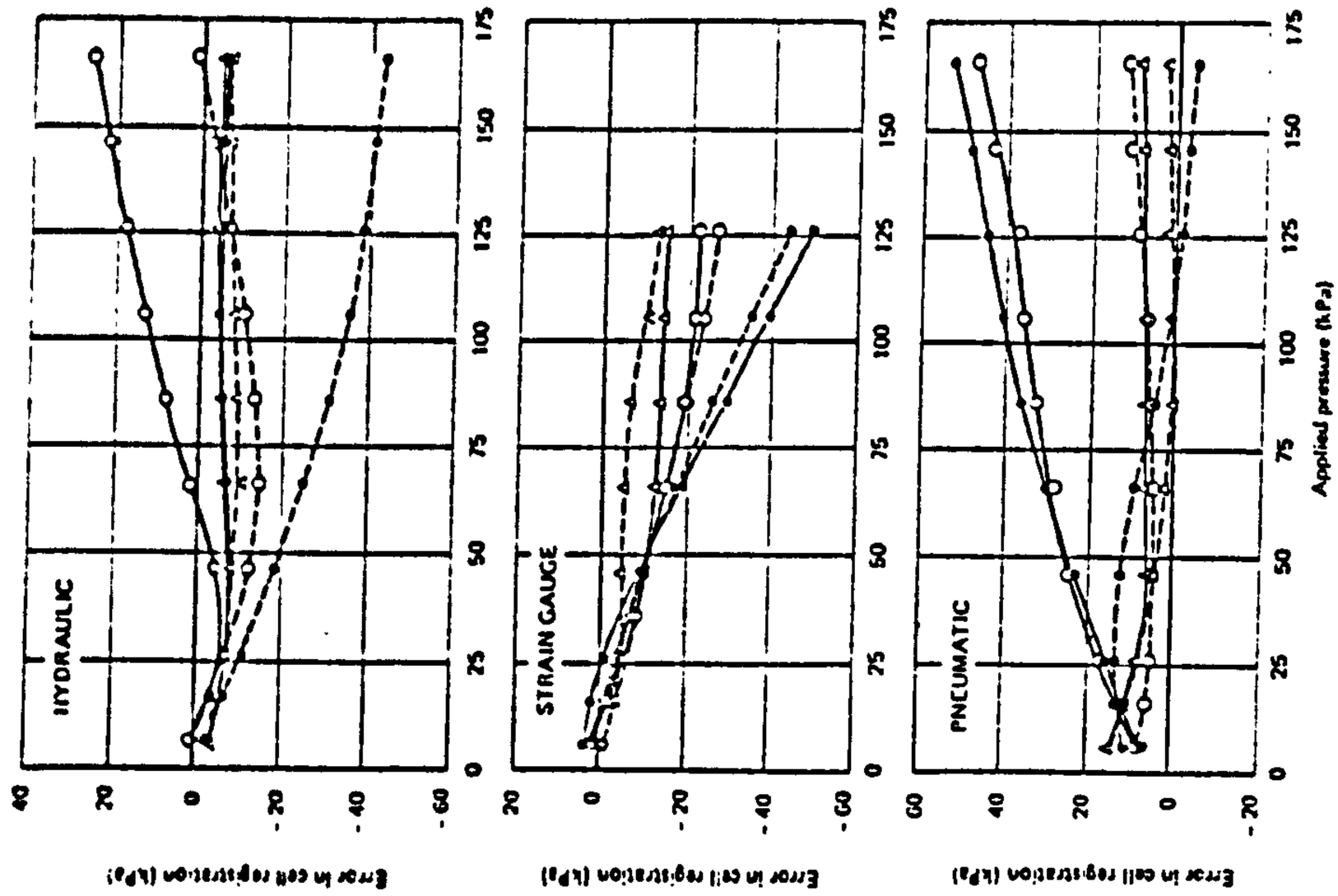
The test results are also shown in Figure A5.16. The strain-gauged instrument (i.e. the Cambridge load cell) under-registered the applied stress by between 5 and 15% in the heavy clay, and by between 5 and 25% in the sandy clay, for applied stresses in the range 25-125kPa.

> "...undrained triaxial tests showed that the initial tangent modulus of both the sandy clay and the heavy clay remained between 18 to 25MPa over a range of lateral pressure from 0 to 200kPa."[31]

This assumes that the soils' behaviour is initially linear, whereas in fact all soils display highly non-linear stress-strain characteristics in the elastic range (see Appendix 3). Hence the conventional interpretation of triaxial tests underestimates the true small-strain stiffness of the soil.

The compliance of the Cambridge load cell was $f = 0.2\mu m/kPa$; the radius of its loading platen $a = 57mm$; and its shape factor $C = 4/\pi$. Substituting $G = E_u/3 \approx 6.67MPa$ and $\mu = 0.5$ into the equation for $\Delta\sigma_{rr}/\sigma_{rr}$ (see p569) gives $\epsilon = 4.8\%$. Encouragingly, this estimate of ϵ is close to the minimum error for both clays over the stress range 25-125kPa. If a more realistic value of G was used in the calculation, then good agreement could be obtained between the results of the laboratory tests and the theoretical cell action.

The laboratory tests at the TRRL demonstrate that cell action effects can be estimated to a reasonable degree of accuracy using simple linear-elastic calculations, provided the soil's stiffness is not under-estimated. Consequently, if theoretical calculations based on over-estimates of G show that the instrument does not significantly under-register the stress, then it becomes unnecessary to measure the cell action effects in time-consuming laboratory tests.



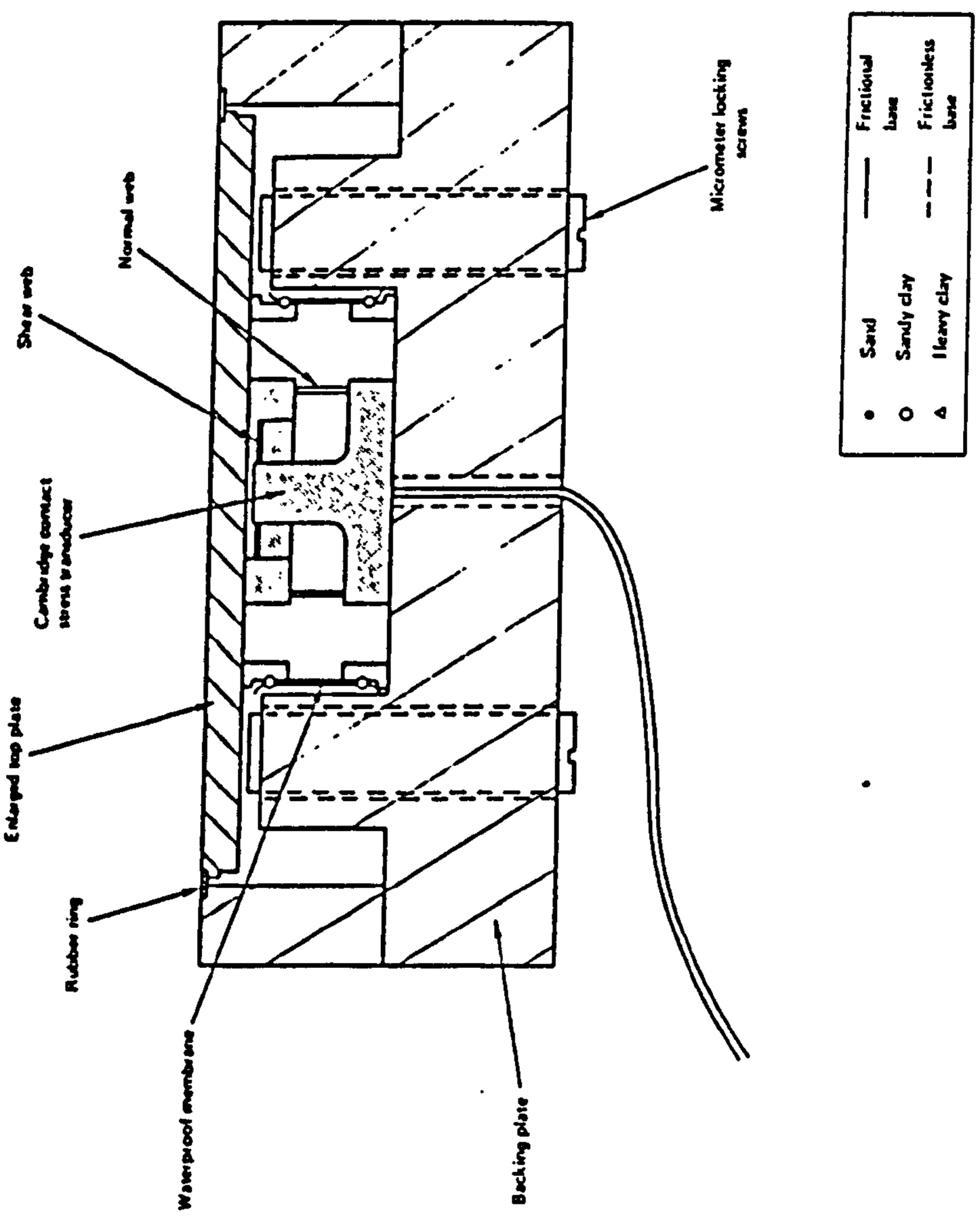


Figure A5.16 Cell action effects as determined in laboratory tests at TRRL

Three different soils were employed: a washed sand; a sandy clay; and a heavy clay. Similar tests were performed on a hydraulic and a pneumatic earth pressure cell.

The test results are also shown in Figure A5.16. The strain-gauged instrument (i.e. the Cambridge load cell) under-registered the applied stress by between 5 and 15% in the heavy clay, and by between 5 and 25% in the sandy clay, for applied stresses in the range 25-125kPa.

> "...undrained triaxial tests showed that the initial tangent modulus of both the sandy clay and the heavy clay remained between 18 to 25MPa over a range of lateral pressure from 0 to 200kPa."[31]

This assumes that the soils' behaviour is initially linear, whereas in fact all soils display highly non-linear stress-strain characteristics in the elastic range (see Appendix 3). Hence the conventional interpretation of triaxial tests underestimates the true small-strain stiffness of the soil.

The compliance of the Cambridge load cell was $f = 0.2\mu m/kPa$; the radius of its loading platen $a = 57mm$; and its shape factor $C = 4/\pi$. Substituting $G = E_u/3 \approx 6.67MPa$ and $\mu = 0.5$ into the equation for $\Delta\sigma_{rr}/\sigma_{rr}$ (see p569) gives $\epsilon = 4.8\%$. Encouragingly, this estimate of ϵ is close to the minimum error for both clays over the stress range 25-125kPa. If a more realistic value of G was used in the calculation, then good agreement could be obtained between the results of the laboratory tests and the theoretical cell action.

The laboratory tests at the TRRL demonstrate that cell action effects can be estimated to a reasonable degree of accuracy using simple linear-elastic calculations, provided the soil's stiffness is not under-estimated. Consequently, if theoretical calculations based on over-estimates of G show that the instrument does not significantly under-register the stress, then it becomes unnecessary to measure the cell action effects in time-consuming laboratory tests.

A5.3 PILE-MOUNTED PIEZOMETERS

A5.3.1 Introduction

This section examines various designs of pore pressure probe that have been mounted on displacement piles installed in clay. The design requirements for these instruments are quite demanding. During pile installation the piezometer should be extremely fast acting, and capable of surviving the effects of cavitation (especially when installed in strongly dilating soils). This requires low system compliance and good saturation procedures.

Technical details about the various pore pressure cells are summarized in Table A5.2, and the probes' response times are calculated in Section A5.4.

A5.3.2 Reese and Seed (1955)

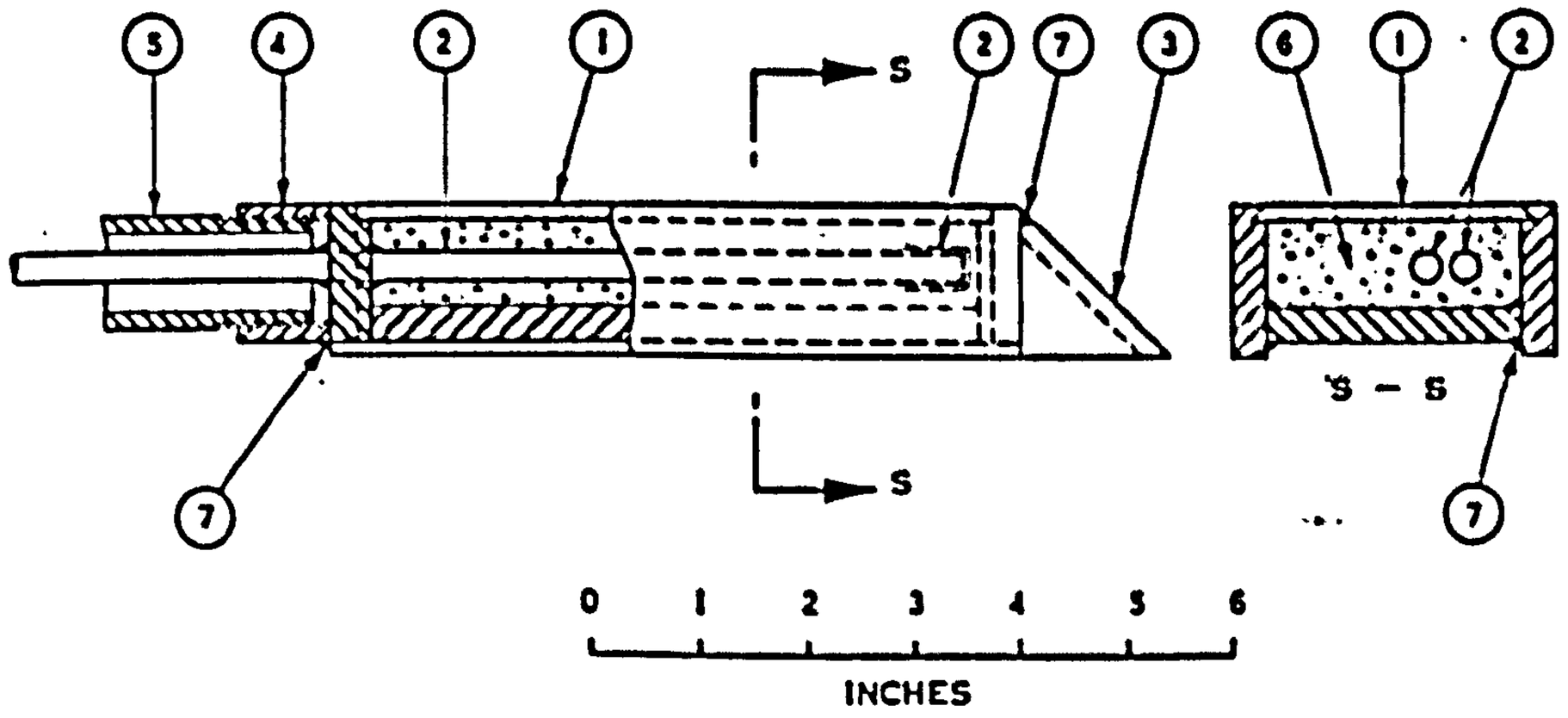
Figure A5.1 (see page 555) shows one of the pore pressure cells employed by Reese and Seed[32] in their instrumented pile test near the San Francisco Bay Bridge.

The transducer's strain-gauged diaphragm was extremely compliant, giving the cell a theoretical response time (t_{95}) of about 5¼ hours, according to Hvorslev's formula - see Section A5.4 for details. This assumes that the soil's permeability is 10^{-10}m/s (which is fairly typical for a clay).

The pore pressure vs time curves presented by Reese and Seed for gauges W-2, W-3, and W-5 show a maximum reading more than 3h after the end of pile installation. Gauge W-1 was the only one to give a fast response. This suggests that the pore pressures acting on the pile were underestimated by the PP cells during installation.

A5.3.3 Hanna (1967)

Hanna[33] describes the design of a pile piezometer which was welded to the outside of two H-section piles. The piles were installed in a firm to stiff, silty clay at Lambton, Ontario; and in a firm, sandy silty clay



1 1/8 INCH DOVETAILED POROUS BRONZE MEMBRANE
2 1/4 INCH I.D. STAINLESS STEEL TUBE WITH END COVERED BY 200 MESH SCREEN
3 3 INCH CHANNEL SECTION PROTECTION TOE
4 3/4 INCH PIPE COUPLING
5 3/4 INCH PIPE
6 MEDIUM SAND
7 WELD

Figure A5.17 Hanna's pile piezometer

at Pickering, also in Ontario. The piezometer is shown in Figure A5.17. Hanna made no attempt to measure the pore pressures during pile installation, and Table A5.2 suggests why. The instrument's response time, even when fully saturated, would be more than 1½h in a low permeability clay (k = 10^{-10}m/s). However, in the sandy-silty clay (permeability[34] between 10^{-6} and 10^{-7}m/s) the response time was probably of the order of one to ten seconds (according to Hvorslev' formula).

A5.3.4 Kenney (1967)

The piezometer used by Kenney[35] is identical to the earth pressure cell shown in Figure A5.2, save for the addition of a porous bronze filter to the front face of the diaphragm. Its technical details are given in Section A5.4.

A5.3.5 Laboratory tests at Cambridge University (1981-83)

Steenfelt et al.[36] and Francescon[37] employed Druck PDCR 81 semi-conductor transducers for their laboratory tests on model piles installed in kaolin. These are extremely stiff devices (compliance ≈ 10^{-8}mm^3/kPa) which also have a very small internal volume (including filter ≈ 21mm^3): together these characteristics give the transducers an extremely rapid response time in low permeability clays.

A5.3.6 O'Neill et al. (1982)

Although they give no details about their PP cells, O'Neill et al.[38] do comment on their attempts to measure the pore pressures next to large-scale instrumented piles installed in the heavily overconsolidated Beaumont clay:

> "During driving, saturation was lost on the piezometers at the surface of the piles. Re-saturation and stabilization of those piezometers was not reached until one to four days after installation so the pore pressures that existed immediately after driving at the pile-soil interfaces were not known."

The value of this information is its warning about the potential problems in measuring pore water pressures in clays that dilate on shearing. Unless the PP cell is able to recover quickly from the effects of cavitation, then very little useful information is obtained.

A5.3.7 The Oxford University IMP (1987)

The Oxford University In-Situ Model Pile[39] (IMP) incorporates two types of PP cell: a Druck PDCR 81 semi-conductor transducer, behind an epoxy/sand filter; and the strain-gauged diaphragm device shown in Figure A5.18. Technical details for the latter cell are given in Table A5.2.

This strain-gauged diaphragm device has a fairly fast response time in low permeability clays (t_{95} ≈ 20s, if c_h = 50m^2/year), provided it's filter and the cavity in front of the diaphragm are thoroughly de-

aerated. In the presence of even a single air bubble of radius 0.17mm (equivalent to 0.01% air in the system), t_{95} increases to about eight minutes (see Table A5.2).

Coop performed tests with the Oxford IMP in two heavily overconsolidated clays: the Gault at Madingley and the London clay at Canons Park. In both deposits, the PP cells located behind the pile tip quite often recorded smooth, almost featureless profiles of pore pressure against depth. Although the transducers were carefully de-aerated in the laboratory, cavitation of the fluid in the piezometers may have occurred during pile installation. Several of Coop's traces registered <u>negative</u> pore pressure (i.e. pressures below atmospheric) during jacking.

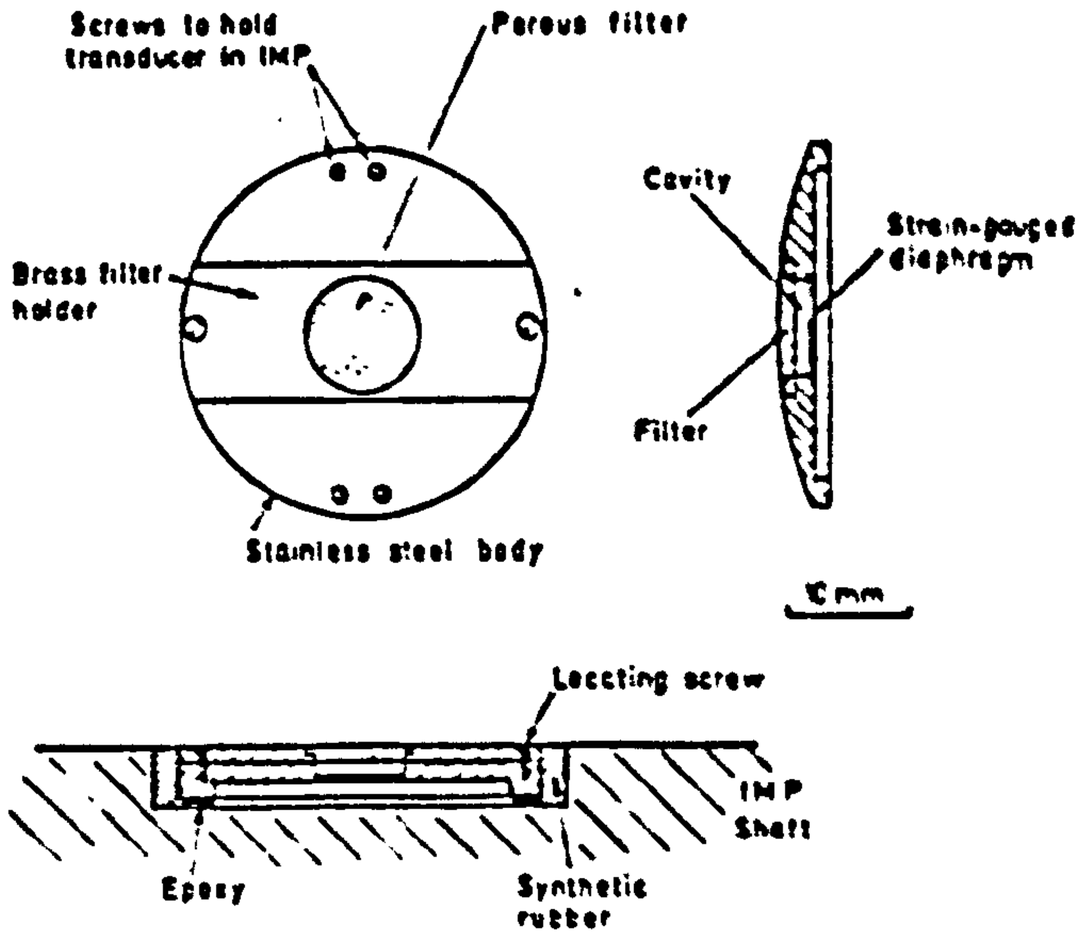


Figure A5.18 Strain-gauged diaphragm pore pressure cell mounted on the Oxford University model pile

Throughout the equalization period, several probes were sluggish in their response, sometimes failing to record a maximum pore pressure until 2½h after the end of installation. Although Coop's pore pressure vs time curves may be in error because of the transducers' inability to survive cavitation, it is feasible that the traces record the actual response of the soil.

The problems noted above for tests in heavily overconsolidated clays were not manifest in Coop's other tests: in a soft silty clay at Huntspill, and in a soft, very silty clay (silt?) at Great Yarmouth. In both of these deposits mainly <u>positive</u> pore pressures were recorded during pile installation, and the pressures reached maximum values about 3¼ minutes into the equalization period. Hence the problems that occurred at Madingley and at Canons Park appear to be linked to the <u>cavitation</u> of

the fluid in the piezometer system caused by the dilation of the clay during pile installation.

These results illustrate the immense difficulties that exist in making reliable measurements of pore pressures next to piles, particularly in heavily overconsolidated clays.

A5.3.8 NGI's instrumented piles (1989)

The pore pressure sensors on the Norwegian Geotechnical Institute's A- and C- piles[40] are given on Figure A5.13 (see p567), and those on their B- piles on Figure A5.19. The sensors on the latter are similar to the pore pressure cell designed by Φien (see Section A5.1.3).

All of these instruments are vibrating wire devices. No other technical details about the probes are available at present.

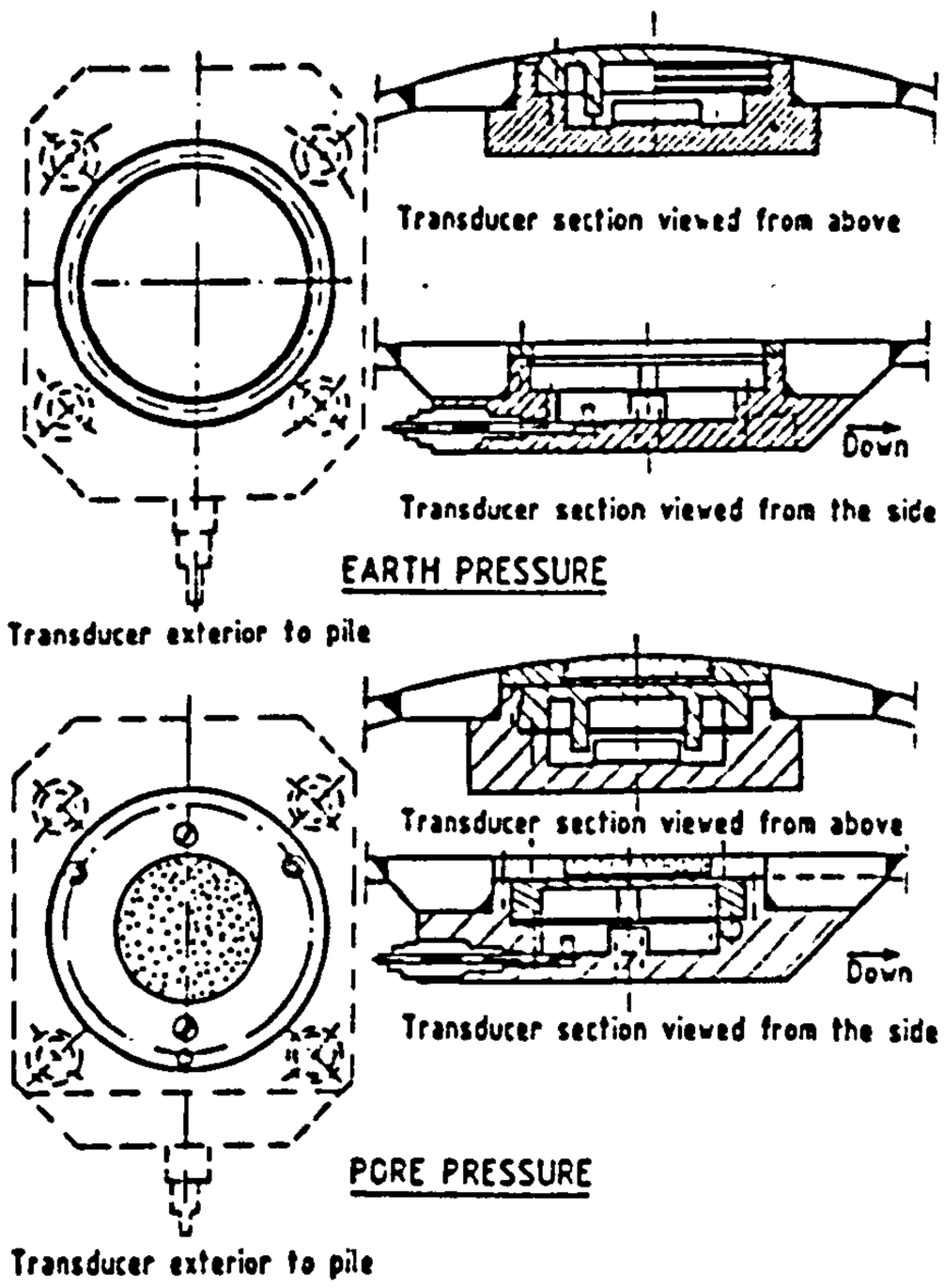


Figure A5.19 Instrument units for the NGI's B- piles

A5.4 RESPONSE TIMES OF PILE-MOUNTED PIEZOMETERS

A5.4.1 Sources of error in pore pressure measurement

Hvorslev[41] described ten sources of error in pore pressure measurements in soils, including:

- Hydrostatic time lag (1)
- Stress adjustment time lag (2)
- General instrument error (3)
- Gas bubbles in open or closed piezometer system (6 and 7)
- Gas bubbles in soil (8)
- Sedimentation and clogging (9)

Two of these cases (1 and 2) are illustrated in Figure A5.20.

Case number 1 assumes that the presence of the piezometer does not alter the pore pressure in the soil, and so the time taken to record the true pressure depends chiefly on the volume compressibility of the piezometer system (C_{ps}) and the soil's permeability (k). This delay is commonly expressed in terms of the time required to register 95% of the change in pressure, and is given by:

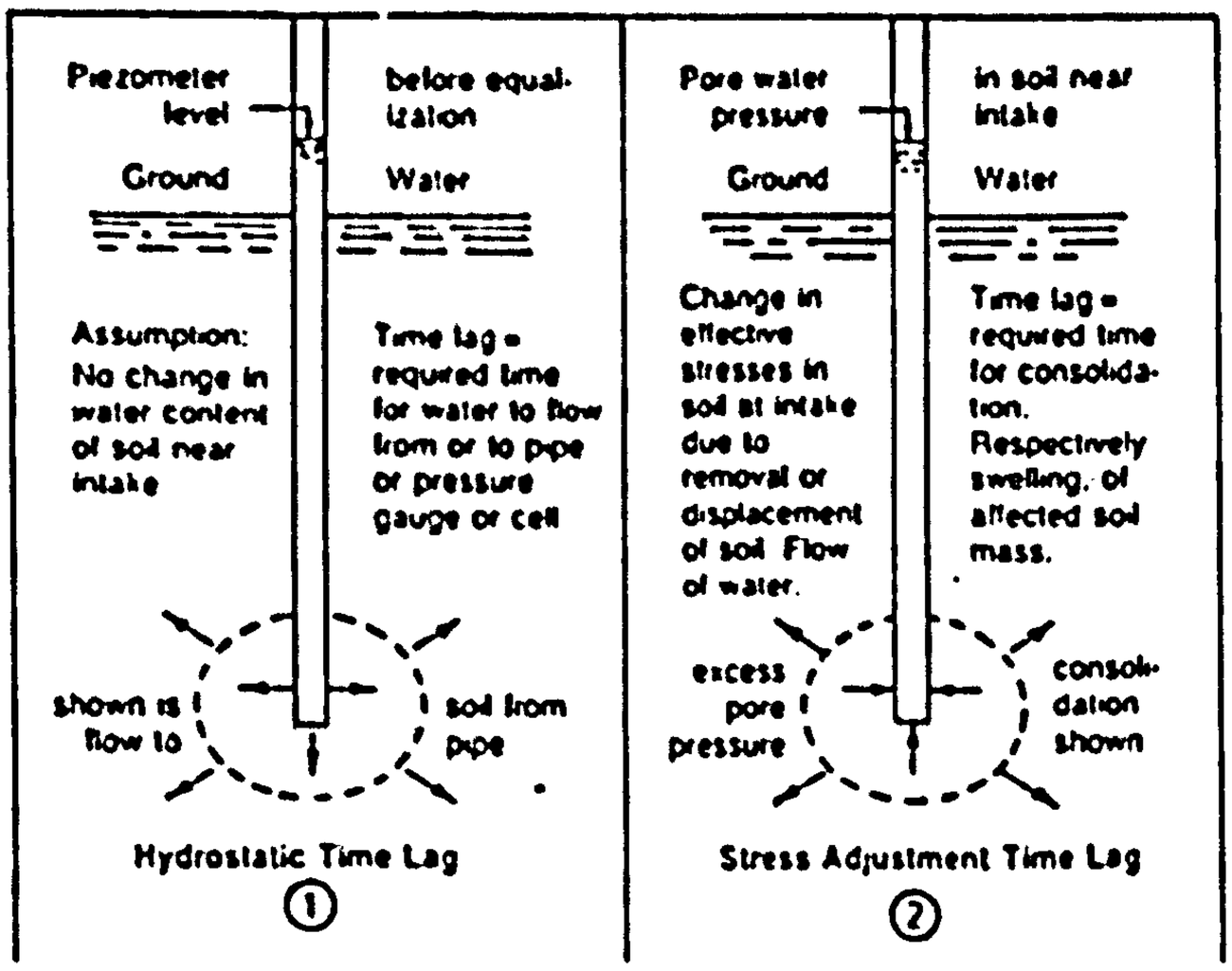


Figure A5.20 Problems associated with measuring pore pressures in soil

$$t_{95} = -\mathrm{Ln}(0.05)C_{ps}\gamma_w/Fk \approx 3C_{ps}\gamma_w/Fk$$

where γ_w is the unit weight of water (9.81kN/m^3), and F is a (non-dimensional) "shape factor",[42] which depends on the geometry of the piezometer intake.

The equation given above is the well-known "Hvorslev formula", implicit in which is the assumption that the soil is incompressible. However, real soils are compressible, and consequently there is a "stress adjustment time lag", as shown in Figure A5.20 (case 2). Gibson[43] has analyzed this situation and has shown that the piezometer's response time depends not only on C_{ps}, k, and F, but also on the soil's compressibility m_v: Values of t_{95} are given in Figure 4 of Gibson's paper and are a function of the parameter μ, defined as:

$$\mu = F^3 m_v / 16\pi^2 C_{ps} = F^3 k / 16\pi^2 C_{ps} \gamma_w c$$

where c is the coefficient of consolidation of the soil ($c = k/m_v\gamma_w$). The parameter μ reflects the relative compressibility of the soil to that of the piezometer ($\mu \propto m_v/C_{ps}$): for an incompressible soil, or an extremely compliant piezometer, $\mu \to 0$; whereas for a very soft soil, or an extremely stiff piezometer system, $\mu \to \infty$. (As $\mu \to 0$ so Gibson's formula becomes equivalent to Hvorslev's.)

In assessing the performance of pile-mounted pore pressure cells, it is necessary to know their volume compressibility and shape factor, and the consolidation coefficient of the soil in which they are to be installed.

The compressibility of the piezometer system (C_{ps}) comprises two separate components: that of the transducer (C_{tr}) and that of the saturating fluid between the transducer and the soil (C_{fl}). The latter is equal to the volume of fluid (V_{fl}) divided by its bulk modulus (K_{fl}). Values of K_{fl} are strongly dependent on the amount of air in the fluid. For pure water, K_{fl} = 2GPa, whereas with 0.01% air in it K_{fl} = 0.0048GPa.[44]

A5.4.2 Comparing pile-mounted piezometers

Table A5.2 compiles detailed technical information for a wide range of piezometer systems, as employed on open- and closed-ended piles, and on

various forms of cone penetrometer. The design details of many of these instruments are discussed in Section 5.3.

Included in the Table are values of the shape factor (F) and the compressibility (C_{ps}) of each piezometer system. From this information, I have calculated the response times (t_{95}) of the piezometers by assuming the soil's permeability is 10^{-10}m/s, and its coefficient of horizontal consolidation, c_h, is 50m^2/yr (1.59mm^2/s). These are typical values for the London clay at Canons Park.

Two separate calculations of t_{95} are included in Table A5.2: that for a fully saturated piezometer and that for a piezometer which has 0.01% air in the system. The purpose of this second calculation is to demonstrate the potentially serious effects of incomplete saturation of the piezometer fluid. For some instruments (e.g. Hanna's and Kenney's), the response time increases enormously if there is even a small amount of air in the piezometer system.

Inspection of Table A5.2 also reveals the following:

- The internal cavity in many piezometers is quite large, and quite often the majority of this volume is contained within the porous filter
- The compliance of the fluid (C_{fl}) typically accounts for 50-100% of the total compliance of the system (C_{ps})
- Most of the modern instruments (post 1975) give response times in clay of ≈1 second when fully de-aerated
- During penetration through dilating soils, however, these systems are likely to become de-saturated and their compliance to increase - in which case the response times may well be much greater than 1 second
- The response time is critically sensitive to the quantity of free air trapped inside the piezometer; hence good saturating procedures, and the avoidance of 'bubble traps' in the design of pore pressure cells, therefore of paramount importance

Table A5.2(a) Response times of various piezometer systems, as used on piles and piezocones

1	Authors	Reese & Seed (1955)	Hanna (1967)	Kenney (1967)	Piegnaud (1979)	Battaglio et al. (1981)	Tumay et al. (1981)	Zuidberg et al.
2	Organization	Univ. of California	Hydro-Electric, Ontario	NGI	LRPC d'Angers	TUT	LSU	Fugro
3	Instrument	Pile	Pile	Pile	Piezo probe	Piezo probe*	Piezocone	Piezocone
	Filter							
4	Type	Porous bronze	Porous bronze	Porous bronze	Ceramic	Sintered stainless steel	Not given	Aerolith ceramic
5	Shape	Circle	Rectangular	Circle	Cylinder	Cylinder	Tapered cylndr	Tapered cylndr
6	Size (mm)	(ϕ15?)	≈146 x ≈57	(ϕ115)	ϕ44 x 50	ϕ15 x 5	ϕ22 x 3.5?	ϕ28 x 6.5
7	Intake (mm^2)	(177)	8387	(10390)	6911	236	≈240	567
8	Shape fctr (mm)	(39)	270	(151)	338	96.7	≈140	177
9	Location	B	B	B	S	S	F	F
10	Fluid used	Water	Water	Water	Water	Water & silicone fluid	Water	Water
	Transducer							
11	Type	Strain gauged diaphragm	Bourdon gauge	Vibrating wire diaphragm ϕ75	Bell & Howell	Statham	Not given	Not given
	Piezo volume							
12	Ex filter (mm^3)	-	(49 800)	-	?	(v small)	(≈1000)	180
13	+ filter (mm^3)	(>3200)	(58 100)*	(≈40 000)	(≈10^4)	(<265[e])	(≈1260)	1600
	Compliance (mm^3/MPa)							
14	Fluid C_{fl}	(1.6)	(29)	(20)	≈5	<0.13	≈0.6	0.8
15	Transducer[f] C_{tr}	2506	7130[g]	(≈150)	?	≈1	1	0.02-0.5
16	Total C_{ps}	2508	≈7160	(170)	≈5	≈1.1	1.5-2.6	≈0.8
	Response time							
17	Gibson's μ	≈10^{-3}	0.11	0.82	157	33.5	55.9	280
18	t_{95}	5½h	1.9h	6.2min	1.8s	2.1s	1.9s	0.2s
	With 0.01% air							
19	C_{fl} (mm^3/MPa)	(>667)	(12104)	(≈8 333)	≈2080	<55	≈263	333
20	Gibson's μ	≈7.5×10^{-4}	0.042	0.017	0.76	0.67	0.43	0.68
21	t_{95}	>6½h	5.8h	4.6h	31min	≈3min	≈9½min	≈9½min

*Assuming porosity of "medium sand" = 30%; and porosity of filter = 30%

[f]Silver (1979) recommends that a transducer's compliance should not exceed 2.5mm^3/MPa

[g]Including 22.9m of nylon tubing i.d. 1.59mm

*The instrument due to Torstensson (1975)

[e]Assuming a filter porosity of 30%

Table A5.2(b) Response times of various piezometer systems, as used on piles and piezocones

	Francescon (1983)	Fahey & Foley (1987)		Coop (1987)
2	Cambridge University	Univ. of W. Australia		Oxford University
3	Model pile	Probe 1*	Probe 2	Model pile
	Filter			
4	Porous ceramic	Sintered stainless steel	Sintered stainless steel	Plastic/sintered bronze
5	Circle	Cylinder	Circle	Circle
6	ϕ6.4	ϕ44 x 40	ϕ8	ϕ10
7	32.2	5027	50.3	78.5
8	16.8	297	21.0	26.3
9	B	B	B	B
10	(Water)	Water	Water	Glycerine/ H_2O mixture
	Transducer			
11	(Druck PDCR 81)	Not given	Druck PDCR 81	Strain-gauged diaphragm
	Piezo volume			
12	(≈1)	≈4600	(32)	(83)
13	(≈21)	≈8900	(62)	(201)
	Compliance			
14	(≈0.01)	≈4.5	0.03	0.1
15	(≈10^{-6})	?	(10^{-6})	(1.2^{ϕ})
16	(≈0.01)	≈4.5	0.03	1.3
	Response time			
17	19.3	237	12.6	0.57
18	0.15s	0.70s	0.37s	16.6s
	With 0.01% air			
19	(≈4.4)	≈1855	12.9	41.9
20	0.044	≈0.58	≈0.029	≈0.018
21	1.3min	≈31½min	≈3min	≈8min

*Fahey & Foley report that this version of their probe gave an unsatisfactory response.

ϕCompliance of diaphragm = $\pi(1-\mu^2)d^6/1024Et^3$, where d = 13mm, t = 0.0375 ±0.025mm, E = 210GPa, and μ = 0.3. Dimensions provided by Freeman (1988, priv. comm.).

	Borg Hansen et al. (1989)	This Thesis		
2	NGI	Imperial College		
3	Pile	Fast probe	Flushable probe	
4	Epoxy	Sintered stainless steel	Sintered stainless steel	
5	Circle	Circle	Circle	
6		ϕ12.7	ϕ12.7	
7		127	127	
8		33.4	33.4	
9	B	B	B	
10	Water	Silicone fluid	Water	
11	Vibrating wire diaphragm	Druck PDCR 81	Druck PDCR 200	
12		182	≈25 000	
13		291	≈25 000	
14		0.29	≈12.5	
15		10^{-6}	10^{-6}	
16		0.29	≈12.5	
17		5.23	0.12	
18		2.9s	≈100s	
19		60.6	≈5200*	
20		0.025	≈3 x 10^{-6}	
21		≈9min	≈13h	

*Measured compliance = 1000mm³/MPa, which implies t_{95} = 2½h

Notes to accompany Table A5.2

LRPC = Laboratoire Régional des Ponts et Chaussées, France; TUT = Technical University of Turin, Italy; LSU = Louisiana State University, USA; NGI = Norwegian Geotechnical Institute.

Shape factors calculated according to the formulae given by Brand & Premchitt (1980a and 1980b): for cylinders, $F = 2.4\pi L/Ln(1.2L/d+\sqrt{(1+[1.2L/d]^2)})$, where d = average diameter and L = length; and for circles, $F = 2.63d$.

Location of filter: T = at tip of cone; F = on face; S = on shoulder; B = behind (i.e. along the shaft).

C_{ps} = compliance of the piezometer system, otherwise known as the "volume factor", V. Compliance of fluid alone = volume of internal cavity + bulk modulus of the fluid. For fully saturated water, K = 2GPa; with 0.01% air dissolved in it, K ≈ 0.0048GPa (Fredlund, 1976).

$\mu = F^3k/16\pi^2C_{ps}\psi_w c$, where $k = 10^{-10}$m/s and $c = 50m^2/yr$ (typical values for the London clay at Canons Park), and $\psi_w = 9.81kN/m^3$. $\mu = 0$ implies an incompressible soil (or an extremely compliant transducer); $\mu = \infty$ implies an infinitely stiff transducer.

For $\mu \geq 0.1$, $t_{95} = (F^2/16\pi^2)(T_{95}/c)$, where T_{95} is obtained from Figure 4 of Gibson's paper; for $\mu < 0.1$, $t_{95} \approx 3C_{ps}\gamma_w/Fk$, which is Hvorslev's formula.

A5.5 NOTES AND REFERENCES

[1]Reese L.C. and Seed H.B. (1955). Pressure distribution along friction piles. Proc. Am. Soc. for Testing Materials, 55, pp1156-1182. See Figure 7, pp1163-1166, and pp1172.

[2]Kenney T.C. (1967). Field measurements of in situ stresses in quick clays. Proc. Geotech. Conf. on Shear Strength Properties of Natural Soils and Rocks, Oslo, 1, pp45-55.

[3]Φien K. (1962). Vibrating-wire measuring devices used at strutted excavations. Norwegian Geotechnical Institute, Technical Report No 9, Oslo, 151pp.

[4]The components shown on Figure A5.2 are as follows: 1) steel wire; 2) diaphragm; 3) clamping pin; 4) arm; 5) steel ball; 6) & 7) O-ring; 8) sheet pile; 9) cable; 10) copper tube; 11) fitting screw; 12) housing; 13) locking nut; 14) Unbrako Z screw; 15) insulation strip; 16) electromagnet; 17) screw; 18) hole for a guide pin.

[5]Agarwal S.L. and Venkatesan S. (1965). An instrument to measure skin friction and normal earth pressure on deep foundations. Symp. on "Instruments and apparatus for soil and rock mechanics", 68th Annual Meeting of Am. Soc. for Testing Materials, Lafayette, Indiana. ASTM Special Tech. Publ. No 392, pp152-169.

[6]Koizumi Y. and Ito K. (1967). Field tests with regard to pile driving and bearing capacity of piled foundations. Soils and Foundations, 7(3), pp30-53.

[7]Sutton V.J., Rigden W.J., James E.L., St John H.D., and Poskitt R.J. (1979). A full scale instrumented pile test in the North Sea. Proc. 11th Offshore Technology Conf., Houston, Texas, 2, pp1117-1133 (Paper OTC 3489).

[8]St John H.D. (1983). The measurement of performance of offshore piled foundations - a review. Ground Engng, 16(2), March, pp24-30.

[9]Rigden W.J., Pettit J.J., St John H.D., and Poskitt T.J. (1979). Developments in piling for offshore structures. Proc. 2nd Int. Conf. on the Behaviour of Offshore Structures (BOSS '79), Imperial College, London, pp279-296.

[10]Gallagher K.A. and St John H.D. (1980). Field scale model studies of piles as anchorages for buoyant platforms. Proc. European Offshore Petroleum Conf. and Exhibition, London, Paper EUR 135, 20pp.

[11]Johnston I.W. (1972). Electro-osmosis and porewater pressures; their effect on the stresses acting on driven piles. PhD Thesis, Southampton Univ.

[12]McAnoy R.P.L., Cashman A.C., and Purvis D. (1982). Cyclic tensile testing of a pile in glacial till. Proc. 2nd Int. Conf. on Num. Methods in Offshore Piling, Austin, Texas, pp257-291.

[13]Ponniah D.A. and McAnoy R. (1985). Pile jacking in glacial tills. Proc. Int. Conf. on Construction in Glacial Tills and Boulder Clays, Edinburgh University, pp137-146.

[14]O'Neill M.W., Hawkins R.A., and Audibert J.M.E. (1982a). Installation of pile group in overconsolidated clay. J. Geotech. Engng Div., Am. Soc. Civ. Engrs, 108(GT11), pp1369-1386.

[15]O'Neill M.W., Hawkins R.A., and Mahar L.J. (1982b). Load transfer mechanisms in piles and pile groups. J. Geotech. Engng Div., Am. Soc. Civ. Engrs, 108(GT12), pp1605-1623.

[16]See O'Neill, Hawkins, and Audibert (1982a), loc. cit., p1371; and O'Neill, Hawkins, and Mahar (1982b), loc. cit., p1621.

[17]Maddocks D.V. (1981). The development of a transducer to measure the effective soil stresses and the pore water pressure acting on the surface of a driven, steel pile. Cambridge Univ. Engng Dept Report CUED/D-SOILS/TR113; and Maddocks D.V. (1983a). A transducer to measure the radial effective soil stress and the pore water pressure acting on the surface of a driven, steel pile. Cambridge Univ. Engng Dept Report CUED/D-SOILS/TR131, 18pp+.

[18]Francescon M. (1983). Model pile tests in clay. Stresses and displacements due to installation and axial loading. PhD Thesis, Univ. of Cambridge, 110pp + figures.

[19]Baligh M.M., Martin R.T., Azzouz A.S., and Morrison M.J. (1985). The Piezo-Lateral Stress cell. Proc. 11th Int. Conf. Soil Mech. & Fdn Engng, San Francisco, 2, pp841-844.

[20]Morrison M.J. (1984). In-situ measurements on a model pile in clay. PhD Thesis, Massachusetts Institute of Technology, c687pp.

[21]Wersching S.N. (1987). The development of shaft friction and end bearing for piles in homogeneous and layered soils. PhD Thesis (CNAA), Polytechnic of Wales.

[22]Coop M.R. (1987). The axial capacity of driven piles in clay. DPhil Thesis, Univ. of Oxford.

[23]Coop (1987), loc. cit. See pp3-8.

[24]Borg Hansen S., Solheim K., and Norum P. (1989). Instrumentation of driven model test piles for determination of capacity of cyclically loaded offshore piles. Proc. Conf. on Geotech. Instrumentation in Civ. Engng Projects, Nottingham, April 1989, Paper 53 (in press).

[25]Formula given by Kallstenius T. and Bergau W. (1956). Investigations of soil pressure measuring by means of cells. Proc. Roy. Swedish Inst., Stockholm, no 12, 50pp. See p8.

[26]Poulos H.G. and Davis E.H. (1974). Elastic solutions for soil and rock mechanics. John Wiley & Sons Inc., New York, 411pp.

[27]Baligh M.M. (1984). The Simple-Pile Approach to pile installation in clays. In "Analysis and Design of Pile Foundations" (ed. J.R. Meyer). Proc. Symp. on Codes and Standards, ASCE National Conv., San Francisco, 1984, pp310-330.

[28]Maddocks (1983a), loc. cit.

[29]Argument based on energy transfer

Consider an earth pressure cell moving through a soil deposit in which σ_{rr} is constant (equals σ). For the cell to register a stress σ, it must deflect by a finite amount, and in so doing it must receive a finite amount of energy (E) from the soil. If the pile is stationary, the energy comes from a small element of soil adjacent to the cell. Consequently the stress in that element (of volume ΔV) falls by an amount $\Delta\sigma$ (from σ to $[\sigma - \Delta\sigma]$). If the pile is *moving*, then the energy E can be taken from a much larger volume of soil ($V \gg \Delta V$). Hence the energy given up by any one element of soil is $\Delta E = (\Delta V/V)E$. Since $\Delta\sigma$ is proportional to ΔE, so $\Delta\sigma \to 0$ as $V \to \infty$.

(The weakness in this argument is that it assumes that energy can only be transferred from the soil to the load cell, and not vice versa.)

Argument based on large strains during installation

Consider an element of soil which is just below the current level of the load cell. The cell registers a stress $(\sigma - \Delta\sigma)$, whilst that in the soil is σ. For the cell to register a stress $(\sigma - \Delta\sigma)$, it must already have deflected by an amount $\delta = (\sigma - \Delta\sigma)f$, where f is the cell's compliance. As the soil element comes into contact with the cell, so it expands to fill the recess in front of the instrument, and the stress in the soil drops by $\Delta\sigma$. Hence even though the loading platen does not move, the instrument still under-registers σ by an amount $\Delta\sigma$.

The value of $\Delta\sigma$ depends on the soil's stiffness. Since the soil is unloading, when the pile is *stationary* this stiffness could be quite large. However, it seems reasonable to assume that, while the pile is *moving* (i.e. during pile installation), the disturbance is great enough for the soil's stiffness to be small.

[30]Carder D.R. and Krawczyk J.V. (1975). Performance of cells designed to measure soil pressure on earth retaining structures. TRRL Lab. Report 689, Dept of Environment, TRRL, Crowthorne, England, 7pp+.

[31]Carder and Krawczyk (1975), loc. cit., p2.

[32]Reese and Seed (1955), loc. cit.

[33]Hanna T.H. (1967). The measurement of pore water pressures adjacent to a driven pile. Can. Geotech. J., 4(3), pp313-325.

[34]As reported by: Ismael N.F. and Klym T.W. (1979). Pore-water pressures induced by pile driving. J. Geotech. Engng Div., Am. Soc. Civ. Engrs, 105(GT11), pp1349-1354. Ismael and Klym also used Hanna's pile piezometer.

[35]Kenney (1967), loc. cit.

[36]Steenfelt J.S., Randolph M.F., and Wroth C.P. (1981). Instrumented model piles jacked into clay. Proc. 10th Int. Conf. Soil Mech. & Fdn Engng, Stockholm, 2, pp857-864.

[37]Francescon (1983), loc. cit.

[38]O'Neill et al. (1982a, b), loc. cit.

[39]Coop (1987), loc. cit., pp3-16 and 3-17, plus Figure 3.10. Additional technical information provided by the instrumented pile's designer, Mr Tim Freeman (personal communication, 1988).

[40]Borg Hansen et al. (1989), loc. cit.

[41]Hvorslev M.J. (1951). Time lag and soil permeability in ground-water observations. Bulletin No 36, Waterways Experimental Station, Corps of Engineers, Vicksburg, Mississippi, 50pp.

[42]Values of F for various piezometer shapes have been given by: Brand E.W. and Premchitt J. (1980a). Shape factors of cylindrical piezometers. Géotechnique, 30(4), pp369-384; and Brand E.W. and Premchitt J. (1980b). Shape factors of some non-cylindrical piezometers. Géotechnique, 30(4), pp536-537.

[43]Gibson R.E. (1963). An analysis of system flexibility and its effect on time-lag in pore-water pressure measurements. Géotechnique, 13(1), pp1-11.

[44]Fredlund D.G. (1976). Density and compressibility characteristics of air-water mixtures. Can. Geotech. J., 13(4), pp386-396.

Appendix 6

Details of instrument design: axial load cells

CONTENTS OF APPENDIX 6

A6.1 AXIAL LOAD CELLS MKS I-III 596

A6.2 TECHNICAL DATA: AXIAL LOAD CELLS 597

A6.2.1 General information 597

A6.2.2 Basic properties 597

A6.2.3 Calibration coefficients 598

A6.2.4 Other properties 598

A6.3 DESIGN DRAWING 599

A6.4 NOTES AND REFERENCES 600

A6.1 AXIAL LOAD CELLS MKS I-III

Three designs of axial load cell (ALC) have been used in the instrumented pile tests at Canons Park. The original (Mk I) load cell was designed by Johnston[a] at Southampton University (see Appendix 5 for details of his design), and was employed in the Pilot experiment (CP0) by Jardine.[b] A higher capacity version of this cell (Mk II) was manufactured at Imperial College prior to Test Series CP1, and replaced the two ALCs that had been buckled during installation of CP0 (see Appendix 9).

A completely new axial load cell was designed for the Imperial College Instrumented Pile, and this device (the Mk III ALC) was used throughout experiments CP2-5.

A6.2 TECHNICAL DATA: AXIAL LOAD CELLS

A6.2.1 General information

Load cell	Mk I	Mk II	Mk III
Design type	Unsleeved	Unsleeved	Sleeved
Capacity[c]	Low	High	Highest
Designed by...	Johnston[d]	Johnston	Bond
Manufactured by...	Southampton University	Imperial College	Imperial College
Date	Early 1970s	c.1984	1986

A6.2.2 Basic properties

Material used	1½% manganese molybdenum steel[e]	As for Mk I	As for Mk I
Wheatstone bridge	Poisson[f]	Poisson	Poisson
Gauges	120Ω	120Ω	120Ω
Strain gauges fixed to...	External wall	External wall	Internal wall
Sensitive to σ_{rr}?	Yes	Yes	No
Wall thickness	0.89mm	1.27mm	2.25mm
X-sectional area of wall	281.3mm^2	400.3mm^2	496.6mm^2
Wall length L	≈20mm	≈20mm	≈7mm
'Shell' length[g]	Moderately long	Moderately long	Short
Load at 0.2% strain[h] Q_{max}	118kN	168kN	209kN
Buckling load[i] Q_f	128kN	194kN	Yields first

A6.2.3 Calibration coefficients[j]

a) Direct sensitivity a_1 (MN)

Theoretical[k]	43.7 ±3.1	62.4 ±4.5	78.8 ±5.6
Measured	41.5-44.4	61.8-63.8	93.2-108.9

b) Cross-sensitivity a_2 (cm^2)

Theoretical[l]	162	162	0
Measured	188-234	133-149	c.0.1

A6.2.4 Other properties

2nd moment of area of wall	$36cm^4$	$50cm^4$	$31cm^4$
Cell's axial compliance[m]	0.44μm/kN	0.33μm/kN	0.37μm/kN
Load lost through seal[n]	Not applicable	Not applicable	0.6%

A6.3 DESIGN DRAWING

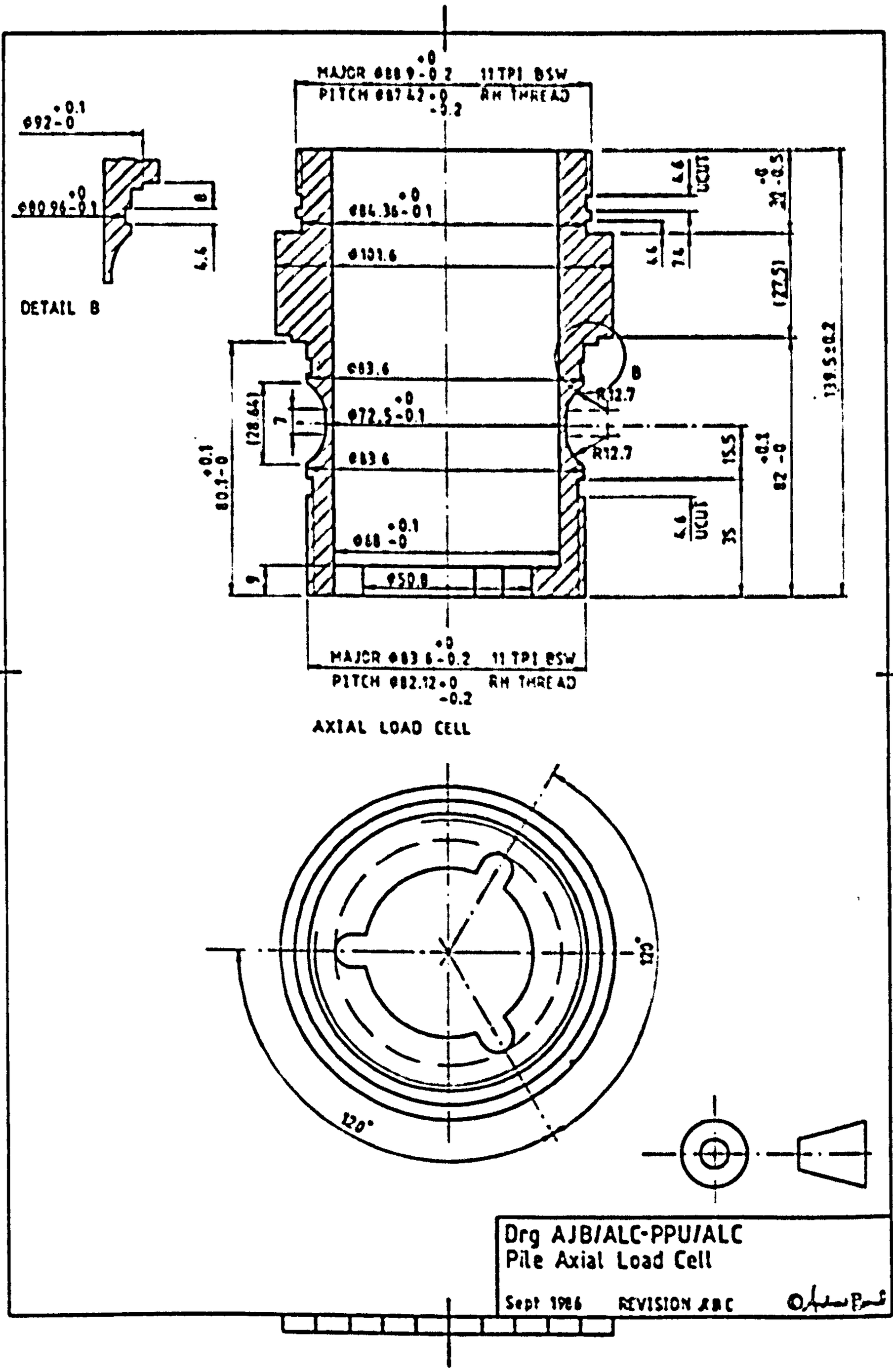


Figure A6.1 Design drawing for Mk III axial load cell

A6.4 NOTES AND REFERENCES

[a]Johnston I.W. (1972). Electro-osmosis and porewater pressures; their effect on the stresses acting on driven piles. PhD Thesis, Southampton Univ.

[b]Jardine R.J. (1985). Investigations of pile-soil behaviour, with special reference to the foundations of offshore structures. PhD Thesis, Univ. of London (Imperial College), 2 vol., 789pp.

[c]Low ≈118kN; high ≈168kN; highest ≈209kN.

[d]See Chapter 5 of: Johnston I.W. (1972). Electro-osmosis and porewater pressures; their effect on the stresses acting on driven piles. PhD Thesis, Southampton Univ.

[e]605M36 condition S. See British Standards Institution (1970). British Standard Specification for Wrought steels for mechanical and allied engineering purposes. BS970: Part 2: 1970. (This steel was formerly known as En16S, according to BS970: 1955.) Yield strength R_o = 585MPa (min.); Young's Modulus E assumed to be 210 ±10GPa.

[f]Poisson bridge: four gauges aligned axially to sense the axial strain; four gauges aligned circumferentially to sense the hoop strain.

[g]See Chajes A. (1985). Stability and collapse analysis of axially compressed cylindrical shells. Chapter 1 (pp1-17) of "Shell Structures. Stability and Strength", ed. R. Narayanan. Elsevier Applied Science Publishers, London, 345pp. Moderately long shells fail at loads well below those given by linear theory (which applies to short shells). A cylindrical shell is 'short' if $Z = (L/R)^2(R/h)\sqrt{(1-\mu)} < 2.85$, where h is the thickness of the thinned wall, and L its length. For the unsleeved cells R = 50.8mm; for the sleeved cell R = 36.25mm. (Poisson's ratio μ assumed to be 0.3.)

[h]$Q_{max} = AE\epsilon_{0.2} = 0.002AE$.

[i]Calculated according to the AISI design criterion (see Chajes, 1985, loc. cit.).

[j]Coefficients for use in the formula:

$$Q = a_o + a_1(V_o/V_i) + a_2\sigma_{rr}$$

where Q = axial load; V_o, V_i = output, input bridge voltages; and σ_{rr} = total radial stress.

[k]$a_1 = (2\pi RhE/(1+\mu))(2/k)$, where k = strain gauge factor (taken as 2.1 ±0.05). The error band quoted in the table accounts only for the uncertainty in the values of E (±10GPa) and k - not for the uncertainty in the values of R, h, and μ.

[l]$a_2 = 2\pi R^2$.

[a]Axial compliance calculated from the formula $\delta/Q = (1/E)\Sigma(\delta l/A)$.

[b]The soil seal used with the sleeved axial load cell carries some of the axial load passing through the cell. The seal used is a Pioneer Nu-Lip Ring (ref. no. 4-045), whose stiffness is about 3kN/mm. To shorten the thinned wall by 1μm (δ) requires a load $Q = AE\delta/L$ of about 15kN; a further 0.003kN would be required to compress the rubber seal by 1μm. Therefore the loss of load through the rubber should be ≈0.02% of Q. During calibration this value was found to be around 0.6% (i.e. the seal's stiffness is greater than estimated).

Appendix 7

Details of instrument design: surface stress transducers

CONTENTS OF APPENDIX 7

A7.1 SURFACE STRESS TRANSDUCERS MKS I-IV 606
A7.1.1 Background 606
A7.1.2 Circuit diagram 607
A7.2 TECHNICAL DATA: SURFACE STRESS TRANSDUCERS 608
A7.2.1 General Information 608
A7.2.2 Details of the main housing 608
A7.2.3 Basic features of the load cells 608
A7.2.4 Radial total stress circuits 609
A7.2.5 Shear stress circuits 609
A7.2.6 Calibration coefficients 610
A7.2.7 Load cell compliance 610
A7.3 DESIGN DRAWINGS 611
A7.4 NOTES AND REFERENCES 617

A7.1 SURFACE STRESS TRANSDUCERS MKS I-IV

A7.1.1 Background

The surface stress transducers used in the Pilot experiment were designed by Johnston[a] at Southampton University in the early 1970s (see Appendix 5 for details). Johnston's design suffered from two major weaknesses: the lack of an adequate water-proofing system; and the load cells' complicated method of assembly. For Test Series CP1 the original Cambridge load cells were replaced by new instruments manufactured at Imperial College. These devices (the "Horseshoe" and "Oval" load cells) were designed with the assistance of Dr R Bassett of King's College, London. Figure A7.1 shows the "Oval" load cell in cut-away view.

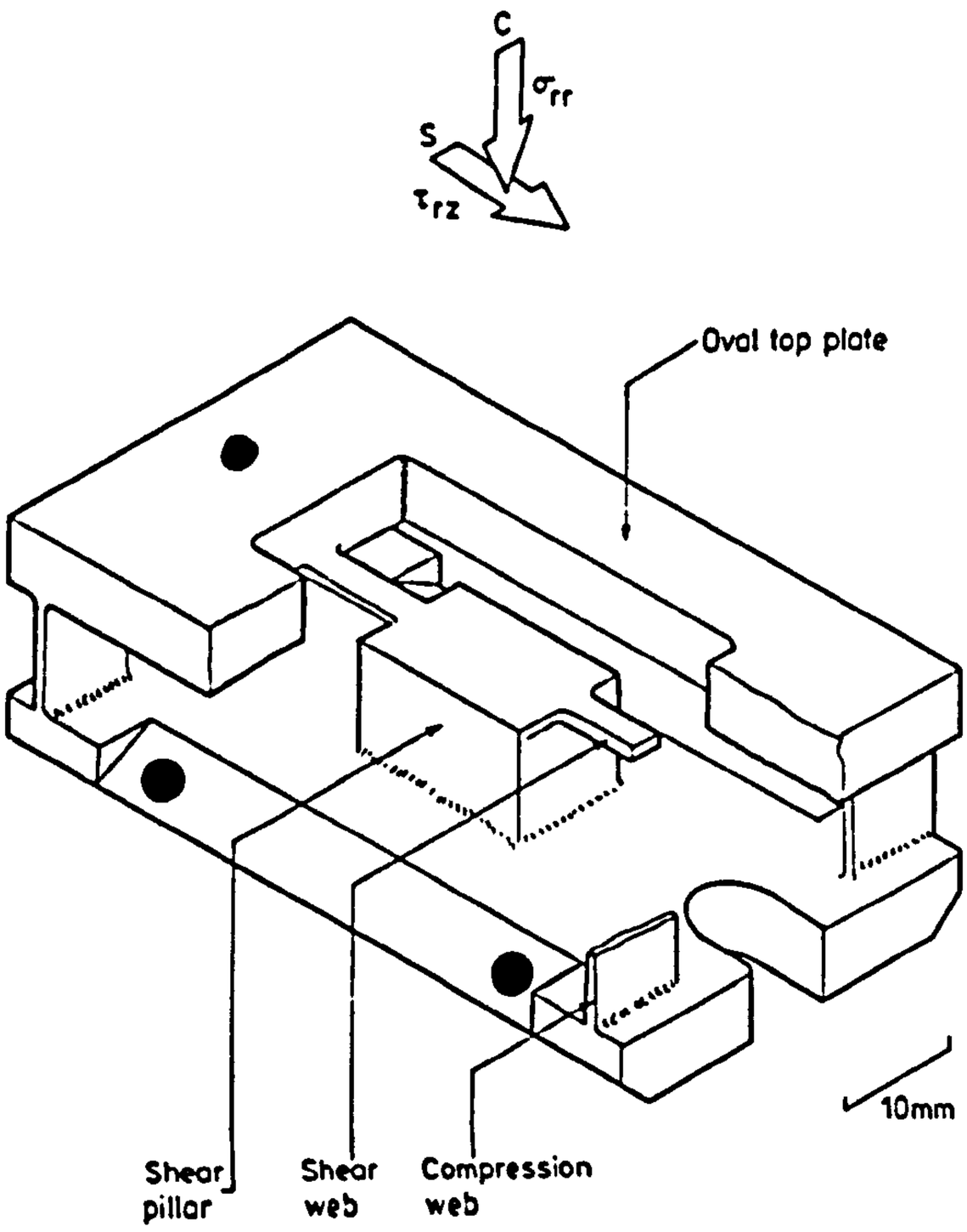


Figure A7.1 The "Oval" Cambridge earth pressure cell

These improvements to Johnston's original instruments did not overcome the waterproofing problem, and so a completely new device, the "surface stress transducer", was designed with the help of Mr Clive Dalton of Cambridge Insitu Ltd. This instrument is described at length in Chapter 6.

A7.1.2 Circuit diagram

Figure A7.2 shows the circuit diagram for the surface stress transducers (and all the instruments mounted on the pile).

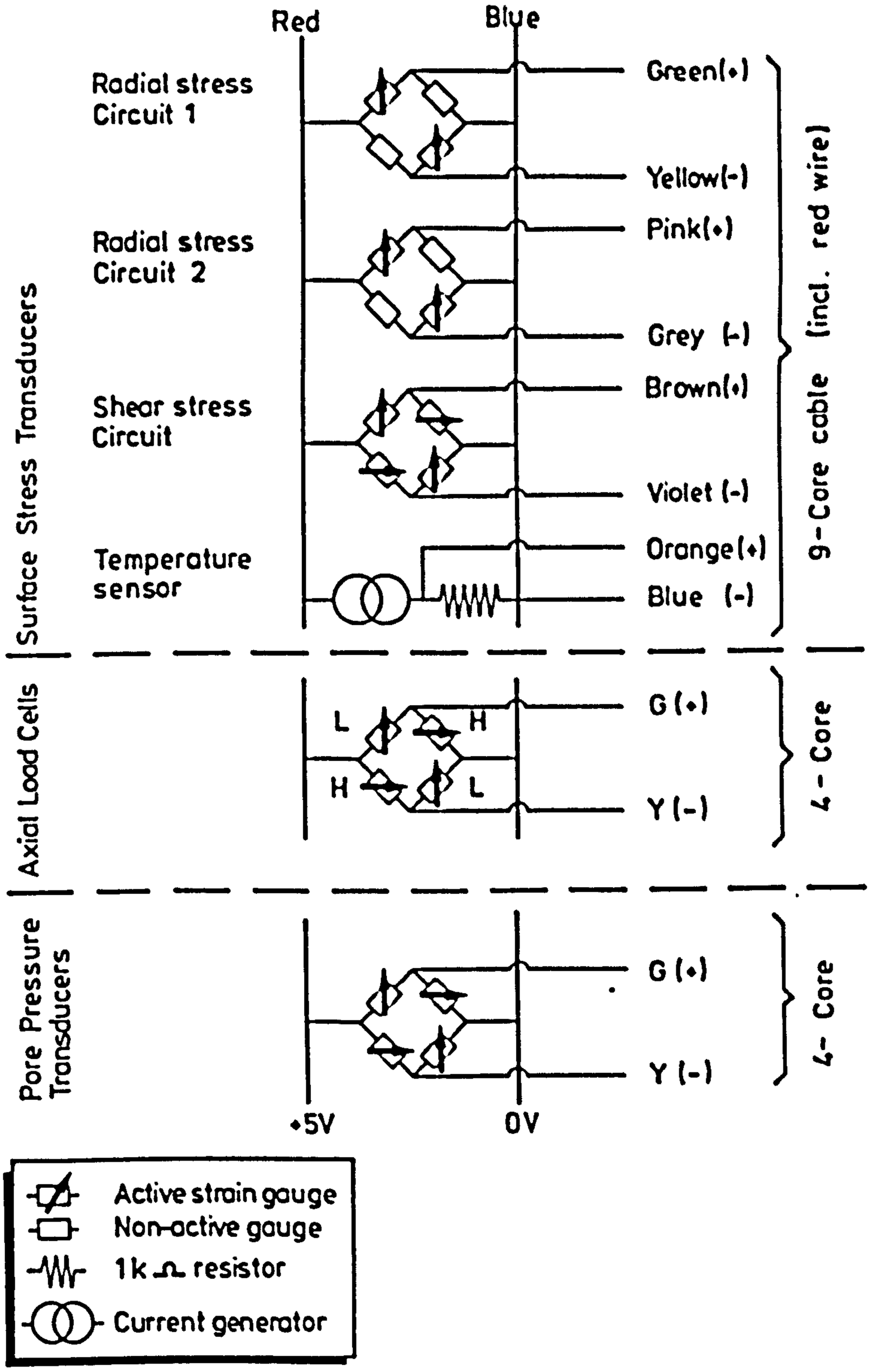


Figure A7.2 Circuit diagram for surface stress transducers, axial load cells, and pore pressure probes

A7.2 TECHNICAL DATA: SURFACE STRESS TRANSDUCERS

A7.2.1 General Information

SST	Mk I	Mk II	Mk III	Mk IV
Manufactured by...	Southampton University	Imperial College	Imperial College	Cambridge Insitu[b]
Date	Early 1970s	1986	1986	1986

A7.2.2 Details of the main housing

Design type	No name	No name	No name	Window
Designed by...	Johnston[c]	Johnston	Johnston	Bond/Dalton
No of cells	2	2	2	1
Size of cover plate (W x L)	63.5mm x 76.2mm	63.5mm x 76.2mm	63.5mm x 76.2mm	77.5mm x 97.5mm[d]
Waterproofing arrangements	Cover plate sealed by fillet of RTV rubber and epoxy coal-tar; gauges coated with RTV rubber and whole cell surrounded by soft paraffin wax[e]	Cover plate sealed against rubber mould by Bostik 1752 sealing compound; strain gauges sealed locally by M-Coats D and G[f]	Cover plate sealed against rubber mould by Bostik 1752 sealing compound; strain gauges sealed locally by M-Coats D and G	"Window" system[g] of waterproofing cover plate; gauges locally sealed by M-Bond 610 and M-Coat D
Axial compliance[h]	0.17μm/kN	0.17μm/kN	0.17μm/kN	0.21μm/kN
Second moment of area	≈118cm^4	≈118cm^4	≈118cm^4	160-194cm^4

A7.2.3 Basic features of the load cells

Load cell	(No name)	"Horseshoe"	"Oval"	"Dogbone"
Designed by...	Johnston	Bassett/Bond	Bond/Bassett	Bond
Material used	"Ground flat stock" and feeler-gauge steel	Armco 17-4PH stainless steel[i]	Armco 17-4PH stainless steel	2014A aluminium alloy[j]
Cell's basic form	Six pieces bolted together	2 ¼-cells bolted to base plate	One piece	One piece
Distance a	63.5mm	54.25	56.25	67.0
Distance b	19.05	17.25	15.4	15.8
Ratio[k] b/a	0.30	0.32	0.27	0.24

A7.2.4 Radial total stress circuits

SST	Mk I	Mk II	Mk III	Mk IV
No webs n_c	4	4	4	4
Wheatstone bridge:	Half active[l]	Half active[m]	Half active[n]	Half active[o]
Gauges	120Ω	120Ω	120Ω	120Ω
Dimensions of webs[p] (w_c x t_c x l_c)	6.35mm x 1.52mm x 15.0mm	8mm x 0.75mm x 8mm	8mm x 0.75mm x 10mm	11mm x 1.0mm x 10mm
X-sectional area[q]	38.6mm^2	24.0mm^2	24.0mm^2	44.0mm^2
Area factor[r]	4839mm^2	4839mm^2	4839mm^2	7556mm^2
Load at 0.1% web strain	7.7kN	4.8kN	4.8kN	3.1kN
σ_{rr} at 0.1% web strain[s]	1591kPa	992kPa	992kPa	435kPa
Buckling load of webs[t]	58-232kN	139kN	89kN	101kN

A7.2.5 Shear stress circuits

SST	Mk I	Mk II	Mk III	Mk IV
No webs n_s	1 plate	2	2	4
No pillars n_p	3	2	1	2
Wheatstone bridge	Fully active	Fully active[u]	Fully active	Fully active
Gauges	120Ω	120Ω	120Ω	120Ω
Dimensions of webs (w_s x t_s x l_s)	13mm x 0.45mm x 27.0mm	3mm x 0.75mm x 9mm	3mm x 0.75mm x 9mm	5mm x 0.75mm x 10mm
X-sectional area	11.7mm^2	4.5mm^2	4.5mm^2	15.0mm^2
Area factor	5227mm^2	5227mm^2	5227mm^2	8015mm^2
Load at 0.1% web strain	2.3kN	0.90kN	0.90kN	1.05kN
τ_{rz} at 0.1% web strain	446kPa	172kPa	172kPa	131kPa
Buckling load of webs	0.53-2.14kN	20.6kN	20.6kN	19.4kN

A7.2.6 Calibration coefficients[v]

a) Direct sensitivity, c_{11} (μV/V per kPa)

SST	Mk I	Mk II	Mk III	Mk IV
Theoretical[w]	0.66 ±0.05	1.06 ±0.08	1.06 ±0.08	2.43 ±0.13
Measured	0.73-0.81	0.87-0.89	0.79-1.00	2.26-2.56

b) Cross-sensitivity, c_{12} (μV/V per kPa)

Measured[x]	0.18 max	0.26 max	0.23 max	0.10 max

c) Direct sensitivity, c_{22} (μV/V per kPa)

Theoretical	4.69 ±0.35	12.2 ±0.9	12.2 ±0.9	16.0 ±0.8
Measured	3.83-4.18	6.50-6.59	8.93-10.88	13.32-18.05

d) Cross-sensitivity, c_{21} (μV/V per kPa)

Measured	0.047 max	0.27 max	0.34 max	0.075 max

A7.2.7 Load cell compliance

SST	Mk I	Mk II	Mk III	Mk IV
Radial compliance[y] δ_c/σ_{rr}	0.0095?μm/kPa[z]	0.0081μm/kPa	0.0101μm/kPa	0.0231μm/kPa
Lost signal[aa]	0.005%	0.12%	0.14%	0.19%
Shear compliance δ_s/τ_{rz}	0.0603? μm/kPa[bb]	0.0523μm/kPa	0.0523μm/kPa	0.0763μm/kPa
Lost signal[cc]	5.1%	5.3%	2.7%	2.9%
Dimensions of shear pillar[dd] (d_p x w_p x h_p)	(1) 12.7mm x 12.7mm x 3.2mm; (2) 6.35mm x 12.7mm x 5.4mm	5mm x 3mm x 8.75mm	16mm x 10mm x 10.75mm	25mm x 10mm x 14mm
Lost signal[ee]	<2%	38%	8.7%	11%

A7.3 DESIGN DRAWINGS

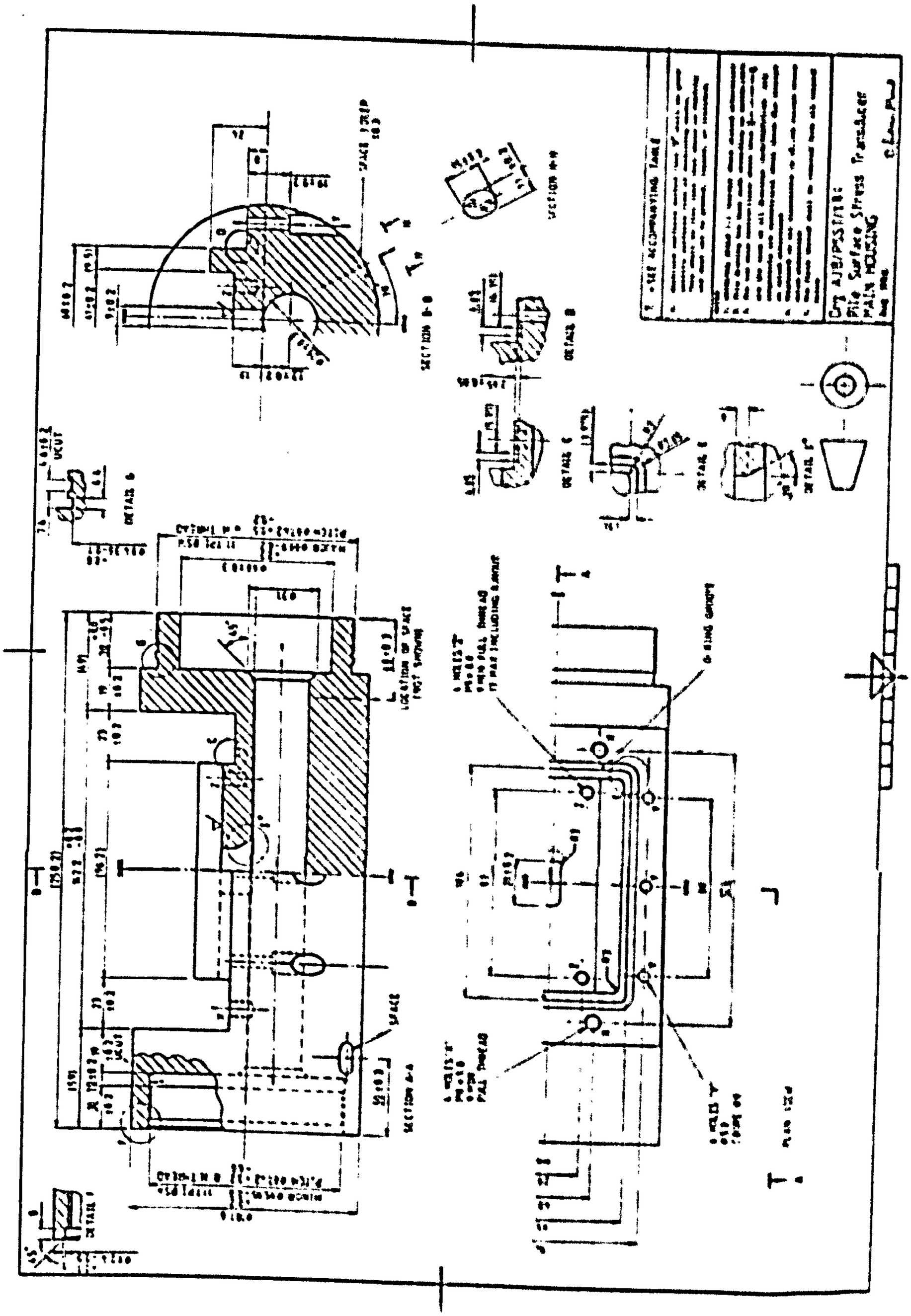


Figure A7.3 Surface stress transducer: design drawing AJB/PSST/1

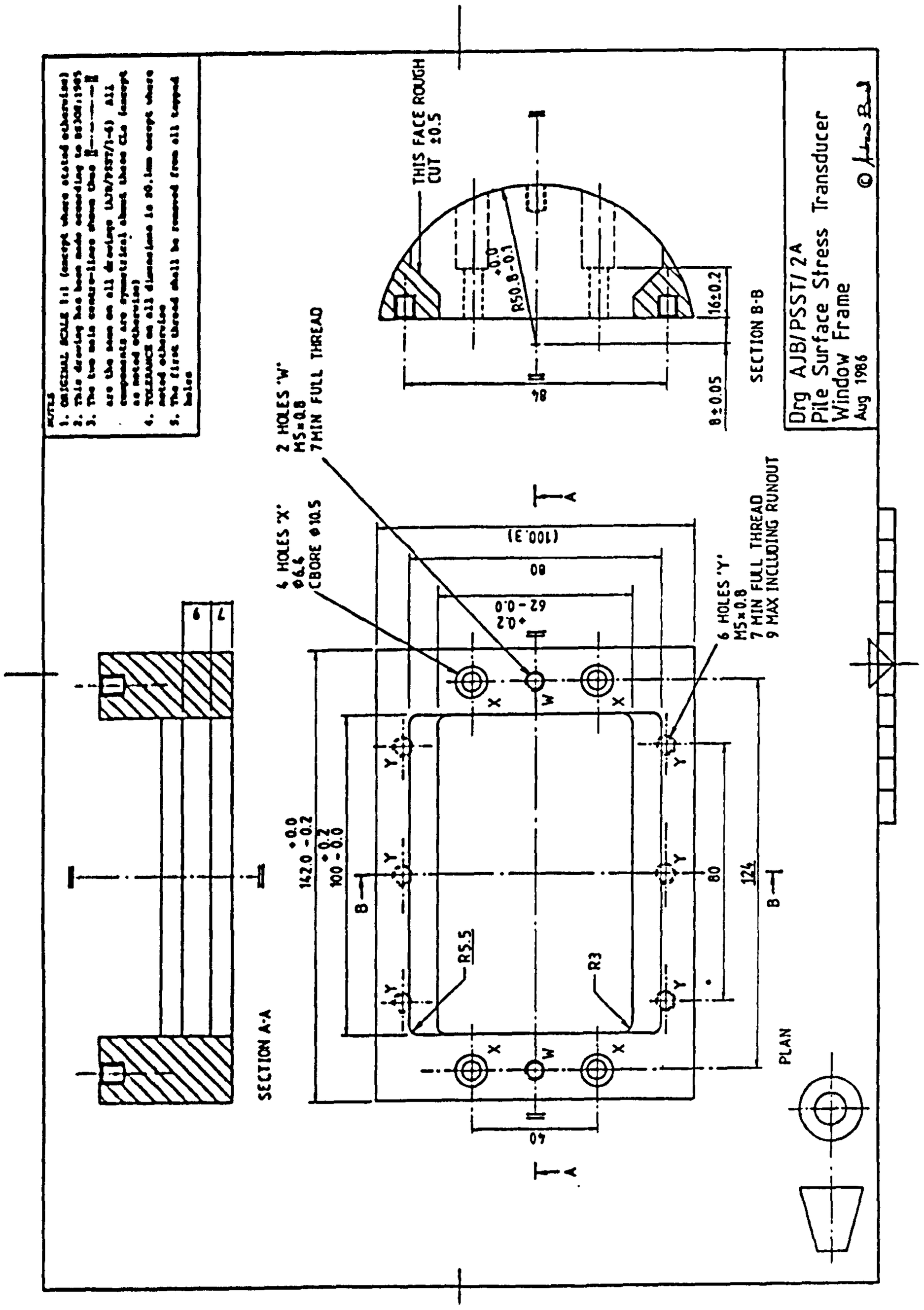


Figure A7.4 Surface stress transducer: design drawing AJB/PSST/2

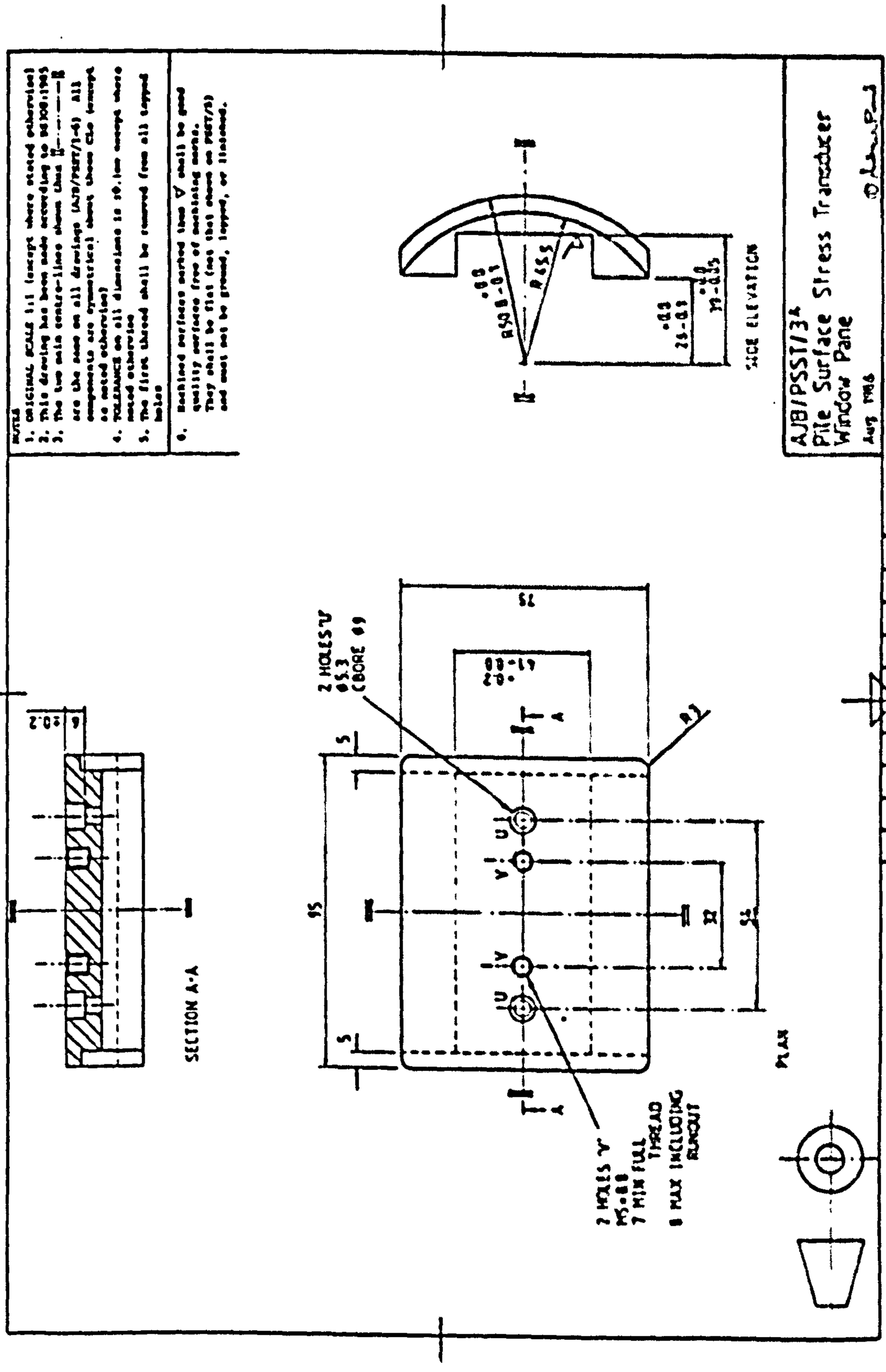


Figure A7.5 Surface stress transducer: design drawing AJB/PSST/3

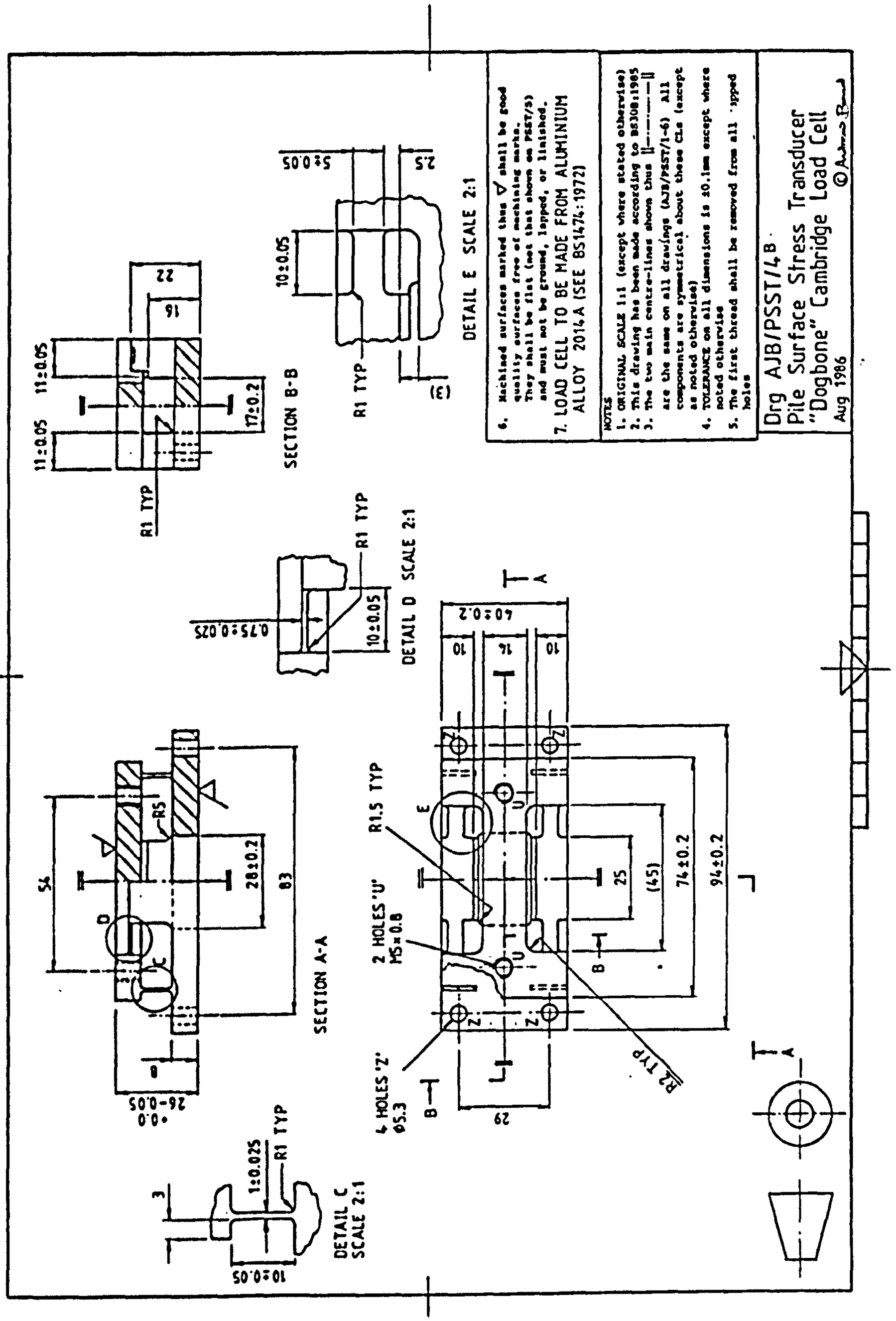


Figure A7.6 Surface stress transducer: design drawing AJB/PSST/4

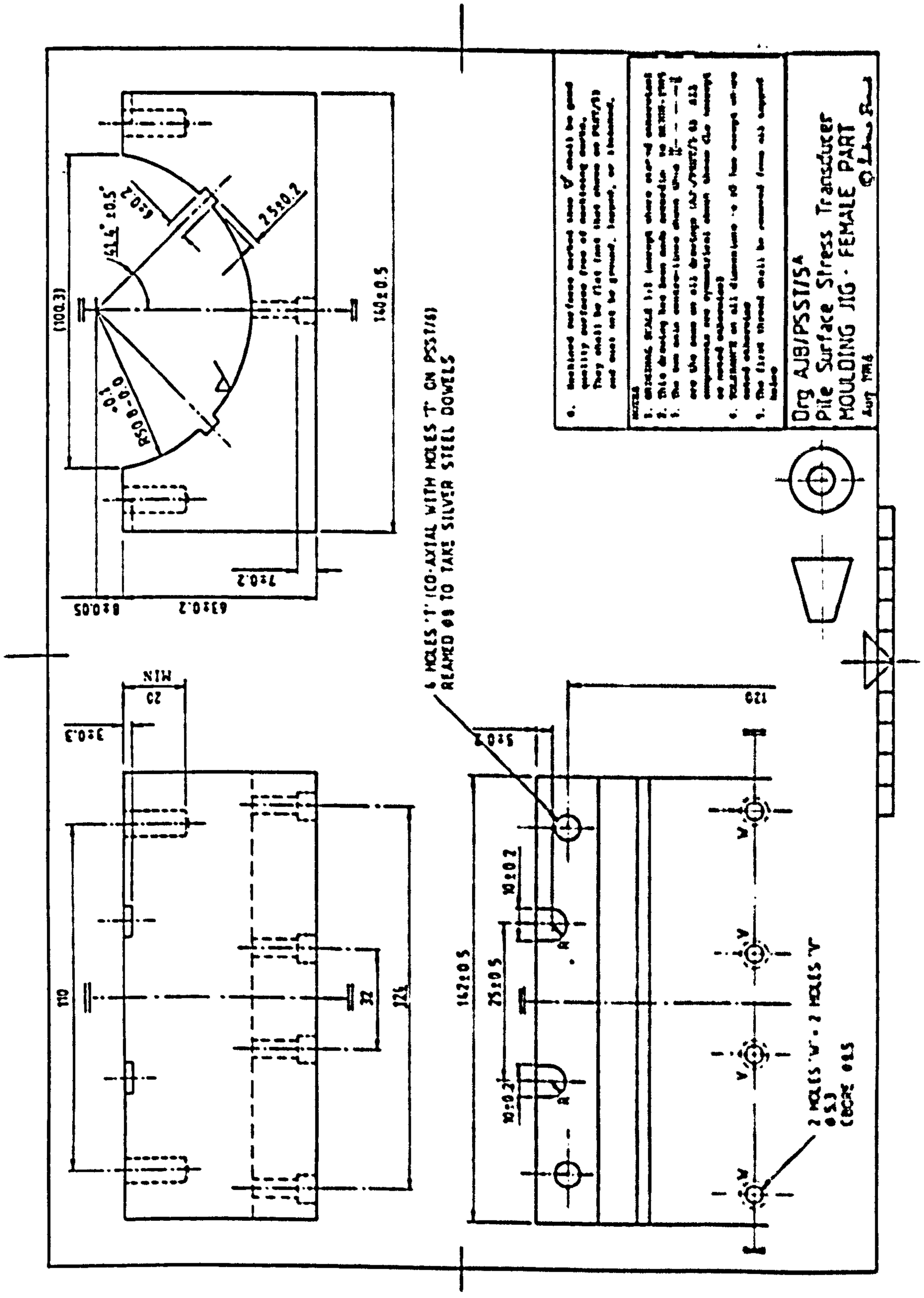


Figure A7.7 Surface stress transducer: design drawing AJB/PSST/5

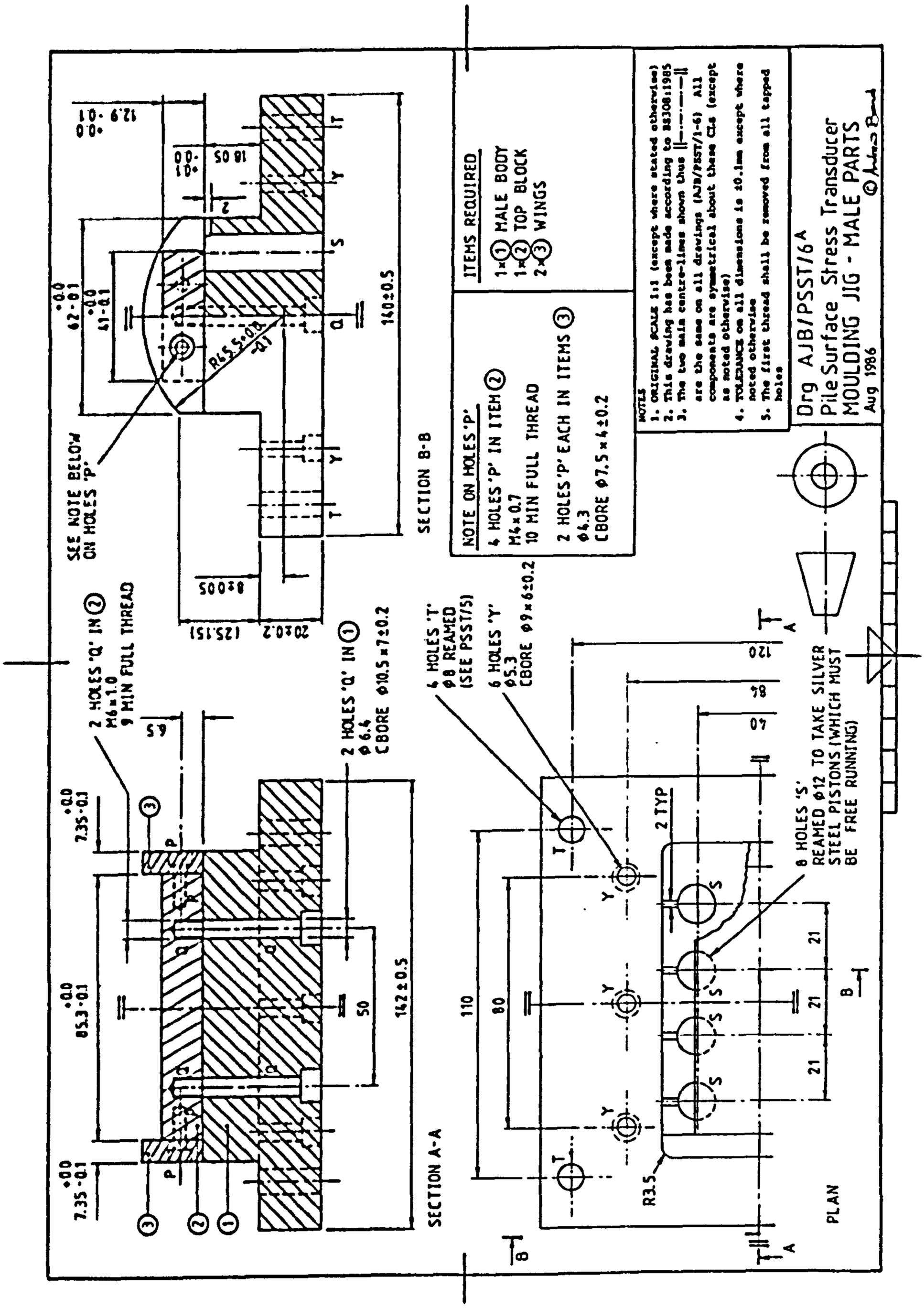


Figure A7.8 Surface stress transducer: design drawing AJB/PSST/6

A7.4 NOTES AND REFERENCES

[a]Johnston I.W. (1972). Electro-osmosis and porewater pressures; their effect on the stresses acting on driven piles. PhD Thesis, Southampton Univ.

[b]Made on a CNC milling machine.

[c]See Chapter 5 of: Johnston I.W. (1972). Electro-osmosis and porewater pressures; their effect on the stresses acting on driven piles. PhD Thesis, Southampton Univ.

[d]These dimensions include for half the width of the rubber between the window pane and the window frame (width = 2.5mm).

[e]See Jardine R.J. (1985). Investigations of pile-soil behaviour, with special reference to the foundations of offshore structures. PhD Thesis, Univ. of London (Imperial College), 2 vol., 789pp., Chapter 9.5. This waterproofing system failed during the equalization period: the first circuit went down after 100 hours, and a further three (of a total of ten) were lost during the next 600 hours (25 days).

[f]The rubber mould was specially formed to fit each cover plate. Bostik 1752 sealing compound is a solvent-borne nitrile rubber; M-Coat D an acrylic paint which insulates the strain gauges; and M-Coat G a two-part, 100% solids, polysulphide-epoxy compound. M-Bond 610 is an epoxy-phenolic adhesive.

[g]The "Window" system comprises a window pane (which serves as a loading platen) surrounded by a window frame. The pane is bolted to a Cambridge load cell (which in turn is bolted onto the main housing); there is a hot-bonded rubber seal between the pane and frame; and the frame compresses an O-ring seal when it is bolted down onto the main housing. See Chapter 8 for full details of the "Window" system.

[h]Axial compliance calculated from the formula $\delta/Q = (1/E)\Sigma(\delta l/A)$.

[i]See Armco Bulletin Number S-6d. 17-4PH is a precipitation hardened stainless steel which can be machined to the final dimensions because the hardening temperatures are low (482°C). This property is especially useful when machining Cambridge type load cells from one piece of metal. Young's Modulus E = 200 (±10)GPa; Poisson's ratio μ = 0.29.

[j]See British Standards Institution (1972). Specification for wrought aluminium and aluminium alloys for general engineering purposes. Bars, extruded round tube and sections. BS1474: 1972. BSI, London, 38pp. Young's Modulus E = 70 (±2) GPa; Poisson's ratio μ = 0.33.

[k]For the definition of b and a, and for a discussion of why the ratio b/a should be kept as small as possible, see: Branaby P.L. (1972). Cambridge contact stress transducers. Lecture notes for the course "Research techniques and equipment in soil mechanics", Cambridge, March 1972. Cambridge Univ. Engng Dept Report CUED/C-SOILS/LN2.

[l]Two bridges, one at each end of the load cell. Each bridge contains gauges from two webs (two gauges per web) and four dummy gauges (for temperature compensation).

[m]One bridge, comprising gauges from all four webs (two per web) and eight dummy gauges.

[n]One bridge, comprising gauges from all four webs (two per web) and eight dummy gauges.

[o]Two bridges, one at each end of the load cell. Each bridge contains gauges from two webs (two gauges per web) and four dummy gauges (for temperature compensation).

[p]w - width, t - thickness; l - length. Subscripts: c for radial compression, s for shear.

[q]Total cross sectional area - n x w x t.

[r]Area factor A_c - 2RLsin θ - WL; A_s - 2RLθ, where θ - arcsin(W/2R) and R - 50.8mm.

[s]Load at 0.1% web strain - 0.001nwtE; radial stress σ_{rr} - $0.001n_cw_ct_cE/A_c$; shear stress τ_{rz} - $0.001n_sw_st_sE/A_s$.

[t]Buckling load of webs - $kn\pi^2Ewt^3/12l^2$, where k - 4 for fully encastré webs, and k - 1 for pin-ended webs. The fixity of the original load cells' webs would be somewhere between k - 1 and k - 4.

[u]One bridge comprising eight gauges, two gauges per web.

[v]The coefficients quoted are those in the formulae:

$$(V_o/V_i)_c - c_{11} \times \sigma_{rr} + c_{12} \times \tau_{rz}$$
$$(V_o/V_i)_s - c_{21} \times \sigma_{rr} + c_{22} \times \tau_{rz}$$

where V_o, V_i - bridge output and input voltages respectively; and c and s denote the radial compression and shear circuits. By inverting these equations in c_{ij}, the coefficients d_{ij} can be found for use in the following formulae:

$$\sigma_{rr} - d_{11} \times (V_o/V_i)_c + d_{12} \times (V_o/V_i)_c$$
$$\tau_{rz} - d_{21} \times (V_o/V_i)_c + d_{22} \times (V_o/V_i)_s$$

In particular, if $c_{11}c_{22} >> c_{12}c_{21}$ (which is generally the case): d_{11} - $1/c_{11}$; d_{12} - $-c_{21}/c_{11}c_{22}$; d_{21} - $-c_{12}/c_{11}c_{22}$; and d_{22} - $1/c_{22}$.

[w]c_{11} - $kA_c/2n_cw_ct_cE$ and c_{22} - $2kA_s/2n_sw_st_sE$, where k - strain gauge factor (taken as 2.1 ±0.05). The error band accounts only for the uncertainty in E and k - not for that in A_c, w_c, and t_c; or A_s, w_s, and t_s.

[x]The cross-sensitivity is not amenable to calculation as it depends upon the exact positioning of the strain gauges on the webs. If the gauges were aligned perfectly then the cross-sensitivity would be zero.

[y]Radial compliance $\delta_c/\sigma_{rr} = l_c A_c/n_c w_c t_c E$; shear compliance $\delta_s/\tau_{rz} = l_s A_s/n_s w_s t_s E$.

[z]0.0083μm/kPa according to Johnston.

[aa]Signal lost through bending of shear webs = $n_s w_s t_s^3 l_c/n_c w_c t_c l_s^3$.

[bb]0.174μm/kPa according to Johnston.

[cc]Signal lost through bending of radial compression webs = $n_c w_c t_c^3 l_s/n_s w_s t_s l_c^3$.

[dd]d_p = depth of pillar (in direction of web); w_p = width; h_p = height (from base to web).

[ee]Signal lost through shear deformation of shear pillar is given by $2(1+\mu)n_s w_s t_s h_p/n_p w_p d_p l_s$, where μ = Poisson's ratio.

Appendix 8

Details of instrument design: pore pressure probes

CONTENTS OF APPENDIX 8

A8.1 PORE PRESSURE PROBES MKS I-IV 624
A8.1.1 Background 624
A8.2 TECHNICAL DATA: PORE PRESSURE PROBES 626
A8.2.1 General information 626
A8.2.2 Housing 626
A8.2.3 Pore pressure block 626
A8.2.4 Fluid used in system 626
A8.2.5 Transducer 627
A8.3 DESIGN DRAWINGS 628
A8.4 NOTES AND REFERENCES 632

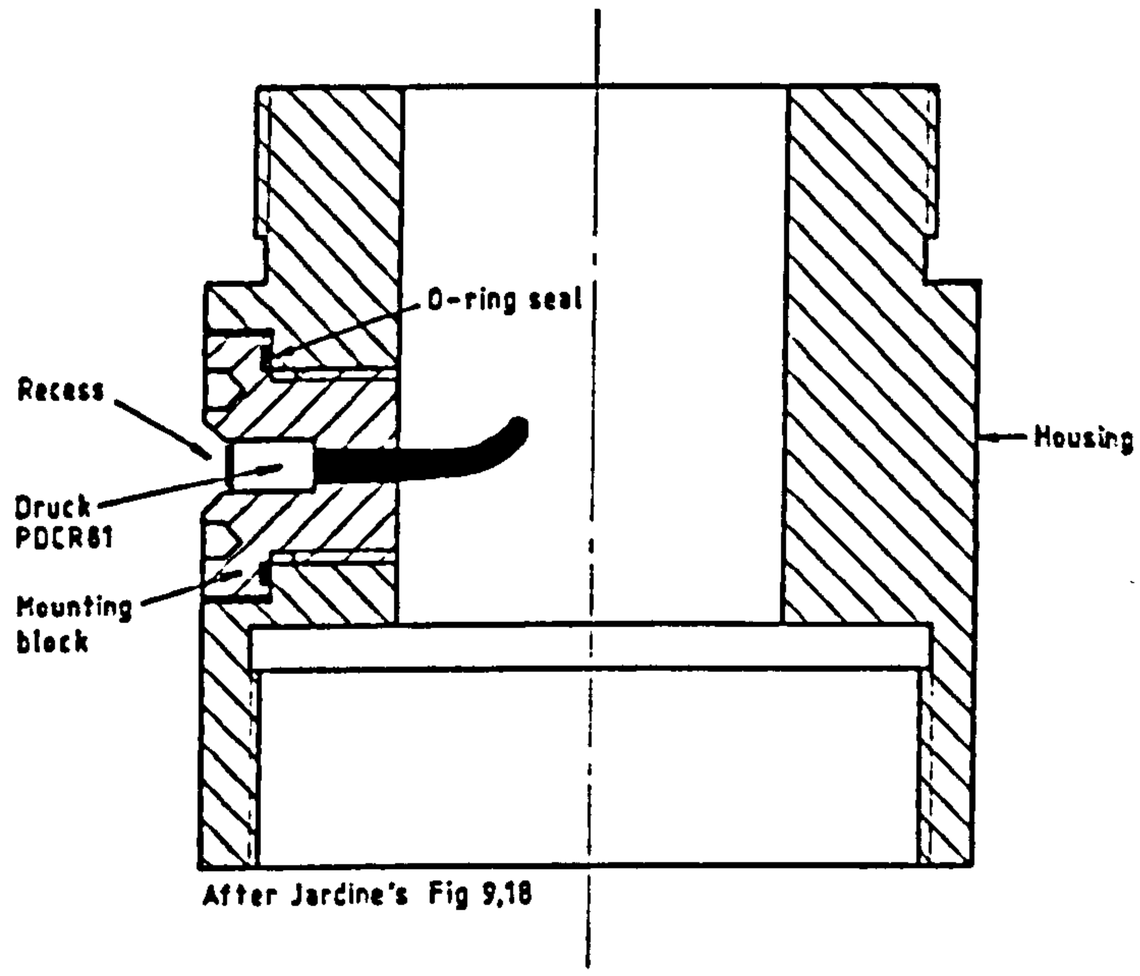
A8.1 PORE PRESSURE PROBES MKS I-IV

A8.1.1 Background

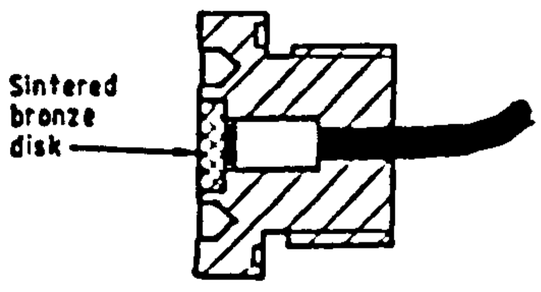
For the Pilot experiment at Canons Park, the instrumented pile carried three pore pressure probes, of the type illustrated in Figure A8.1(a). A Druck PDCR 81 semi-conductor transducer was mounted in a plated steel block, and the recess in front of its ceramic filter was filled with de-aerated soft London clay.

For the next experiment, CP1s, the probe was re-designed so that a sintered bronze disk replaced the pad of soft clay and prevented the transducer from coming into contact with the soil outside the pile. This re-designed probe (Mk II) is shown in Figure A8.1(b).

Both the Mark I and Mark II probes were saturated with water.



a) Jardine's (1985) pore pressure unit (Mk I)



b) Mark II Pore Pressure Probe

Figure A8.1 Pore pressure probes, Mks I and II

The Imperial College Instrumented Pile, as used in Test Series CP2-5, was equipped with "fast-acting" pore pressure probes (Mk III probes), whose mounting blocks were made from acetal copolymer. This was intended to prevent galvanic action between the transducer (titanium), the porous disk (stainless steel), and the pile (molybdenum steel). See Chapter 6 for further details. The fast-acting probes were saturated with silicone fluid.

The Mark IV pore pressure probes were used in Test Series CP4f only. These were designed so that they could be flushed with de-aerated water. The pore pressure blocks were the same as those used for the fast-acting probes, only with a different insert. The transducers (PDCR 200s) were mounted half-way up the pile, in a special brass housing. See Chapter 6 for further details.

A8.2 TECHNICAL DATA: PORE PRESSURE PROBES

A8.2.1 General information

PPU	Mk I	Mk II	Mk III	Mk IV
Designed by...	Jardine	Jardine/Bond	Bond	Bond
Date	1983/4	1986	1986	1986/87

A8.2.2 Housing

Type	'Simple'[a]	'Simple'	Combined with axial load cell[b]	Special "half-way housing"
Material	1¼% manganese molybdenum steel[c]	As for Mk I	As for Mk I	Brass
Portholes	1	2	2	N/a
Block secured by...	Screw thread	Screw thread	Bolting	Bolting

A8.2.3 Pore pressure block

Block design	One piece	One piece	Two piece[d] (block and thrust ring)	Two piece (block and insert)
Material	Steel[e]	Stainless steel	Acetal copolymer[f]	As Mk III + brass insert
Filter	1mm pad soft de-aired clay[g]	Sintered bronze disk[h]	Sintered stainless steel disk	Sintered stainless steel disk
Pore size D_e	?	5μm[i]	5μm	5μm
Permeability[j] ϕ	?	1mm^2	1mm^2	1mm^2
Porosity n	?	30%	≈27%	≈27%
Filter clamping...	Pressed by hand	Glued with Araldite	Pressed/shrunk fit[k]	Pressed/shrunk fit
Piezometer volume[l] V_p	?	175mm^3	≈291mm^3	

A8.2.4 Fluid used in system

Fluid	De-aired water	De-aired water	Silicone fluid[m]	De-aired water
Bulk modulus K	≈2GPa[n]	≈2GPa	0.8-1.0GPa[o]	≈2GPa

Kinematic viscosity	1.00mm^2/s	1.00mm^2/s	20-30mm^2/s[P]	1.00mm^2/s
Surface tension[Q] σ	72.7mN/m	72.7mN/m	20.6mN/m	72.7mN/m
Air entry value of filter	?	5kPa	16kPa	5kPa
AEV of transducer's own filter[r]	214kPa	214kPa	-	-

A8.2.5 Transducer

Type	Druck PDCR81[S]	Druck PDCR81	Druck PDCR81	Druck PDCR200
With/without own filter	With	With	Without	Without
Filter type	Aerox "Celleton" grade VI ceramic[t]	As Mk I	-	-
Pore size D_o	1.4μm	As Mk I	-	-
Permeability ϕ	0.003mm^2	As Mk I	-	-
Porosity n	46.4%	As Mk I	-	-
Sensitivity of transducer	11.11-11.96μV/V per kPa	As Mk I	As Mk I	-
Transducer compliance	$10^{-11}mm^3$/kPa	As Mk I	As Mk I	

A8.3 DESIGN DRAWINGS

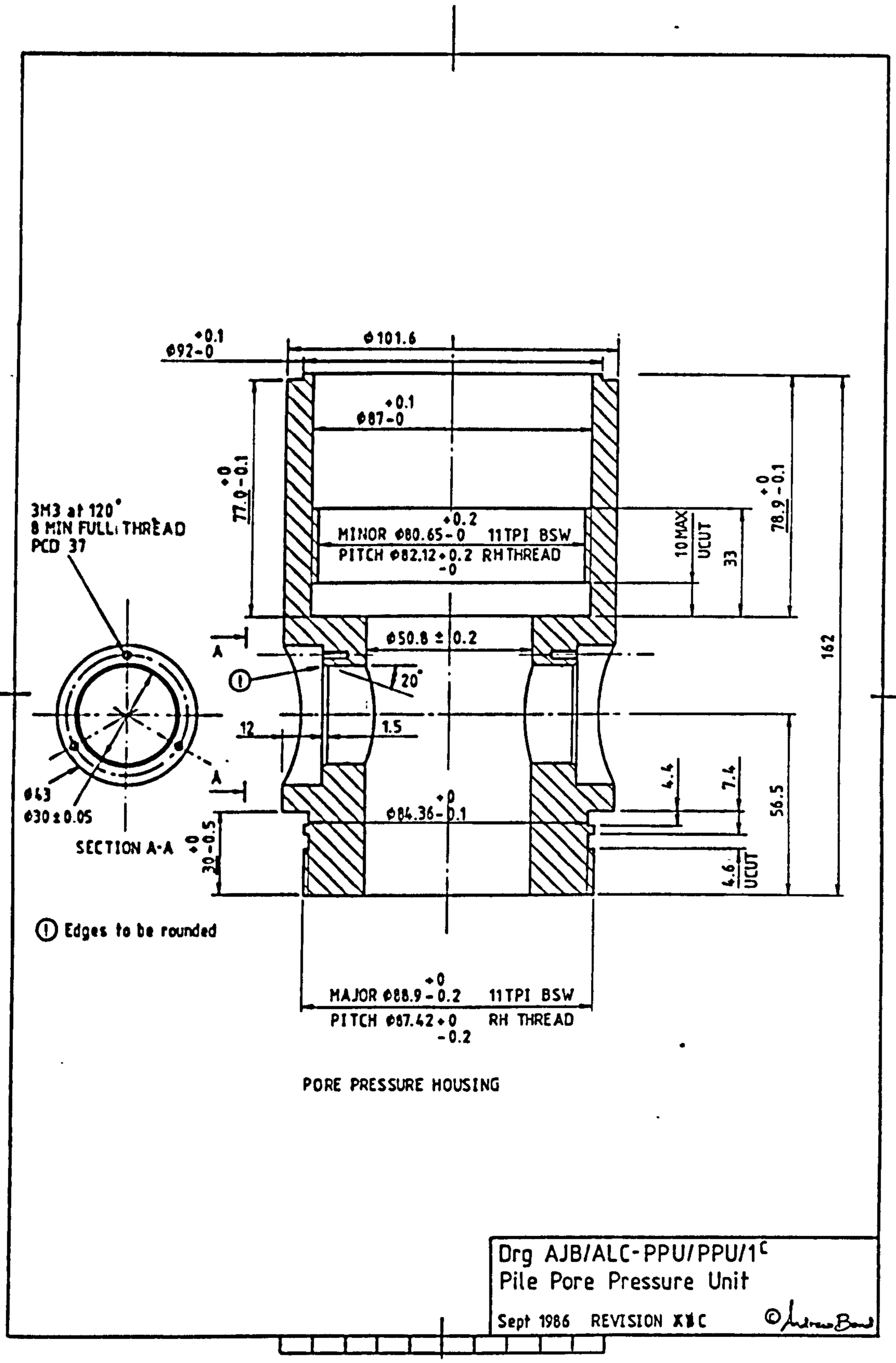


Figure A8.2 Pore pressure probes: design drawing AJB/PPU/1

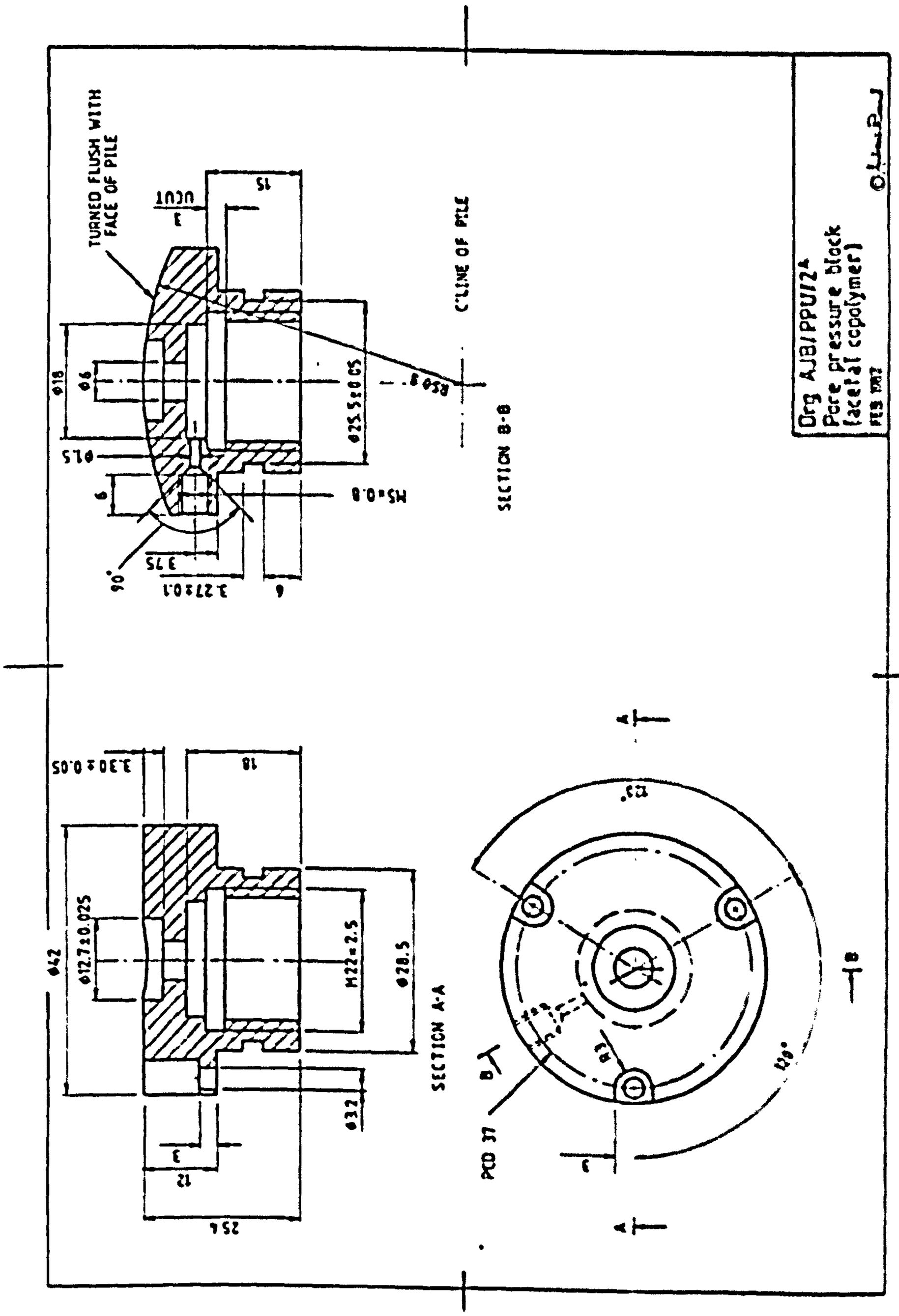


Figure A8.3 Pore pressure probes: design drawing AJB/PPU/2

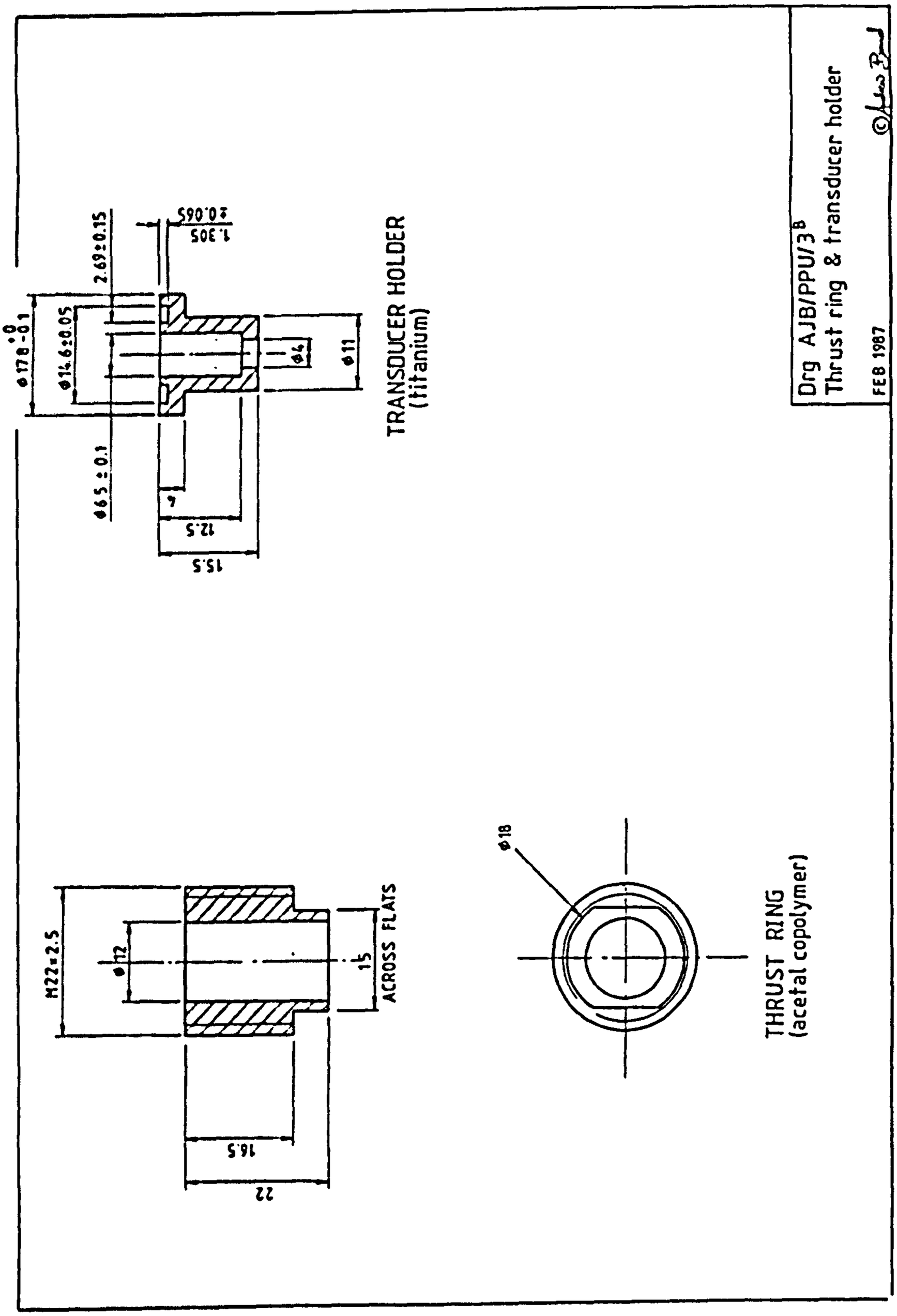


Figure A8.4 Pore pressure probes: design drawing AJB/PPU/3

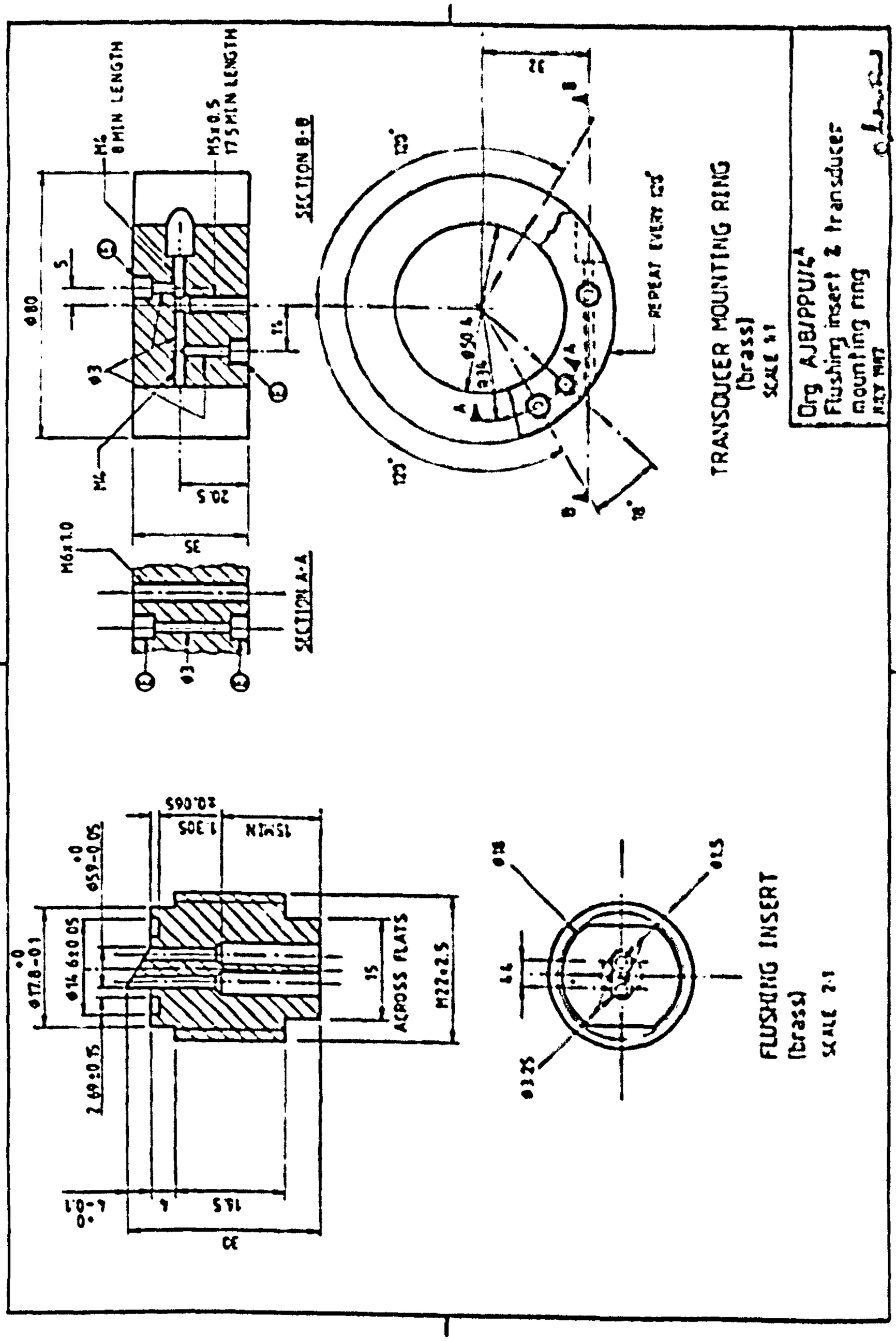


Figure A8.5 Pore pressure probes: design drawing AJB/PPU/4

A8.4 NOTES AND REFERENCES

[a]See Jardine R.J. (1985). Investigations of pile-soil behaviour, with special reference to the foundations of offshore structures. PhD Thesis, Univ. of London (Imperial College), 2 vol., 789pp., Figure 9.18. The 'simple' housing is a length of steel tubing (outside diameter 101.6mm; inside diameter 50.8mm) with portholes cut through the side wall (into which the pore pressure blocks are screwed).

[b]See Chapter 8 for details.

[c]605 M36S. See British Standards Institution (1970). British Standard Specification for Wrought steels for mechanical and allied engineering purposes. BS970: Part 2: 1970. (This steel formerly known as En16, according to BS970: 1955.)

[d]The thrust ring screws into the back of the pore pressure block, thereby clamping the flange of the transducer holder into its correct position. See Chapter 8 and the design drawings for details.

[e]The steel was plated with nickel in order to prevent corrosion (unsuccessfully).

[f]Acetal copolymer was chosen because it is strong and rigid, its abrasion and chemical resistance is good, and its water absorption is low. See Farago P.J. (1969) (editor). Plastics handbook. Design Engineering Handbooks, Product Journals Ltd, West Wickham, Kent, 235pp. Trade name of plastic used: Delrin (produced by Du Pont de Nemours).

[g]See Jardine (1985), loc. cit., Section 9.7: assuming a coefficient of consolidation of $0.3m^2$/year the London clay pad would consolidate to a time factor T of unity in 1.8 minutes.

[h]Sintered discs supplied by Sheepbridge Sintered Products Ltd. Discs used: Porosint Bronze Grade A (ϕ12.7mm x 3.175mm thick); Porosint Stainless Steel Grade P/2½ (same dimensions).

[i]As determined by the 'First Bubble Point Method' (see BS5600: Part 3: 1979): the porous disk is saturated with a liquid (isopropanol) of known surface tension σ, and the pressure p needed to force a channel of air through it is measured. The effective or threshold pore size* (diameter) D_e is given by the formula $p\pi D_e^2/4 = \sigma\pi D_e$; i.e. $D_e = 4\sigma/p$. (The manufacturer also quotes a 'micron rating' for these filters: this is the size of the largest solid particle that can pass through them, as measured by "the filtration method". The micron rating for both types of filter is 2.5μm.)

*Values given in Sheepbridge Sintered Products Ltd's technical data sheet entitled 'Sintered Filter Elements' (1986?).

[j]ϕ is the viscous permeability in the formula: $Q/A = (\phi/\eta)(-dp/dl)$, where Q = volume of flow through area A; $-dp/dl$ = rate of pressure drop with distance; and η = fluid's dynamic viscosity. The viscous permeability is

independent of the fluid used to saturate the filter, something that is not true of the permeability k (which is more familiar to soils engineers), as utilized in Darcy's law: $Q/A = ki = (k/\rho g)(-dp/dl)$, where i = hydraulic gradient $-d(p/\rho g)/dl$; g = acceleration due to gravity; and ρ = fluid density. The dynamic viscosity is related to the kinematic viscosity ν by $\nu = \eta/\rho$, and so: $k = g\rho\phi/\eta = g\phi/\nu$. Hence, in water the permeability of the sintered discs is $k \approx 10^{-5}$m/s; whereas in silicone fluid $k \approx 5\times10^{-7}$m/s. The SI units for ϕ are m^2; in the cgs system they are darcies: 1 darcy = $10^{-12}m^2$.

[k]The plastic block is heated to 80°C and the porous disk (not heated) is pressed into place.

[l]The piezometer volume (V_p), between the transducer's sensing element and the soil, is given by:

$$V_p = V_d + V_b + V_{ps} + V_g,$$

where V_d = volume of voids in the porous disc; V_b = volume of the cylindrical bore in front of the transducer*; V_{ps} = volume within the transducer's porous stone, if fitted (or of the gap left if the stone isn't fitted); and V_g = volume of gap between transducer's porous stone and its sensing element. (*In order to prevent physical contact between the transducer and the porous disc, there is a small gap between the two. See the design drawings for exact details.) From the discs' dimensions and porosity (see the text): $V_d \approx 121mm^3$ (bronze discs) or $109mm^3$ (stainless steel discs). For the one piece block, $V_b \approx 33mm^3$; for the two piece block, $V_b \approx 152mm^3$. If the porous stone is fitted, $V_{ps} \approx 20mm^3$. If not, $V_{ps} \approx 29mm^3$. $V_g \approx 1mm^3$, according to Hight D.W. (1983). Laboratory investigations of sea bed clays. PhD Thesis, Univ. of London (Imperial College).

[m]Dow Corning 200 Fluid, nominal viscosity $\nu = 20mm^2/s$. N.b. $1mm^2/s$ = 1cSt (centistoke). See Dow Corning's data sheet number 22-069I-01 (Dec 1985). This fluid is a dimethyl siloxane polymer which exhibits little change in physical properties over a wide temperature span. It has excellent water repellency, low surface tension, and low toxicity. Its density is $949kg/m^3$.

[n]See Fredlund D.G. (1976). Density and compressibility characteristics of air-water mixtures. Can. Geotech. J., 13(4), pp386-396.: the bulk modulus of water K_w (= $1/C_w$, where C = compressibility) varies dramatically with the amount of air dissolved in it. Pure water has $K_w \approx$ 2GPa, whereas with 1% (by volume) of dissolved air $K_w \approx 0.003$GPa (at atmospheric pressure).

[o]The compressibility of Dow Corning 200 Fluid has been determined (by the manufacturer) at pressures much greater than those being studied in this research project. The values quoted in the table are therefore only approximate.

[p]The viscosity of silicone fluid varies with temperature: the nominal viscosity ($20mm^2/s$) is that at 25 C; at 10°C $\nu \approx 30mm^2/s$.

[q]Values taken from: Tennent R.M. (1971). (Editor.) Science data book. Oliver & Boyd, Edinburgh, 104pp.

[f]The air entry value (AEV) is analogous to the 'blow through pressure' or 'first bubble pressure' p, defined in note i above. The AEV of a filter depends on the surface tension of the fluid used to saturate it. The values quoted in the text relate to the particular fluid (i.e. water or silicone fluid) used in each piezometer system.

[g]The PDCR81 is a miniature pore water pressure transducer which consists of a single crystal, silicon diaphragm, with a fully active strain gauge bridge diffused into its surface. The transducer is housed within a titanium capsule and can be supplied with or without a ceramic filter in front of the diaphragm. Details of the transducer's construction may be found in the PhD Thesis by Hight D.W. (1983), loc. cit.

The following information has been taken from Druck's data sheet for the PDCR81:

Diameter of titanium capsule	6.4mm
Length of capsule (without filter)	11.4mm
Overall length of capsule and filter (max.)	11.9mm
Weight (including 5m of cable)	30g
Nominal full-scale output*	15mV/V
Output impedance	1kΩ
Combined non-linearity & hysteresis	0.2%
Operating temperature range	-20 to +120°C
Thermal zero shift	0.05% FSO/°C
Thermal sensitivity shift	0.2% FSO/°C
Overload capacity	x3

*The transducer's maximum operating pressure is 1500kPa (for the particular transducers used.

[t]Properties of Aerox "Celloton" grade VI ceramic as determined by Blight G.E. (1961). Strength and consolidation characteristics of compacted soils. PhD Thesis, Univ. of London (Imperial College), 111pp + figures. Permeability k quoted as 2.93×10^{-8}m/s, which implies $\phi = 0.003mm^2$.

Appendix 9

Notes on instrumented pile tests CP0-5

CONTENTS OF APPENDIX 9

A9.1 JARDINE'S PILOT TEST (CPOF) 638
A9.1.1 Main sequence of events 638
A9.1.2 Instrument performance 639
A9.2 TEST SERIES CP1s - REJUVENATING THE SOUTHAMPTON PILE . . 640
A9.2.1 Aims of the first Test Series 640
A9.2.2 Main sequence of events 640
A9.2.3 Instrument performance 641
A9.3 TEST SERIES CP2f - INAUGURATION OF THE IMPERIAL COLLEGE INSTRUMENTED PILE 644
A9.3.1 Aims of the second Test Series 644
A9.3.2 Main sequence of events 645
A9.3.3 Instrument performance 645
A9.4 TEST SERIES CP3fs - PROVING THE SIGNIFICANCE OF JACKING RATE 647
A9.4.1 Aims of the third Test Series 647
A9.4.2 Main sequence of events 648
A9.4.3 Instrument performance 648
A9.5 TEST SERIES CP4f - LONG-TERM MEASUREMENTS OF PORE PRESSURE 649
A9.5.1 Aims of the fourth Test Series 649
A9.5.2 Main sequence of events 649
A9.5.3 Special procedure for installing CP4f 650
A9.5.4 Instrument performance 651
A9.6 TEST SERIES CP5f - "CONTROL" EXPERIMENT FOR DRIVEN PILES 652
A9.6.1 Main aims of the fifth Test Series 652
A9.6.2 Main sequence of events 652
A9.6.3 Instrument performance 652
A9.7 ORIENTATION OF INSTRUMENTS 653
A9.8 CONFIGURATION OF INSTRUMENTS 654
A9.8.1 Test Series CP0-2 654
A9.8.2 Test Series CP3-5 655
A9.9 NOTES AND REFERENCES 656

A9.1 JARDINE'S PILOT TEST (CPOF)

A9.1.1 Main sequence of events

The Pilot Test at Canons Park was conducted by Jardine[1] in the summer of 1984. The pile was installed at a fast rate of jacking, and was load tested in tension just over 3¼ months later. The level of instrumentation is shown in Figure A9.1 and the pile's key features are summarized in the box on page 639.

The Pilot pile was installed in a series of approximately eighty 35mm pushes. "In each push the full capacity of the pile was mobilised for ...around 15 seconds".[2] The total time taken for installation was 1h 10min, and the rate of jacking was typically 500mm/min (accurate to ±20% at best).

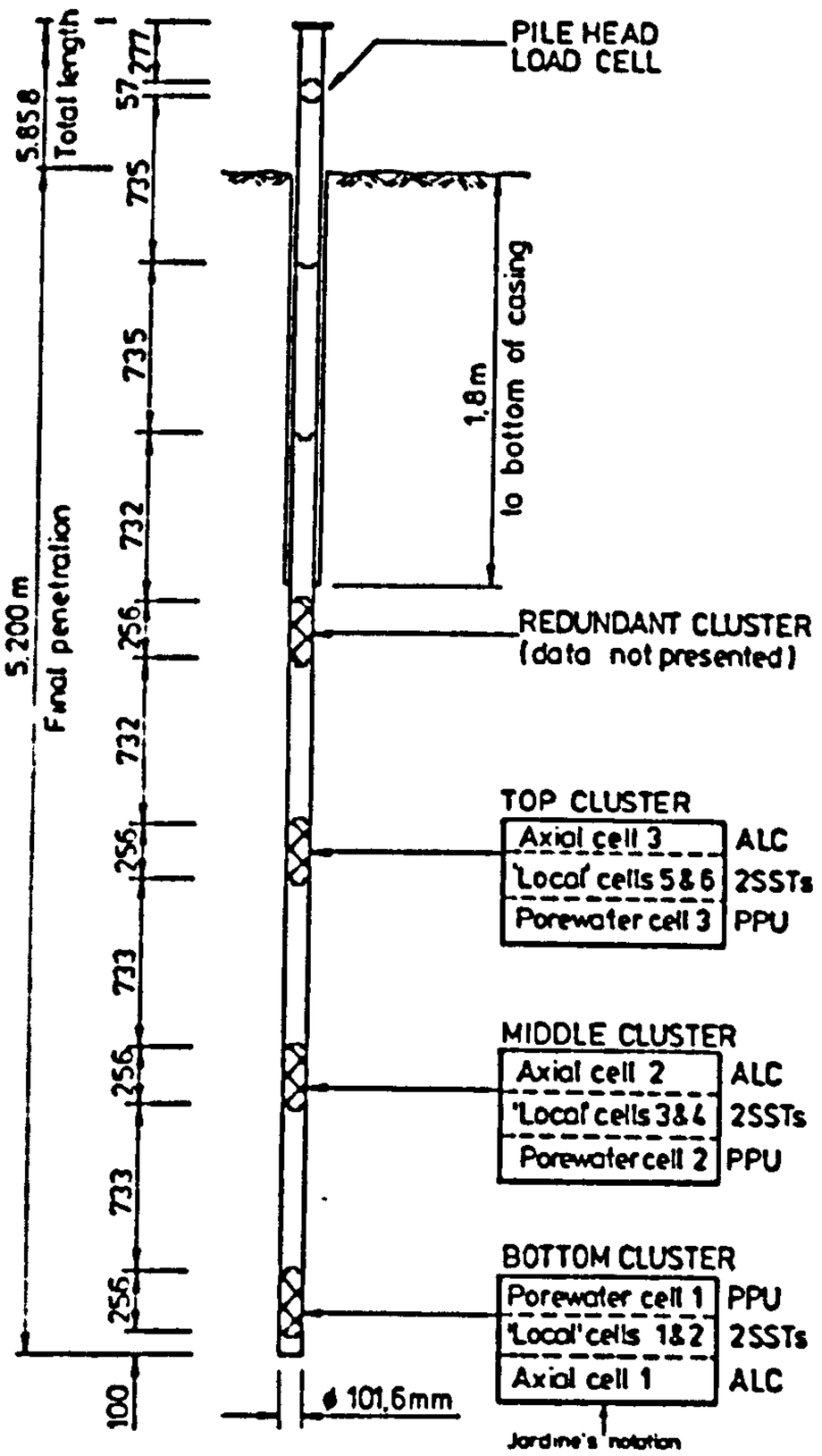


Figure A9.1 Configuration of instruments - Pilot Test

During installation, the top two axial load cells buckled when the jacking force exceeded their load capacities (≈130kN). One of the cells could be replaced (that at the pile head), but the other could not (cell 3). Therefore the subsequent load test was conducted in tension (LlT) rather than in compression. (The buckled cell had an overwhelming influence on the pile's load-displacement characteristics, although it should not have altered its overall load capacity.)

Key features of the Pilot pile

Pile design	Southampton
Overall length	5.86m
Penetration	5.20m
Embedded length L	3.11m
Ratio L/D	30.6
ALCs (unsleeved)	5
SSTs (original)	8
PPPs (original/H_2O)	4
TSs	0
Installation	Fast
Equalization	Long
Load tests	LLT

Jardine's test procedure was different to the LPC method described in Chapter 8. The load was increased in increments of 6kN at the rate of one increment a minute; it took a total of ≈32 minutes to reach the pile's peak capacity. As the test was load controlled the displacement rates varied continuously, "but 0.15mm/min can be considered typical before failure".[3]

CP0 was extracted from the ground on day 109. The pile had a coating of clay (≈3mm thick) on its surface as it emerged from the ground.

A9.1.2 Instrument performance

During installation, the pore pressures probes suffered from slow response times; and, during equalization, they were affected by consolidation of a pad of soft clay that Jardine had placed in front of the transducer's ceramic filter. Since the readings bear no resemblance to the results of later tests at Canons Park, they are ignored in this Thesis.

Readings of shear stress were obtained at two instants only during pile installation, but seem reliable.

The radial total stress during installation appear trustworthy. For the equalization period, Jardine presents[4] traces showing the variations in σ_{rr} over a total of 600h (25 days). However, the first radial stress circuit became unstable after ≈100h and by the twenty-fifth day 40% of the circuits had been lost. Comparing the results with those of CP2f/EQ (see Chapter 10) suggests that the radial stress circuits went awry perhaps as early as the seventh day.

A9.2 TEST SERIES CP1s - REJUVENATING THE SOUTHAMPTON PILE

A9.2.1 Aims of the first Test Series

The main aim of the first experiment was to obtain reliable readings of the earth pressures and pore water pressures acting on the pile over a period of 2¼ months following installation. Test CP1 was intended to repeat the Pilot Test (CP0f), except that the first load test would be in compression and not in tension. The importance of the rate of installation on the pile's behaviour was not appreciated at the time: hence the jacking rate of CP0 was not matched.

Figure A9.2 shows the level of instrumentation carried by CP1s and the box on page 641 lists the pile's key features.

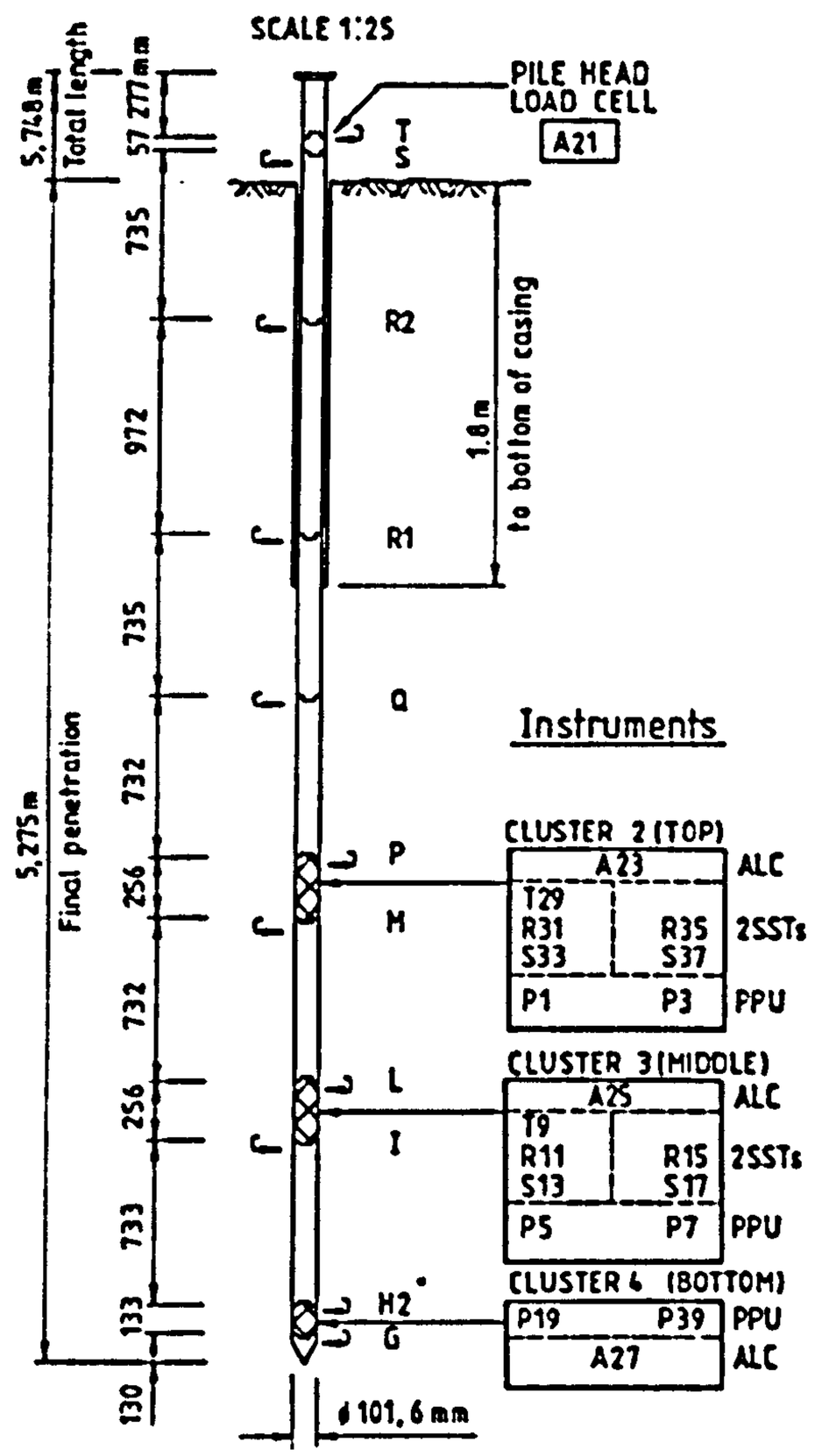


Figure A9.2 Configuration of instruments - pile CP1

A9.2.2 Main sequence of events

Pile CP1 was jacked at a slow rate (94 ±22mm/min) in just under 2½h, and was left for 79 days (≈2¼ months) before load testing in compression (CP1s/L1C). The pile was extracted on day 80 at a rate of 107 ±26mm/min.

A9.2.3 Instrument performance

Key features of pile CP1

Pile design	Southampton
Overall length	5.75m
Penetration	5.28m
Embedded length L	3.19m
Ratio L/D	31.4
ALCs (unsleeved)	4
SSTs (Oval/11'shoe)	4
PPPs (original/H_2O)	6
TSs	2
Installation	Slow
Equalization	Long
Load tests	LIC

The surface stress transducers gave reliable readings during pile installation and for a short time thereafter. Throughout equalization, however, their signals drifted intolerably, owing to moisture entering the load cells' housings. Consequently the data gathered during equalization has been disregarded. Changes in radial total stress and shear stress during the load test should not have been affected by the signals drifting, and so these are reported herein (see Chapter 11).

There were two main problems with the pore pressure readings. The first was the probes' slow response times during installation, following cavitation in the disturbed London clay. To illustrate this point, Figure A9.3 presents the traces obtained with the leading probes, P19 and P39. Throughout the head material (1.5 to 2.5m deep) the instruments respond in unison, but do not register such high positive values

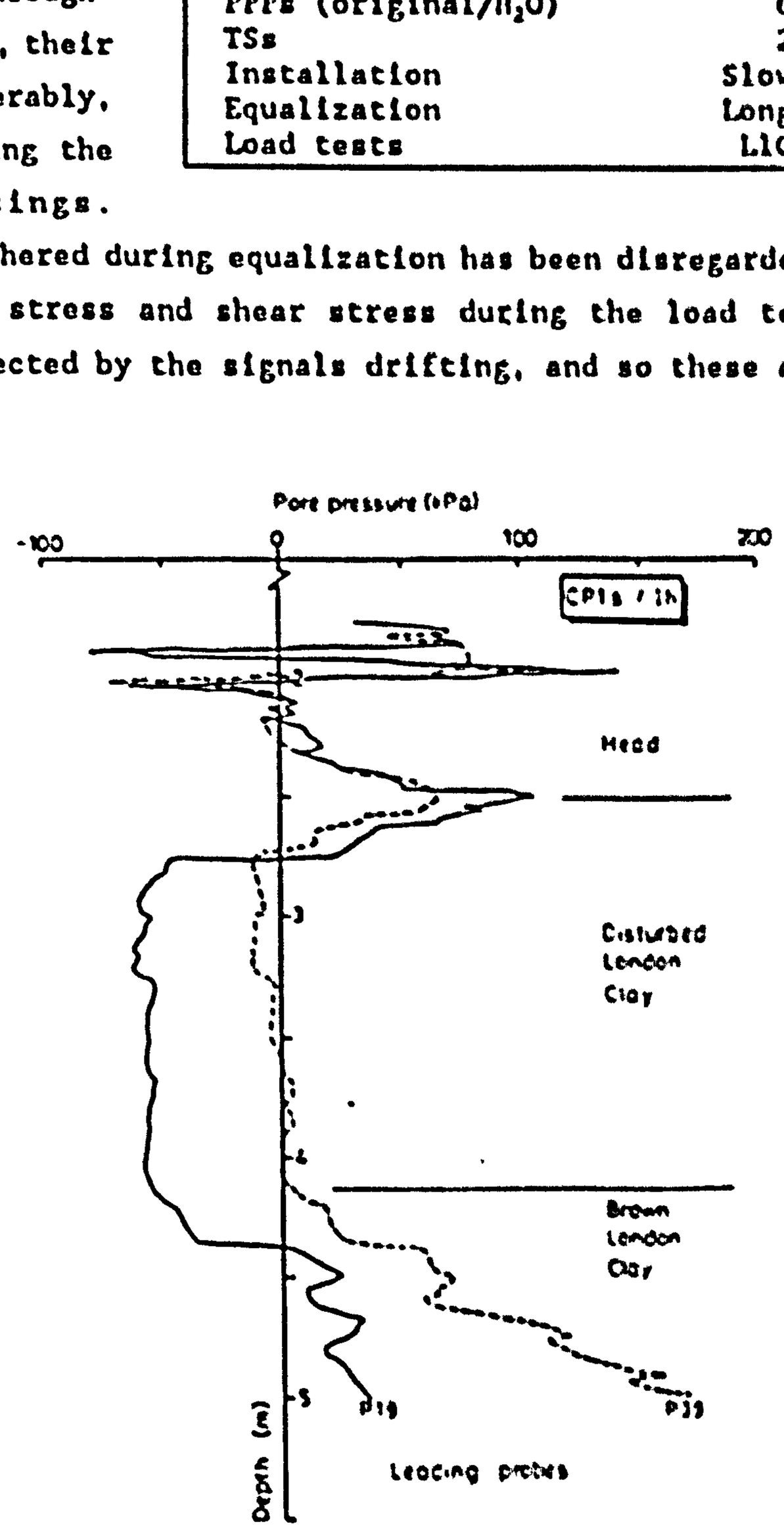


Figure A9.3 Pore pressures recorded during installation, Test CP1

as were obtained in subsequent tests (using the fast-acting probes). Between 2.75 and 4.0m the traces are listless, failing to show any changes in pore pressure during the pause periods between pushes (of up to 15 minutes). Piezocones with filters located behind the cone tip give similar traces in heavily overconsolidated clays.[5]

The second problem occurred after the pile had been in the ground for six days, when the probes started to record highly erratic signals, as shown in Figure A9.4. Note from this diagram that:

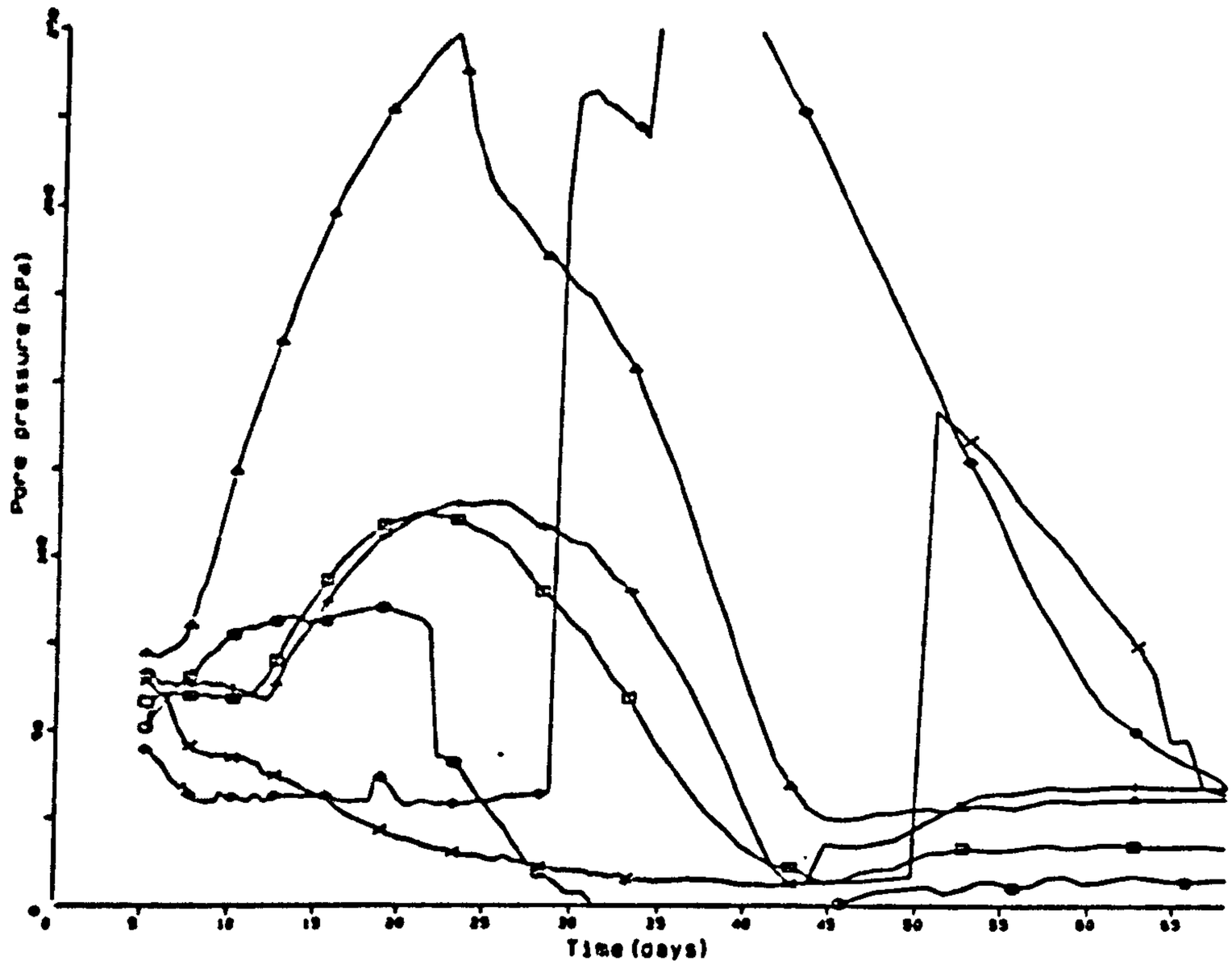


Figure A9.4 Erratic pore pressure signals during Test Series CPIs

- The traces become erratic only after six days have elapsed; some drift badly whilst others show sudden and large changes in the recorded pore pressure
- After about 70 days all of the readings have returned to near hydrostatic values

Erratic pore pressure readings such as these have been reported by DiBiaggio[6] and attributed by him to gases generated inside the piezometer

system. The cause of the problem was galvanic action between dissimilar metals. Figure A9.5 shows the data reported by DiBiaggio: trace A suffers a sudden jump of +30kPa, and trace B a gradual drift of ≈100kPa. Neither symptom could be attributed to any "external" cause.

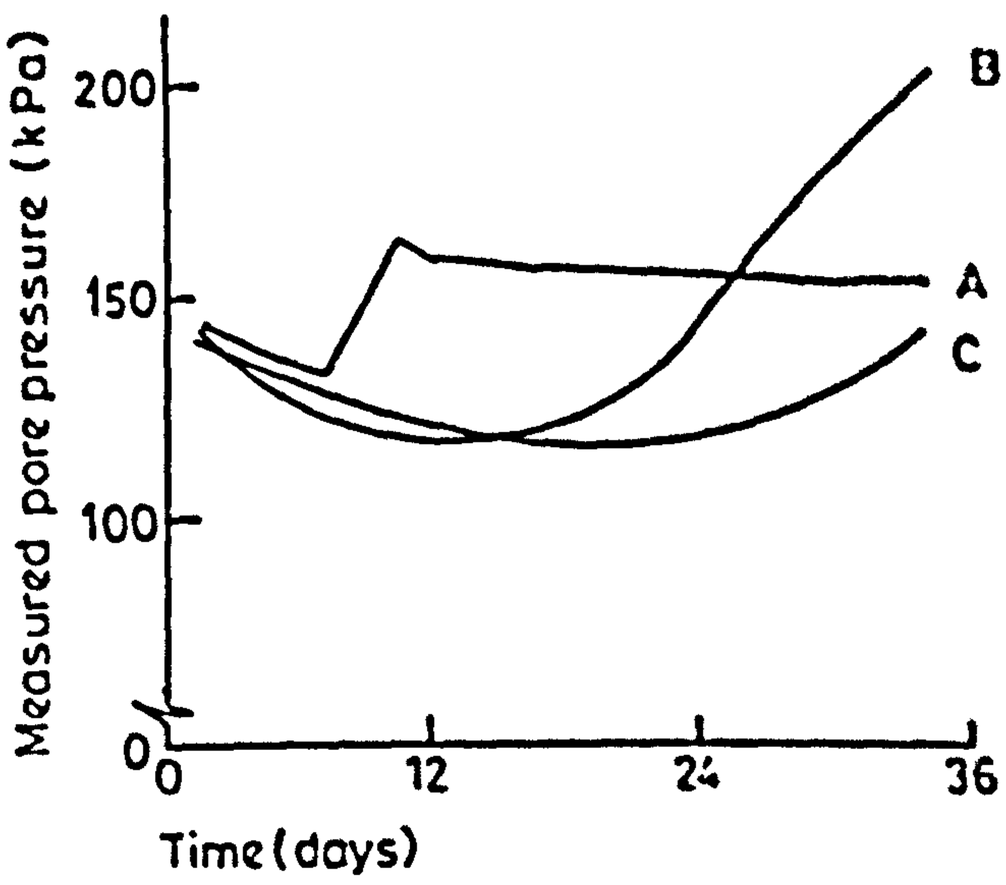


Figure A9.5 Erratic pore pressure observations reported by DiBiaggio

Two-metal corrosion liberates hydrogen gas at the cathode of the galvanic cell, and also produces an electric current that may cause electro-osmosis of the pore water. Both of these processes would tend to increase the pore pressure inside the piezometer.

Based on DiBiaggio's findings, the erratic readings obtained during Test CP1 have been attributed to two-metal corrosion between the molybdenum steel of the pile (the anode) and the stainless steel of the pore pressure block (the cathode). To overcome this problem, the probes were completely re-designed with plastic components (to break the galvanic circuit) and were saturated with silicone fluid (which, unlike water, is <u>not</u> an electrolyte). See Chapter 6 for further details.

Since the pore pressure readings over the first 60h of equalization are highly credible (see Appendix 12), they have been accepted at face value <u>for this period only</u>, and all the subsequent data has been ignored.

Several components suffered from corrosion during test CP1, caused by condensation inside the pile. In later experiments bags of silica gel were used and dry nitrogen was trickled through the pile, in order to absorb any water vapour that might be present.

A9.3 TEST SERIES CP2f - INAUGURATION OF THE IMPERIAL COLLEGE INSTRUMENTED PILE

A9.3.1 Aims of the second Test Series

Test Series CP2 was the inaugural experiment with the newly designed Imperial College Instrumented Pile (ICIP). The main aim of the Test was to obtain the reliable readings of earth and pore pressures that had so far proved elusive. CP2 was designed as a long-term experiment to match both the Pilot Test (CP0) and CP1. The pile was jacked at a fast rate, to confirm the load capacity obtained in the Pilot experiment.

In order to prove the reliability of the new instruments, duplicate readings were taken of all the parameters being measured. At each level there were two pore pressure probes, two surface stress transducers (and temperature sensors), and one axial load cell. The readings of axial load could be checked by comparing the shaft friction between each level (as deduced from the axial load cell readings) with the shear stresses measured by the surface stress transducers.

A sequence of load tests were planned to investigate the effect on the pile's load-

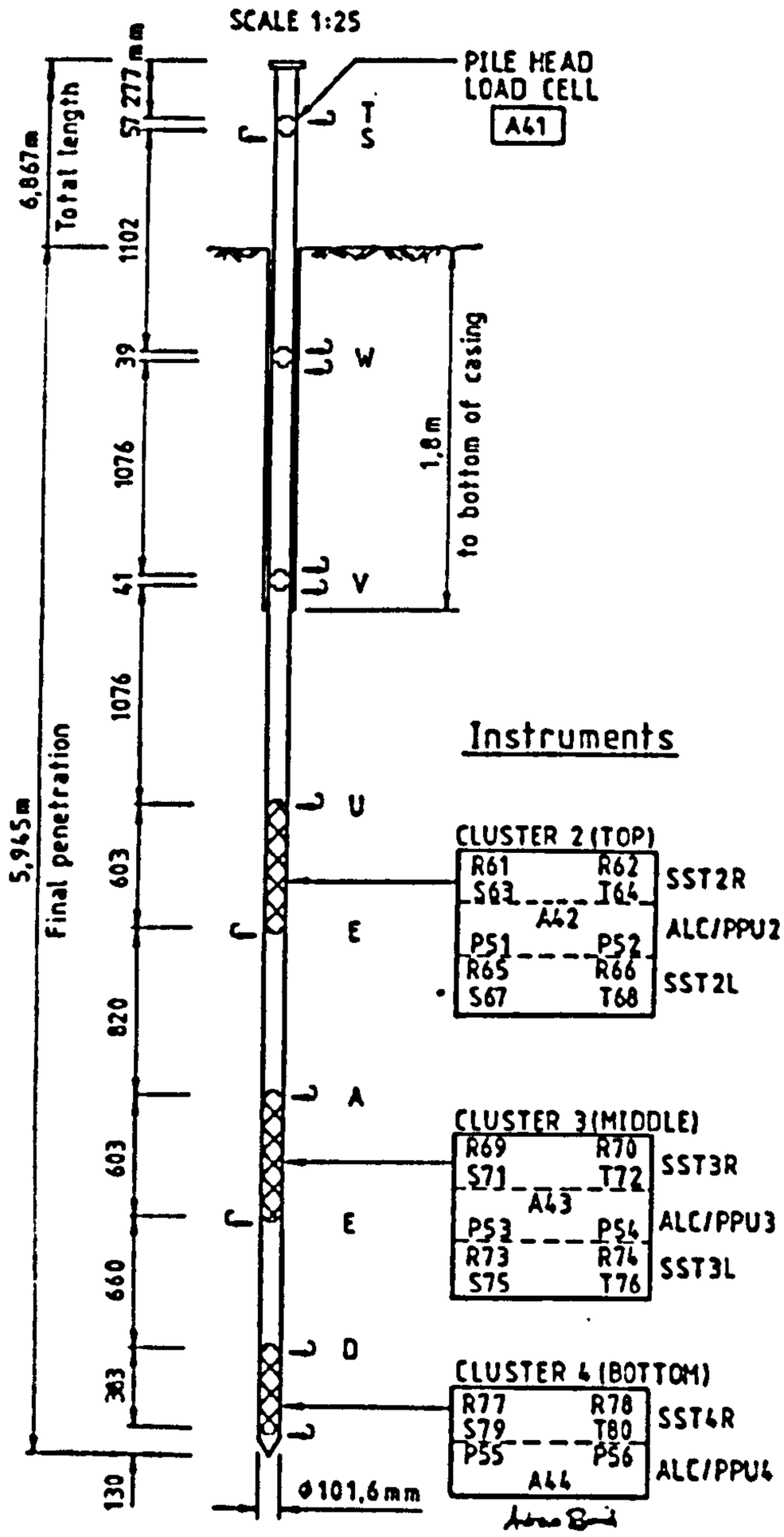


Figure A9.6 Configuration of Pile CP2

displacement characteristics of loading direction (i.e. whether in compression or in tension). In addition, the feasibility of conducting cyclic loading tests was checked.

Key features of pile CP2f

Pile design	Imperial
Overall length	6.87m
Penetration	5.95m
Embedded length L	3.86m
Ratio L/D	38.0
ALCs (sleeved)	4
SSTs (window)	5
PPPs (fast-acting)	6
TSs	5
Installation	Fast
Equalization	Long
Load tests	L1C, L2C, L3T

A9.3.2 Main sequence of events

Pile CP2 was installed on 4th June 1987, at a fast rate of jacking (426 ±34mm/min). Installation took just over 6¼h to complete, owing to major delays (of 1¾ and 2¼h) when the wiring to one of the load cells was damaged (see below).

The pile was left for 63 days before load testing. It was tested on three occasions, twice in compression (L1C and L2C) and once in tension (L3C). Experiment L2C included a limited sequence of cyclic loading. The pile was extracted on day 92.

A9.3.3 Instrument performance

The new instruments performed extremely well throughout experiment CP2. The surface stress transducers gave such consistent results that the number carried in subsequent tests was reduced to one per cluster. This permitted two piles to be commissioned, thereby speeding up the field work significantly.

Unfortunately, during pile installation the wiring to the head axial load cell (A21) was badly damaged, and the readings obtained from it are not trustworthy (and have been ignored). The cell was completely overhauled and re-calibrated before being used again.

On this occasion, the pore pressure traces remained alive throughout pile installation but once again suffered from erratic readings (after three days), as witnessed in Test Series CP1s (see Appendix 9.2.3 above). The absolute values of pore pressure after three days have been ignored,

therefore.

Inspection of the erratic pore pressure traces from both CP1 and CP2 (not shown) reveals:

- Probes situated in the intact, brown London clay produce erratic readings, whereas those in the disturbed London clay do not
- The "lift-off" point for the erratic readings is typically between 3½ and 7 days after pile installation

The design of the fast-acting probes (as used on CP2) prevents galvanic action taking place inside the piezometer system. However, it can still occur elsewhere along the pile - and in particular between the stainless steel housing of the surface stress transducers (SSTs) and the molybdenum steel of the remainder of the pile. Any gases that build up on the SSTs may then diffuse into the adjacent pore pressure probes (which are only ≈25mm away). Also, if electro-osmosis occurs, the resultant higher pore pressures next to the SSTs could in turn be registered by the probes.

Fortunately, from a practical point of view, these problems are not important. Results from all five tests suggest that 95% of the excess pore pressures caused by pile installation have dissipated within three days. Hence, the subsequent erratic readings are of little consequence provided the load tests are planned for the "window" between days three and five (when the signals first go awry).

A9.4 TEST SERIES CP3fs - PROVING THE SIGNIFICANCE OF JACKING RATE

A9.4.1 Aims of the third Test Series

The evidence from the first three experiments at Canons Park (CP0-2) was that the rate of installation of a jacked pile has an overwhelming influence on its subsequent load capacity. To prove this point conclusively, pile CP3 was jacked at a fast rate to a depth of 4.08m, and thereafter jacked at a slow rate (for a further 1.79m). A marked drop in the shear stress measured by the surface stress transducers was expected, together with a significant drop in the axial load needed to push the pile.* A key question to be answered was whether these phenomena were linked to sudden changes in radial total stress or pore pressure. It was better to switch the rate of jacking from fast to slow (rather than vice versa) since it is unlikely that fast (turbulent) shearing can overcome the effects of slow shearing (sliding friction).

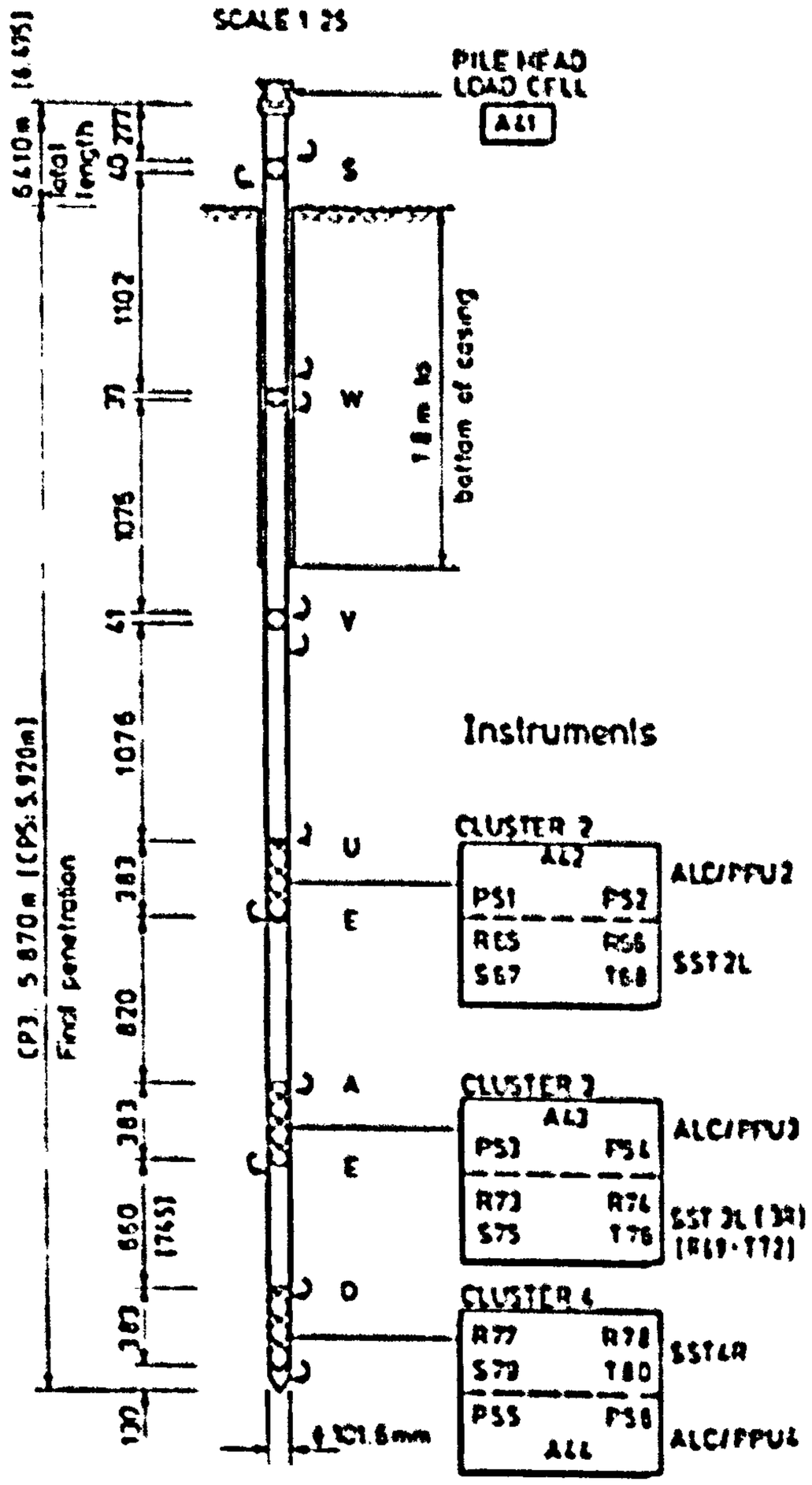


Figure A9.7 Configuration Pile CP3

The only other slow installed pile (CP1s) had been tested following a long equalization period (see Chapter 7). To investigate the effects of

*At least initially: the axial load would build up once more with further penetration of the pile

different set-up times CP3fs was tested in the short term. All three load tests on CP3fs were performed in the space of four days, to avoid the erratic pore pressure readings that had marred the first three tests.

Key features of pile CP3fs

Pile design	Imperial
Overall length	6.41m
Penetration	5.87m
Embedded length L	3.78m
Ratio L/D	37.2
ALCs (sleeved)	4
SSTs (window)	3
PPPs (fast acting)	6
TSs	3
Installation	Fast/slow
Equalization	Short
Load tests	L1C, L2T, L3C

A9.4.2 Main sequence of events

Pile CP3fs was jacked to 4.08m at a fast rate (403 ±94mm/min*); and from 4.08m to 5.87m at a slow rate (81 ±15mm/min†). Installation took 3h 10min in total. The pile was tested in compression (L1C) on day 2; in tension (L2T) on day 3; and finally in compression again (L3C) on day 4. CP3 was extracted from the ground on day 107.

A9.4.3 Instrument performance

The instruments' performance throughout Test Series CP3 was very good, only one circuit being lost (through a wire coming loose). The pore pressure probes showed no signs of gassing up over the restricted time allowed for equalization prior to the first load test. This experiment was the first one to give dependable pore pressure measurements during load testing.

---

*Measured from 3.105 to 4.08m penetration

†Measured from 4.87 to 5.87m

A9.5 TEST SERIES CP4f - LONG-TERM MEASUREMENTS OF PORE PRESSURE

A9.5.1 Aims of the fourth Test Series

Test Series CP4 had one overriding aim: to prove that the sudden increases in pore pressure after 3-5 days that had been witnessed in experiments CP1 and CP2 were in fact spurious. If this was the case then the pore pressures around the pile appeared to reach equilibrium values within a few days of installation.

The pile carried two types of pore pressure probe, one of which was the fast-acting type used in the previous two experiments and the other a flushable probe that could be de-aerated whilst the pile was in the ground. Full details of these probes' design are given in Chapter 6 and Appendix 8. One of each type was mounted at every level to afford direct comparison of the readings obtained.

A9.5.2 Main sequence of events

Pile CP4 was jacked at a fast rate (488 ±45mm/min), over a period of two days. The pile was left for 20 days before load testing in

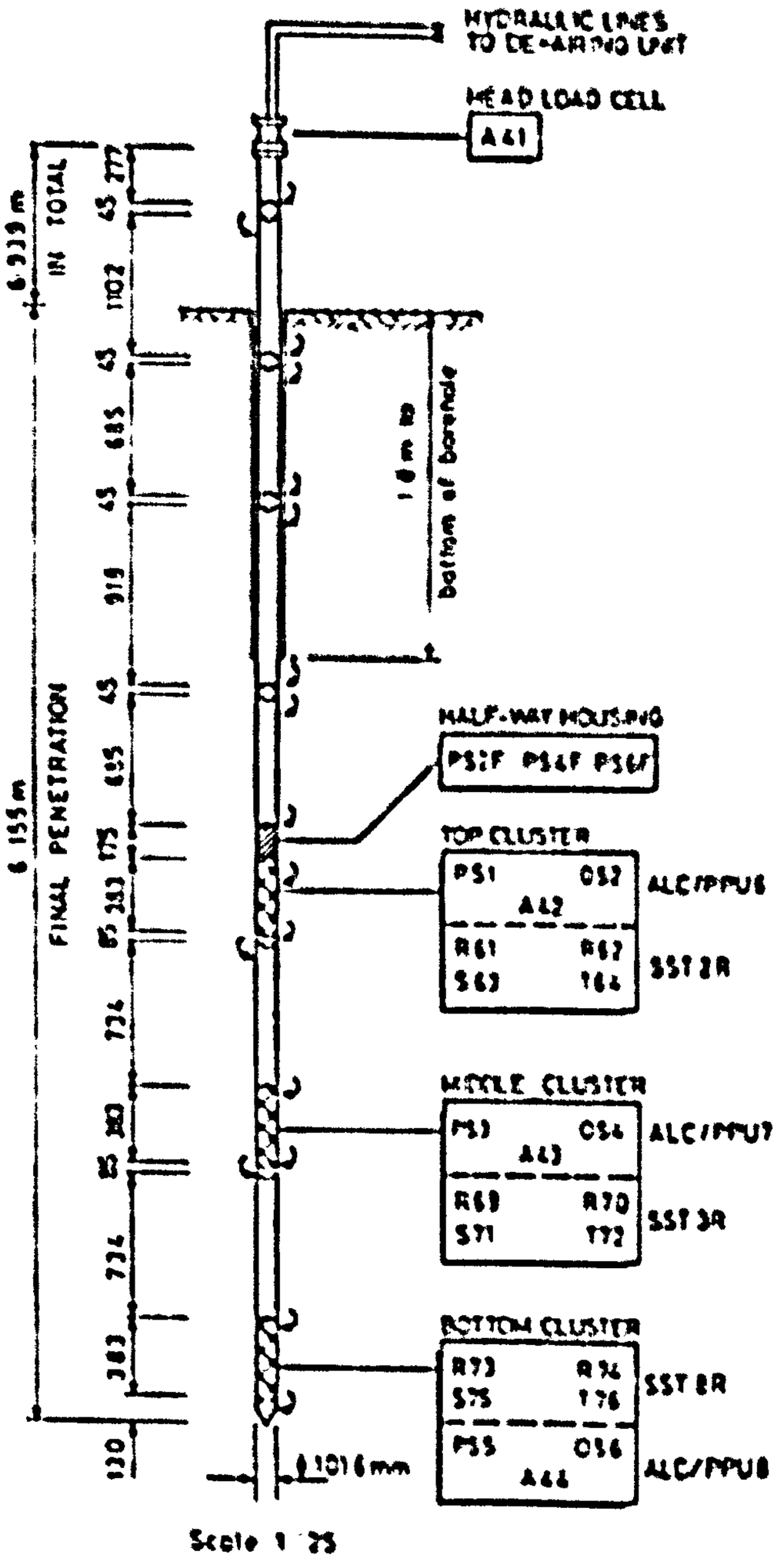


Figure A9.8 Configuration of Pile CP4

tension (CP4f/L1T); and a second load test in compression (L2C) was conducted on day 40. The probes were flushed with de-aerated water on days 5, 18, 27, and 34. Three falling-head permeability tests (CP4f/FHK) were run concurrently from day 34 to day 40 (i.e. between the first and second loading tests); and all three flushable probes were used for hydraulic fracture tests (CP4f/HF), on the day that CP4 was extracted from the ground (day 42).

A9.5.3 Special procedure for installing CP4f

In comparison with previous tests, installation of pile CP4 was made far more difficult by the presence of the six hydraulic tubes running through the pile. The main danger was that some of these tubes might be severed accidentally during the site operations.

Key features of pile CP4f

Pile design	Imperial
Overall length	6.94m
Penetration	6.16m
Embedded length L	4.07m
Ratio L/D	40.0
ALCs (sleeved)	4
SSTs (window)	3
PPPs (fast acting)	3
PPPs (flushable)	3
TSs	3
Installation	Fast
Equalization	Medium
Load tests	L1T, L2C

Installation proceeded as follows. Once the pile had been lifted upright into the loading frame all of the hydraulic lines were flooded with de-aerated water, and their valves closed. A small pat of saturated clay was smeared on the face of the probes' porous discs to prevent water discharging from them. As each of the flushable probes became submerged beneath the water in the borehole, its hydraulic lines were re-charged with de-aerated water to remove any air that had managed to get past the clay.

The pile was then jacked to a depth of 3.49m, and left at this position overnight. It was jacked to its final penetration of 6.16m on the following morning.

Overnight, all of the instruments were monitored. The leading pore pressure probes P55 and O56 (see Figure A9.8) were left at a position midway through the disturbed London clay layer (see Chapter 5); the

following probes P53 and O54 just above the bottom of the 2m deep borehole; and the trailing probes ≈0.6m below ground level.

The hydraulic lines to O52 and O54 were both flushed with de-aerated water at the end of the first day, but O56 was not (in case the pore pressure regime around the tip of the pile was altered). The valves at the top of the hydraulic lines were kept closed throughout installation on the second day.

A9.5.4 Instrument performance

The waterproofing to surface stress transducer 2R failed when the rubber between its window pane and window frame became un-bonded, owing to faulty manufacture. All of its circuits were lost and a significant degree of noise was added to the other instruments' signals, until the offending instrument had been disconnected from the power supply.

The fast-acting pore pressure probes displayed the expected erratic readings after five to six days. The signals from the flushable probes showed a consistent and strong daily cycle, believed to be caused by the expansion and contraction of the hydraulic lines with changes in temperature.

Despite this problem, the trends were clear enough, especially following de-airing, to establish that the values of pore pressure during the medium term were in fact hydrostatic.

A9.6 TEST SERIES CP5f - "CONTROL" EXPERIMENT FOR DRIVEN PILES

A9.6.1 Main aims of the fifth Test Series

CP5 was a dual-purpose experiment, designed to provide reliable pore pressure readings during load testing on a fast-jacked pile, and to act as the control experiment for the subsequent driven pile tests. CP5 was identical to CP3 except for the substitution of the surface stress transducer SST3R for SST3L (see Figure A9.7).

Reliable pore pressure readings had not been obtained during load testing in any of the previous experiments with fast-jacked piles (CP0f, CP2f, and CP4f); the only reliable readings were those from the fast-and-slow pile CP3fs. Therefore, CP5 was installed at a fast rate and load tested after a short equalization period.

The driven piles CP6 and 7 would carry no instruments, and so I were tested in tension to avoid any uncertainty in estimating their end-bearing. CP5f was also tested in tension, to allow direct comparison with the results obtained with the driven piles.

A9.6.2 Main sequence of events

CP5f was jacked at a rate of 445 ±55mm/min, over a period of 2¾h. It was tested twice: once in tension (CP5f/L1T) on day 2; and once in compression (L2C) on day 3. The pile was extracted on day 7, at 520 ±25mm/min.

A9.6.3 Instrument performance

Throughout all stages of CP5f the instruments' performance was exemplary, not a single circuit being lost or causing any problems whatsoever. CP5f is - therefore - an ideal choice to use as the "model" or reference test.

Key features of pile CP5f

Pile design	Imperial
Overall length	6.50m
Penetration	5.92m
Embedded length L	3.83m
Ratio L/D	37.7
ALCs (sleeved)	4
SSTs (window)	3
PPPs (fast acting)	6
TSs	3
Installation	Fast
Equalization	Short
Load tests	L1T

A9.7 ORIENTATION OF INSTRUMENTS

Figure A9.9 records the orientation of the instruments on each pile (CP1-5), looking down their centre-lines (as viewed from above). The common reference line shown on the figure is the line adjoining the centres of

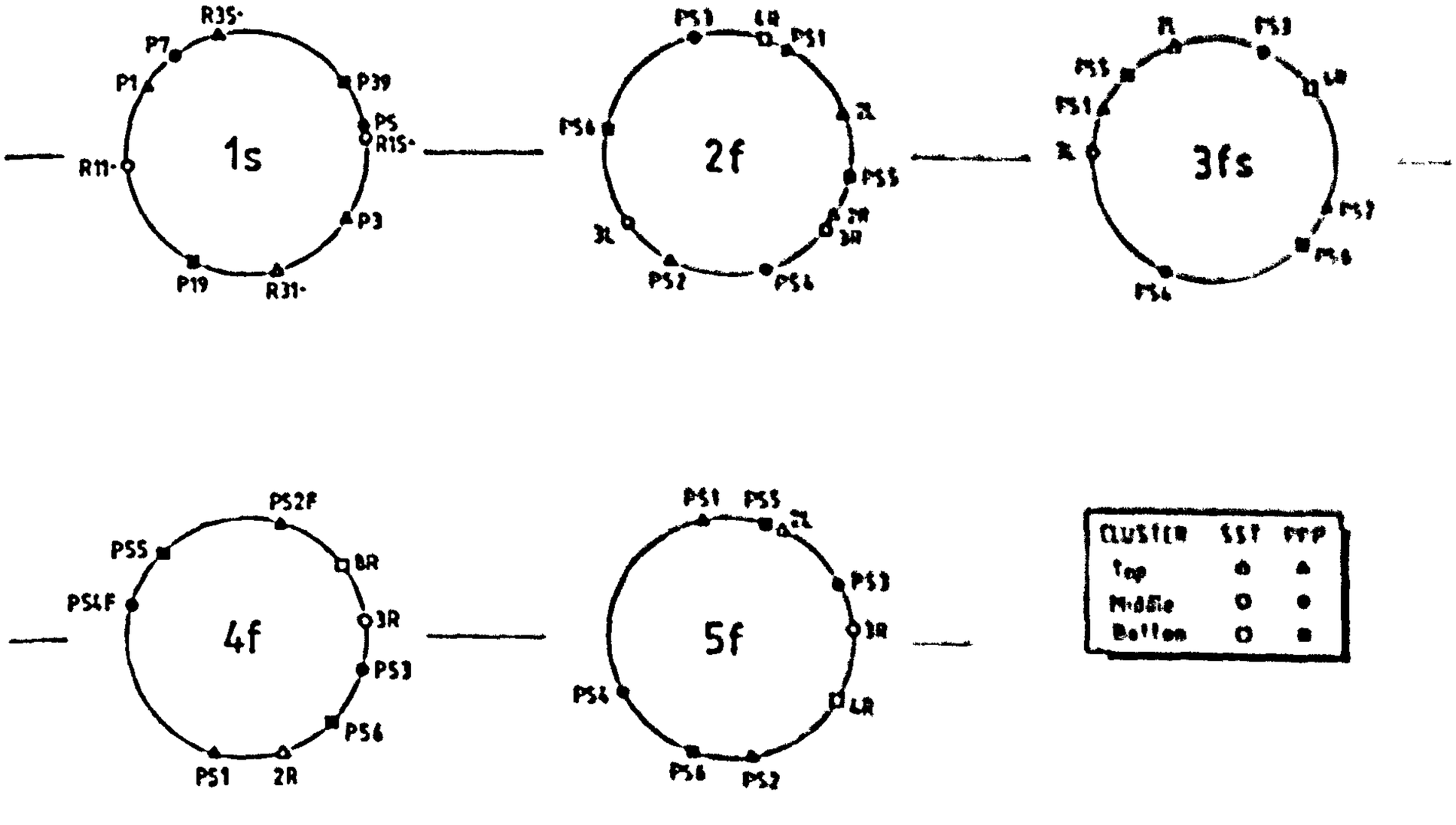


Figure A9.9 Orientation of instruments, Test Series CP1-5

the boreholes through which the piles were installed (see Chapter 7).

A9.8 CONFIGURATION OF INSTRUMENTS

A9.8.1 Test Series CP0-2

General information	CP0f	CP1s	CP2f
Overall length (m)	5.858	5.748	6.867
Diameter D (mm)	101.6	101.6	101.6
Wall thickness (mm)	9.525	9.525	9.525
Depth of penetration (m)	5.200	5.275	5.945
Embedded length L (m)	3.112	3.187	3.857
L/D	30.6	31.4	38.0
D/h	10.7	10.7	10.7
Axial load cells	**Mk I**	**Mks I/II**	**Mk III**
Design type	Unsleeved	Unsleeved	Sleeved
Capacity*	Low	Low/High	Highest
Number used	5	4 (2+2)	4 (3+1)#
Surface stress transducers	**Mk I**	**Mks II/III**	**Mk IV**
Design of housing	Original	Original	"Window"
Cambridge load cell	Original	Horseshoe/Oval+	Dogbone
Number used	8	4 (1+3)	5
Pore pressure units	**Mk I**	**Mk II**	**Mk III**
Design of housing	Original	Original	Combined$
Mounting block	Steel	Stainless steel	Acetal copolymer
Porous stone	Clay	Bronze	St. steel
Saturating fluid	Water	Water	Silicone fluid
Transducer type (Druck)	PDCR 81	PDCR 81	PDCR 81
Number used	4	6	6
Temperature sensors			
Number used	0	2	5

---

*Load cell capacities are: low ≈118kN; high ≈168kN; highest ≈209kN

#Three Mk III cells, plus one Mk II cell at the pile head

+The Horseshoe cell is the Mark II, the Oval the Mark III design

$Combined with the sleeved axial load cell

A9.8.2 Test Series CP3-5

General information	CP3fs	CP4f	CP5f
Overall length (m)	6.410	6.939	6.495
Diameter D (mm)	101.6	101.6	101.6
Wall thickness (mm)	9.525	9.525	9.525
Depth of penetration (m)	5.870	6.155	5.920
Embedded length L (m)	3.782	4.067	3.832
L/D	40.1	42.9	37.7
D/h	10.7	10.7	10.7
Axial load cells	**Mk III**	**Mk III**	**Mk III**
Design type	Sleeved	Sleeved	Sleeved
Capacity	Highest	Highest	Highest
Number used	4 (3+1)	4 (3+1)	4 (3+1)
Surface stress transducers	**Mk IV**	**Mk IV**	**Mk IV**
Design of housing	"Window"	"Window"	"Window"
Cambridge load cell	Dogbone	Dogbone	Dogbone
Number used	3	3	3
Pore pressure units	**Mk III**	**Mks III/IV**	**Mk III**
Design of housing	Combined	Combined	Combined
Mounting block	Acetal copolymer	Acetal copolymer	Acetal copolymer
Porous stone	St. steel	St. steel	St. steel
Saturating fluid	Silicone fluid	Silicone fl./water*	Silicone fluid
Transducer type (Druck)	PDCR 81	PDCR 81/200	PDCR 81
Number used	6	6 (3+3)#	6
Temperature sensors			
Number used	3	3	3

*The Mark III system was saturated with silicone fluid: the Mark IV with de-aired water

#One Mark III system (with the PDCR 81) and one Mark IV (with the PDCR 200) in each instrumented section; the Mark IV system can be flushed through with de-aired water when the pile is underground, whereas the Mark III cannot

A9.9 NOTES AND REFERENCES

[1]See Chapter 9, pp210-249 of: Jardine R.J. (1985). Investigations of pile-soil behaviour, with special reference to the foundations of offshore structures. PhD Thesis, Univ. of London (Imperial College), 2 vol., 789pp.

[2]Jardine (1985), loc. cit., p232, Section 9.9.1.

[3]Jardine (1985), loc. cit., p241, paragraph 9.12.3.

[4]Jardine (1985), loc. cit., Figures 9.25, 9.26, and 9.27.

[5]In particular, at Brent Cross, north London (London clay); Cowden, North Humberside (glacial till); and Madingley in Cambridge (Gault clay). See Lunne T., Powell J.J.M., Quarterman R.S.T., and Eidsmoen T.E. (1986). Piezocone testing in overconsolidated clays. Proc. 39th Can. Geotech. Conf. on 'Insitu Testing and Field Behaviour', Carlton Univ., Ottawa, Canada, pp209-218.

[6]DiBiaggio E. (1977). Field instrumentation - a geotechnical tool. Proc. 1st Baltic Conf. on Soil Mech. & Found. Engng, Gdansk, 1, pp29-40.

Appendix 10

Instrument performance (tests CP1-5)

CONTENTS OF APPENDIX 10

A10.1 INSTRUMENT RELIABILITY: TEST SERIES CP1S 660
A10.2 INSTRUMENT RELIABILITY: TEST SERIES CP2F 661
A10.3 INSTRUMENT RELIABILITY: TEST SERIES CP3FS 662
A10.4 INSTRUMENT RELIABILITY: TEST SERIES CP4F 663
A10.5 INSTRUMENT RELIABILITY: TEST SERIES CP5F 664

A10.1 INSTRUMENT RELIABILITY: TEST SERIES CP1S

Instrument	Circuit number	FSO	Non-linearity & hysteresis (%FSO)	Temperature sensitivity (per °C)	Zero shift	Response time t_{99} (ms)
Axial load cells						
		kN		kN	kN	
MCB/MRE	MCB	+199	0.24	?	?	-
S-T	A21	+144	0.20	-0.011	+4.9	-
		-120	0.16			-
O-P	A23	+140	0.24	+0.034	+5.8	-
		-120	0.21			-
K-L	A25	+80	1.34	-0.004	-6.2	-
		-80	0.80			-
G-H1	A27	+110	1.48	-0.0001	+1.2	-
		-80	0.59			-
Surface stress transducers						
		kPa		kPa	kPa	
Oval 1	R11	+555*	2.12	+0.39	-472.8	-
Oval 2	R15	"	2.39	N/A#	-969.1	-
Oval 3	R31	"	0.59	+0.30	-128.5	-
H'shoe	R35	"	1.49	+1.21	+817.6	-
Oval 1	S13	±200	0.70	-0.20	-1.6	-
Oval 2	S17	"	0.51	N/A	-5.2	-
Oval 3	S33	"	1.15	-0.053	-21.7	-
	S35	"	1.50	+0.36	-26.9	-
Pore pressure transducers						
		kPa		kPa	kPa	
	P1	1035	0.23	+0.27	-1.6	<1 000+
	P3	"	0.50	-1.24	-16.1	51 000
	P5	"	0.46	-1.26	-4.8	33 000
#2575	P7	"	0.25§	-0.23	-8.8	<1 000
#3432	P19	"	0.17§	+0.73	-28.6	?**
#3434	P39	"	0.15	+0.47	+27.0	?
Displacement transducers						
		mm				
D1		38	0.07	?	-	-
D2		"	0.08	?	-	-
D3		"	0.04	?	-	-

*This is the maximum load applied using dead weights. Further testing was done using a lever arm to obtain higher loads (of up to 1000kPa). No change in sensitivity occurred at the higher loads

#Not available: wiring accidently disconnected during temperature calibration

+The response times of these transducers were measured rather crudely, by recording signals on the data-logger (at 1s intervals), as a sudden step in pressure (of 345kPa) was applied. The figures given are the 99% response times. With this method response times of less than 1s could not be resolved

§The Manufacturer's figure for combined non-linearity and hysteresis is ±0.2% My calibrations for P19 and P39 gave sensitivities +2.9% higher than those given by Druck (Manufacturer's figures were not available for the other transducers)

**Although the response times of transducers P19 and P39 were not actually measured, it is clear from the values for non-linearity and hysteresis that they were of the same order as those of P1 and P3 (i.e. <1s)

A10.2 INSTRUMENT RELIABILITY: TEST SERIES CP2F

Instrument	Circuit number	FSO	Non-linearity & hysteresis (IFSO)	Temperature sensitivity (per °C)	Zero shift	Response time t_{95} (ms)
Axial load cells						
		kN		kN	kN	
NCB/MRE	NCB*	+198	0.13	?	?	-
Head	A41*	+140	1.16	?	2.2	-
ALC2	A42#	+160	0.14	+0.072	-0.66	-
		-99	0.20			-
ALC3	A43	+160	0.24	-0.040	-0.84	-
		+99	0.20			-
ALC4	A44	+160	0.13	+0.034	-1.46	-
		-99	0.28			-
Surface stress transducers						
		kPa		kPa	kPa	
SST2R	R61/62	+500	0.40	-2.37	+5.8	-
SST2L	R65/66	"	0.54	-1.68	-14.4	-
SST3R	R69/70	"	0.26	-1.87	-0.33	-
SST3L	R73/74	"	0.53	N/A$	-	-
SST4R	R77/78	"	0.58			-
SST2R	S63	±146	1.17$	?	-82.4	-
SST2L	S67	"	1.01	-0.019	-0.22	-
SST3R	S71	"	0.85	-0.041	-1.03	-
SST3L	S75	"	1.93	N/A	-	-
SST4R	S79	"	?			-
Pore pressure transducers						
		kPa		kPa	kPa	
#3440	PS1	1034	0.18		-5.1	10-30**
#3437	PS2	"	0.18		+0.3	50-65
#3433	PS3	"	0.21		+17.8	+100
#3431	PS4	"	0.22		+18.4	150-400
#3439	PS5	"	0.22		+172.5##	23-64
#3438	PS6	"	0.16		+3.0	100-250

Displacement transducers
Same as for Test Series CP1s

---

*This is the same load cell as was used in Test Series CP1s, under the designation A21. The change in sensitivity between the two calibrations was +0.11% in compression, and -0.22% in tension. This cell's wiring was damaged during pile installation, necessitating some hasty repairs on site. The re-wired cell was calibrated after the end of the Test Series, with the less reliable values of non-linearity and hysteresis given here

#This axial load cell was tested with and without the "Nu-Lip" rubber ring in place. The presence of the ring changed the sensitivity by -0.06% This cell was also tested for cross-sensitivity to radial total stress, by applying a water pressure of up to 1.1MPa to its protective sleeve. There was no discernible cross-sensitivity

+The wiring of this transducer was damaged during pile assembly, prior to temperature calibration

$These values are not reliable because they include errors due to misalignment of the transducer in its calibration cradle. An angular mis-alignment of just 0.25° produces additional noise in the signal of around 1.6% FSO. This noise does not systematically affect the calibration coefficients, but it does obscure the degree of non-linearity and hysteresis that the circuit suffers from. The values given for non-linearity and hysteresis are, therefore, much exaggerated

**The response times for these transducers were measured using an oscilloscope. The time quoted is that taken to record fully a step in pressure of ±80kPa

##The major proportion of this zero shift occurred between calibration and installation, namely +131.2kPa. Somewhat surprisingly, this transducer was well-behaved during Test Series CP1fs

A10.3 INSTRUMENT RELIABILITY: TEST SERIES CP3FS

Instrument	Circuit number	FSO	Non-linearity & hysteresis (IFSO)	Temperature sensitivity (per °C)	Zero shift	Response time t_{99} (ms)
Axial load cells		kN		kN	kN	
MCB/MRE	MCB	As CP2f (q.v.)				
Head	A41*	As CP1s/A23		?	?	-
ALC2	A42	As CP2f		<0.06	-0.91	-
ALC3	A43	As CP2f		<0.06	-0.03	-
ALC4	A44	As CP2f		<0.06	-0.66	-
Surface stress transducers		kPa		kPa	kPa	
SST2L	R65/66	+586	0.48#	-1.62	-14.1+	-
SST3L	R73/74§	"	0.38	-1.65	-0.18	-
SST4R	R77/78	"	0.39	-2.12	+0.48	-
SST2L	S67	±146	0.66	-0.004	-0.57	-
SST3L	S75	"	0.64	+0.15	-0.58	-
SST4R	S79	"	0.74	-0.03	-5.71	-
Pore pressure transducers		kPa		kPa	kPa	
#3440	PS1	1034	0.36**	-0.26	+1.1	?
#3437	PS2	"	0.34	-1.33	-0.4	?
#3433	PS3	"	0.37	+0.46	-6.8	?
#3431	PS4	"	0.17	+0.31	+8.7	?
#3439	PS5	"	0.13	-0.04	-3.5	?
#3438	PS6	"	0.15	-0.59	+7.9	?

Displacement transducers
Same as for Test Series CP1s

---

*This is the same cell as was used in Test Series CP1s, under the designation A23

#The wiring to these transducers was damaged during Test Series CP2f, and so they were re-calibrated prior to CP3fs, giving direct sensitivities that differed from the original values by the following percentages:

Instrument	Change in sensitivity	Instrument	Change in sensitivity
R65/66	-0.10%	S67	-0.39%
R73/74	-0.31%	S75	-0.83%
R77/78	+0.25%	S79	+0.30%

+One of the two circuits appears to be drifting slowly but steadily with time (a similar zero shift occurred in Test Series CP2)

§This transducer was tested for cross-sensitivity to axial load, Q, and gave a roughly bi-linear response:

Axial load (kN)	$\Delta\sigma_{rr}/\Delta Q$ (kPa/kN)	$\Delta r_{rr}/\Delta Q$ (kPa/kN)
$0 \leq Q \leq 40$	-0.55	-0.015
$40 \leq Q \leq 100$	-0.13	-0.015

Note that these figures were measured with the transducer standing unsupported (in air). When below ground level the cross-sensitivity to axial load would be much reduced, particularly in stiff soils

**On re-calibrating these transducers, the following changes in sensitivity (from that recorded prior to CP2b) were noted:

Instrument	Change in sensitivity
PS1	+0.28%
PS2	+0.21%
PS3	-1.39%
PS4	-3.57%
PS5	+1.00%
PS6	-0.03%

A10.4 INSTRUMENT RELIABILITY: TEST SERIES CP4F

Instrument	Circuit number	FSO	Non-linearity & hysteresis (IFSO)	Temperature sensitivity (per °C)	Zero shift	Response time t_{95} (ms)
Axial load cells		kN		kN	kN	
MCB/MRE	MCB	+200	0.24	?	?	*
Head	A41	As CP1s/A23 (q.v.)				
ALC6	A42	+199	0.38		+4.74	*
		-120	0.34			*
ALC7	A43	+159	0.14		+2.73	*
		-120	0.36			*
ALC8	A44	+150	0.24		+2.86	*
		-60	0.31			*
Surface stress transducers		kPa		kPa	kPa	
SST2R	R61/62	As CP2f (q.v.)			N/A*	
SST3R	R60/70	As CP2f (q.v.)			+23.6	
SST8R	R73/74	+621	0.49		-238.8	*
SST2R	S63	As CP2f (q.v.)			-	
SST3R	S71	As CP2f (q.v.)			-3.78	
SST8R	S75	±144	1.37		+0.23	*
Pore pressure transducers		kPa		kPa	kPa	
#3440	P51	1035	0.11		-0.98	?
#2913	P52F[#]	690	0.13	See 16	-4.0	<100
#3433	P53	1035	0.12		-17.9	?
#2915	P54F[+]	690	0.18	See 16	+3.25	<100
#3439	P55	1035	0.14		+33.3	?
#2922	P56F[§]	690	0.10	See 16	+1.84	<100

Displacement transducers
Same as for Test Series CP1s

---

*Not available: circuits R61, R62, and S63 all became unstable when SST2R's waterproofing failed. Note that S63 also displayed a large zero shift in Test Series CP2

#Volume of hydraulic lines (as measured) = 23.6 x 10^3mm^3

+Volume of hydraulic lines (as measured) = 28.4 x 10^3mm^3; compliance 1.3mm^3/kPa; creep rate 1.8mm^3/kPa in 12.2h

§Volume of hydraulic lines (as measured) = 32.5 x 10^3mm^3; compliance 0.73mm^3/kPa; creep rate 0.28mm^3/kPa in 12.2h

A10.5 INSTRUMENT RELIABILITY: TEST SERIES CP5F

Instrument	Circuit number	FSO	Non-linearity & hysteresis (%FSO)	Temperature sensitivity (per °C)	Zero shift	Response time t_{99} (ms)
<u>Axial load cells</u>		kN		kN	kN	
MCB/MRE	MCB	+200	0.24	?	?	-
Head	A41	As CP1s/A23 (q.v.)				
ALC2	A42	As CP3fs (q.v.)			-0.42	-
ALC3	A43	As CP3fs (q.v.)			+0.52	-
ALC4	A44	As CP3fs (q.v.)			-0.26	-
<u>Surface stress transducers</u>		kPa		kPa	kPa	
SST2L	R65/66	As CP3fs (q.v.)			-1.08	-
SST3R	R73/74	+690	0.15		-10.6	-
SST4R	R77/78	As CP3fs (q.v.)			+13.9	-
SST2L	S67	As CP3fs (q.v.)			+1.75	-
SST3R	S75	As CP4f (q.v.)			+0.50	-
SST4R	S79	As CP3fs (q.v.)			+1.15	-
<u>Pore pressure transducers</u>		kPa		kPa	kPa	
#3440	PS1	1035			+0.87	?
#3437	PS2	"			+0.10	?
#3433	PS3	"			-1.43	?
#3433	PS4	"			+4.63	?
#3439	PS5	"			-2.04	?
#3438	PS6	"			+6.91	?

<u>Displacement transducers</u>
Same as for Test Series CP1s

Appendix 11

Further test results: pile installation

CONTENTS OF APPENDIX 11

A11.1 PORE PRESSURE RESPONSE DURING PILE INSTALLATION 668

A11.1.1 Introduction 668

A11.1.2 Test Series CP1s 668

A11.1.3 Test Series CP2f 669

A11.1.4 Test Series CP3fs 670

A11.1.5 Test Series CP4f 671

A11.2 RELIABILITY OF THE PORE PRESSURE READINGS 673

A11.3 SUMMARY OF RESULTS FROM CANONS PARK EXPERIMENTS 675

A11.4 NOTES AND REFERENCES 676

A11.1 PORE PRESSURE RESPONSE DURING PILE INSTALLATION

A11.1.1 Introduction

This section presents the pore pressures traces from *leading* instrument positions in Test Series CP1-4. (The corresponding traces for Test Series CP5 are shown in Chapter 9.) Brief notes are given about any unusual features of these records.

A11.1.2 Test Series CP1s

See Figure A11.1. Probes saturated with water; note how the traces "die" on entering the disturbed London clay - cf. records from later tests using fast-acting probes saturated with silicone fluid.

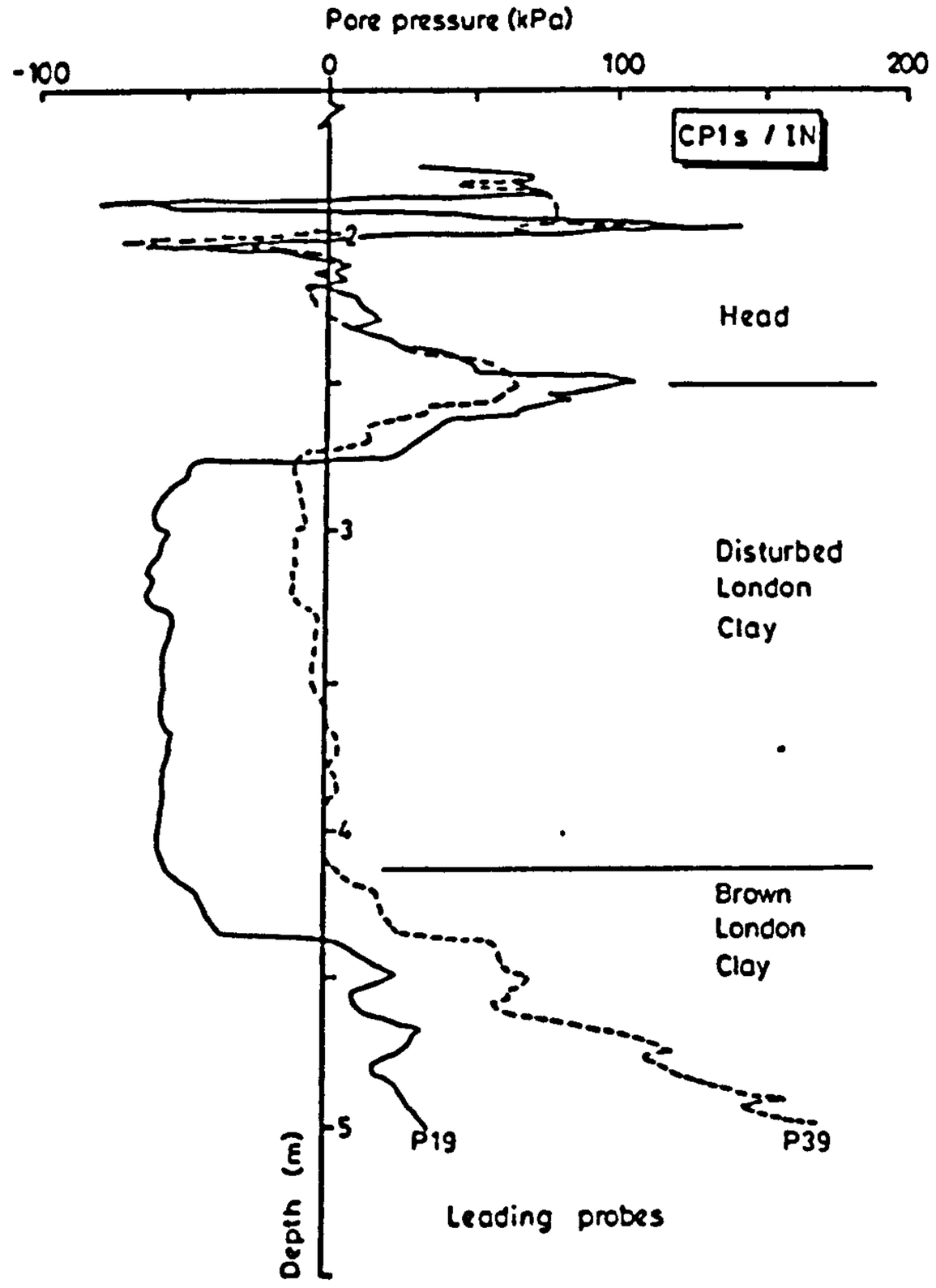


Figure A11.1 Pore pressures recorded at leading instrument positions during pile installation, Test Series CP1s

A11.1.3 Test Series CP2f

See Figure A11.2. First experiment using fast-acting probes (saturated with silicone fluid). Note how traces remain "alive" during installation, recording the changes in pore pressure during pauses in jacking. The

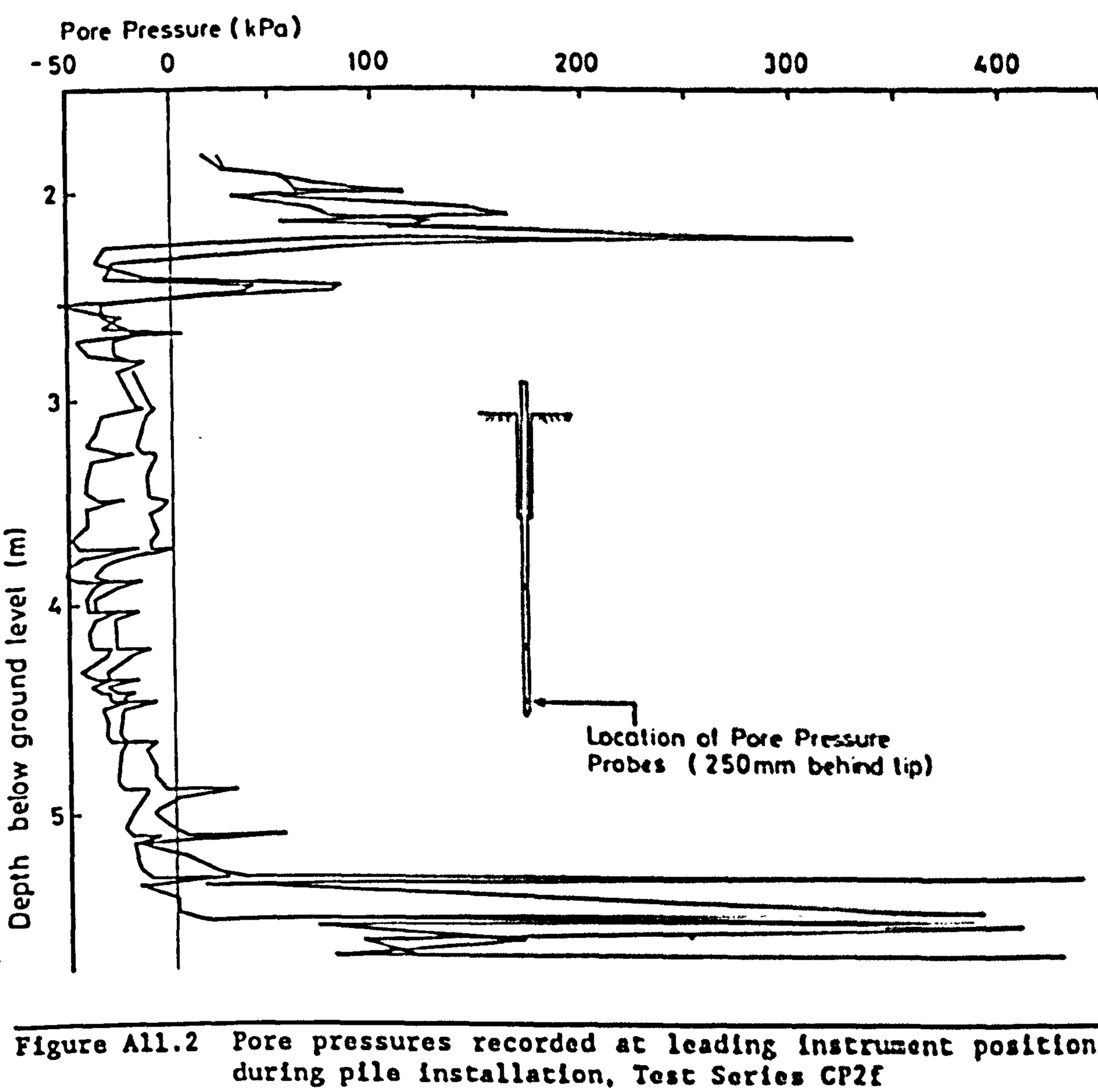


Figure A11.2 Pore pressures recorded at leading instrument positions during pile installation, Test Series CP2f

change in response below 5m is believed to be the result of a change in permeability of the soil (pause periods were, if anything, *shorter* below 5m than above).

A11.1.4 Test Series CP3fs

See Figure A11.3. Note the excellent agreement with the pressures recorded in CP2f/IN. The change in jacking rate from fast to slow, when the leading probes were at 3.81m, has no obvious effect on the pore

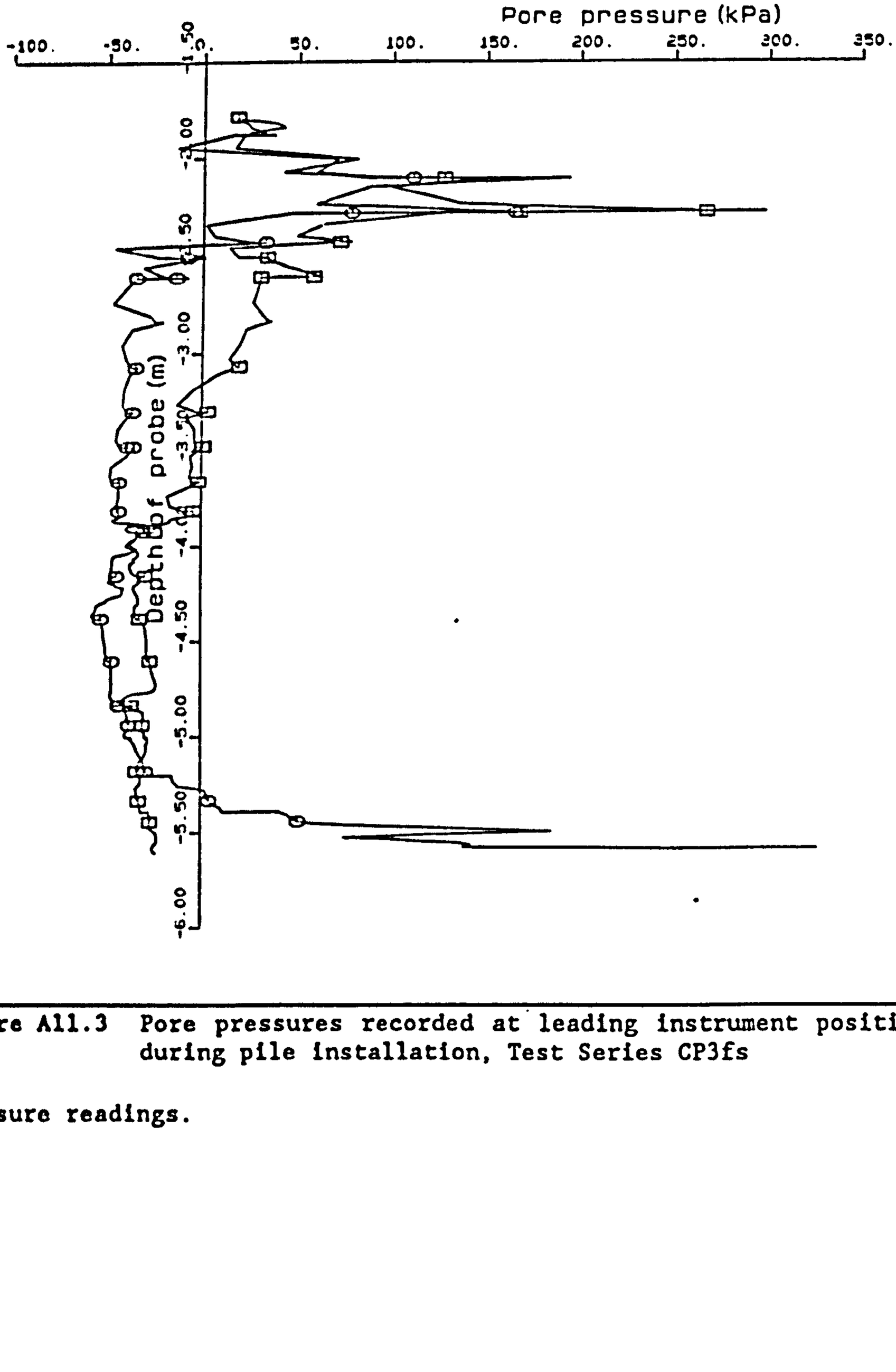


Figure A11.3 Pore pressures recorded at leading instrument positions during pile installation, Test Series CP3fs

pressure readings.

A11.1.5 Test Series CP4f

See Figure A11.4. Note only one fast-acting pore pressure probe at each level (there being a flushable probe on the other side of the pile). Much higher pore pressures were recorded in CP4f/IN (in the pause periods between pushes) than in any other test (see Section A11.2) for a discussion of this point). The reason for this is uncertain, but the following are possible causes:

- The presence of the flushable probe may have affected the response of the fast-acting one on the other side of the pile. The flushable probes were filled with water during installation, although their valves (at the head of the pile - see Figure 6.13, p257) were closed. Maybe the free water in the flushable probes prevented de-saturation of the fat-acting ones?
- The fast-acting probes may have been better saturated prior to CP4f than prior to the other tests. However, I am aware of no change in the saturation procedure between tests, so this seems unlikely.

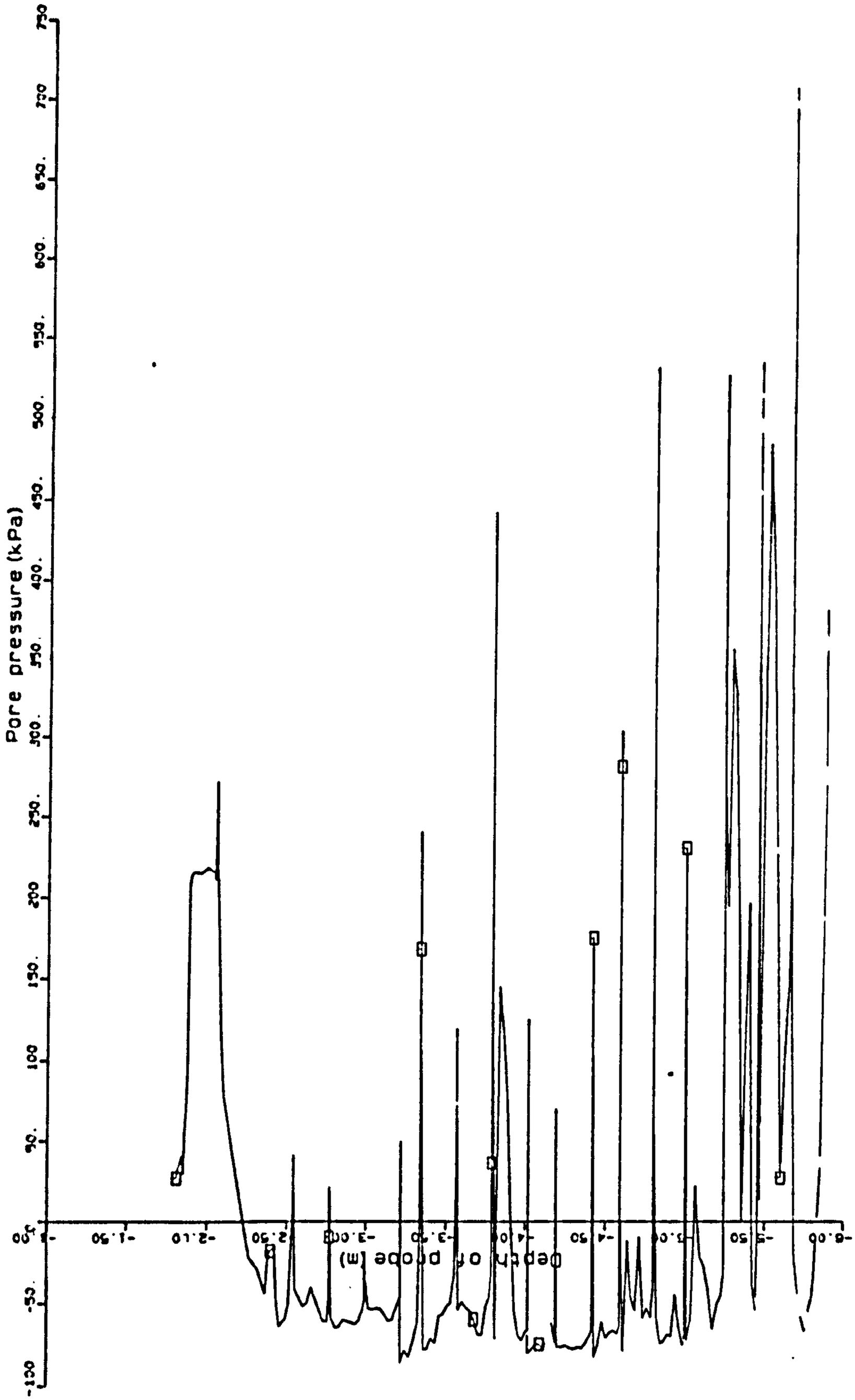


Figure A11.4 Pore pressures recorded at leading instrument positions during pile installation, Test Series CP4f

A11.2 RELIABILITY OF THE PORE PRESSURE READINGS

The measurement of negative pore pressures is fraught with difficulties Fluids are unable to sustain tension, except when they are confined in extremely small spaces and can benefit from the effects of surface tension. It follows that, even if the water in the soil can exist at a pressure below absolute zero (-100kPa gauge pressure), the fluid in the piezometer cannot. The consequence is that pore pressure readings in dilating soils experience a "cut-off" when the piezometer fluid cavitates, at about -50kPa.*

Cavitation has at least two adverse effects. The first is that the pore pressure <u>in the soil</u> is not known. Is it the same as that in the piezometer (i.e. -50kPa)? Or does the soil sustain a pore water suction whose magnitude might be tens or even hundreds of kilopascals? Does Terzaghi's principle of effective stress[1] still hold if the pore water cavitates? If not, what laws of physics govern the soil's behaviour during shear?

The second problem concerns the piezometers' response times after they have cavitated. During cavitation any air in the piezometer fluid will come out of solution, thereby de-saturating the device and rendering it slow to respond. Hence it is essential to saturate pore pressure probes with a thoroughly de-aerated fluid every time they are used.

Even if they are thoroughly de-aerated, the pore pressure probes can still obtain air from the water in the ground. Any suction that exists in the soil when it dilates has the effect of emptying the piezometer cavity of some of its original saturating fluid. When the dilation stops, the suction disappears and the device fills up with <u>water</u> (from the soil). If this water contains air then the probe becomes de-saturated. *One thing I observed at the end of each test at Canons Park was the presence of small amounts of water inside all the fast-acting pore pressure probes.*

---

*Owing to impurities in the fluid, the cavitation pressure is in practice between -50 and -80kPa

The ability of a piezometer to *recover* from cavitation depends on how well it resists the inflow of air during installation. The probes that were saturated with silicone fluid (Tests CP2-5) performed this task extremely well, whereas those saturated with water (CP1) did not. (Note that Lunne et al.[2] also obtained a far better response from piezocones saturated with silicone fluid than from those saturated with water.) The reason for this is probably the fact that silicone fluid and water are not miscible, and hence any vaporized fluid in the probe is encouraged to stay there by the presence of water in the soil.

I have great confidence in the performance of the fast-acting probes during Test Series CP2-5. As demonstrated in Chapter 9, the traces recorded by these instruments remained alive throughout pile installation, and - in CP4f - were able to register changes in pore pressure of up to ±500kPa in less than six seconds (see Table A11.1.)

Table A11.1 Pore pressure response in CP4f/EQ

Time (h:m:s)	Reading (kPa)
12:45:54.4	13.4
12:45:57.4	297.8
12:46:00.4	484.9
12:53:29.6	660.5
12:53:32.6	168.4
12:53:35.6	-20.7

Proof that the pressures recorded by the fast-acting probes are reliable in the other tests (CP2f, CP3fs, and CP5f) is provided by the sudden change in the soil's response at a depth of ≈5.5m. For example, in CP5f (see Figure 9.1 on p305) the probes recorded a rise in pore pressure of ≈300kPa in less than 2¼ minutes, whereas at *shallower* depths no such increase was noted during pauses of up to 1h 10min. It is inconceivable that a slow-responding instrument could fail to register a large (positive) pore pressure at a depth of (say) 4½m, and then do so later within a few minutes.

A11.3 SUMMARY OF RESULTS FROM CANONS PARK EXPERIMENTS

Table A11.2 summarizes some of the key parameters that were recorded in the instrumented pile tests at Canons Park. These include:

- The value of z/R at each instrument position
- The overconsolidation ratio, based on an assumed overburden of 155m of submerged clay (OCR_{155})
- The coefficient of earth pressure at rest (K_0)
- The soil's undrained strength ratio (c_{uo}/σ'_{vo}), based on unconsolidated undrained (UU) triaxial compression tests
- The normalized horizontal total stress at the end of pile installation (H_i)
- The excess pore pressure ratio at the end of installation ($\Delta u_i/\sigma'_{vo}$)
- The maximum excess pore pressure ratio during equalization ($\Delta u_{max}/\sigma'_{vo}$)
- The lateral stress coefficient at the end of installation (K_i)
- The lateral stress coefficient at the end of equalization (K_e)

Table A11.2 Summary of results from the Canons Park pile tests

Test	Depth (m)	z/R	OCR_{155}	K_0[¶]	c_{uo}/σ'_{vo}	H_i	$\Delta u_i/\sigma'_{vo}$	$\Delta u_{max}/\sigma'_{vo}$[¶¶]	K_i	K_e
CP1s	3.17	41.5	39 ±9	2.51	1.90	5.1-6.0	?	?	?	?
	4.14	22.1	32 ±7	2.33	1.85	7.6	?	?	?	?
CP2f	2.84	61.2	42 ±9	2.58	2.06	2.62	$u_i < 0$	≈0.00	3.77	4.63
	3.26	52.9	38 ±8	2.48	1.86	4.03	$u_i < 0$	≈0.00	5.70	5.87
	4.26	24.9	31 ±7	2.30	1.84	8.93	$u_i < 0$	4.05	10.2	7.33
	5.52	8.3	25 ±6	2.12	1.89	17.6	0.56 1.23	5.08	17.1	13.0
CP3fs	3.40	51.6	37 ±8	2.46	1.80	2.55	$u_i < 0$	≈0.24	3.46*	3.09
	4.61	24.9	29 ±6	2.24	2.21	8.94	$u_i < 0$	≈0.83	10.30#	7.12
	5.45	8.3	26 ±6	2.15	1.91	13.3	1.48 $u_i < 0$	6.89	11.3-14.0	11.0
CP4f	3.53	51.7	36 ±8	2.43	1.75	3.00?	$u_i < 0$	≈0.53	?	?
	4.73	28.0	29 ±6	2.24	2.16	11.8	$u_i < 0$	≈0.35	12.1	?
	5.73	8.3	24 ±5	2.08	1.84	10.6?	2.07	11.1§	?	?
CP5f	3.37	50.2	37 ±8	2.46	1.81	3.20	$u_i < 0$	≈0.88	3.60†	3.38
	4.57	26.5	29 ±6	2.24	2.23	13.0	$u_i < 0$	≈0.21	14.8	9.67
	5.50	8.3	25 ±6	2.12	1.90	17.4	$u_i < 0$	5.36	17.8†	12.8

? = data not reliable (problems with instrumentation)
[¶]In general, values quoted are accurate to ±0.22
[¶¶]Higher of the two values measured at each depth
*±0.07; #±0.22; †±0.47; ‡±0.32
§σ_{rr} = 736kPa, u = 783kPa = σ'_{rr} < 0! (u measured slightly nearer to the pile tip)

A11.4 NOTES AND REFERENCES

[1]Terzaghi K. (1936). The shearing resistance of saturated soils and the angle between the planes of shear. Proc. 1st Int. Conf. Soil Mech. & Fdn Engng, Cambridge, 1, pp161-165.

[2]Lunne T., Powell J.J.M., Quarterman R.S.T., and Eidsmoen T.E. (1986). Piezocone testing in overconsolidated clays. Proc. 39th Can. Geotech. Conf. on 'Insitu Testing and Field Behaviour', Carlton Univ., Ottawa, Canada, pp209-218.

Appendix 12

Further test results: equalization

CONTENTS OF APPENDIX 12

A12.1 PORE PRESSURE DISSIPATION CURVES CP1-4 680
A12.2 LONG-TERM MEASUREMENTS WITH FLUSHABLE PROBES 684

A12.1 PORE PRESSURE DISSIPATION CURVES CP1-4

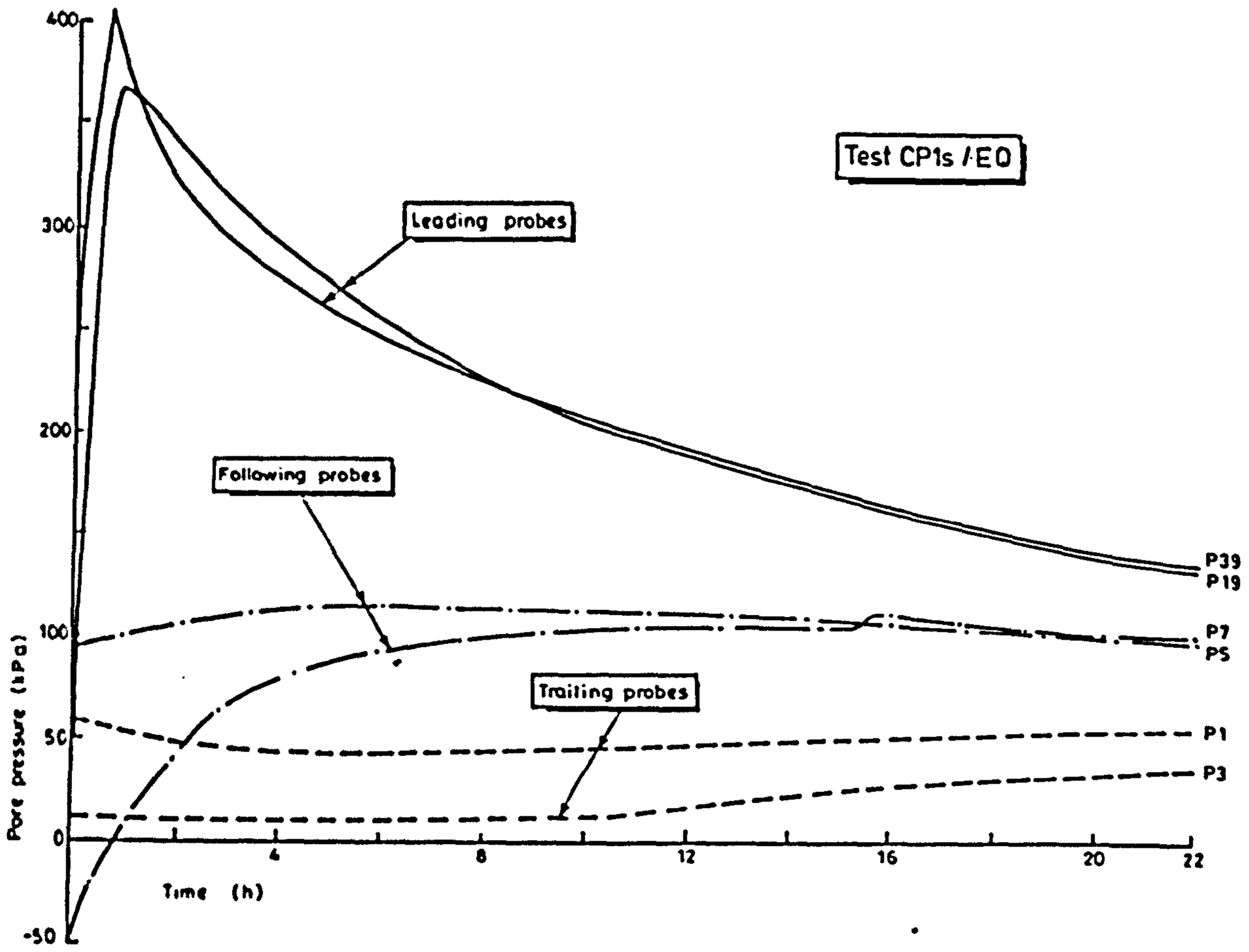


Figure A12.1 Pore pressure dissipation curves for Test Series CP1s

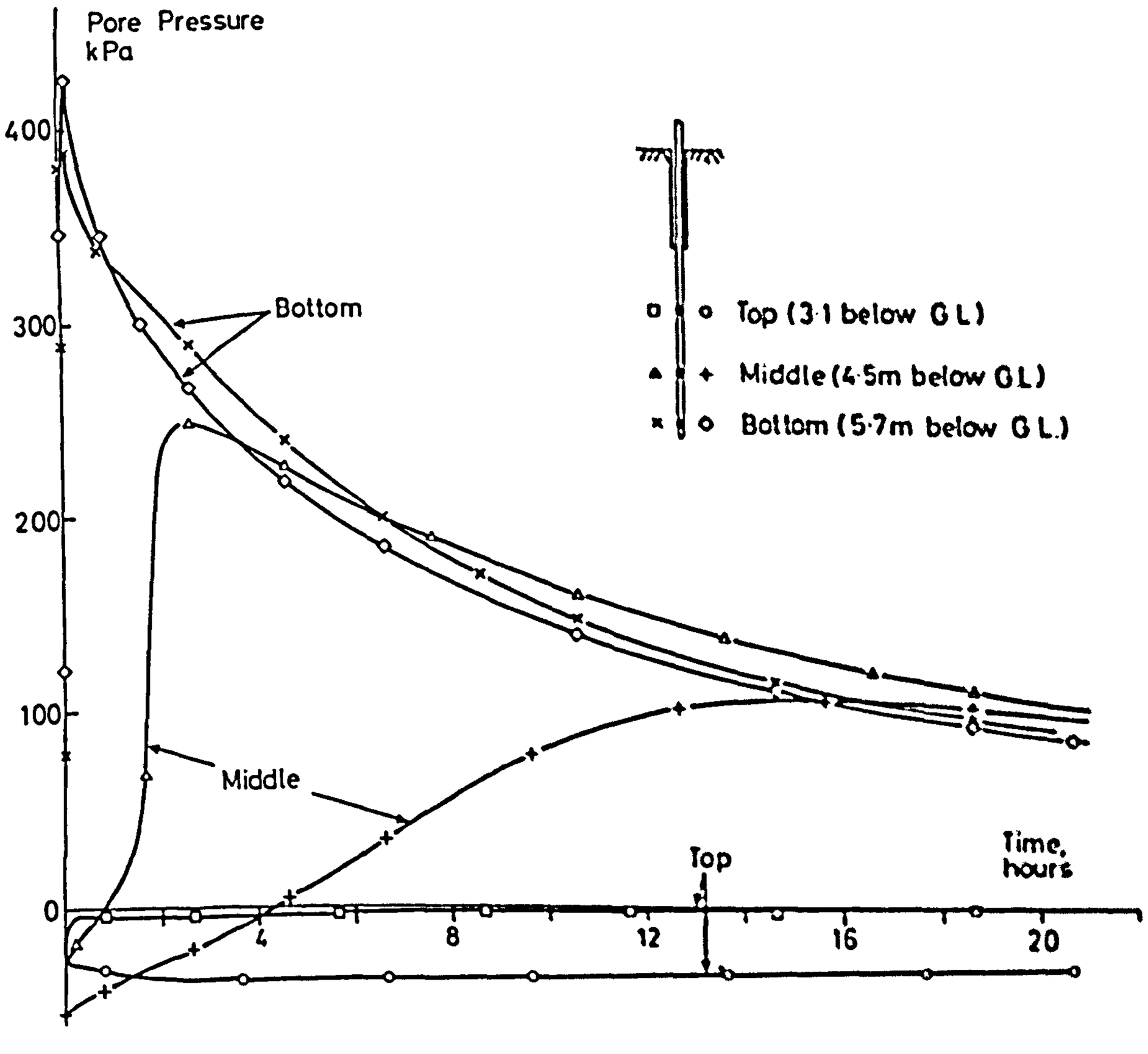


Figure A12.2 Pore pressure dissipation curves for Test Series CP2f

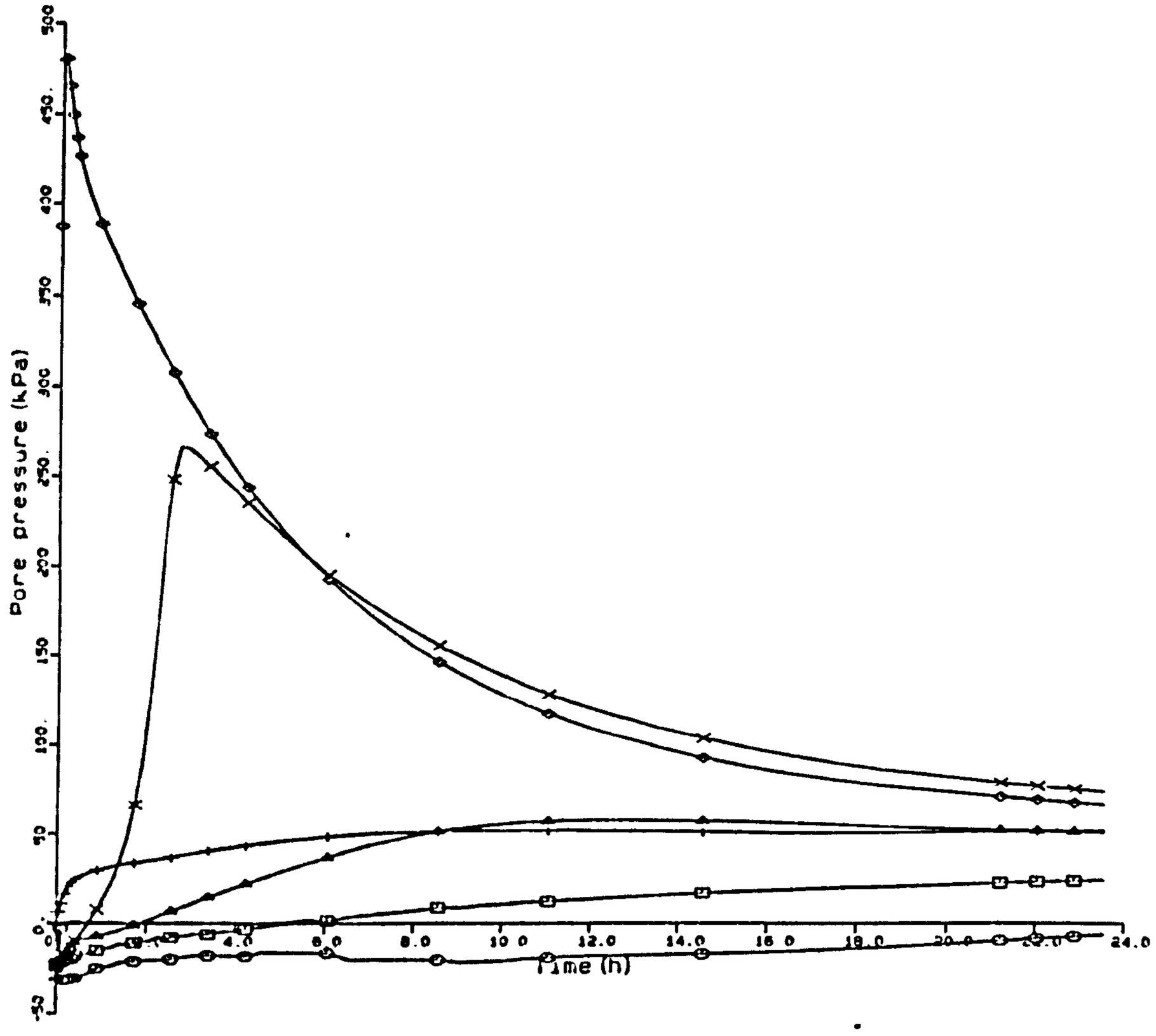


Figure A12.3 Pore pressure dissipation curves for Test Series CP3fs: (top) leading, (middle) following, (bottom) trailing probes

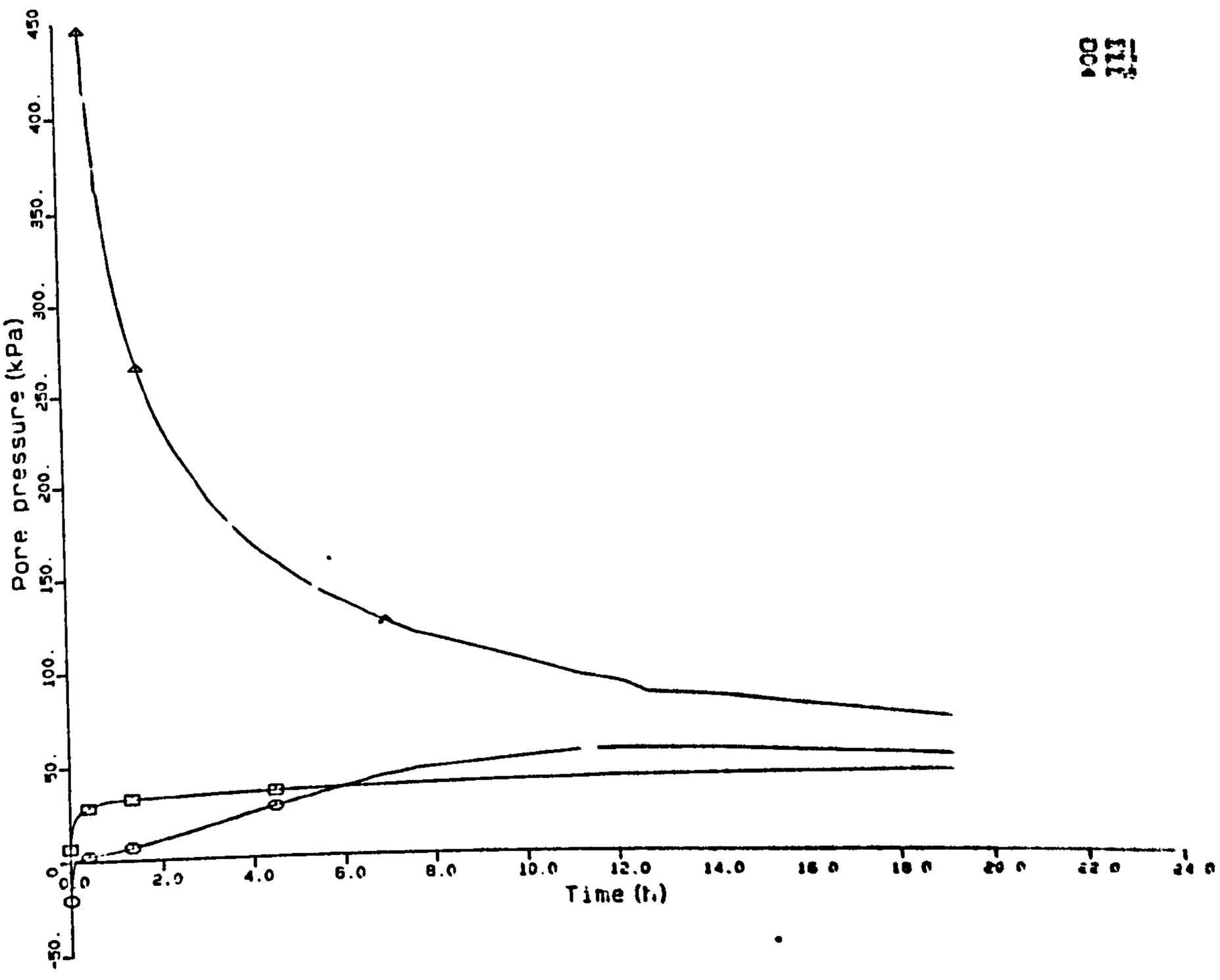


Figure A12.4 Pore pressure dissipation curves for Test Series CP4f: (triangle) leading, (circle) following, (square) trailing probes

A12.2 LONG-TERM MEASUREMENTS WITH FLUSHABLE PROBES

Figure A12.5 shows the pore pressures recorded by the flushable probes in Test Series CP4f. Their hydraulic lines were flushed with de-aerated water on day 27, and the transducers left for seven days to come into equilibrium with the ambient pore pressure in the soil.

During this period, the *leading* and *following* traces oscillated with daily changes in air temperature. The readings from the *leading* probe had the greatest amplitude of oscillation, since it had the greatest length of tubing. The *trailing* probe appears to have malfunctioned.

The *average* pressure recorded by the leading and following probes was 10-15kPa. Note that this is the pressure <u>at the level of the transducer</u>, <u>not</u> at the probe. The corresponding pore pressure in the far-field is ≈20kPa, i.e. slightly higher. The main conclusion to be drawn from these results is that the enormous long-term pressures recorded by the fast-acting probes (see Figure A9.4, p642) are indeed fallacious.

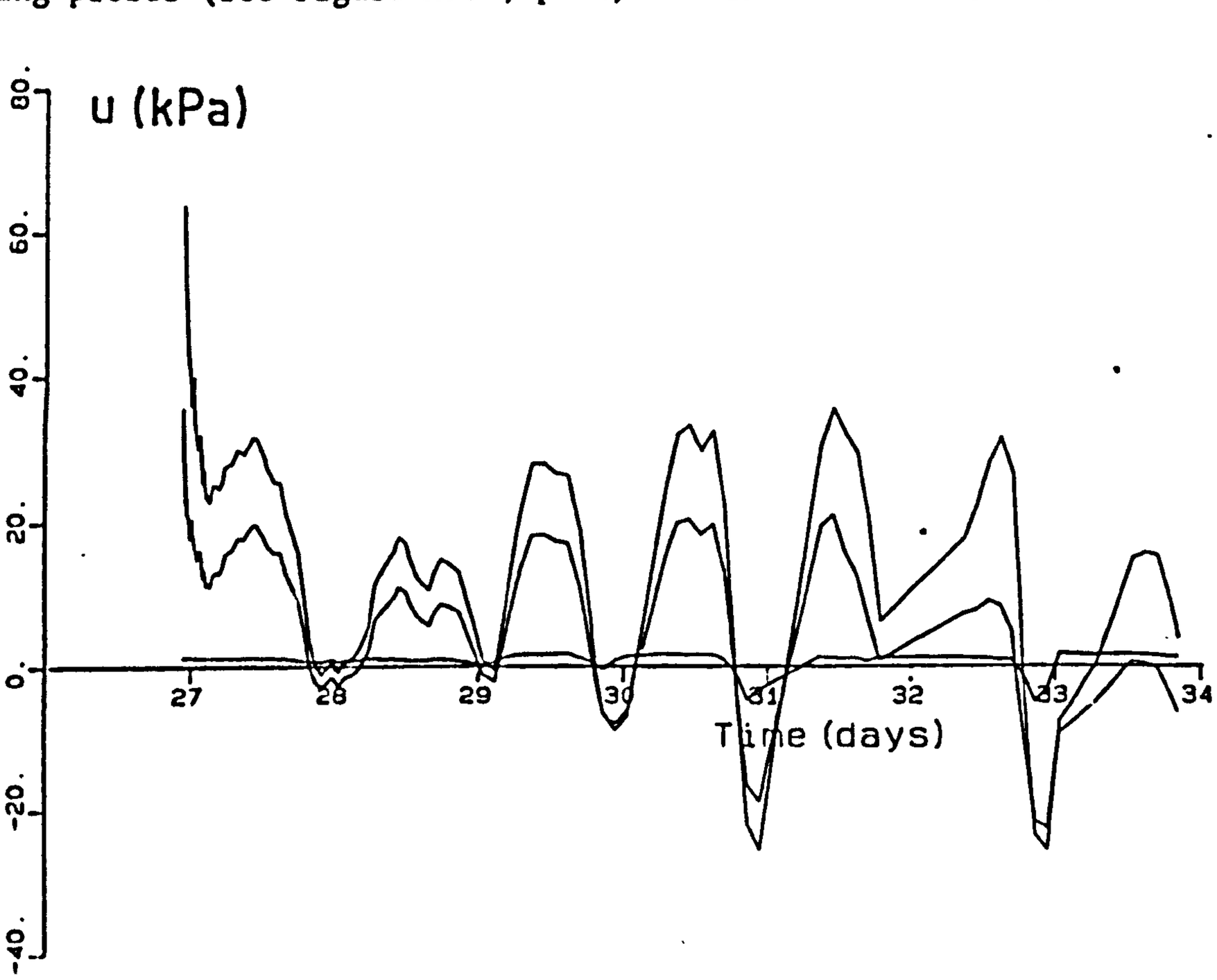


Figure A12.5 Pore pressures recorded by flushable probes in Test Series CP4f: (top) leading, (middle) following, (bottom) trailing probes (n.b. pressure at transducer, <u>not</u> probe)

Appendix 13

Further test results: pile loading

CONTENTS OF APPENDIX 13

A13.1 LOAD-DISPLACEMENT DIAGRAMS 688
A13.2 FURTHER INSTRUMENTED PILE DATA: TEST SERIES CP3C 700
A13.3 FURTHER INSTRUMENTED PILE DATA: TEST SERIES CP3C . . . 704

A13.1 LOAD-DISPLACEMENT DIAGRAMS

This section presents load-displacement diagrams for Test Series CP1-7. The diagrams are largely self-explanatory, giving information about the pile's head load (Q_{head}) and toe load (Q_{toe}) in each test. Also indicated on the figures is the rate of pile displacement at various stages during loading.

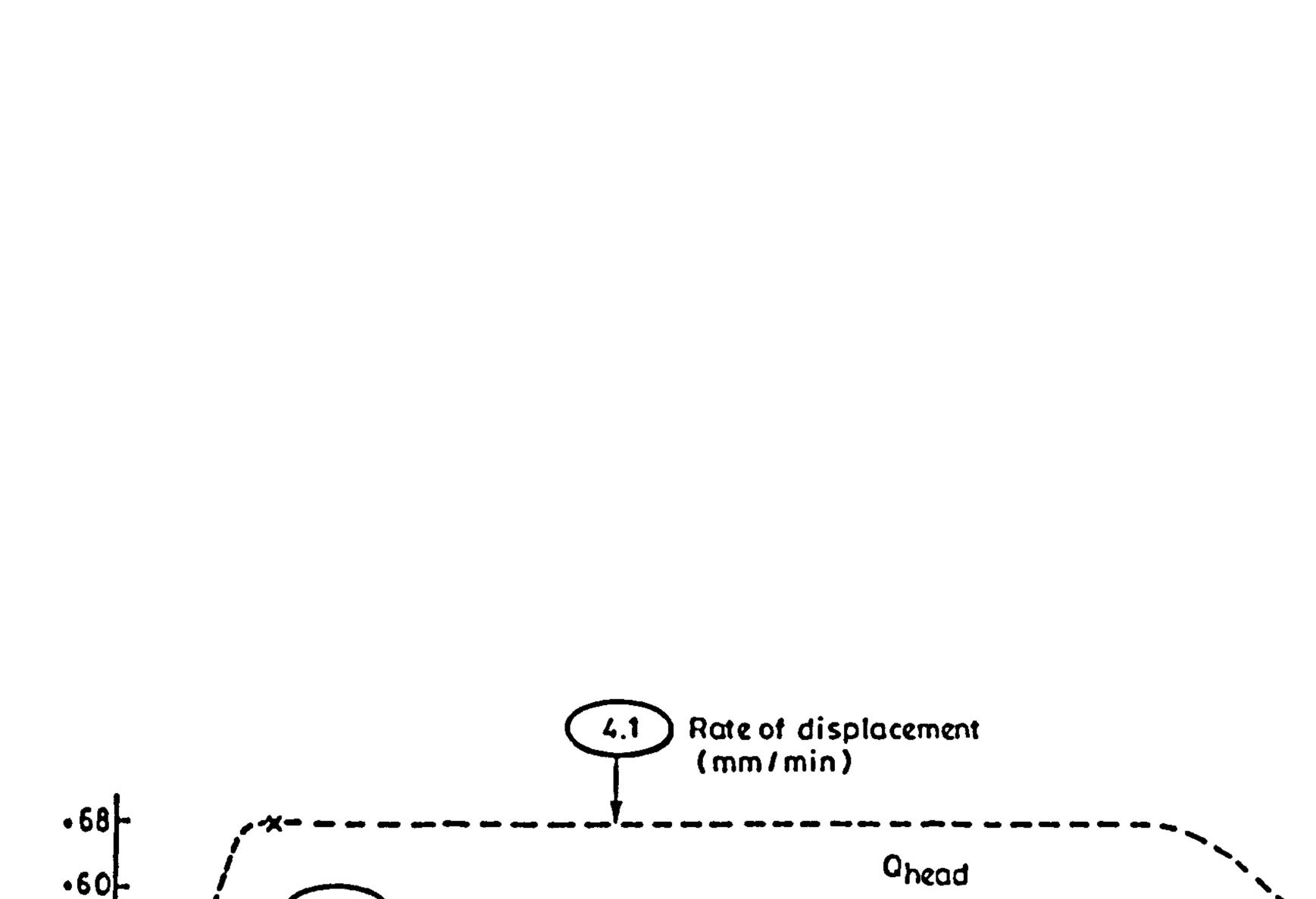


Figure A13.1 Load-displacement diagram for load test CP1s/L1C

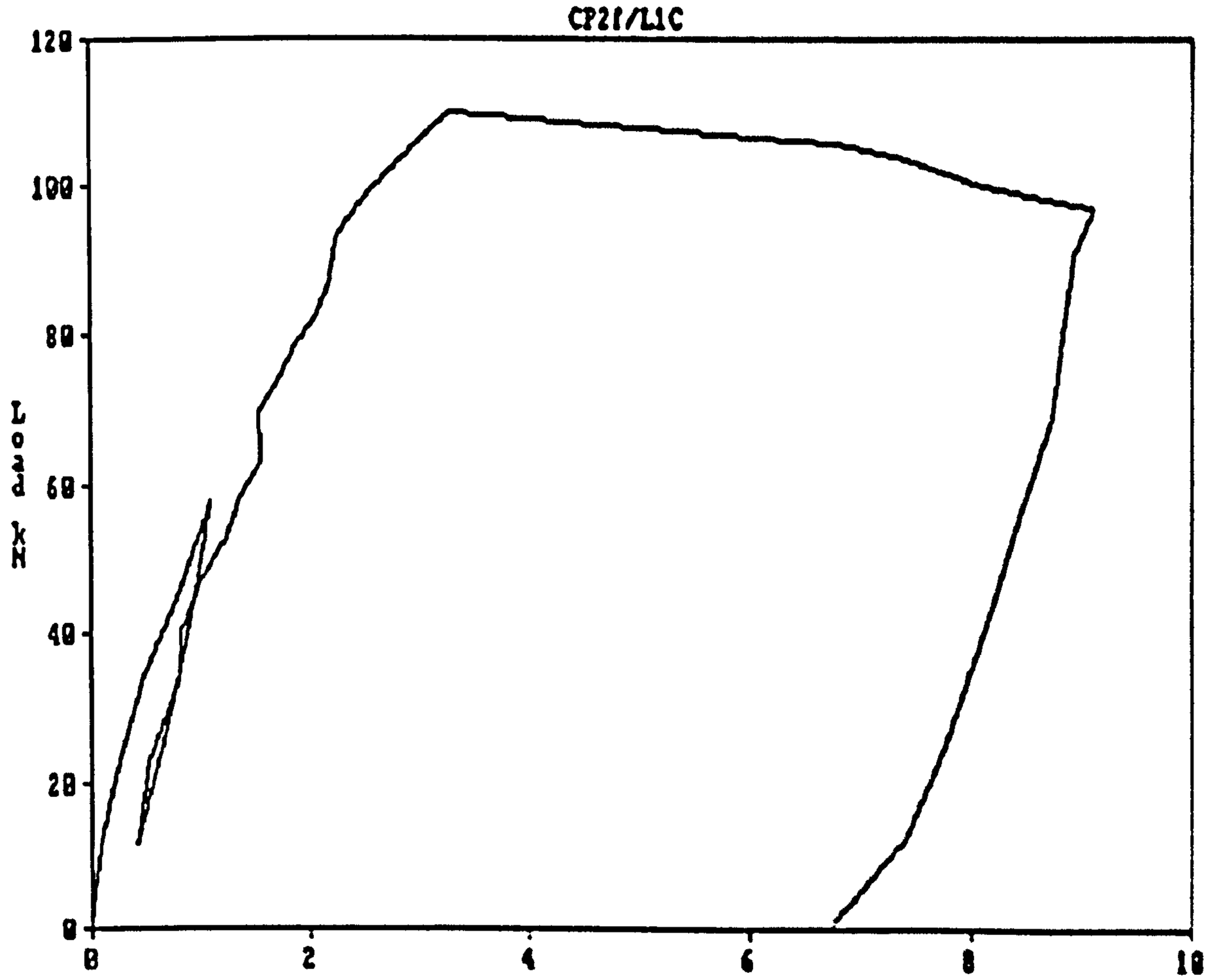


Figure A13.2 Load-displacement diagram for load test CP2f/L1C

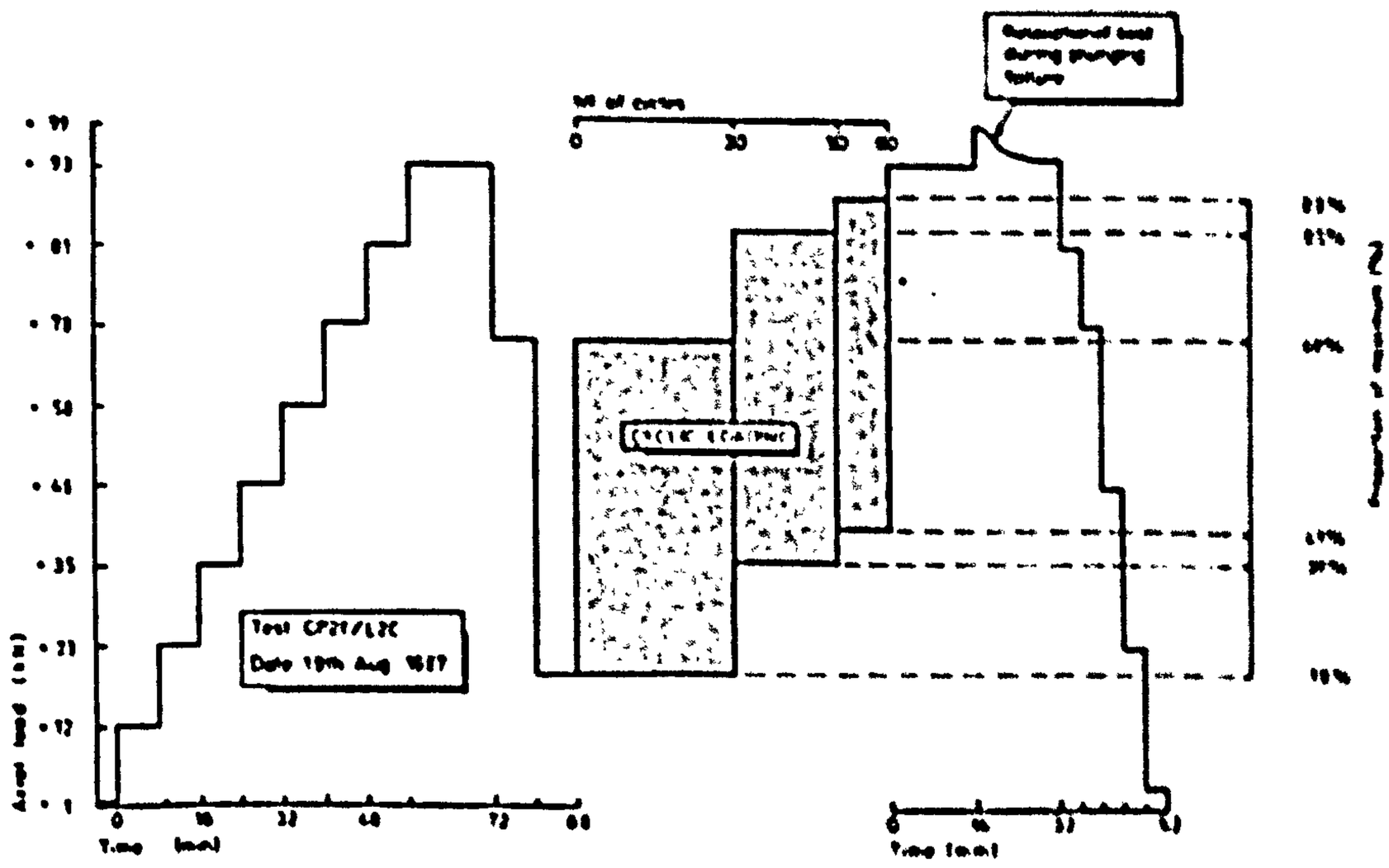


Figure A13.3 Pattern of loads applied in load test CP2f/L2C

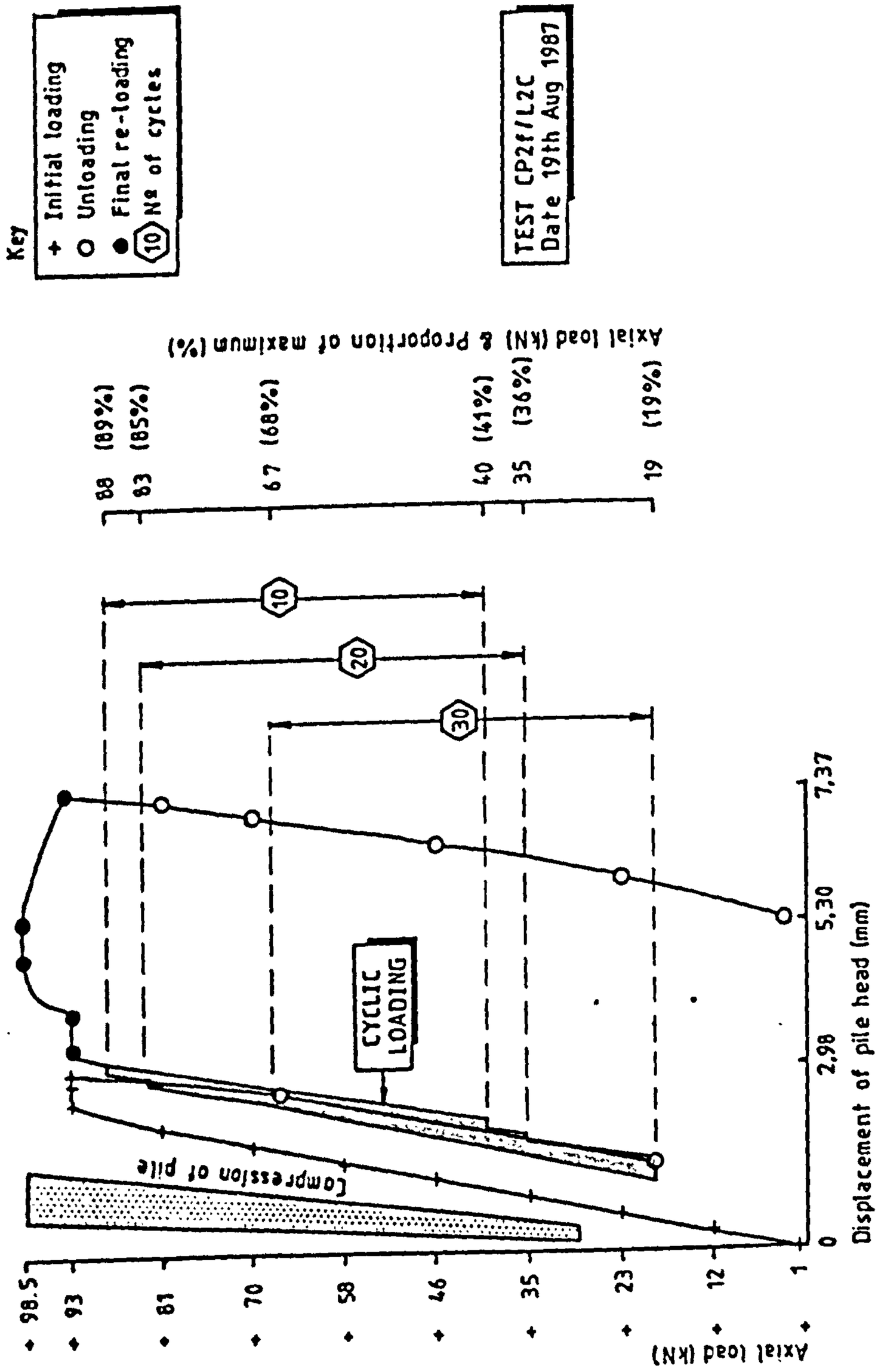


Figure A13.4 Load-displacement diagram for load test CP2f/L2C

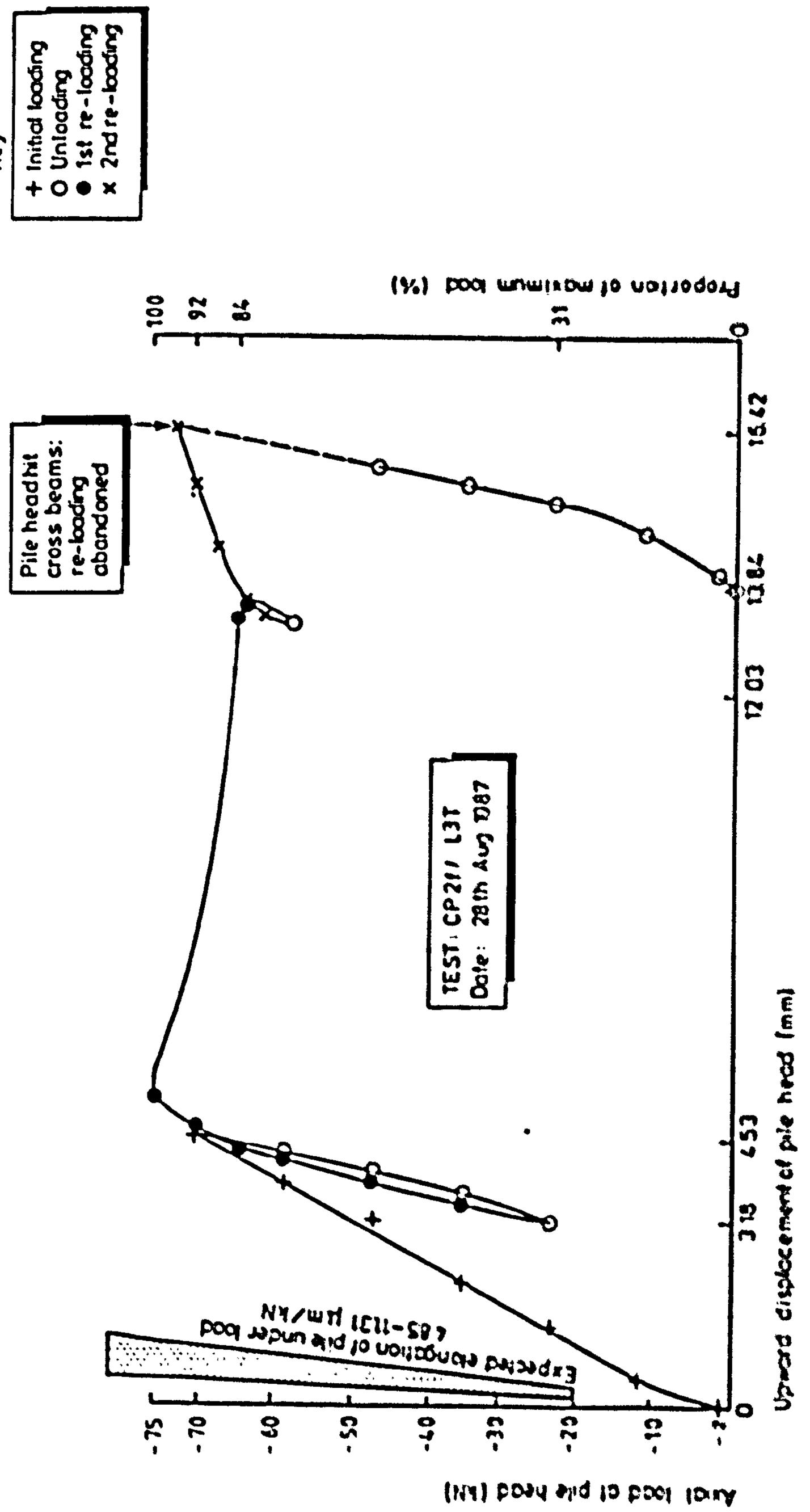


Figure A13.5 Load-displacement diagram for load test CP2f/L3T

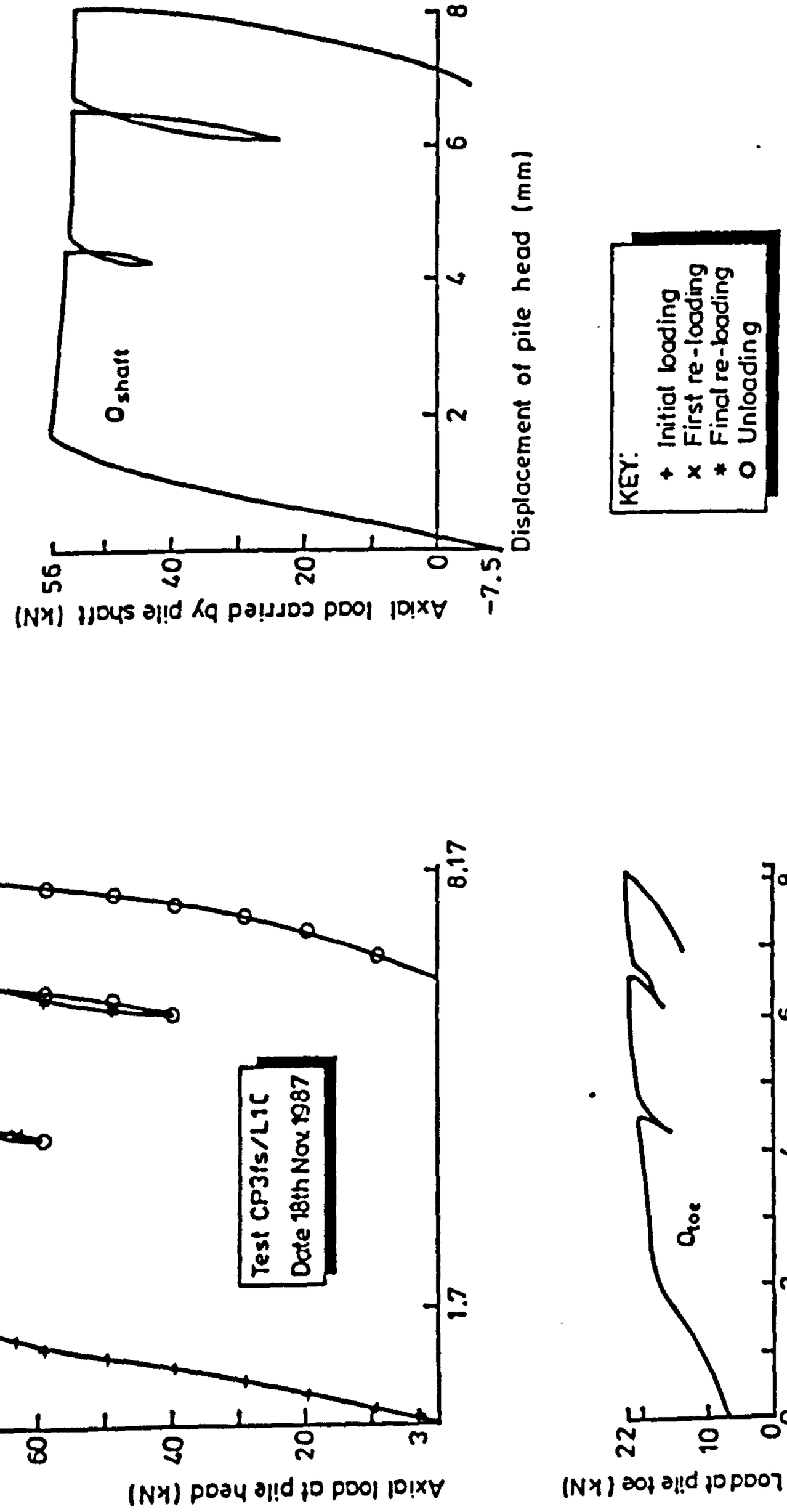


Figure A13.6 Load-displacement diagram for load test CP3fs/L1C

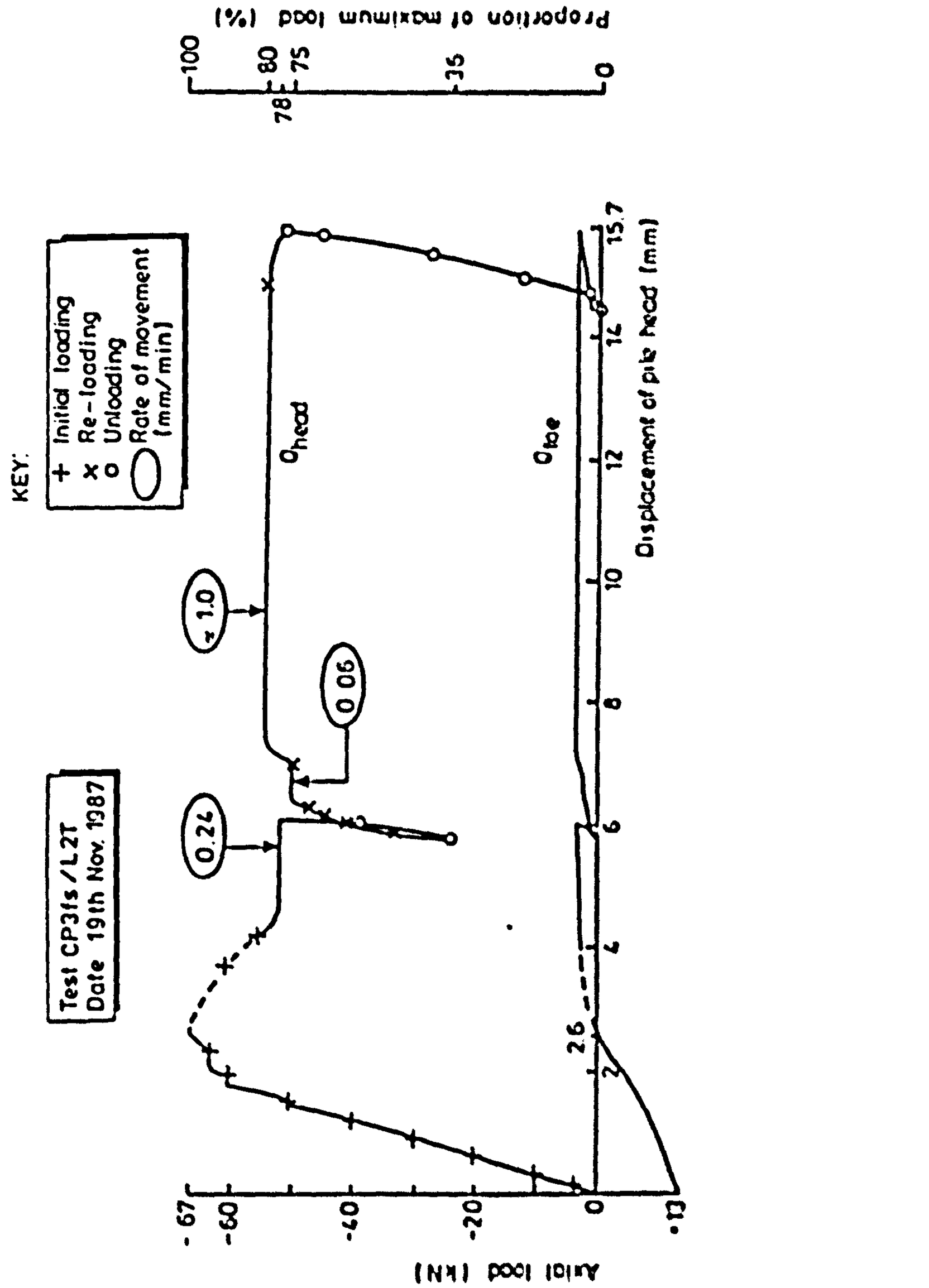


Figure A13.7 Load-displacement diagram for load test CP31s/L2T

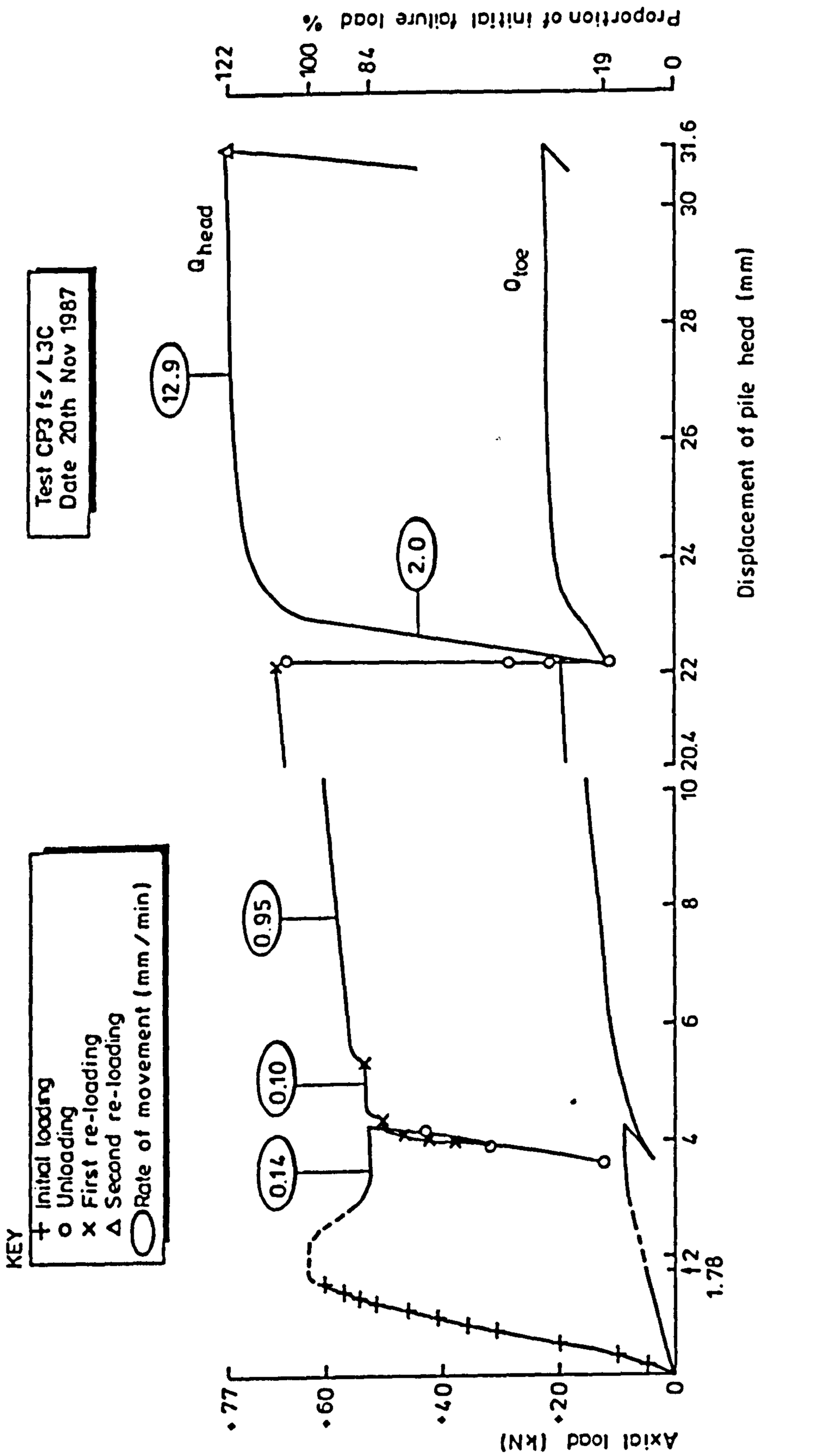


Figure A13.8 Load-displacement diagram for load test CP3fs/L3C

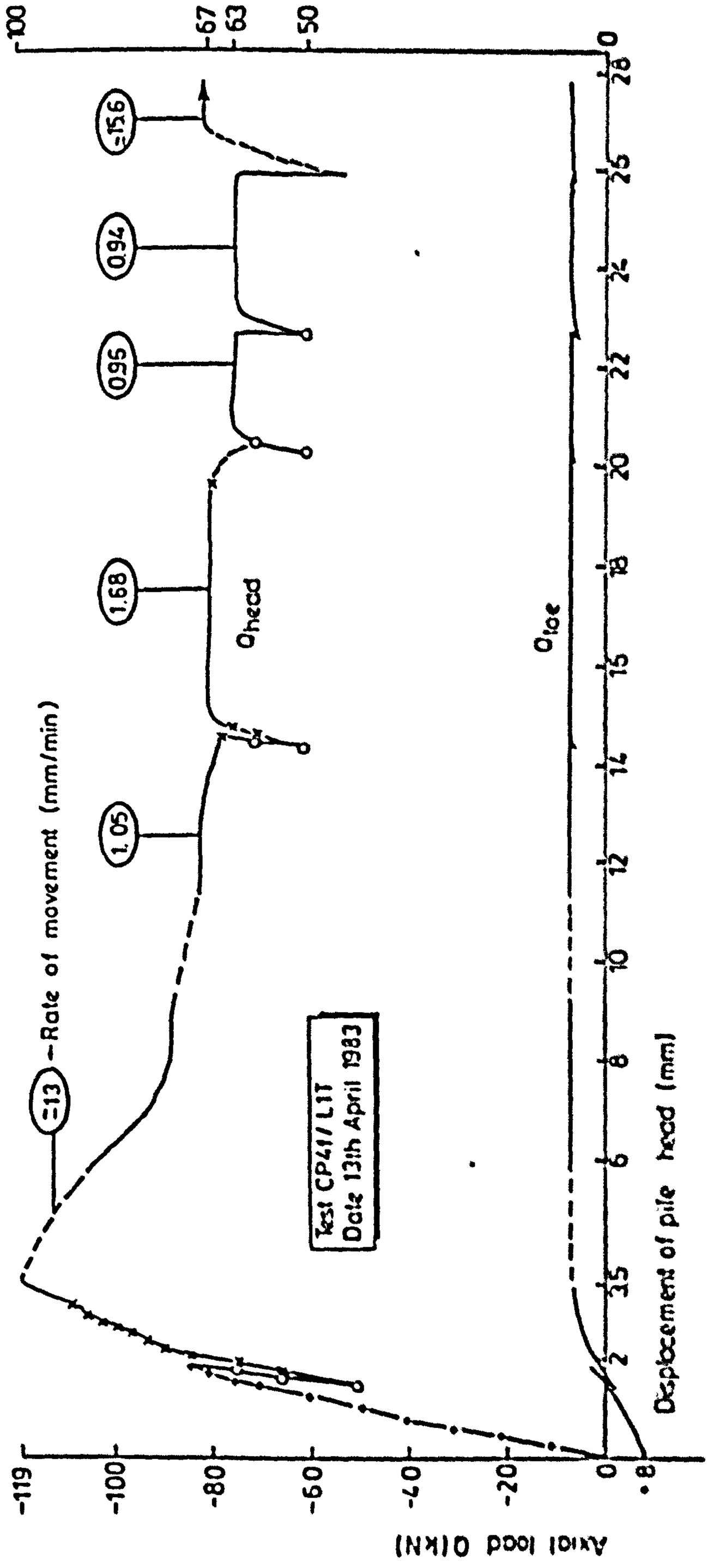


Figure A13.9 Load-displacement diagram for load test CP41/L1T

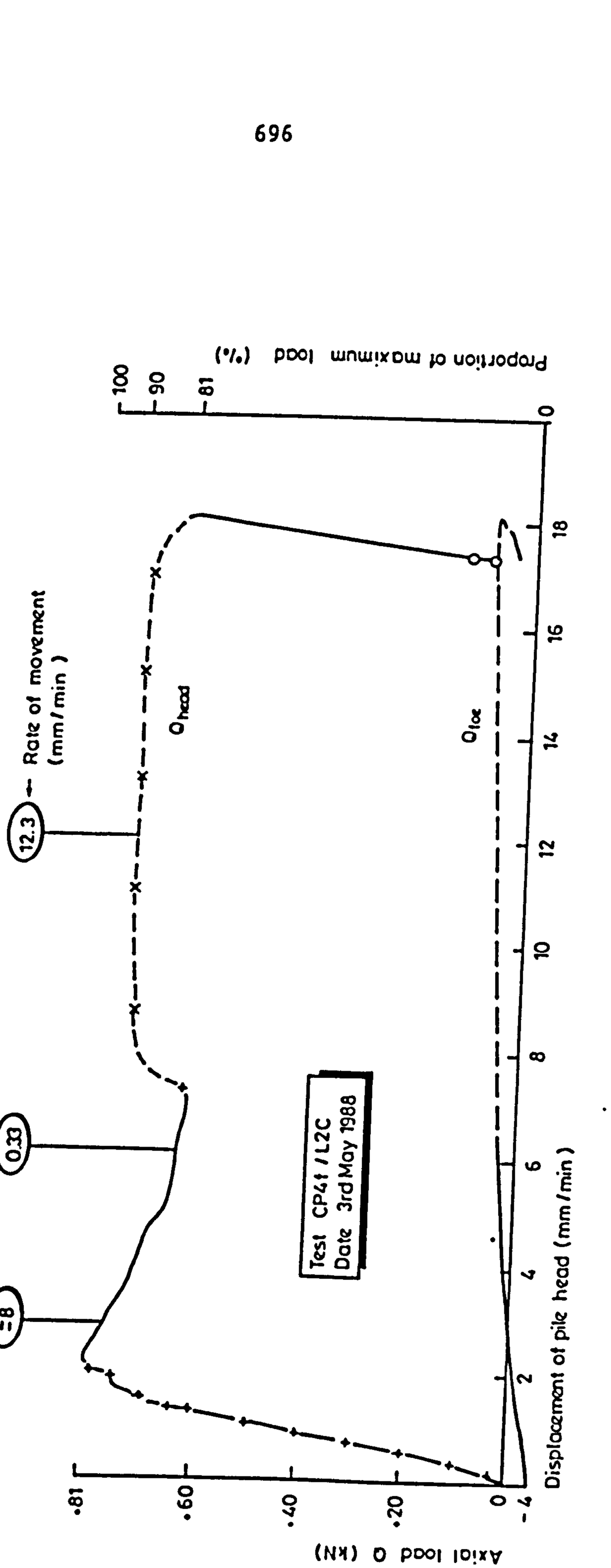


Figure A13.10 Load-displacement diagram for load test CP4f/L2C

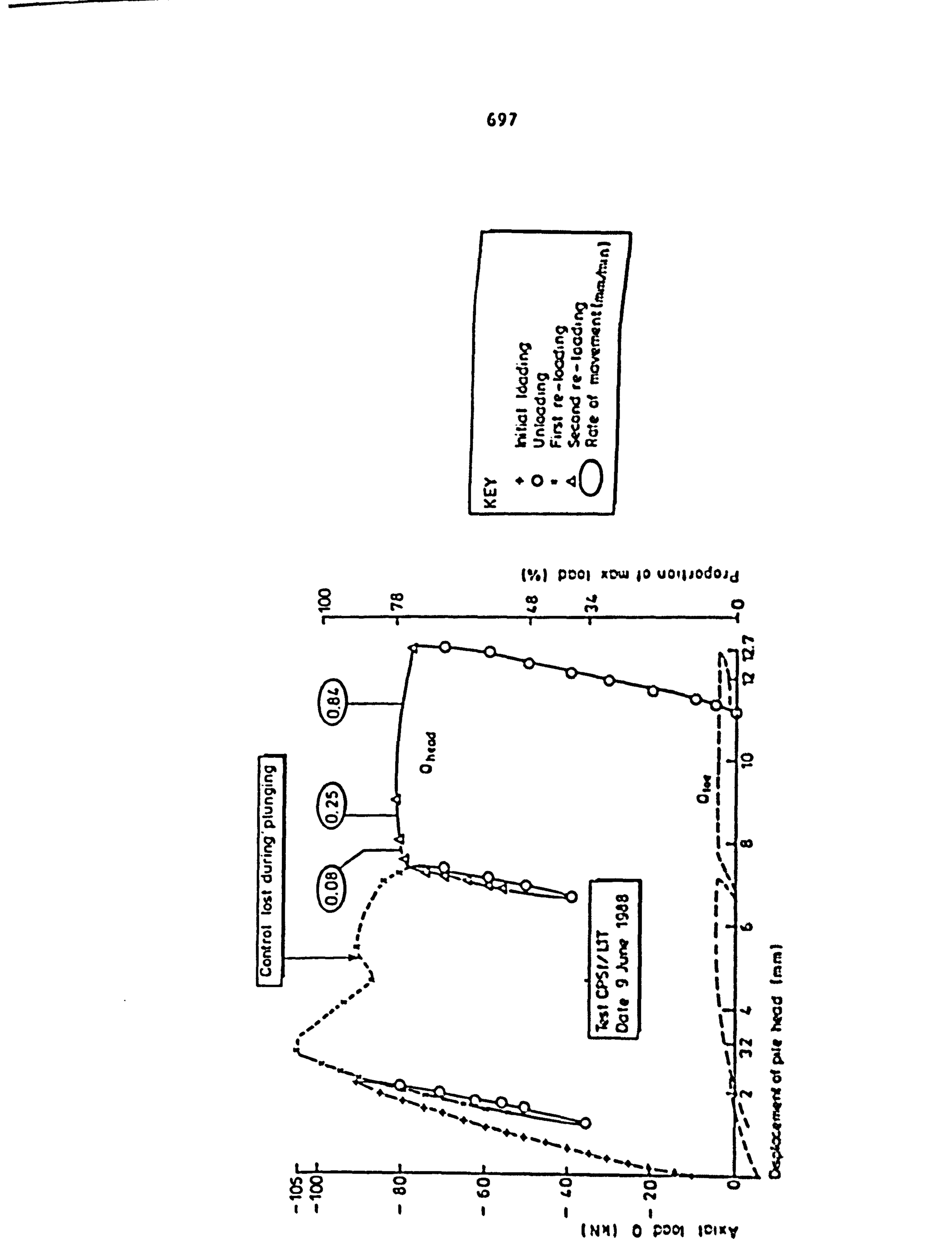


Figure A13.11 Load-displacement diagram for load test CPSf/LIT

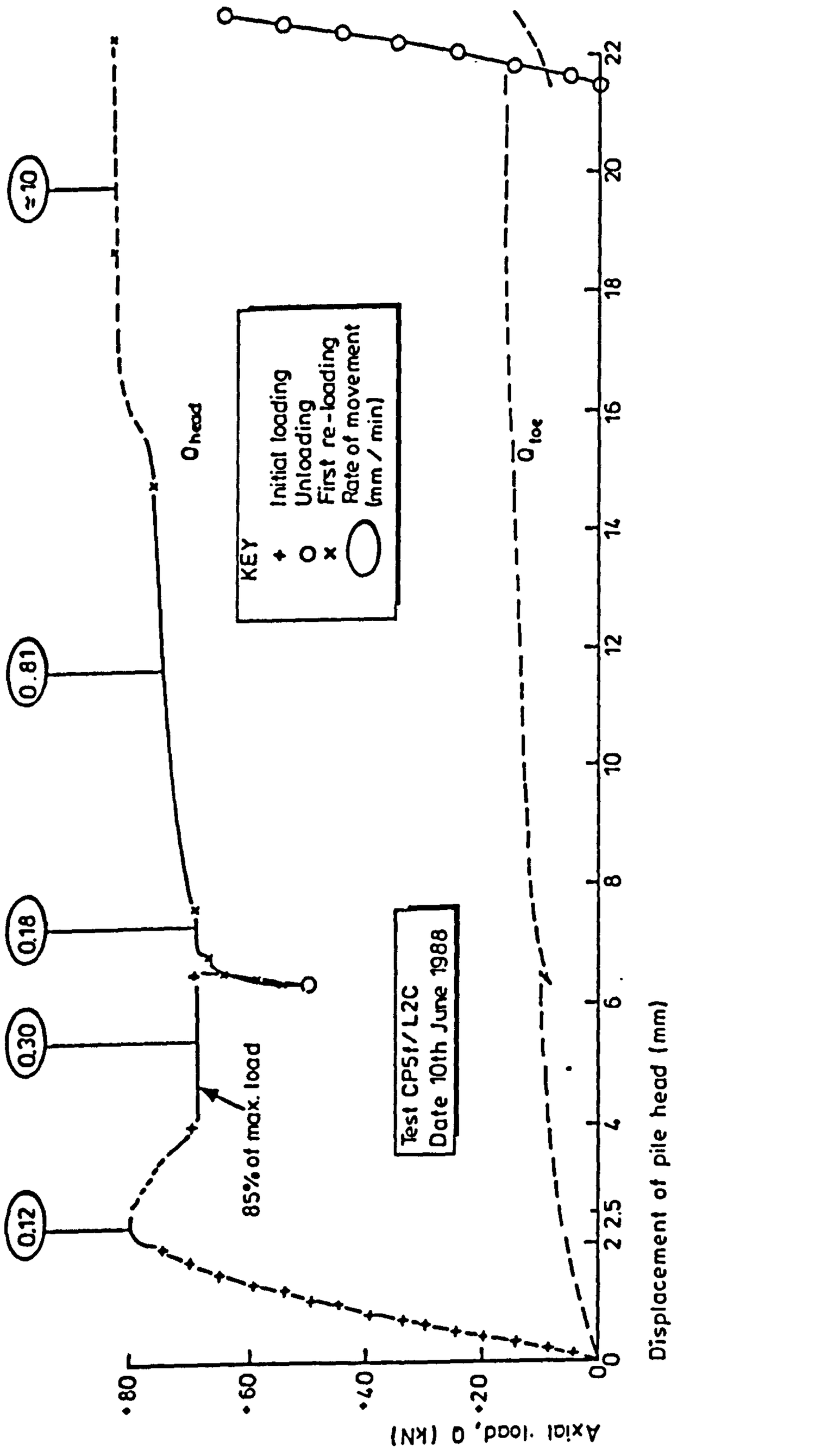


Figure A13.12 Load-displacement diagram for load test CP5f/L2C

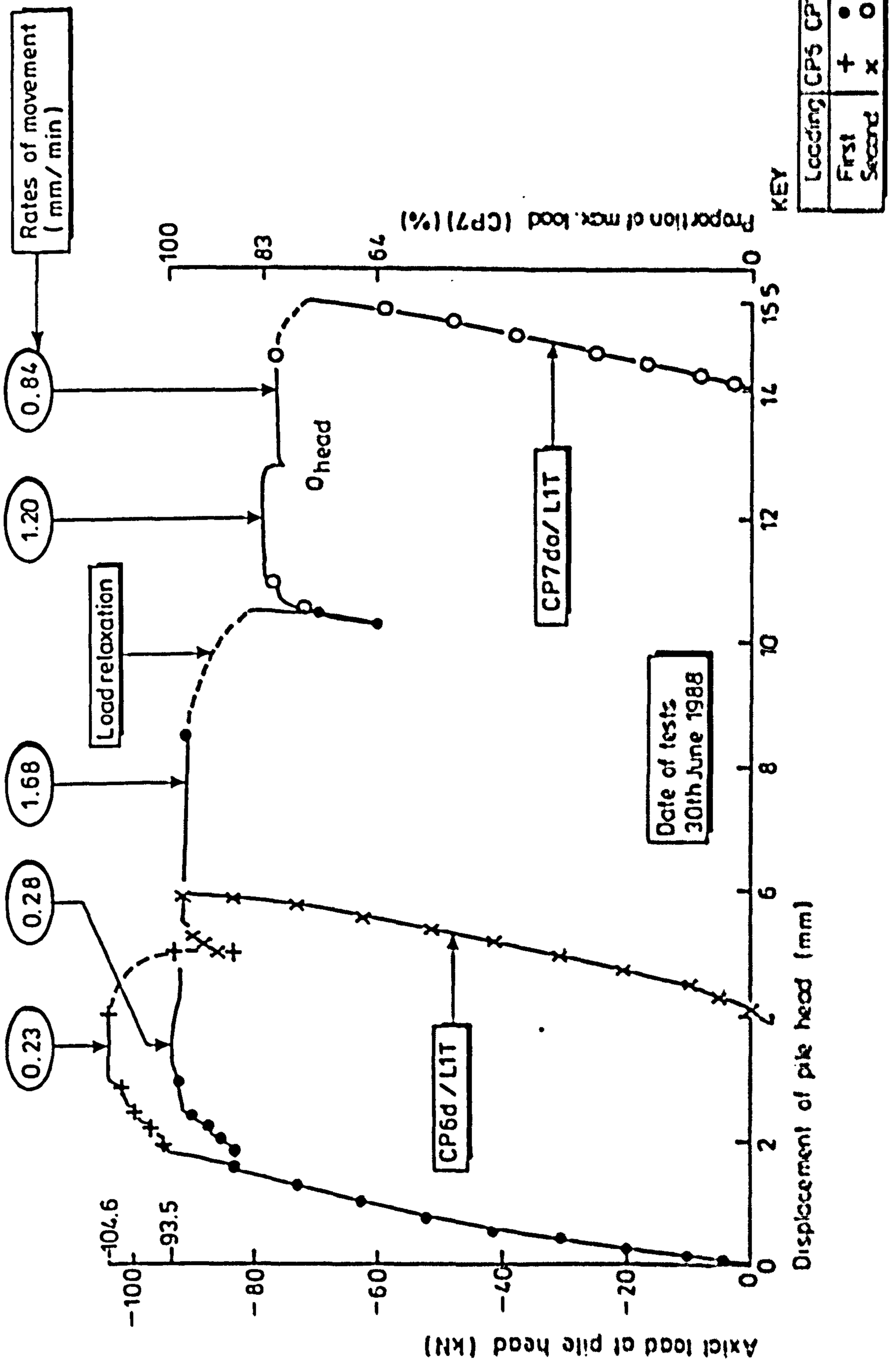


Figure A13.13 Load-displacement diagrams for load tests CP6d/L1T and CP7do/L1T

A13.2 FURTHER INSTRUMENTED PILE DATA: TEST SERIES CP5f

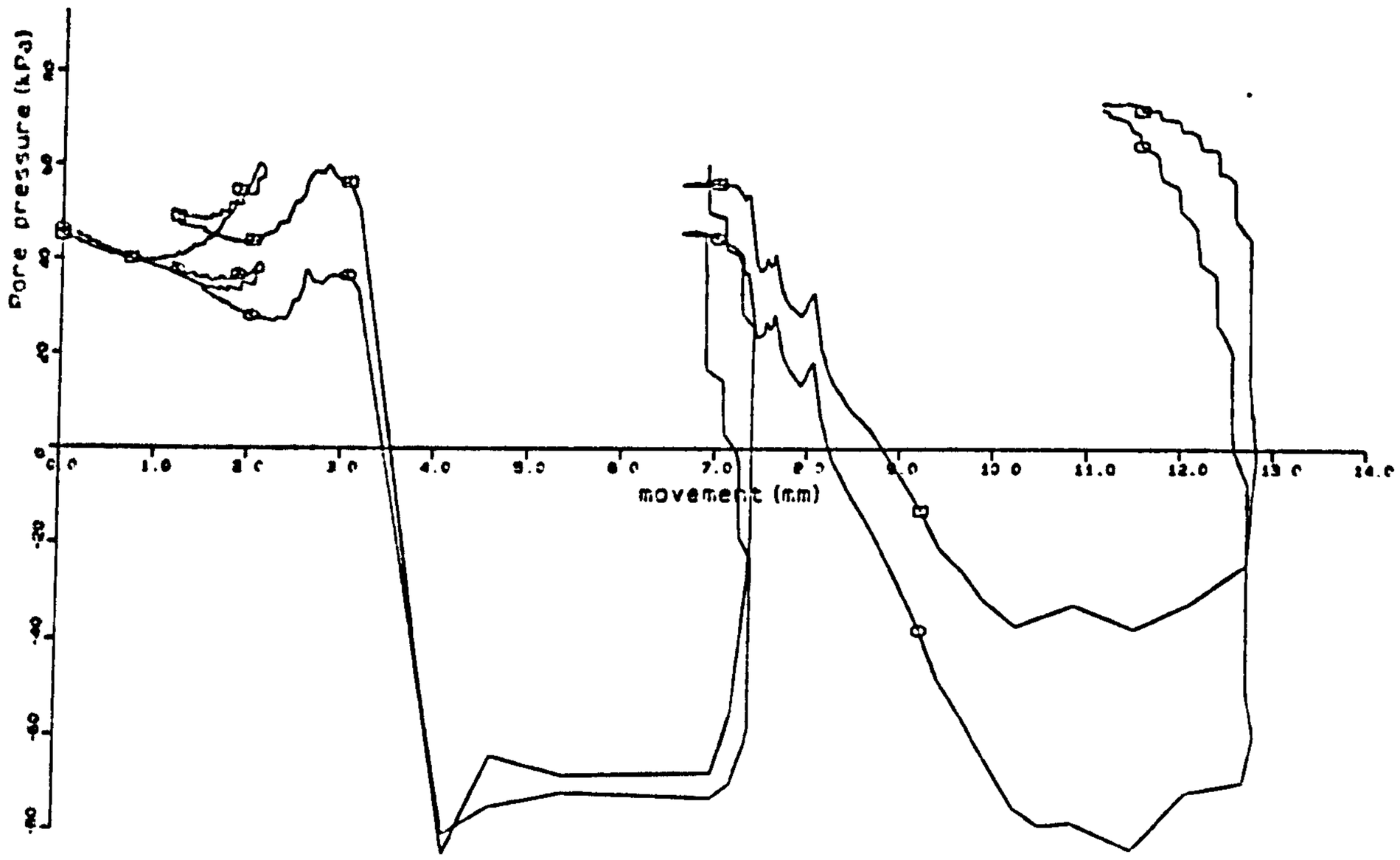


Figure A13.14 Variations in pore pressure with pile displacement during load test CP5f/L1T: (top) trailing, (bottom) following instruments

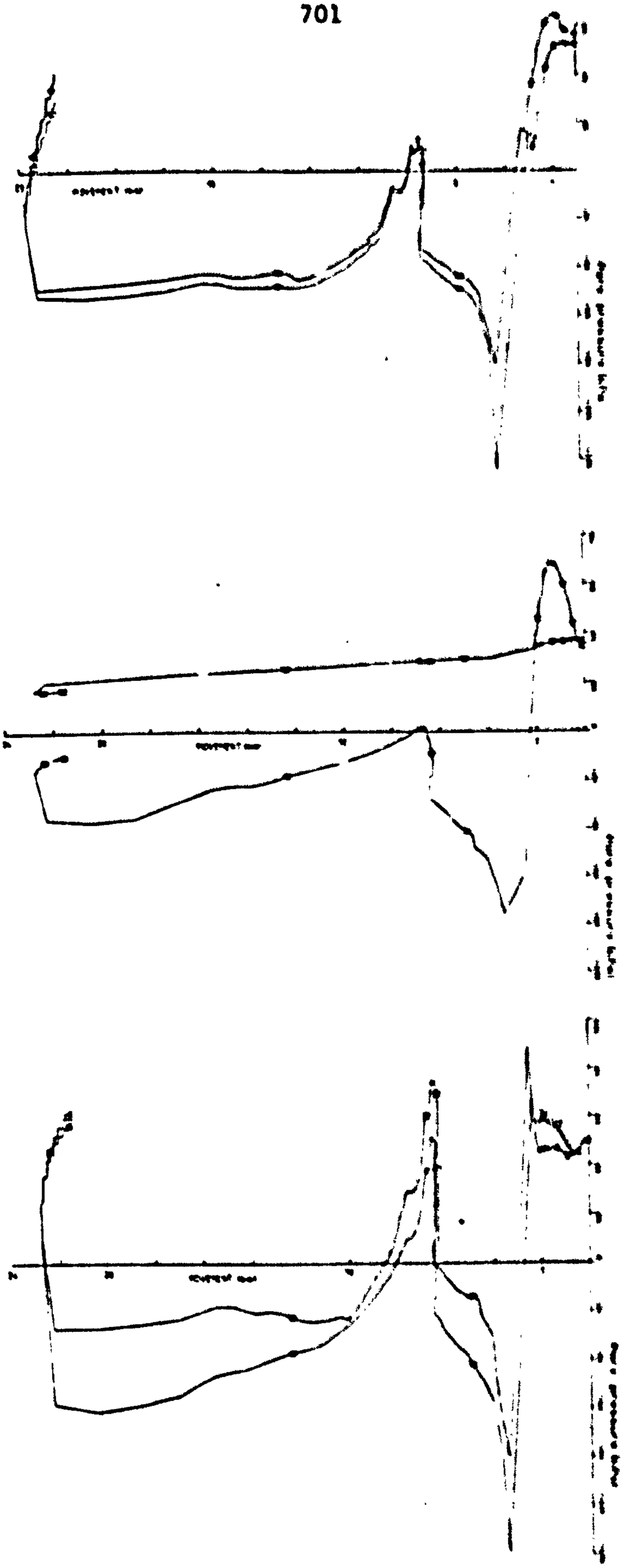


Figure A13.15 Variations in pore pressure with pile displacement during load test CP5f/L2C: (top) trailing, (middle) following, (bottom) leading instruments

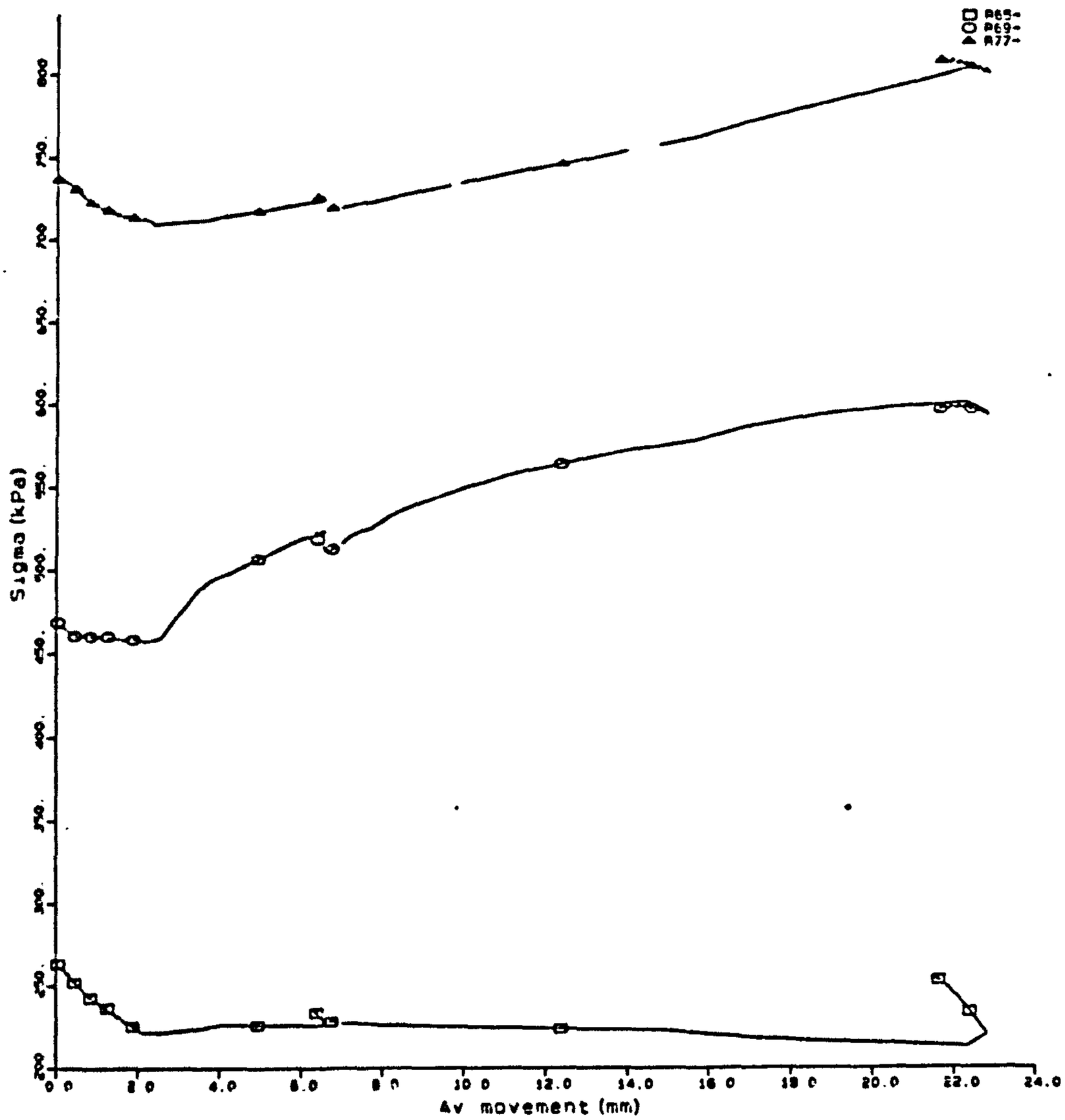


Figure A13.16 Changes in radial total stress, load test CP5f/L2C: (top) leading, (middle) following, (bottom) trailing instruments

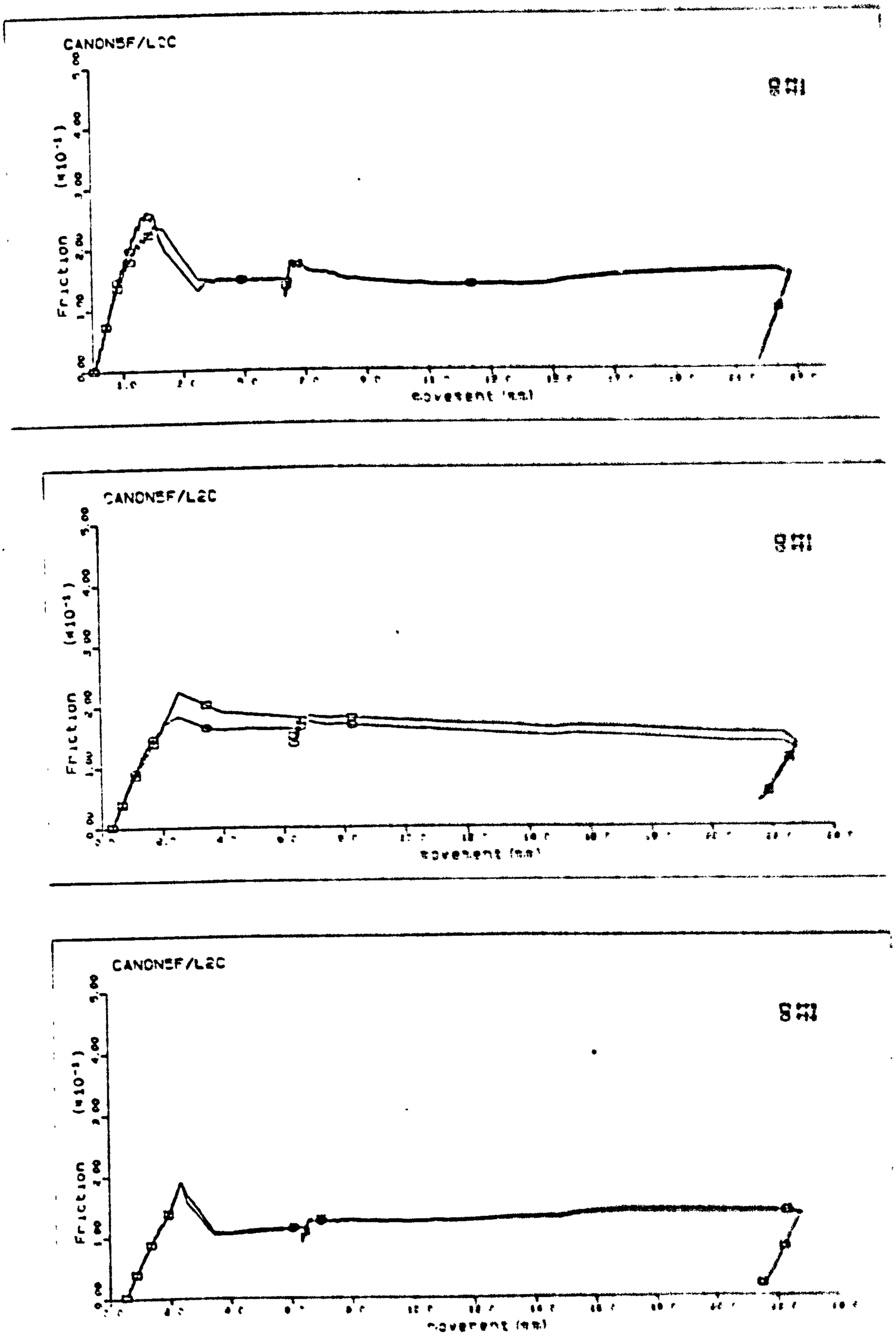


Figure A13.17 Coefficients of friction, load test CF5f/L2C: (top) trailing, (middle) following, (bottom) leading instrument positions

A13.3 FURTHER INSTRUMENTED PILE DATA: TEST SERIES CP3fs

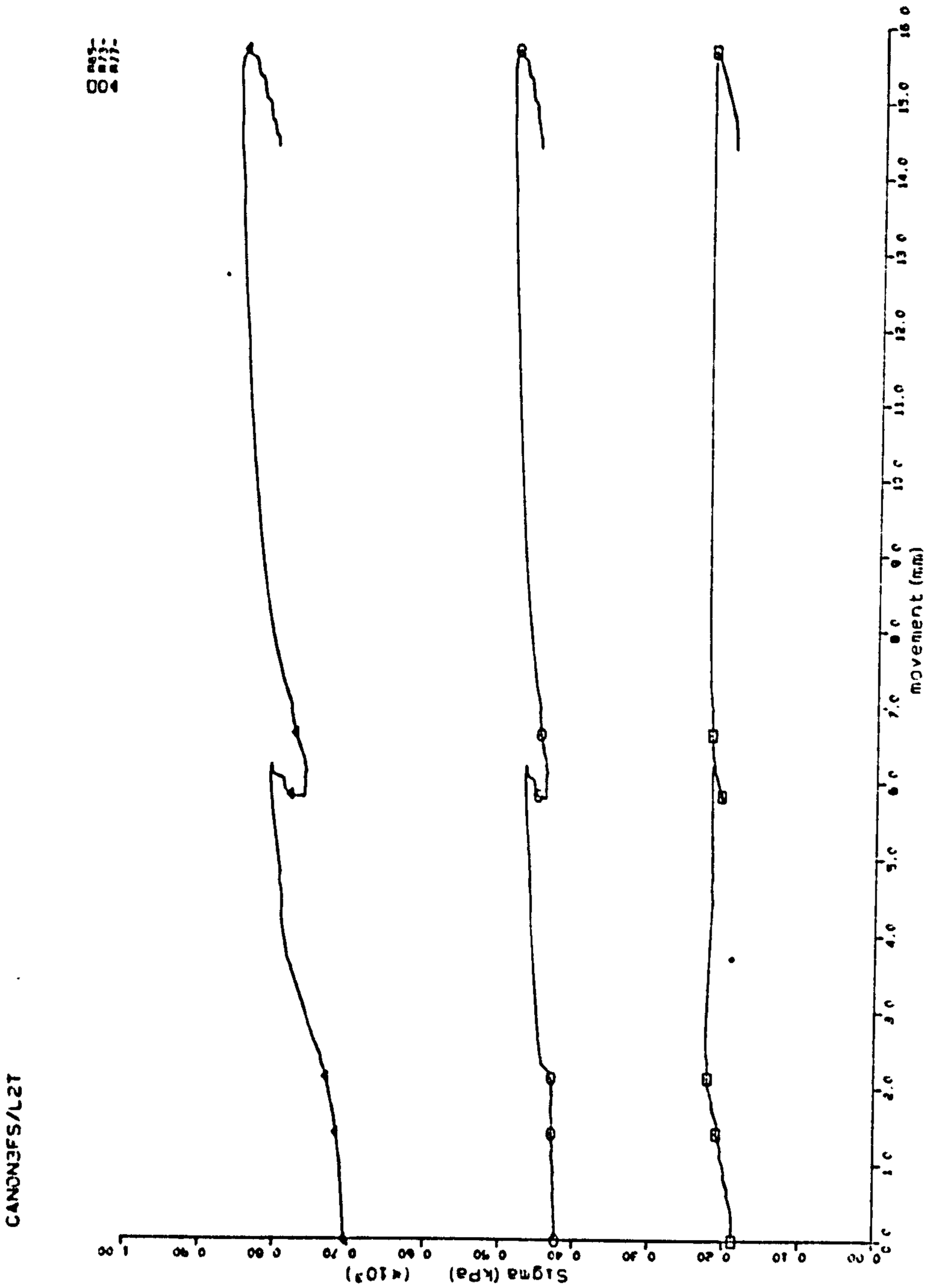


Figure A13.18 Changes in radial total stress, load test CP3fs/L2T: (top) leading, (middle) following, (bottom) trailing instruments

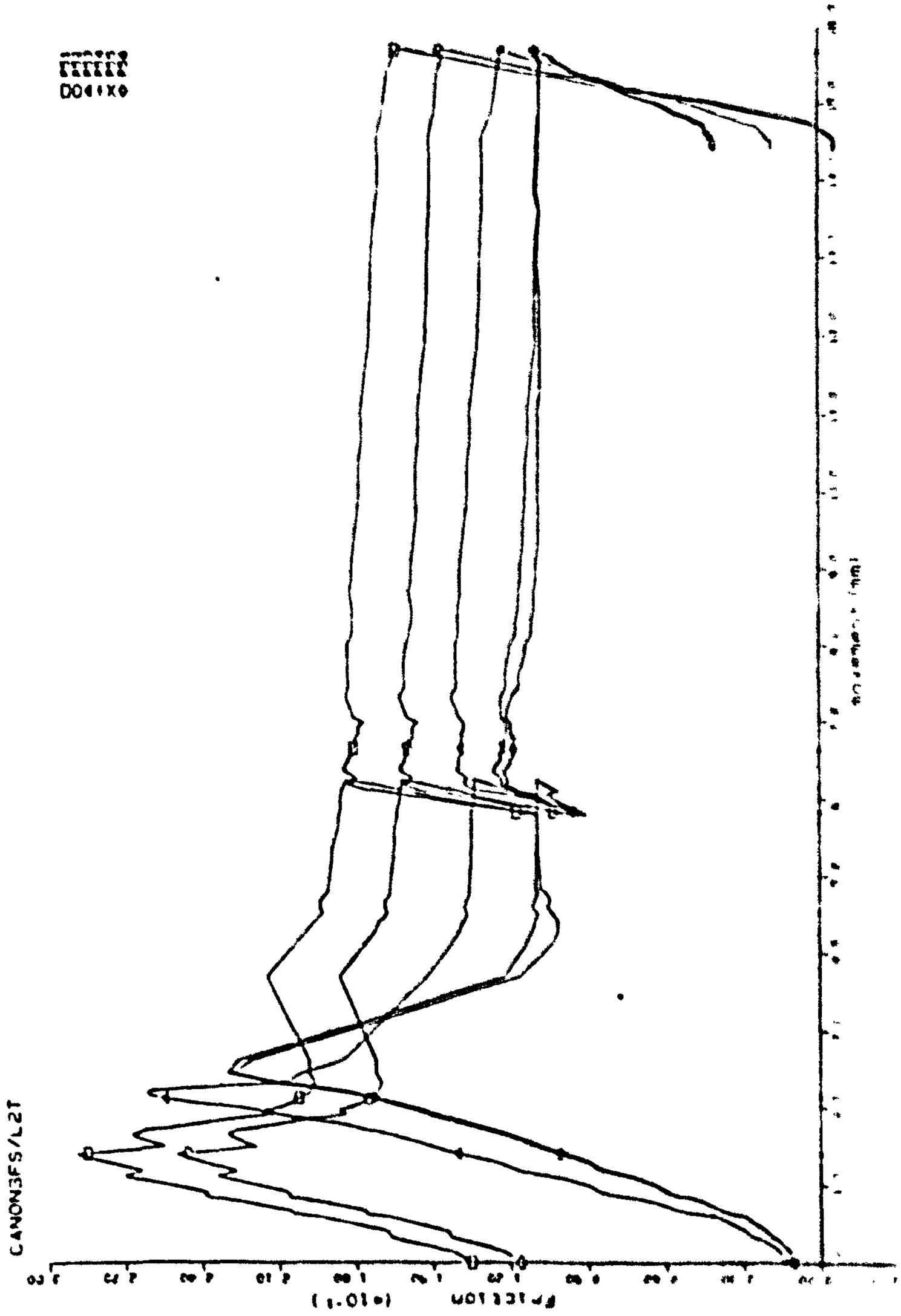


Figure A13.19 Coefficients of friction, load test CP3fs/L2T: P51 & P52 - trailing, P53 - following, P55 & P56 - leading instrument positions (P54 not shown)

Appendix 14

Notes on the preparation of thin sections

CONTENTS OF APPENDIX 14

A14.1 PREPARATION OF THIN SECTIONS 710
A14.1.1 Sampling procedure 710
A14.1.2 Sample impregnation 710
A14.2 NOTES AND REFERENCES 712

A14.1 PREPARATION OF THIN SECTIONS

A14.1.1 Sampling procedure

As noted in Chapter 13 (see pp414-415), thin-sections were made from samples of soil that had been cut from adjacent to either the driven pile CP6d or Kitching's jacked pile. Some samples were cut from the remains of the X-ray specimens (see Figure 13.4, p413), whilst others were recovered from the ground specifically for the purpose. The procedure followed in obtaining these samples was as follows.

Soil was removed from between the two piles in such a way as to leave an upstanding bench of clay. The bench was typically 100mm high x 100mm wide x 350mm long. Hand-held spades were used to make the final cuts to the bench's top surface and its two side faces (i.e. the pneumatically operated clay-spades were not used for this purpose). The underside was cut with a cheese wire held taut beneath the heels of our boots. An identical procedure was used for obtaining the samples needed for the measurements of soil suction (see Appendix 15).

Once each sample had been separated from the underlying ground it was immediately wrapped in cling film and then coated with wax. The samples were kept in the site hut for safe-keeping before removing to the laboratory.

Once in the laboratory, each sample was removed from its protective seal and cut into smaller pieces, approximately 45mm high ẋ 90mm long x 25mm thick. Both vertically-aligned and horizontally-aligned specimens were cut - Figure 13.4 (p413) shows one of the vertically-aligned specimens.

A14.1.2 Sample impregnation

All of the samples were impregnated with Carbowax 6000,* following the procedure recommended by Tchalenko.[1] Carbowax is used to replace the

---

*Polyethylene glycol (PeG) with a molecular weight of ≈6000

water in the soil's pores, making the samples rock-hard at room temperature. They can then be ground into thin-sections and mounted on glass slides for microscopic examination.

The samples were placed in a tray of melted Carbowax, and left in a temperature-controlled oven set at 60°C. The total time allowed for impregnation was just over two weeks.* Note that the average time used by Tchalenko[2] was one week, "although stiff clays necessitated longer periods", and that Martins[3] impregnated samples of kaolin for three weeks.

Tchalenko also noted that "excessive impregnation sometimes produced friability in specimens".[4] Several of the samples from Canons Park broke up during impregnation, despite attempts to constrain them against expansion by strapping them with tape. Fortunately, none of the samples that were lost were from positions adjacent to the piles.

On their removal from the Carbowax, the samples were allowed to cool and harden, before being sent for grinding and mounting. This last stage in the manufacture of the thin-sections was undertaken by the Department of Geology at Queen Mary College, London.[5] Paraffin, not water, was used to lubricate the stone used for grinding, since water is known to dissolve hardened Carbowax.

---

*The original Carbowax was replaced with a fresh batch at the end of the first week

A14.2 NOTES AND REFERENCES

[1]Tchalenko J.S. (1967). The influence of shear and consolidation on the microscopic structure of some clays. PhD Thesis, Univ. of London (Imperial College), 2vols, 221pp + 171 figures. See pp36-42; and 196-200.

[2]Tchalenko (1967), loc. cit., p197.

[3]Martins J.P. (1983). Shaft resistance of axially loaded piles in clay. PhD Thesis, Univ. of London (Imperial College), 435pp. See p75.

[4]Tchalenko (1967), loc. cit., p197.

[5]I am grateful to Mr Kevin Schrapel for doing this work.

Appendix 15

Notes on the measurement of soil suction

CONTENTS OF APPENDIX 15

A15.1 FILTER PAPER TECHNIQUE 716
A15.1.1 Sampling procedure 716
A15.1.2 Testing procedure 716
A15.1.3 Notes on the formulae used to calculate soil suction 717
A15.1.4 Further test results 720
A15.2 PRESSURE-PLATE MEASUREMENTS 723
A15.2.1 Testing procedure 723
A15.3 NOTES AND REFERENCES 724

A15.1 FILTER PAPER TECHNIQUE

A15.1.1 Sampling procedure

The procedure for cutting the filter-paper samples was as follows. Soil was removed from between the two piles in such a way as to leave an upstanding bench of clay (see Figure A15.1), from which the samples could be obtained. The bench was typically 100mm high x 100mm wide x 350mm long. Hand-held spades were used to make the final cuts to the bench's top surface and its two side faces (i.e. the pneumatically operated clay-spades were not used for this purpose). The underside was cut with a cheese wire held taut beneath the heels of our boots.

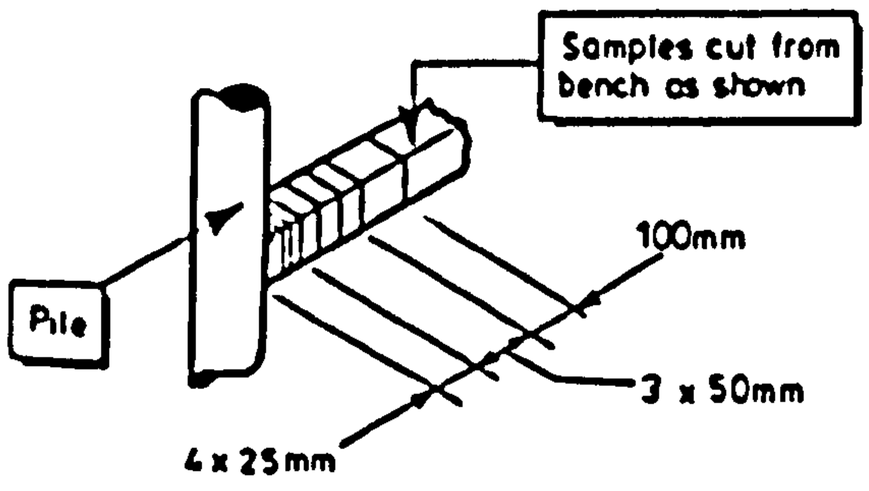


Figure A15.1 Bench of clay for obtaining filter-paper samples

Once the bench had been separated from the underlying ground it was cut with the cheese wire into slices of different thicknesses (as shown in Figure A15.1). Each slice was immediately wrapped in cling film and then coated with wax. Finally, the samples were transported to the laboratory for testing.

A15.1.2 Testing procedure

In the laboratory, each sample was removed from its protective seal before being split into two halves. Filter-papers were placed against the sample's two outer surfaces; and on its inside (between the newly cut faces). The specimen's two halves were then re-joined, and the whole thing wrapped in cling film and waxed. The filter-papers used were Whatman's No 42, as employed by Chandler and Gutierrez.[1]

The samples were left for two weeks for the water content in the filter-paper (w_{fp}) to come to equilibrium with the suction in the sample. The papers were then removed from the soil and weighed.

Special precautions were necessary to prevent the filter-papers from drying out between uncovering and weighing. A simple test showed that wet filter-papers quickly lose moisture[2] if no precautions are taken, leading to unacceptable errors in w_{FP} and hence in p_k. Therefore, each sample was placed inside a sealable plastic bag (which itself had already been weighed) and the filter-paper and bag were weighed together.

Finally, the filter-paper's dry weight was measured, once it had been dried overnight in an oven. Other precautions that were taken included: i) cutting off the any pieces of filter-paper that soil had adhered to; ii) placing the dry filter-paper in a plastic bag prior to weighing, to reduce its uptake of moisture from the atmosphere; and iii) taking care not to handle the filter-papers with greasy hands (cutting the samples out of their cling film/wax coating inevitably led to my hands becoming greasy).

The papers were weighed using an Oertling R42 analytical balance, which was accurate to ±0.0005g. For the range of values of w_{FP} measured this creates an uncertainty in the value of w_{FP} of ±0.5% (absolute), i.e. an uncertainty of ±7½% (relative) in p_k.

A15.1.3 Notes on the formulae used to calculate soil suction

a) Correlations between p_k and w_{FP}

There are several correlations between a filter-paper's water content (w_{FP}) and soil suction (p_k). That due to Chandler and Gutierrez[3] is:

$$p_k = \gamma_w \times 10^{(3.83-6.22w)}$$

(which is restricted to the range $0.17 \leq w \leq 0.47$, i.e. $6000 \geq p_k \geq 80$kPa); and that due to Fawcett and Collis-George:[4]

$$p_k = \gamma_w \times 10^{(4.03-6.86w)} \quad \text{...for } w < 0.475, \text{ i.e. } p_k > 58\text{kPa}$$
$$p_k = \gamma_w \times 10^{(1.40-1.32w)} \quad \text{...for } w \geq 0.475, \text{ i.e. } p_k \leq 58\text{kPa}$$

In all these equations p_k is in pascals, γ_w in newtons per cubic metre, and w is expressed as a *fraction* (<u>not</u> a percentage).

Since many of the soil samples from Canons Park had water contents greater than 0.475, I have used the Fawcett/Collis-George correlations to calculate p_k.

In Chapter 13 (see p401), it is argued that the measured suction in the filter-paper sample is related to the mean effective stress in the soil (p'). However, there are errors in assuming that $p' = p_k$, as explained in Section A15.1.3.b below. In addition, there is at least one systematic error in the calculated value of suction, owing to water transfer between the soil and the filter-paper itself (see Section A15.1.3.c).

b) Error due to anisotropy

Consider an element of soil that exists in the ground under effective stresses (σ'_1, σ'_2, σ'_3) and pore pressure u. The mean effective stress in the soil is $p' = (\sigma'_1 + \sigma'_2 + \sigma'_3)/3$, and the mean total stress $p = p' + u$.

When the sample is removed from the ground, the mean total stress (p) is reduced to zero (i.e. $\Delta p = -p$). If the soil unloads elastically <u>and is isotropic</u>, then the change in pore pressure (Δu) is given by $\Delta u = B\Delta p$, where B is Skempton's pore pressure parameter and Δp the change in mean total stress (i.e. -p). Assuming the sample remains fully saturated (B = 1) allows the soil suction (p_k) to be written as:

$$p_k = -(u + \Delta u) = -(u + B\Delta p) = +(p - u) = p'$$

In other words, the suction in the sample is equal to the mean effective stress in the ground prior to sampling.

If, however, the soil is <u>anisotropic</u>, then the precise value of Δu depends on the relative magnitudes of σ'_1, σ'_2, and σ'_3. For simplicity, consider a transversely isotropic soil, i.e. one that has different

properties in the horizontal and vertical directions. For this case, Bishop and Hight[5] have derived the following equation for Δu:*

$$\Delta u = (B/E_h C)(\Delta\sigma_1(E_h/E_v - 2\mu_{hv}) + [\Delta\sigma_2 + \Delta\sigma_3](1 - \mu_{hv} - \mu_{hh}))$$

where C is the compressibility of the soil structure, given by:

$$C = (E_h/E_v - 4\mu_{hv} - 2\mu_{hh} + 2)/E_h$$

Numerical values for the parameters that appear in these formulae are given by Bishop and Hight for the London clay, and are: $E_h/E_v = 2.00$, $\mu_{hv} = 0.38$, and $\mu_{hh} = 0.00$. Substituting these numbers into the equations for Δu and C gives:

$$\Delta u = B(0.5\Delta\sigma_1 + 0.25\Delta\sigma_2 + 0.25\Delta\sigma_3)$$

Hence, for fully saturated soil (B = 1), the measured soil suction, $p_k = -(u + \Delta u)$, is:

$$p_k = (0.5\sigma'_1 + 0.25\sigma'_2 + 0.25\sigma'_3)$$

Far away from the pile, $K_0 \approx 2\text{-}2\frac{1}{2}$, and hence $p' \approx 1.11\text{-}1.14p_k$. Hence, if we ignore the anisotropic nature of the London clay by treating it as *isotropic* (i.e. by assuming $p' = p_k$), then we *under*-estimate p' by 11·14% (in the far-field).

The error in assuming the soil is isotropic is not so great as we move in towards the pile. Theoretical predictions for the ratio of the principal stresses close to the pile are given in Chapter 3 (see Table 3.9, p107). According to the cavity expansion method, $\sigma'_{zz} = \sigma'_{\theta\theta} \approx K_0^{nc}\sigma'_{rr}$ (where $K_0^{nc} \approx 0.62$ for London clay); whereas the strain path method predicts $\sigma'_{\theta\theta} \approx K_0^{nc}\sigma'_{zz} \approx K_0^{nc}\sigma'_{rr}$. The former implies $p' \approx 1.04p_k$ and the

---

*E_v and E_h are Young's moduli in the vertical and horizontal directions (respectively); μ_{hv} is Poisson's ratio for strain in the vertical direction due to a horizontal direct stress; and μ_{hh} is Poisson's ratio for strain in any horizontal direction due to a horizontal direct stress at right angles. Bishop and Hight's equation assumes that $\Delta\sigma_1$ acts in the *vertical* direction, and $\Delta\sigma_2$ and $\Delta\sigma_3$ in the horizontal directions.

latter $p' \approx 0.97p_k$. In other words the likely error in p_k if we ignore the anisotropic nature of the clay is - next to the pile shaft - less than 5%.

c) Error due to water transfer from sample to filter-paper

At the same time as the *dry* filter-papers remove water from the sample, so they increase the suction that acts inside the sample. A simple calculation[6] shows that, for the size of samples and number of filter-papers used in the Canons Park experiments, the likely error in the measured suction is between 4 and 22kPa (p_k over-estimated). The higher figure is appropriate for samples taken from adjacent to the piles (where p_k itself is large), and the lower figure for those from further away (where p_k is small). On average, p_k is over-estimated by about 10%. Of course, the inevitable loss in suction through handling the samples leads to the true p_k being *under*-estimated. It seems likely that the latter effect is greater than that due to the transfer of water to the dry filter-papers.

A15.1.4 Further test results

The results of the filter-paper measurements of soil suction next to the driven pile are shown in Figure A15.2 for soil at two depths, 3.10m and 3.86m. (The diagram for 3.86m is also shown in Chapter 13.) Figure A15.3 gives the corresponding measurements for the jacked pile.

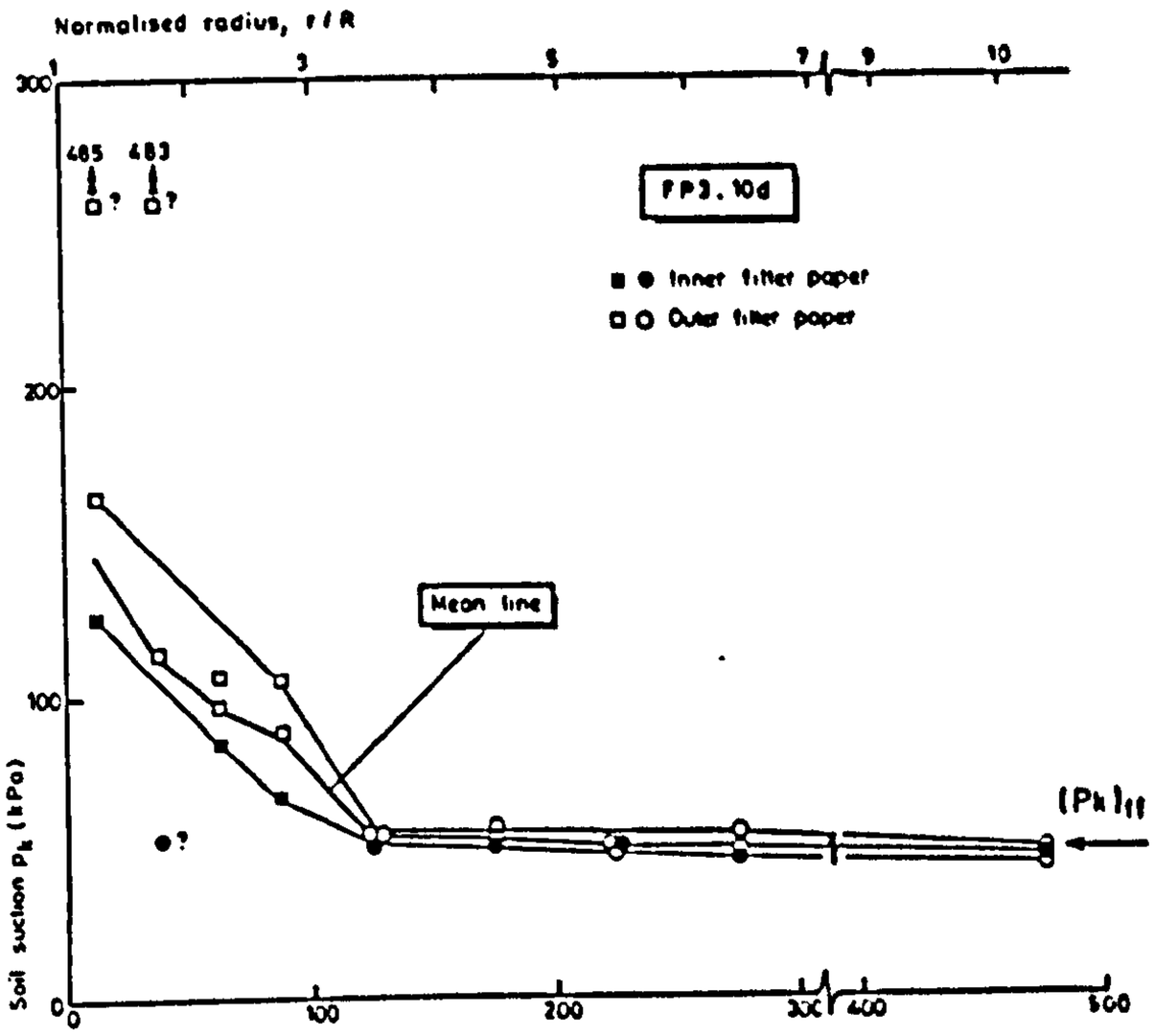
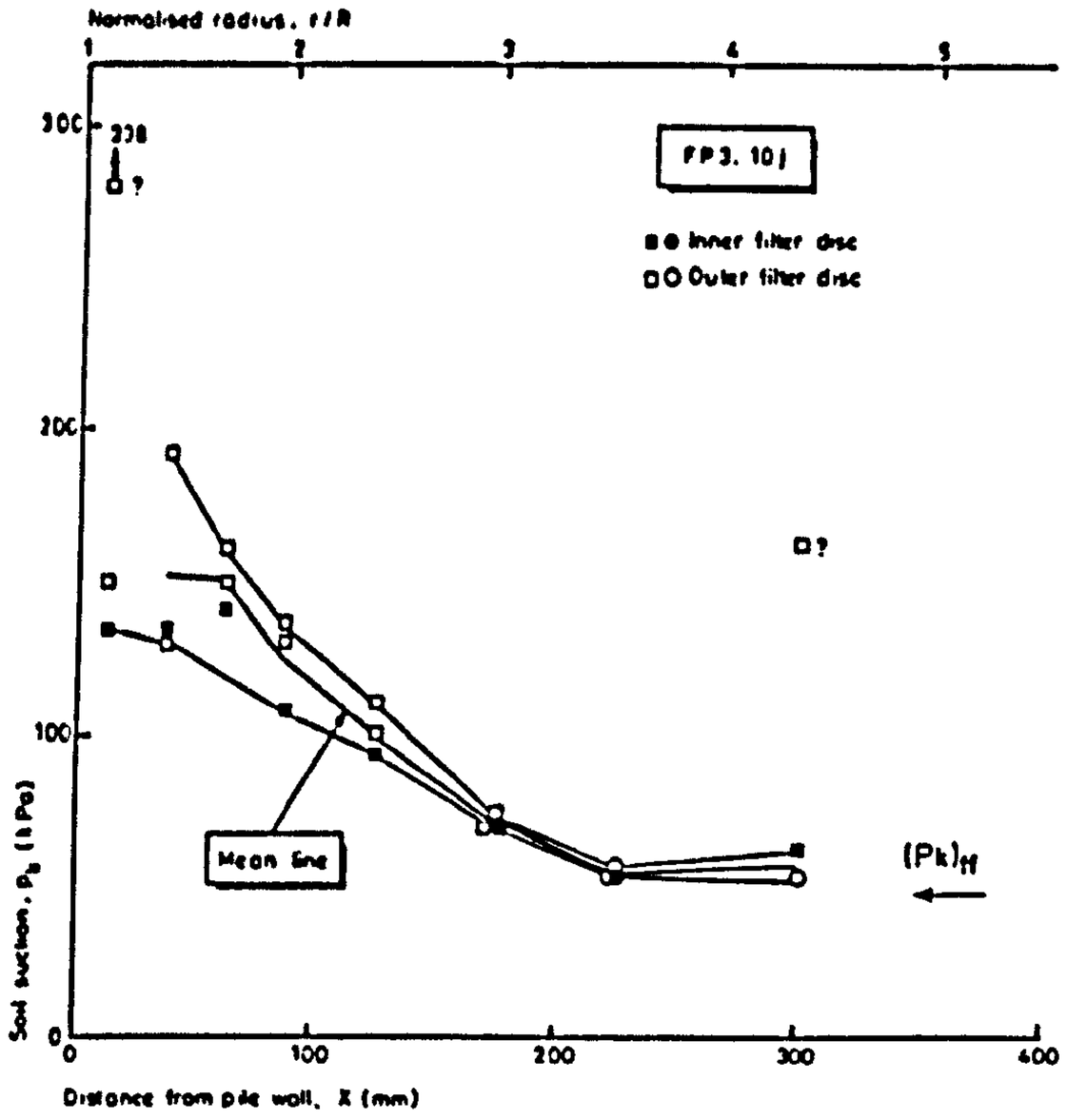


Figure A15.2 Filter-paper measurements of soil suction next to the driven pile CP6d: (top) 3.10m; (bottom) 3.86m



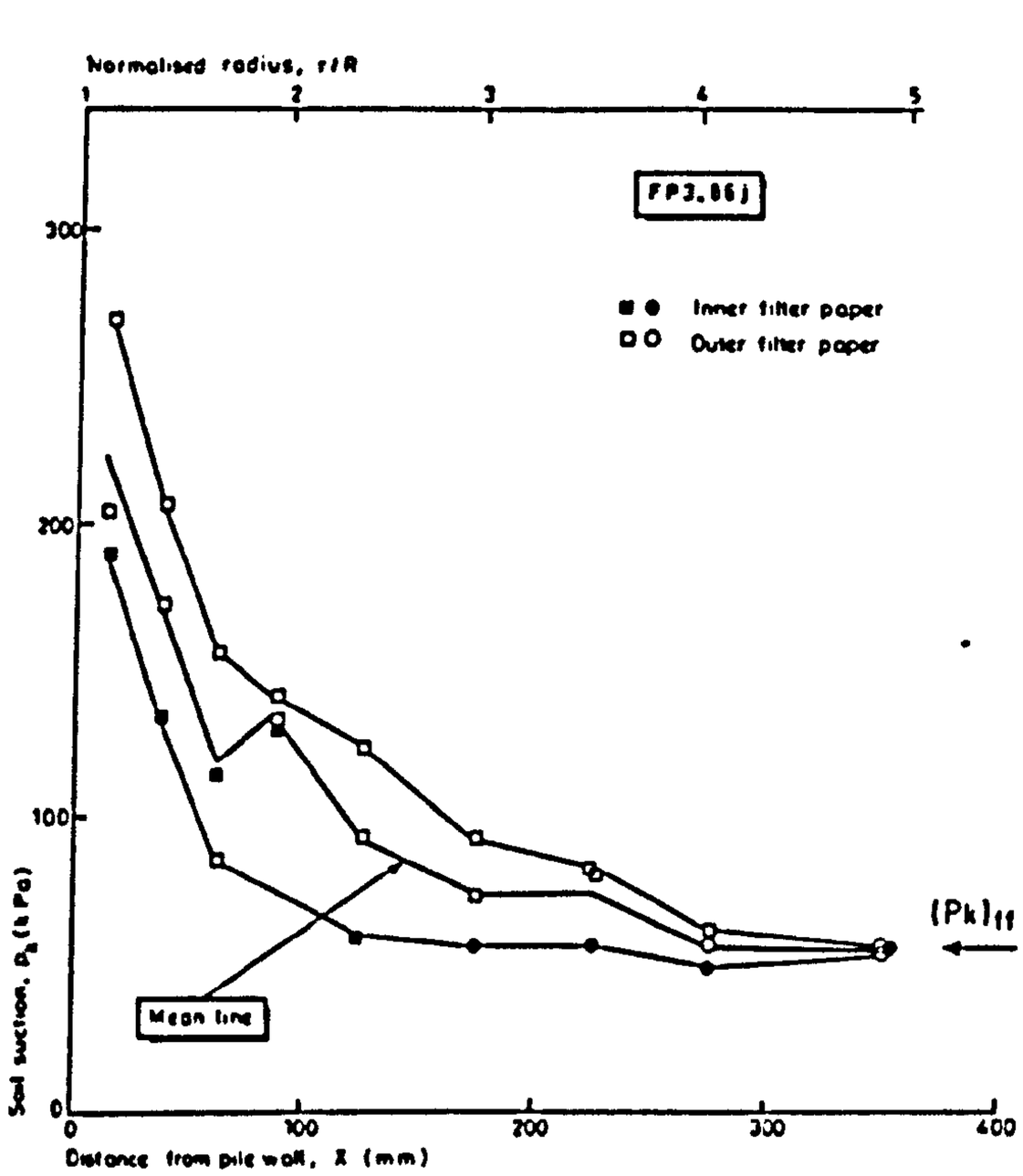


Figure A15.3 Filter-paper measurements of soil suction next to Kitching's jacked pile: (top) 3.10m; (bottom) 3.86m

A15.2 PRESSURE-PLATE MEASUREMENTS

A15.2.1 Testing procedure

Each specimen was trimmed with a sharp knife to the (approximate) dimensions 75mm x 75mm x 12½mm high. Great care was taken to produce top and bottom faces that were parallel and extremely flat: this is essential for accurate measurements of the soil's suction.

The specimen was then placed in contact with the pressure plate,* and enclosed in a high pressure container. A constant air pressure (u_a) between 100 and 400kPa was applied to the outside of the specimen; and the sample's water pressure (u_w) - as transmitted to the pressure plate - was recorded at frequent intervals over the next 24h, as the sample came into equilibrium under the applied air pressure. The sample was not allowed to drain.

*A high air-entry ceramic disc, previously saturated with water

A15.3 NOTES AND REFERENCES

[1]Chandler R.J. and Gutierrez C.I. (1986). The filter-paper method of suction measurement. Géotechnique, 36(2), pp265-268.

[2]Moisture was lost at the rate of ≈0.003g/min; a dry filter-paper weighs 0.36g, and a wet one 0.54g. Hence the error in w_{FP} would have been -0.8% per minute had no precautions been taken to prevent moisture being lost. (Chandler and Gutierrez (1986), loc. cit., report errors of about 1½%/min for both the drying out of wet papers and the wetting up of dry ones - see their Figure 3). An error of -1% in w_{FP} leads to a +15% error in p_k.

[3]Chandler and Gutierrez (1986), loc. cit., p266. The correlation is based on suction measurements made with a conventional oedometer; the scatter in the water content measurements was rather large (see their Figure 1).

[4]Fawcett R.G. and Collis-George N. (1967). A filter-paper method for determining the moisture characteristics of soil. Aust. J. Exp. Agric. Anim. Husb., 7, pp162-167.

[5]Bishop A.W. and Hight D.W. (1977). The value of Poisson's ratio in saturated soils and rocks stressed under undrained conditions. Géotechnique, 27(3), pp369-384. See equations 38 and 41, on p380.

[6]Since the filter-paper was originally dry, the *mass* of water that must be taken out of the soil sample to give it a water content w_{FP} is:

$$\Delta m_w = w_{FP} N m_{FP} \qquad \ldots.(1)$$

where N is the number of filter-papers used, and m_{FP} their mass. The resultant change in volume of the soil is:

$$\Delta V = -(\Delta m_w/\rho_w) = -w_{FP} N m_{FP}/\rho_w \qquad \ldots.(2)$$

where ρ_w is the density of water. This loss of water increases the suction by:

$$\Delta p_k = -K(\Delta V/V) = +K w_{FP} N m_{FP}/V\rho_w \qquad \ldots.(3)$$

where K is the soil's bulk modulus; and V the original volume of the sample. V is given by:

$$V = (m_s/G_s\rho_w) + (m_w/\rho_w) \qquad \ldots.(4)$$

where m_s is the mass of *dry* soil; m_w the <u>original</u> mass of water in the sample; and G_s the specific gravity of the dry soil.

Combining equations 3 and 4, and noting that the *original* water content of the soil sample is given by $w_o = (m_w)/m_s$, produces:

$$\Delta p_k = +K w_{FP} N m_{FP}/(m_s[1/G_s + w_o]) \qquad \ldots.(5)$$

The filter-paper comes into equilibrium with the sample's changed suction, i.e. $(p_k + \Delta p_k)$, hence the true suction is over-estimated by Δp_k.

For the Canons Park samples, appropriate numerical values for these parameters are: K = 10MPa; N = 3; m_{fp} = 0.36g; m_s = 0.4-1.5kg; G_s = 2.7; and $w_o \approx 0.3$. Substitution into equation (5) gives the following errors in p_k:

For a 25mm thick sample: $\Delta p_k \approx$ 14kPa if w_{fp} = 35%, or ≈22kPa if w_{fp} = 55%.
For a 100mm thick sample: $\Delta p_k \approx$ 4kPa if w_{fp} = 35%, or ≈6kPa if w_{fp} = 55%.